University of Naples Federico II
Department of Molecular and Cellular Biology and Pathology
"L. Califano"
Pathology and Physiopathology Doctorate Program- XXIII cycle

Multifunctional roles of microRNAs in human glioblastoma

Candidate:
Cristina Quintavalle

Supervisor:
Prof. Gerolama Condorelli

Coordinator:
Prof. Vittorio Enrico Avvedimento

Naples 2010

TABLE OF CONTENTS

LIST OF PUBLICATIONS 4

ABSTRACT 6

1. BACKGROUND 7
1.1 Central nervous System tumours 7
1.2 Pathogenic Pathway involved in gliomagenesis 9
1.2.1 Altered Growth signalling 9
1.2.2 Altered cell cycle arrest 9
1.2.3 Invasion and cell motility 10
1.3. Protein Tyrosine Phosphatase in glioma 12
1.4 Glioblastoma treatments 16
1.4.1 Alkylating agent: temozolomide 16
1.4.2 Reactivation of apoptosis:TNF-related apoptosis inducing ligand (TRAIL) 17
1.4.3 Antiangiogenetic therapy 18
1.5 MicroRNAs 20
1.6 Function of miRNAs in animals 22
1.6.1 Evolution and physiological function 22
1.6.2 Cancer 23

2. AIMS OF STUDY 25

3. MATERIALS AND METHODS 26
3.1 Cell Culture and transfection 26
3.2 Soft Agar Assay 26
3.3 Injection of glioma cells in nude mice 26
3.4 Virus Production 26
3.5 Protein Isolation and Western Blotting 27
3.6 miRNA microarray expreriments 27
3.7 Glioma cancer samples 27
3.8 RNA extraction and Real Time PCR 28
3.9 Luciferase Assay 28
3.10 miRNA locked nucleic acid in situ hybridization of formalin fixed, paraffin-embedded tissue section 28
3.11 Migration Assay 29
3.12 Cell death quantification 29
3.13 Colony Assay 30
3.14 Statistical Analysis 30

4. AIM I: Identification and Characterization of miRNAs involved in glioma tumorigenesis- Results 31
4.1 miRNA expression in glioma cell lines 31
4.2 Identification of PTPμ as a new target of miR-221 and -222 33
4.3 Expression of PTPμ and miR-22 and -221 in glioma 35
4.4 miR-221 and -222 regulate cell motility in glioma cells 36
4.5 miR-222 and PTPμ mRNA levels in glioma 37

5. AIM II: Identification of miRNAs involved in TRAIL resistance in glioma cells: Results 40
5.1 Selection of TRAIL sensitive and TRAIL resistance glioma cell lines 40
5.2 miRNA expression screening in TRAIL resistance vs. sensitive glioma cell lines 40
5.3 Roles of miRNAs in TRAIL resistance in glioma 41
5.4 Identification of cellular targets of miR-30c and miR-21in glioma cells 42
5.5 Validation of miR-21 and miR-30c mechanism of action 45

6. AIM III: Role of miR-221 and -222 in temozolomide resistance in glioma cells: Results 46
6.1 Temozolomide sensitivity of human glioma cell lines 46
6.2 MGMT is target of miR-221 and -222 47
6.3 miR-221 and -222 modulate temozolomide sensitivity in glioma cell lines 48
6.4 miR-221 and -222 and MGMT mRNA levels in glioma samples 49

7. DISCUSSION AND CONCLUSION 51

8. ACKNOWLEDGMENT 54

9. REFERENCES 55

LIST OF PUBLICATIONS

This dissertation is based upon the following publications:

- Michela Garofalo, Giulia Romano, **Cristina Quintavalle**, MariaFiammetta Romano, Federico Chiurazzi, Ciro Zanca, Gerolama Condorelli. Selective inhibition of PED protein expression sensitizes B-cell chronic lymphocytic leukaemia cells to TRAIL-induced apoptosis. Int J Cancer. 2007; 120(6):1215-22.

- Ciro Zanca, Michela Garofalo, Giulia Romano, Pia Ragno, Nunzia Montuori, **Cristina Quintavalle**, Luigi Tornillo, Daniel Baumhoer, Luigi Terracciano, and Gerolama Condorelli. PED mediates TRAIL resistance in human non-small cell lung cancer. J Cell Mol Med. 2008; 12(6A):2416-26.

- Michela Garofalo, **Cristina Quintavalle**, Gianpiero Di Leva, Ciro Zanca, Giulia Romano**,** Cristian Taccioli, C G Liu, Carlo M. Croce, and Gerolama Condorelli. MicroRNAs signatures of TRAIL resistance in human Non-Small Cell Lung Cancer. Oncogene. 2008;27(27):3845-55.

- Michela Garofalo*, **Cristina Quintavalle***, Ciro Zanca, Assunta De Rienzo, Giulia Romano, Mario Acunzo, Loredana Puca, MariaRosaria Incoronato, Carlo Maria Croce, and Gerolama Condorelli . Akt regulates drug-induced cell death through Bcl-w downregulation. PLoS ONE. 2008;3(12):e4070. *The first two authors contributed equally to this paper.

- MariaRosaria Incoronato, Michela Garofalo, Loredana Urso, Giulia Romano, **Cristina Quintavalle**, Ciro Zanca, Margherita Iaboni, Gerald Nuovo, Carlo Maria Croce and Gerolama Condorelli. *miR-212 increases* TRAIL sensitivity in non-small cell lung cancer by targeting the anti-apoptotic protein PED. Cancer Research. 2010 ;70(9):3638-46.

- **Cristina Quintavalle**, MariaRosaria Incoronato, Loredana Puca, Mario Acunzo, Ciro Zanca, Giulia Romano, Michela Garofalo, Margherita Iaboni, Carlo Maria Croce and Gerolama Condorelli. *c-FLIPL enhances anti-apoptotic Akt functions by modulation of Gsk3β activity*. Cell Death and differentiation. Cell Death Differ.2010; 17 (12):1908-16.

Other publications :

- Giulia Romano, Carlo Briguori, **Cristina Quintavalle**, Ciro Zanca, Natalia V Rivera, Antonio Colombo, and Gerolama Condorelli. *Iodinated contrast agents and renal cells apoptosis* European Heart Journal , Eur Heart J. 2008 Oct;29(20):2569-76.

- Ciro Zanca, Flora Cozzolino, **Cristina Quintavalle**, Stefania Di Costanzo, Lucia Ricci-Vitiani, Maria Monti, Piero Pucci, Gerolama Condorelli. *PED regulates cell migration process in human Non Small Cell Lung Cancer cells through Rac1*. Journal of Cellular Physiology. 2010; 225 (1):63-72.

- Carlo Briguori, **Cristina Quintavalle**, Francesca De Micco and, Gerolama Condorelli. *Nephrotoxicity of contrast media and acetylcysteine*. Archieves of Toxicology. 2010; Review in press

Abstract

Glioma are among the most deadly types of cancer. In spite of the enormous improvements made in neurosurgery, chemotherapy, and radiotherapy the prognosis of malignant glioma has remained poor over the last decade. Such bad efficacy in the management of glioma is largely attributable to resistance to therapeutic drugs and to the highly invasive nature of glioma cells capable of diffusely infiltrating and widely migrating in the surrounding brain tissue, leading to restricted and incomplete surgical resection and, thus, high recurrence rates. MicroRNAs (miRNA) represent a novel class of small RNAs that function as negative regulators of gene expression, deeply involved in the pathogenesis of several types of cancer. Different evidences indicate that miRNAs might play a fundamental role in tumorigenesis, cell proliferation, migration and apoptosis. The objective of this study is the identification and the functional characterization of microRNAs and their targets involved in resistance to therapeutics drugs (TRAIL, temozolomide) and in tumorigenesis of glioma cells.

1. BACKGROUND

1.1 Central nervous system tumours

Tumours of the central nervous system (CNS) or gliomas are a large collection of primary brain tumours that have characteristics similar to glia, astrocytes and oligodendrocytes (and their precursors) which together support the function of neurons in the brain. Because these tumours arise in the central nervous system and affect the surrounding brain structure, patients affected commonly develop symptoms that include headaches, local neurologic alteration or languages disturbance. CNS tumours are usually detected by computed tomography (CT) and magnetic resonance imaging (MRI) scans (Tran and Rosenthal; 2010).
Malignant gliomas may manifest at any age including congenital and childhood cases. Peak incidence is, however, in adults older than 40 years. Males are more frequently affected then females (Ohgaki and Kleihues; 2005, Ohgaki and Kleihues; 2005).
Excepted for inherited tumour syndromes (10% of all brain tumours) the etiology is still largely unknown. The only unequivocal risk factor is therapeutic ionizing irradiation in fact children receiving prophylactic CNS irradiation for acute lymphatic leukemia (ALL) may develop malignant glioma. No association of exposure to electromagnetic fields or viral infection or diet and glioma has been proven so far (Ohgaki and Kleihues; 2005).
Classification of brain tumours is based on histology and prognosis. The most recent classification of brain tumours is the World Health Organization (WHO) classification which was first formalized in 1979 and updated in 2007 (Louis et al; 2007). In addiction to a morphological grouping of brain tumours on the basis of presumed histogenesis, the WHO schemes have been notable for their grading of individual tumour classes (I, II, III and IV) as a means of reflecting anticipated biological behaviour. In this way higher grade tumours, are expected to follow a more aggressive clinical course than their lower grade counterparts (Huse and Holland; 2010). The WHO scheme divides the brain tumours into astrocytic, oligodendroglial and mixed categories. Additionally, the presence of histological features such as nuclear atypia, increased proliferation, microvascular proliferation and necrosis typically result in higher grade classification as either anaplstic glioma or gliobalstoma (Figure 1).
Grossly, glioblastoma multiforme are heterogeneous intraparenchymal masses that show evidence of necrosis and haemorrhage. Microscopically they consist of several cell types: the glioma cells proper, hyperproliferative endothelial cells, macrophages and trapped cells of the normal brain structures that are overrun by the invading glioma. The blood vessels both within and adjacent to the tumour are hypertrophied. Furthermore, the nuclei of tumour cells are extremely variable in size and shape, a characteristic called nuclear pleomorphism. Tumours cells characteristically invade the adjacent normal brain parenchyma, migrating through the white matter tracts to collect around blood vessels and neurons. The extent to

which these tumours invade adjacent structures is variable, at its extreme, large portion of the brain are diffusely infiltrated by individual tumour cells with no clear focus of tumour. Glioblastoma may develop from diffuse low grade or anaplastic astrocytomas (secondary glioblastoma), but more frequently, they manifest de novo, without a less malignant precursor lesion (primary glioblastoma) (Figure 1).
Low grade gliomas are divided into two histological variants: astrocytomas and oligodendrogliomas.
Anaplastic astrocytoma arise from low grade astrocytomas, but are diagnosed at first biopsy without a less malignant precursor lesion. This kind of tumor consist of cell with a large amounts of cytoplasm and which express the astrocyte-spercific marker gene GFAP (GLIAL FIBRILLARY ACIDIC PROTEIN).This tumours tend to progress to glioblastoma.
Anaplastic oligodendroglioma is a diffusely infiltrating tumour composed of oligodendroglia-like tumour cells which have small rounded nuclei a minimal cytoplasm and do not express GFAP, with focal or diffuse histological features of malignancy (Huse and Holland; 2010).

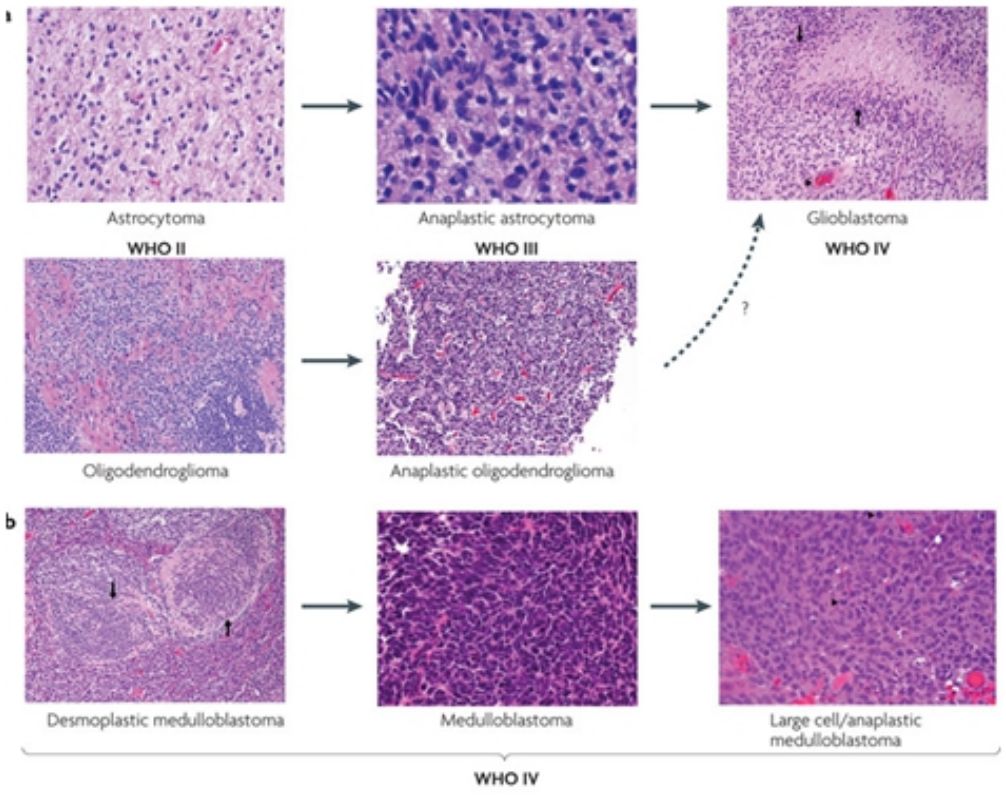

Figure 1-Current World Health Organization classification for diffuse glioma and medulloblastoma. Adapted from (Huse and Holland; 2010)

1.2 Pathogenic Pathway involved in gliomagenesis

Neoplastic disorders are in general genetic disease. The genetic alterations are associated with alteration of cell proliferation, apoptosis, senescence, migration, and cell-to-cell communication. Genetic alterations in malignant gliomas are extremely complex and diverse. However, distinct molecular pathways show frequent alterations:

1.2.1 Altered growth factor signalling

The genes that encode growth factors and their receptors frequently have elevated expression in gliomas. All grade gliomas usually display an overproduction of growth factor such as FGF2, CNTF and PDGF and their receptors (Noble and Mayer-Pröschel; 1997, Ekstrand et al; 1991). These phenomena usually happen in the same cell inducing an autocrine stimulation of the pathway controlled by those receptors. It seems that the pathways activated by these growth factors have a significant role in gliomagenesis. Mutations (amplification or activating mutation) of the gene encoding for EGF receptor have been found in most malignant gliomas. These mutations usually produce a constitutively active receptor in the absence of EGF ligand (Wong et al; 1992).

In glioma these growth factor receptors activate several common signalling pathways including RAS and AKT pathway.

The RAS pathway is one of the best-studied pathways. RAS is indirectly activated by tyrosine kinase receptor and is active when bound to GTP but inactive when the GTP is hydrolysed to GDP. In the active form RAS activates many pathways such as RAL, RAC and RAF pathways, which lead to the mitogen-activated protein kinases (MAPKs) ERK, Jun Kinase (JNK) and p38. This activated pathways enhance proliferation, progression through cell cycle and inhibition of apoptosis (Hunter; 1995).

The pathway of AKT is also activated by tyrosine kinase receptors and is involved in glial differentiation. AKT is activated through phosphosohatidylinositol-3-OH kinase (PI(3)K) and is modulated by tumour suppressor protein PTEN. Active AKT enhance metabolism by activating glycogen synthase kinase 3 (GSK3β) and alter translation by activating the kinase called mammalian target of rapamycin (mTOR). AKT is also capable to inactivate apoptosis through inactivation of BAD, causing caspase activation to be inhibited. Most gliomas show mutation and frequent loss of expression of the PTEN gene and elevated AKT activity but the specific effect of AKT signalling on glial differentiation have not yet been investigated (Sano et al; 1999) (Figure 2A).

1.2.2 Altered cell cycle arrest

The second group of mutations found in gliomas includes those that disrupt the pathways involved in the control of G1 cell-cycle arrest. The retinoblastoma (Rb) tumour suppressor pathway has been shown to be defective in a significant number of high grade glioma, whether by inactivating mutations in RB1 gene itself or amplification of its negative regulators cyclin-dependent kinase 4 (CDK4) and, less frequently, CDK6. Analogously, amplification of the p53 antagonists

MDM2 and MDM4 have also been found in distinct subsets of TP53-intact glioblastomas. These tumours have mutation and/or deletion in the CDKIN2A locus that encodes for both INK4A and ARF, which are crucial positive regulators of Rb and p53 respectively. Mouse models have provide further evidence in the importance of the perturbance of p53 and Rb pathway in glioma pathogenesis demonstrating that functional loos of either Rb and p53 can directly drive glioma formation, decrease disease free latency and or increase tumour grade (He et al; 1994).

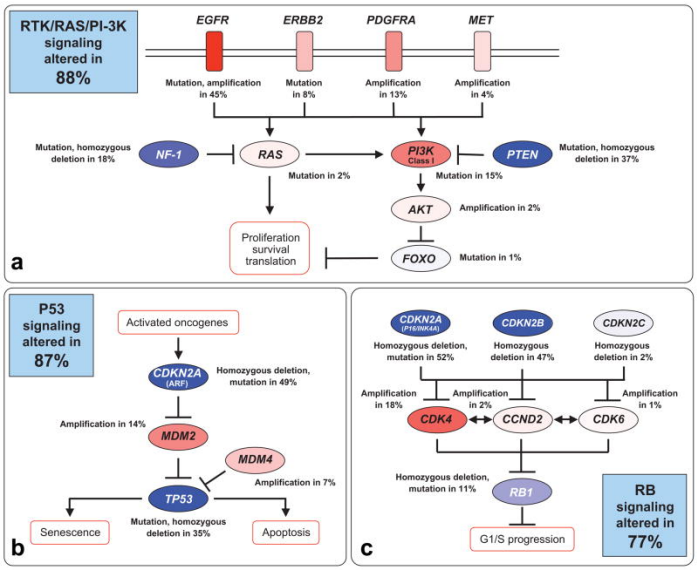

Figure 2- Schematic representation of genetic alterations occurring in glioblastoma in RAS/PI3K, p53 and RB signalling pathway.

1.2.3. Invasion and cell motility

All glial tumours are invasive. The degree of invasiveness does not necessarily correlate with the grade of malignancy. Low-grade astrocytomas often show extensive infiltration of normal brain, which limits surgical resection and eventually leads to recurrence and progression of the disease. The invasion of high-grade gliomas follows similar anatomic structures, but the dynamics of this process seem to be more rapid. After surgical removal of a malignant glioma, invariably a recurrent tumour will manifest; in more than 95% of the cases and frequently immediately adjacent to the resection cavity. Distant lesions far away from the site of the initial tumour may also be found (Giese et al; 2003).

The advent of gene-expression profiling has opened up the opportunity to gain insight into the underlying genetic basis of glioma invasion and motility (Sallinen et al; 2000). Because the elimination of malignant cell with an invasive phenotype remains an elusive therapeutic target, dedicated understanding of migratory and invasive molecular pathologies may be especially supportive for a new treatments of gliomas (Claes et al; 2007).

Invasion is a complex multistep process (Dear and Kefford; 1990). The initial step requires receptor-mediated adhesion of tumour cells to matrix proteins, followed by the degradation of matrix by tumour-secreted proteases and accompanied by biochemical processes supportive of active cell movement. Cell motility is not a de novo feature of cancer cells. Several cell types exhibit active movement during various stages of embryonic development, during wound healing, and in the inflammatory response. This motile behaviour is strictly controlled for this it can be hypothesized that the reappearance of a motile phenotype in cancer cell can be due by the lost of this control (Gressens; 2000). To migrate, the cell body must modify its shape and stiffness to interact with the surrounding extracellular matrix. Cell movement necessitates a change in cell morphology: the cell becomes polarized and membrane protrusions develop, including the extensions of pseudopodia, lamellipodia and filopodia. These extensions contain filamentous actin and various structural and signalling proteins necessary for attachment to the ECM. The formation of membrane anchors allows cytoskeletal contraction, which finally advances a cell forward.

The proteolytic activity of matrix-metalloproteinases has been correlated with invasiveness in tumours of various tissue types and may be an important mediator of glioma invasion. Protease degradation of extracellular matrix creates an intercellular space into which invading cells can migrate by an active mechanism that requires membrane synthesis, receptor turnover, and rearrangement of cytoskeletal elements. This process also requires dissociation from adjacent cells and detachment from previous matrix adhesion sites.

Glioma cells in vitro are highly migratory cells, and the migration rate of these cells can be profoundly regulated by extracellular matrix components. Motility rates positively correlate with substrate adhesion, demonstrating that matrix receptors, which link the cellular membrane to the extracellular space, facilitate migration by providing adhesion and traction on a given matrix substrate.

Recently, a study was presented by Mariani et al who harvested 20,000 glioma cells by a laser-capture micro dissection technique from invaded brain as well as the highly cellular tumour mass of a human glioblastoma specimen. Differential gene-expression profiles of invading and non-invading tumour cells were analyzed, and some 60 candidate genes differentially expressed in invasive cells were identified. One gene over expressed in invasive cells was identified as *P311*, which localizes to focal adhesion areas and serves a structural function by linking the F-actinin bundles through a chain of linking proteins to the cell membrane. This process plays a critical role in cell motility. Over expression of this gene was confirmed in a number of glioblastoma specimens, and antisense oligonucleotide treatment decreased motility of glioma cells in a monolayer-migration assay. This demonstrates that mechanisms regulating cell motility contribute to the invasive phenotype of malignant gliomas (Mariani et al; 2001).

Recently work suggest an important role in glioma cell migration and invasion also for protein tyrosine phosphatase (Mori et al; , Blanquart et al).

1.3. Protein tyrosine phosphatase in glioma

As indicated before, gliomas are characterized by diffuse infiltrative growth in the surrounding brain parenchyma. This characteristic precludes curative treatment by surgery or radiotherapy alone, and together with their relative resistance to common chemotherapy place these tumours among the most incurable human malignancies (Claes et al; 2007). As described before, most of the alteration in glioma tumorigenesis leads to aberrant growth factor signalling and deregulation of cell cycle control in which, the phosphorylation of proteins on tyrosine residues plays a fundamental role. This reliance on protein tyrosine kinase (PTK) activity requires a closer look on the role played by protein tyrosine phosphatases (PTPs) in glioma biology. The opposing actions of PTK and PTP enzymes provide the cell with a functional dial that regulates the activity of mutual substrates through phosphorylation of tyrosine residue in a reversible manner. This phosphorylation itself may regulate the activity of PTKs and PTPs themselves.

The PTP enzyme family has emerged as an important regulator of developmental and disease-related signalling pathways, and multiple members are directly linked to malformation syndromes and tumorigenesis (Hendriks et al; 2008). Reversible tyrosine phosphorylation of proteins plays an important role in the regulation, proliferation and differentiation of cells (Tonks; 2006). There are 107 genes in the human genome that belong to the PTP super family of enzymes. These super families have been divided into four different classes basing on the sequence homology of their catalytic domains. Class I comprises 38 so called 'classical' PTPs (enzymes that exclusively dephosphorylate phosphotyrosine residues, as well as 61 dual-specificity PTPs (DSPs). DSPs can also dephosphorylate phosphoserine and phosphothreonine residues. The 38 classical PTPs can be further subdivided into transmembrane, receptor-like (RPTPs) and non-receptor-type PTPs. In human genome, there is only a single class II gene that encodes the low-molecular weight PTP, termed LMPTP, that is specific for phosphotyrosine residues. Class III comprises three CDC23 homologs that dephosphorylate tyrosine and threonine residues within cyclin-dependent kinases, which participate in cell cycle regulation. Class IV consists of the eyes absent (Eya) proteins, which recognizes phosphorylated tyrosine, or dual serine and tyrosine residues and function as transcriptional regulators. Each PTP class is believed to originate from a distinct ancestral gene and because of similarity in the dephosphorylation mechanism they provide an impressive example of convergent evolution (Alonso et al; 2004).

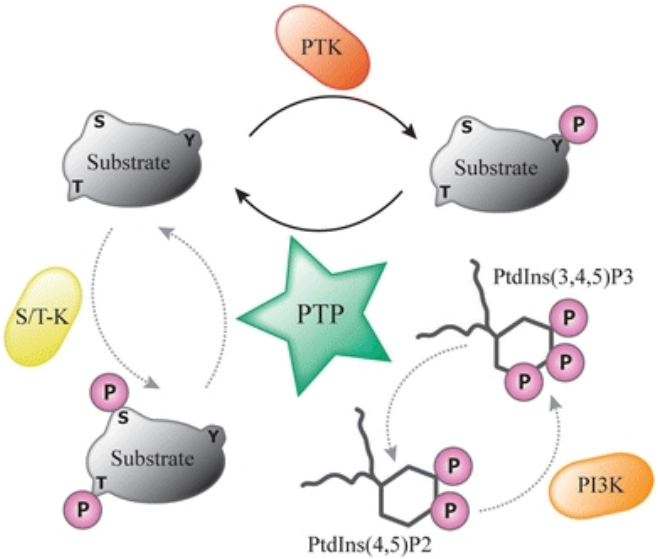

Figure 3-Signalling pathway by tyrosine phosphatase activity: opposing action of PTK (protein tyrosine phosphatase) and PTP (protein tyrosine phosphatase).

A common feature of the PTP class I, II and III is the PTP signature motif (H/V)C(X)R(S/T) in their catalytic domain. The cysteine residue is essential for catalytic activity; the target phosphate group is transferred from the substrate onto this catalytic site, producing a thiol intermediate, and is subsequently released via hydrolysis. The Class IV uses a slight different mechanism, in which aspartate instead cysteine plays a crucial role in the reaction. Outside the catalytic domain, PTPs are very diverse in their structure (Tabernero et al; 2008).

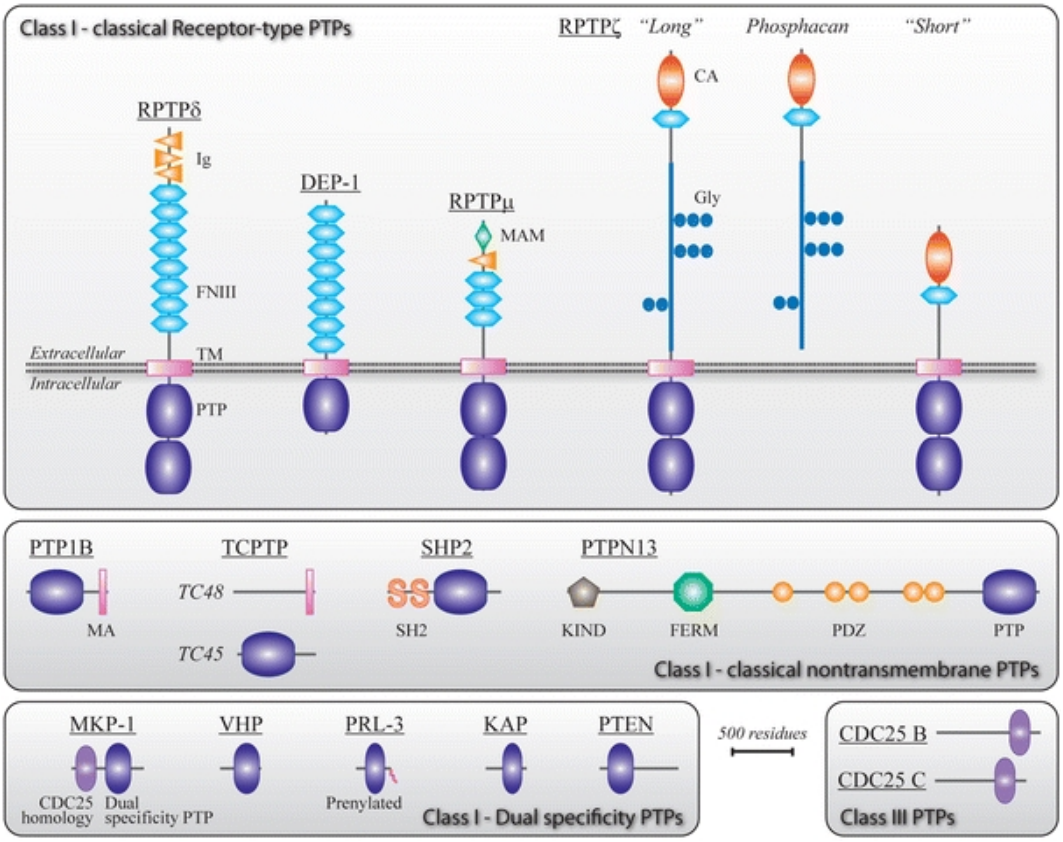

Figure 4- Domain structure of the PTP super family members implicated in glioma biology.

PTPs are been studied for their role in glioma development. 15 out of 107 PTP genes are implicated in some way. Between these a major attention in the last year has been acquired by the cell surface receptor RPTPμ. PTPμ is a member of the PTPμ-like subfamily which includes PTPμ, PTPk, PTPd and PCP-2. The extracellular segment of the PTPμ-like RPTPs contains motifs found in cell adhesion molecules including a MAM (Meprin/A5-protein/PTPMu) domain, an Ig domain, and four FNIII repeats. PTPμ mediates cell-cell aggregation via homophilic binding (Brady-Kalnay et al; 1993, Gebbink et al; 1993). These events happen when PTPμ on the extracellular surface of one cell binds to PTPμ on the surface of an adjacent cell, forming an adhesive contact. The intracellular segment of PTPμ contains a juxtamembrane sequence with homology to cadherins and two conserved phosphatase domains of which only the most membrane proximal is catalytically active. There are different evidences that both cell adhesion and tyrosine phosphorylation play a role in contact inhibition of cell movement.
Brady-Kalnay and others (Hellberg et al; 2002, Burden-Gulley and Brady-Kalnay; 1999) have demonstrated that PTPμ interacts specifically with N-cadherin, E-

cadherin and R-cadherin and that PTPμ is capable to regulate N-cadherin dependent neurite outgrowth of retinal ganglion cells. PTPμ is expressed in a gradient both in the retina and the tecum (Burden-Gulley et al; 2002). Since the axon of retinal ganglion cells form the optic nerve and are the sole output from the retina to the brain, the expression of PTPμ on these cells indicate a putative role of PTPμ in axonal migration and neurite outgrowth. In addition to PTPμ's role in the regulation of cadherin function, PTPμ appears to either directly or indirectly regulate protein Kinase C. PTPμ was found to interact with the scaffolding protein RACK1 (receptor for activated c Kinase) and this interaction is required for both PTPμ mediated neurite outgrowth and PTPμ mediated axon guidance of retinal ganglion cells (Rosdahl et al; 2002).

PTPμ is expressed as a 200kDa protein that is proteolytically cleaved in the fourth FNIII repeat, resulting in a 100KDa extracellular fragment (E-subunit) and intracellular portion (P-subunit). This cleavage is mediated by a furin like protease in the endoplasmic reticulum during intracellular trafficking. The intracellular fragment of PTPμ translocates to the nucleus. The overexpression of full length PTPμ in glioblastoma cells suppresses cell migration and growth factor independent survival. Recently, it was found that full-length PTPμ is downregulated in primary human glioblastomas (Burgoyne et al; 2009, Burgoyne a,b et al; 2009). While overexpression of full length PTPμ protein reduces glioma cell migration (Burgoyne et al; 2009), the presence of a proteolytically cleaved cytoplasmatic fragment of PTPμ, capable to translocate to the nucleus, increases glioma cell migration (Burgoyne et al; 2009). This consideration implies that the presence of full-length PTPμ suppresses migration. In a recent work Phillips-Mason and colleagues identify PKCdelta and PLCgamma1 as PTPμ substrates in tumour cells involved in regulation of PTPμ cell motility (Phillips-Mason et al).

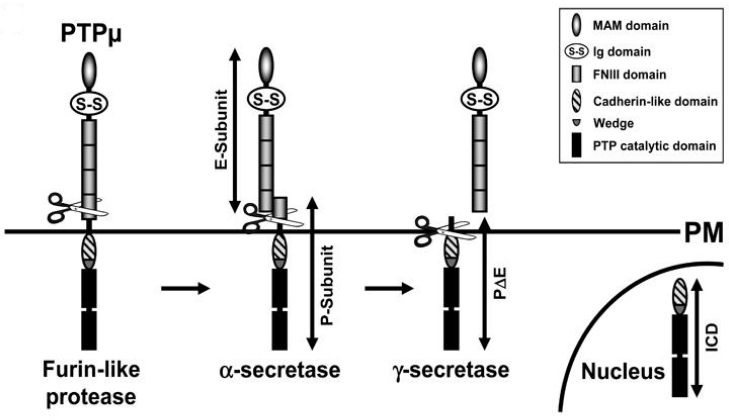

Figure 5- PTPμ structure and mechanisms of activation. PTPμ is cleaved by secretases to generate a fragment that translocates to the nucleus.

1.4. Glioblastoma treatments

Primary brain tumours are widely regarded as being particularly resistant to the most commonly used antineoplastic strategies. Although surgery plays a major role in removing some brain tumours, often the tumour cannot be effectively removed. Both radiation and chemotherapy are compromised because many glial-derived tumours seem to be particularly resistant to apoptosis following DNA damage and are very difficult to reach by the chemoterapic. Recently, the strategies used to fight primary brain tumours are based on the use of alkylalting agent, TRAIL and antiagiogentetic molecules.

1.4.1. Alkylating agent: temozolomide

A new alkylating agent, temozolomide (TMZ) has been recently introduced in clinical trials for treatment of primary or recurrent high grade gliomas (Plowman et al; 1994, Stupp et al; 2005). TMZ has several advantages over other existing alkylating agents because its characteristic: TMZ is a small lipophilic molecule and it can be administrated orally and it crosses the blood brain barrier. Moreover, temozolomide is less toxic to the hematopoietic progenitor cells than convential chemotherapeutic agent because it doesn't result in chemical cross-linking of the DNA strands. For all this characteristics temozolomide is a promising agent for the treatment of malignant gliomas (Agarwala and Kirkwood; 2000, Friedman et al; 2000).

There are different evidences which demonstrate that temozolomide improves median survival and increases the likelihood of long-term survival when given currently with radiotherapy and then following radiotherapy, instead of radiotherapy alone following by surgical resection (Stupp et al; 2005). The cytotoxicity of TMZ has been investigated and recent report suggest that cells treated with temozolomide underwent autophagy cell death and not apoptosis (Kanzawa et al; 2004).

O6-methylguanine DNA methyltransferase (MGMT) is a key enzyme in the DNA repair network that remove mutagenic, cytotoxic adducts from O6-guanine in DNA, the preferred point of attack of alkylating agents. This transfer irreversibly inactivates MGMT. Accordingly, MGMT knockout mice are hypersensitive against alkylating drugs, including TMZ, and depletion of the enzyme by the substrate analog O8-benzylguanine increased the sensitivity of glioma cells against alkylating drugs (Bobola et al; 2004, Liu and Gerson; 2006, Friedman et al; 2002). A direct relationship between MGMT activity and resistance to alkylating agents has also been observed in cell lines and xenografts derived from a variety of human tumours, including gliomas (Esteller et al; 2001) .Therefore, adjuvant chemotherapy based on temozolomide is limited by the action of this enzyme, resulting in the very poor survival of glioblastoma patients.

The loss of MGMT expression is commonly attributable to deletion, mutation, or rearrangement of MGMT gene or messenger MGMT instability. MGMT activity is frequently lost in the presence of CpG island hypermetylation in the promoter region of certain types of human primary neoplasma, including gliomas. Therefore, the methylation status of the MGMT promoter was considered to be

indicative of a good outcome in patients with malignant gliomas treated with an alkylating agent. The most concing data were provided by Hegi et al (Hegi et al; 2005), who investigated the MGMT methylation status in a large cohort of glioblastoma by comparing patients receiving either radiotherapy alone or radiotherapy combined with concomitant and adjuvant TMZ. Patients with methylated MGMT tumours benefited the most from the addition of TMZ, while those with unmethylated MGMT tumours showed only a non significant improvement in survival with TMZ.

1.4.2. Reactivation of apoptosis: TNF-related apoptosis-inducing ligand (TRAIL)

In recent years, a variety of cancer-specific molecular aberration have been identified and explored as potential targets for treatment of patients with glioblastoma. A novel interesting therapeutic approach is the reactivation of apoptosis using member of TNF (tumor necrosis factor) -family, of which TRAIL hold the greatest interest. TRAIL is a relatively new member of the TNF family known to induce apoptosis in a variety of cancers (Schaefer et al; 2007).

TRAIL is an effector molecule involved in immune surveillance by T cell population and NK cells. TRAIL is important for the elimination of virally infected and cancer cells (Hayakawa et al; 2004, Janssen; 2003).

TRAIL is normally expressed on both normal and tumour cells as a transmembrane protein. In addition, a soluble form of TRAIL can be generated due to alternative mRNA splicing or proteolytic cleavage of the membrane form. This molecule acts through four distinct membrane receptors, designed TRAIL-R1, TRAIL-R2, TRAIL-R3 and TRAIL-R4. Of these receptors, only TRAIL-R1 and TRAIL-R2 are functional and transmit the apoptotic signal. These two receptors belong to a subgroup of the TNF receptor family called the death-receptor, and contain the intracellular domain (DD). This domain is critical for the activation of apoptotic signalling of the receptor.

TRAIL, binding one of the two receptors, activates the extrinsic pathway of apoptosis. The activate receptor recruit and activate caspase-8 or -10 through the adaptor protein Fas-associated death domain (FADD; also known as MORT1) at the cell surface. This protein complex is often called the DISC, or Death Inducing Signalling Complex. This recruitment causes subsequent activation of downstream (effector) caspases such as caspase-3, -6 or -7, without any involvement of the BCL-2 family. In some cells, most notably hepatocytes, the extrinsic pathway can intersect the intrinsic pathway through caspase-8 cleavage-mediated activation of the pro-apoptotic BH3-only protein BID. The C-terminal truncated form of BID (tBID) translocates to mitochondria and promotes further caspase activation (caspase-9 and the effector caspases caspase-3, -6 and -7) through the intrinsic pathway. In these situations, loss of BID or overexpression of BCL-XL inhibits cell death (Walczak and Krammer; 2000).

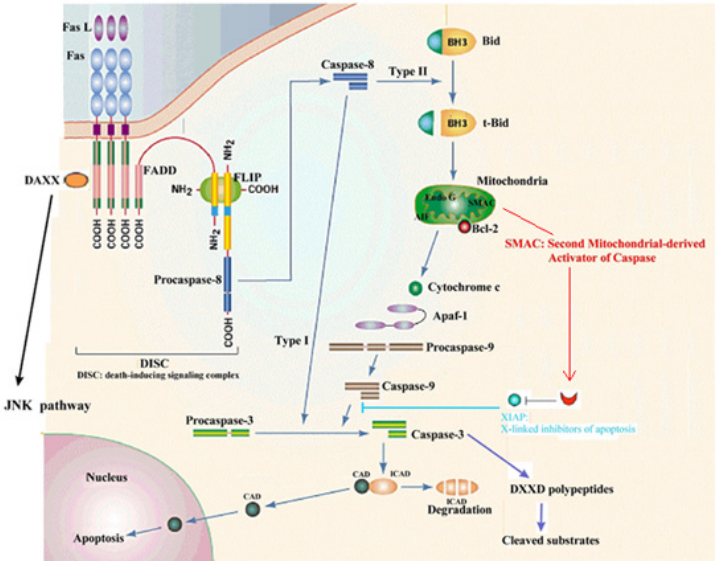

Figure 6- The intrinsic and extrinsic pathway of apoptosis. These two major signalling pathways converge at the level of the effector caspase,

Treatment with TRAIL induces programmed cell death in a wide range of transformed cells, both in vivo and in vitro, without producing significant effects in normal cells (Schaefer et al; 2007, Falschlehner et al; 2007), and for this reason TRAIL is in phase II/III clinical trials for different kinds of tumours. However, a significant proportion of human cancer cells are resistant to TRAIL-induced apoptosis, and the mechanisms of sensitization seem to differ among cell types. Different studies relate resistance to TRAIL-induced cell death to downstream factors. It has been shown that down-regulation of PED or cellular FLICE-like inhibitory protein (c-Flip) can sensitize cells to TRAIL-induced apoptosis (Garofalo et al; 2007, Zanca et al; 2008, Quintavalle et al; 2010). However the mechanism of TRAIL resistance is still largely unknown.

1.4.3. Antiangiogenetic Therapy

One of the prominent features of malignant gliomas is extensive neovascularisation, which is thought to provide oxygen and nutrients to rapidly dividing tumour cells in hypoxic tumour environments. This process is known as angiogenesis. Angiogenesis is regulated by several proteins that promote or prevent the process. During tumour progression, growth is sustained by nutrients and oxygen through passive diffusion. Once new blood vessels form, the tumour start to grow and spread faster. In gliomas, angiogenesis is typically associated with an increase in vascular endothelial growth factor (VEGF), a protein that stimulates new blood vessel formation (Hanahan and Folkman; 1996).

The majority of the anti-angiogenic drugs that have been evaluated in clinical trials to date interfere with the VEGF pathway by directly blocking ligand or

receptor. However, there is increasing interest in targeting proangiogenic molecules that function by alternative mechanisms. For example, the neuropilins are nontyrosine kinase receptors that are activated by VEGF binding and potentiate VEGFR signalling. Neuropilin-1 also facilitates HGF/SF signalling (Hu et al; 2007). The angiopoietins (Ang-1 and Ang-2) are involved in the stability and maintenance of the tumour vasculature. Binding of Ang-2 to its cognate receptor, Tie-2, serves to destabilize vessels, which is a requirement for angiogenesis to proceed. Ang-2 inhibitors are therefore of interest as therapeutic agents (Oliner et al; 2004). Notch inhibitors may also prove effective. Notch receptors on tumour endothelial cells are activated by transmembrane jagged and delta-like ligands on the surfaces of neighbouring cells. Inhibition of delta-like ligand 4 (Dll4) on endothelial cells in preclinical models promotes the growth of an abnormal neovasculature with reduced perfusion and tumour growth (Noguera-Troise et al; 2006). Finally, tumour cells secrete chemokines that serve to recruit proangiogenic myeloid cells to the tumour. For this reason, inhibitors of specific chemotactic signalling may have therapeutic value.

After bevacizumab was approved by the FDA for colon cancer, several neuro-oncology centers began to use it to treat patients with recurrent malignant glioma, often in combination with irinotecan. Different reports demonstrated that bevacizumab therapy leads to rapid reductions in peritumoral edema, often permitting a decrease in dose or even cessation of corticosteroid use. These studies also indicated that bevacizumab treatment is well tolerated in most cases. The risk of intracranial haemorrhage is low. Common toxicities related to bevacizumab therapy in the malignant glioma population include hypertension, proteinuria, fatigue, thromboembolic events, and wound-healing complications (Pope et al; 2006, Poulsen et al; 2009, Narayana et al; 2009).

In addition to VEGF inhibitors, small molecule inhibitors of VEGFR have been tested in recurrent malignant gliomas. Cediranib (AZD2171) inhibits all known subtypes of VEGFR and was evaluated in a phase 2 trial of patients with recurrent GBM. The drug was largely well tolerated, with hypertension, diarrhea, and fatigue as the most common adverse effects. Using dynamic contrast-enhanced magnetic resonance imaging (MRI) scans, the authors demonstrated that cediranib therapy reduced blood vessel size and permeability. In addition to VEGF or VEGFR inhibition, a variety of other approaches may have antiangiogenic activity. Because of its role in pericyte recruitment, inhibition of PDGFR may prove useful. Several trials of PDGFR and dually targeted VEGFR/PDGFR inhibitors are ongoing, as noted earlier. Although antiangiogenic therapies prolong PFS, further progression of disease is inevitable. Tumours that progress during antiangiogenic therapy cannot often be treated successfully thereafter, and most patients die of the disease within a few months

Combining antiangiogenic therapy with anti-invasion therapy may therefore delay disease progression. Another potential mechanism of resistance to antiangiogenic therapies involves increased PDGF signalling. PDGF promotes stabilization of the neovasculature by recruiting pericytes and facilitating pericyte-endothelial cell interactions.

1.5. MicroRNAs

In the last decade, many non-coding RNAs were found to regulate a wide variety of biological processes. Among these, microRNAs (miRNAs) are the best characterized. miRs are a class of endogenous non-coding RNA of 19-24 nucleotides in length that play an important role in the negative regulation of gene expression blocking translation or directly cleaving the targeted mRNA. The biogenesis of miRNAs is a complex and coordinate process in which are involved different enzymes and proteins (Bartel; 2004).
miRNAs gene encoded in the genome are transcribed into long primary miRNAs (pri-miRNAs) by polymerase II or in few rare case, by polymerase III (Lee et al; 2002). Typically, pri-miRNAs display a 33bp stem and a terminal loop structure with flanking segment. Primary miRNA processing begins in the nucleus where an RNAseIII enzyme, Drosha, removes the flanking segments and 11 bp of the stem region, inducing the conversion of pri-miR into precursor miRNAs (pre-miRs). Pre-miRs are 60-70nt long hairpin RNAs with 2-nt overhangs at the 3' end. Pre-miRNAs are transported into the cytoplasm for further processing to become mature miRNAs. The transport occurs through a nuclear pore complexes and is mediated by the RanGTP-dependent nuclear transport receptor exportin-5 (EXP5). EXP5 exports the pre-miRNA out of the nucleus, where hydrolysis of the GTP results in the release of pre-miRNA. In the cytoplasm the pre-miRNA is subsequently processed by Dicer, an endonuclease cypolasmic RNAse III enzyme, to create a mature miRNA. Dicer is a highly specific enzyme that cleaves pre-miRNAs into 21-25 nt long miRNA duplex, of which each strand bears 5' monophosphate, 3' hydroxyl group and 3' 2-nt overhang. Of a miRNA duplex, only one strand, designed the miRNA strand, is selected as the guide of the effector RNA-induced silencing complex (RISC). The core component of RISC is a member of Argonaute (Ago) subfamily proteins. During RISC loading, the miRNA duplexes are incorporated into Ago proteins. RISC loading is not a simple binding of the duplexes and Ago proteins, but also an ATP-dependent active process. After RISC loading, the duplex is unwound and in the complex is maintained only the miRNA strand (Bartel; 2004, Lee et al; 2002, Gregory and Shiekhattar; 2005).

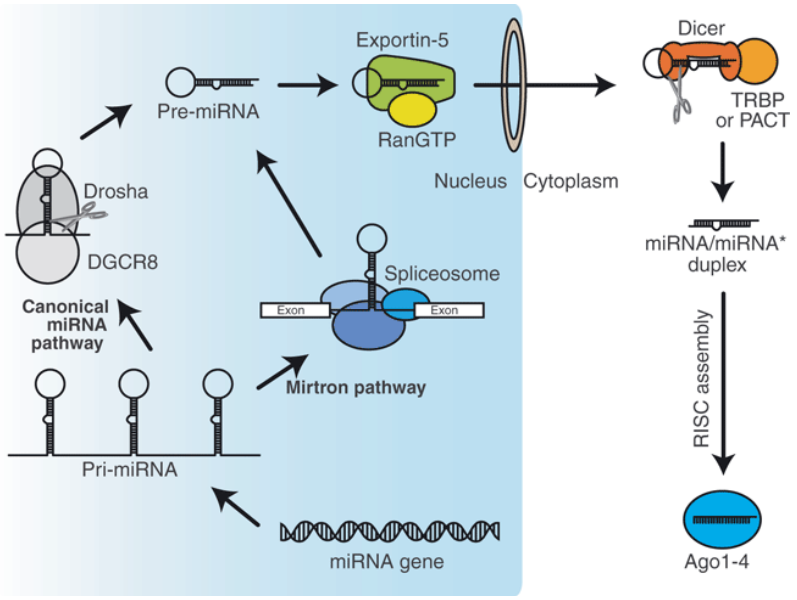

Figure 7- Biogenesis of miRNA

miRNA target sites lie in the 3' untranslated region (UTR) because the movement of ribosome (the translation) counteracts RISC binding. Typically, a target mRNA bears multiple binding sites of the same miRNA and/or several different miRNAs. Not all nucleotides of a miRNA contribute equally to RISC target recognition. The recognition of the target is largely determined by base pairing of nucleotides in the seed region and is enhanced by addional base-pairing in the middle of the 3'UTR region. The binding of RISC to 3' UTR of mRNA, through the action of Ago protein, is capable of RNA cleavage, but this reaction requires extensive base-pairing between the miRNA strand and mRNA target. This is the same mechanisms used by siRNAs. If the complementarity between the miRNA strand and the mRNA is limited, RISC is incapable to cleave target. In such case, Ago protein can recruit other factors required for translation repression and subsequently mRNA deadenylation/degradation (Lewis et al; 2003). To date, the exact mechanisms used by RISC to repress translation are subjects of debate. Between the mechanisms proposed at least six seems to be possible: RISC could induce deadenylation of mRNA which cause decrease the efficiency of translation by blocking mRNA circularization, RISC could block the cap at 5' or the recruitment of ribosomal subunit 60S; RISC could block the initial step of elongation or could induce proteolysis of nascent peptides; RISC could recruits mRNA to processing bodies, in which mRNA is degradated or temporary stored in an inactive form. These models do not necessarily exclude each other (Kwak et al).

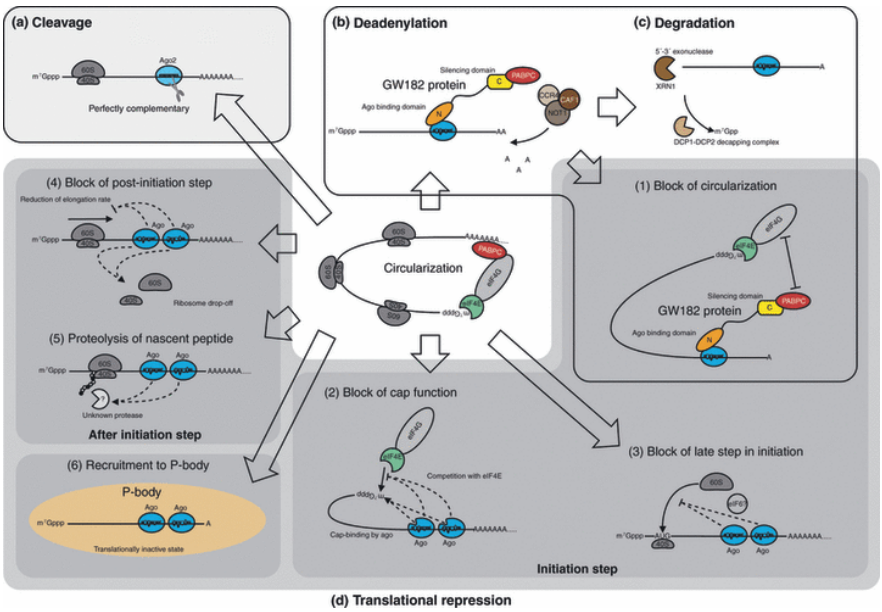

Figure 8-Various mechanisms of regulation of gene expression by RNA-induced silencing complex (RISC)

1.6. Function of miRNA in animals

1.6.1 Evolution and Physiological function

miRNAs have key roles in the regulation of distinct processes in mammals. miRNAs play an evolutionarily conserved role in the development and in the physiological functions in animal.

Knockout gene strategies have been used in different mammals to study the role of miRNAs in developmental processes. A dicer knockout was made in zebrafish (127) and this revealed a role of the family of miR-140 which plays a fundamental role in zebrafish neurogenesis. miRNAs can also control late-stage mouse development by miR-196 which acts upstream Hox B8 and Sonic hedgehog in limb development. miR-1 and miR-133 are important for muscle generation and differentiation of cardiomyocytes and myoblast (Chen et al; 2006). miR-181 is preferentially expressed in B-lymphocytes and regulates mouse hematopoietic lineage differentiation (Chen et al; 2004). miR-181 is also able to regulate homeobox proteins involved in myoblast differentiation (Naguibneva et al; 2006). miR-122a is highly expressed in adult livers and its expression is upregulated during mammalian liver development (Chang et al; 2004). miR-143 is strongly expressed in adipose fat tissue and is upregulated during the differentiation of human pre-adipocytes into adipocytes (Esau et al; 2004). MicroRna are also involved in skin morphogenesis for example, miR-134 acts in dendritic spine development (Schratt et al; 2006).

Some miRNAs regulate diverse physiological processed, for example miR-375 is expressed in pancreatic islet and inhibits glucose-induced insulin secretion, or

miR-16 which controls the ARE-containing mRNAs. Recently, it has been found that some endogenous miRNAs participate in adenoviral defence mechanisms for example miR-32 protects human cells from retrovirus type 1.
Some studies have established a role for miRNAs in cellular processes including apoptosis, proliferation, stress resistance, metabolism,

1.6.2 Cancer

Cancer is characterized by abnormally proliferative cells that undergo rapid and uncoordinated cell growth. Malignant cancer are able to invade adjacent tissues ad/or metastasize to more distant, and sometimes specific, tissues. Genes involved in cancer are generally classified into oncogenes or tumour suppressor genes.
The first evidence for miRNA involvement in human cancer came from a study by Calin et al (Calin et al; 2002). Examining a recurring deletion at chromosome 13q14 in the search for a tumour suppressor gene involved in chronic lymphocytic leukaemia (CLL). In this study was found that the region of deletion encodes two miRNA,miR-15a and miR-16-1. Subsequent investigations have confirmed the involvement of these two miRNAs in the pathogenesis of CLL (Calin et al; 2005, Cimmino et al; 2005).
To date, a lot of miRs have been characterizated for their function in cancer.
Let-7 family contains miRNAs that have been shown to regulate the RAS family of oncogenes (Johnson et al; 2005).
Constinean et al reported, for the first time, that a miRNA by itself could induce a neoplastic disease (Costinean et al; 2006). In fact, by using a transgenic mouse model, they demonstrated that overexpression of miR-155 in B cells induce a lymphoma pre-B leukemia. Petrocca et al (Petrocca et al; 2008) have demonstrated that the miR-106b-25 cluster plays a key role in gastric cancer interfering with proteins involved both in cell cycle and apoptosis.
miRNAs have an important role also in tumour metastasis. miR10-b was found to be highly expressed in metastatic breast cancer cells and Tavazoi et al found that miR-26 and miR-335, whose expression is lost in human breast cancer cells, modulate metastatic potential (Tavazoie et al; 2008).
Deregulation of miRNA expression levels emerges as the main mechanism that triggers their loos or gain of function in cancer cells. The activation of oncogenic transcription factors such as MYC, represents an important mechanisms for altering miRNA expression. Genomic aberrations such amplification, chromosomal deletions, point mutations or aberrant promoter methylation might alter miRNA expressions. Chromosomal abnormalities can trigger oncogenic actions of miRNAs by modulating miRNA expression in the wrong cell type or at wrong time.
Several examples of miRNAs whose expression is deregulated in human cancer have been reported. miR-155 is overexpressed in Hodgkin lymphoma, in pediatric Burkitt lymphoma and in diffuse large B-cell Lymphoma (Eis et al; 2005, Kluiver et al; 2005, Metzler et al; 2004) . miR-21 is upregulated in breast cancer and in glioblastoma, while miR-143 and miR-145 genes are significantly downregulated in colon cancer tissue compared with colonic mucosa (Michael et al; 2003).Evidences now indicate that the involvement of miRNAs in cancer is much

more extensive than initially expected. Studies that investigated the expression of the entire microRNAome in various human solid tumours and hematologic malignancies have revealed differences in miRNA expression between neoplastic and normal tissues (Calin et al; 2005, Ciafrè et al; 2005, Pallante et al; 2006, Weber et al; 2006). These studies show that each neoplasia has a distinct miRNA signature that differs from that of other neoplasms and that of the normal tissue counterpart. Moreover, it has become clear that some miRNAs are recurrently deregulated in human cancer. In most case, miRNAs are upregulated or downregulated in all tumours suggesting a crucial role for these miRNA in tumorigenesis. However, there are some unusual situation: for example members of the miR-181 family are up-regulated in some cancers, such as thyroid (Pallante et al; 2006), pancreatic (He et al; 2005),and prostate carcinomas (Volinia et al; 2006) but downregulated in others, such as glioblastomas and pituitary adenomas (Ciafrè et al; 2005, Bottoni et al; 2007).

2. Aims of the study

Glioblastoma are among the most deadly types of cancer. Advances in standard treatments for this tumour, such as surgery, radiotherapy, and chemotherapy, have not significantly increased patient survival. The most important issues that affect patient survival rate are the resistance to therapeutics drugs and the aggressive phenotype of glioblastoma cancer cells. The present work aims at investigated the role of microRNAs in the malignancy of glioblastoma, especially the role that microRNAs have in regulation of proteins involved in glioma cell motility and tumorigenesis (Aim I) in TRAIL resistance (Aim II) and in temozolomide resistance (Aim III). Therapeutic intervention, involving the use of microRNAs, should not only sensitize tumour cells to drug-inducing apoptosis but also inhibit their survival, proliferation, and invasive capabilities. It can be hypothesized therefore that the modulation of miRNAs might become a viable therapeutic strategy to sensitize cancer cells.

3. Materials and Methods

3.1. Cell culture and transfection. U87MG and T98G and U251 cells were grown in DMEM. Meg01 cells (human, chronic myelogenous leukaemia cells) were grown in RPMI 1640 + 2mM Glutamine + 10%FBS. Media were supplemented with 10% heat-inactivated fetal bovine serum (FBS), 2 mM L-glutamine and 100 U/ml penicillin/streptomycin. LN229 and LN18 were grown in Advanced DMEM (invitrogen) + 2mM Glutamine + 5 %FBS. For miRs transient transfection, cells at 50% confluency were transfected using Oligofectamine (Invitrogen) with 100nM (final) of pre-miR-221, pre-miR-222, pre-miR-30c and/or miR-21, scrambled or Anti miR-222 and Anti miR-221 (Applied Biosystems). For PTPμ transient transfection, cells were transfected using Lipofectamine and Plus Reagent with 5μg of PTPμ cDNA (Origene) for 24 hrs. To knock-down PTPμ gene, specific shRNA were obtained by Open Biosystems (Huntsville, AL, USA) and were transfected using lipofectamine 2000. After 24 hrs the cells were treated for 24hr with 500 ng/ml of puromicine for selection of transfected cells. Two clones stably expressing shRNAi-PTPμ were obtained. TWEEN empty vector, TWEEN miR-221 or TWEEN miR-222 vectors, were obtained from Dr. Ruggero De Maria (Rome).

3.2. Soft Agar Assay. 10^3 cells were plated in 60mm dishes in a solution containing DMEM 2X (Sigma), TPB Buffer (Difco), and 1,25% of Noble Agar (Difco). Briefly, cell were harvested and counted then a layer of 7 ml with the solution containing Noble Agar were left to polymerize on the bottom of the dishes. Then cells were resuspended in 2 ml of same solution and plated. Cells were left grown for 2 weeks in the incubator.

3.3. Injection of glioma cells in nude mice. Nude mice were provided by Charles River. 10^5 cells of T98G and U87MG were subcutaneously injected in one flank of the mice. Were injected 5 mice for each cell type. Mice were followed for 4 weeks and the tumours were measured and photographed.

3.4. Virus production. We produced vector stocks by calcium phosphate transient transfection, cotransfecting three plasmids in 293 T human embryonic kidney cells, since these cells are good DNA recipients. The three plasmids are: the packaging plasmid, pCMVDR8.74 designed to provide the HIV proteins needed to produce the virus particle; the envelope-coding plasmid, pMD.G, for pseudotyping the virion with VSV-G and TWEEN miR-221 or miR-222 vector, the transgene coding plasmids. The calcium phosphate–DNA precipitate was allowed to stay on the cells for 14–16 h, after which the medium was replaced, collected 48 h later, centrifuged at 1000 rpm for 5 min at room temperature and filtered through 0.22 mm pore nitrocellulose filters. On the day of infection, the medium was removed and replaced with viral supernatant to which 4 mg/ml of Polybrene had been added. Cells were then centrifuged in their plate for 45 min in

a Beckman GS-6KR centrifuge, at 1800 rpm and 32°C. After centrifugation, cells were kept for either 1 h 15 min or ON in a 5% CO2 incubator at 32 or 37°C, respectively. After exposure, cells were washed twice with cold PBS and fresh medium added. At either 12 or 48 h after the infection, cells were washed with PBS, harvested with trypsin/EDTA and analyzed by FACS for GFP expression. The GFP positive were sorted by a FACSscan.

3.5. Protein isolation and Western blotting. Cells were washed twice in ice-cold PBS, and lysed in JS buffer (50 mM HEPES pH 7.5 containing 150 mM NaCl, 1% Glycerol, 1% Triton X100, 1.5mM $MgCl_2$, 5mM EGTA, 1 mM Na_3VO_4, and 1X protease inhibitor cocktail). Protein concentration was determined by the Bradford assay (BioRad) using bovine serum albumin as the standard, and equal amounts of proteins were analyzed by SDS-PAGE (12.5% acrylamide). Gels were electroblotted onto nitrocellulose membranes (Millipore, Bedford, MA). For immunoblot experiments, membranes were blocked for 1 hr with 5% non-fat dry milk in Tris Buffered Saline (TBS) containing 0.1% Tween-20, and incubated at 4°C over night with primary antibody. Detection was performed by peroxidase-conjugated secondary antibodies using the enhanced chemiluminescence system (Amersham-Pharmacia Biosciences). Primary antibodies used were: anti-PTPμ (SantaCruz), anti-βActin (Sigma), Ser ^{P}-AKT (Promega), and anti-p27, -AKT, and -PTEN (Cell Signaling), anti-PTEN (Cell Signalling), anti-p85 (Cell Signalling), anti-p53 (Cell Signalling) and anti-Caspase 3, -Tap63 and –Atg5 were from Santa Cruz.

.

3.6. miRNA Microarray experiments- 5 μg of total RNA from each sample was reverse transcribed using biotin end labelled random-octamer oligonucleotide primer. Hybridization of biotinlabeled complementary DNA was performed on a new Ohio State University custom miRNA microarray chip (OSU_CCC version 3.0), which contains 1150 miRNA probes, including 326 human and 249 mouse miRNA genes, spotted in duplicates. The hybridized chips were washed and processed to detect biotin-containing transcripts by streptavidin-Alexa647 conjugate and scanned on an Axon 4000B microarray scanner (Axon Instruments, Sunnyvale, Calif).
Raw data were normalized and analyzed with GENESPRING 7,2 software (zcomSilicon Genetics, Redwood City, CA). Expression data were median-centered by using both the GENESPRING normalization option and the global median normalization of the BIOCONDUCTOR package (www.bioconductor.org) with similar results. Statistical comparisons were done by using the GENESPRING ANOVA tool, predictive analysis of microarray (PAM) and the significance analysis of microarray (SAM) software (http://www-stat.stanford.edu/~tibs/SAM/index.html).

3.7. Glioma cancer samples- A total of 18 paraffined high grade glioma samples were collected at the Federico II University of Naples, Italy at the University

Hospital of Gregorio Marañon, Madrid, Spain. RNA was isolated with RecoverALL™ Total Nucleic Acid Isolation kit from Ambion (Ambion Inc, Austin Texas). The samples were stored at -80°C.

3.8. RNA extraction and Real-Time PCR- Total RNAs (miRNA and mRNA) were extracted using Trizol (Invitrogen) according to the manufacturer's protocol. Reverse transcription of total miRNA was performed starting from equal amounts of total RNA/sample (1μg) using miScript reverse Transcription Kit (Qiagen), for mRNA was used SuperScript® III Reverse Transcriptase (Invitrogen). For cultured cells, quantitative analysis of PTPμ, Caspase-3, MGMT, β-Actin (as an internal reference), miR-221/222, and RNU5A (as an internal reference) were performed by RealTime PCR using specific primers (Qiagen), miScript SYBR Green PCR Kit (Qiagen), and iQ™ SYBR Green Supermix (Biorad), respectively. The reaction for detection of mRNAs was performed as follow: 95°C for 15', 40 cycles of 94°C for 15'', 60°C for 30'' and 72°C for 30''. The reaction for detection of miRNAs was performed as follow: 95°C for 15', 40 cycles of 94°C for 15'', 55°C for 30'' and 70°C for 30''. All reactions were run in triplicate. The threshold cycle (CT) is defined as the fractional cycle number at which the fluorescence passes the fixed threshold. For relative quantization the $2^{(-\Delta CT)}$ method was used as previously described (Livak and Schmittgen; 2001). Experiments were carried out in triplicate for each data point, and data analysis was performed by using software (Bio-Rad).

3.9. Luciferase assay- The 3' UTR of the human PTPμ, Caspase-3 and MGMT genes were PCR amplified using the following primers: PTPμ Fw: 5'-TCTAGACGAGGTGGCCCTGGAATACTTGAATTCT-3' , PTPμ Rv 5'-TCTAGAGCATTTTGTGAATGAGTCCTCCCCCAA-3', Caspase-3 Fw: 5' TCTAGAAGGGCGCCATCGCCAAGTAAGAAA 3', Caspase-3 Rv : 5' TCTAGACCCGTGAAATGTCATACTGACAG 3' ; MGMT Fw: 5' TCTAGAGTATGTGCAGTAGGATGGATG 3' , MGMT Rv: 5' TCCAGAGCTACAGGTTTCCCTTCC 3' and cloned downstream of the Renilla luciferase stop codon in pGL3 control vector (Promega). This construct were used to generate, by inverse PCR, the UTRmut-PTPμ plasmid (primers: PTPμ -mut: Fw 5'-GCATAATATATGCTTGCTTTCCAGGACTAACAGATAAATGTG-3'; Rv 5-' CACATTTATCTGTTAGTCCTGGAAAGCAAGCATATATTATGC-3') and the UTRmut-MGMT (primers: MGMT-mut Fw 5' CTATATCCAAAAGGGAAACCTGTAGCTCTTGC 3' RV 5' GCAGAGCTACACGTTTCCCTTTTGGATATAG 3'). MeG01 cells were cotransfected with 1μg of each generated plasmid and 1 μg of a Renilla luciferase expression construct pRL-TK (Promega) with Lipofectamine 2000 (Invitrogen). Cells were harvested 24 h post-transfection and assayed with Dual Luciferase Assay (Promega) according to the manufacturer's instructions. Three independent experiments were performed in triplicate.

3.10 MiRNA locked nucleic acid in situ hybridization of formalin fixed, paraffin-embedded tissue section- In situ hybridization (ISH) was carried out on deparaffinized human glioma tissues using previously published protocol (Nuovo et al; 2009), which includes a digestion in pepsin (1.3 mg/ml) for 30 minutes. The sequences of the probes containing the six dispersed locked nucleic acid (LNA) modified bases with digoxigenin conjugated to the 5' end were: miR-221-(5') GAAACCCAGCAGACAATGTAGCT; miR-222(5') ACCCAGTAGCCAGATGTAGCT. The probe cocktail and tissue miRNA were co-denatured at 60˚C for 5 minutes, followed by hybridization at 37°C overnight and a low stringency wash in 0.2X SSC and 2% bovine serum albumin at 4°C for 10 minutes. The probe-target complex was seen due to the action of alkaline phosphatase on the chromogen nitroblue tetrazolium and bromochloroindolyl phosphate (NBT/BCIP). Negative controls included the use of a probe which should yield a negative result in such tissues. No counter stain was used, to facilitate co-labelling for PTPμ protein. After in situ hybridization for the miRNAs, as previously described (Nuovo et al; 2009), the slides were analyzed for immunohistochemistry using the optimal conditions for PTPμ (1:200, cell conditioning for 30 minutes). For the immunohistochemistry, we used the Ultrasensitive Universal Fast Red system from Ventana Medical Systems. We used glioma tissues as controls for these proteins. The percentage of tumour cells expressing PTPμ and miR-221 and -222 was then analyzed with emphasis on co-localization of the respective targets.

3.11. Migration assay- Transwell Permeable Supports, 6.5 mm diameter inserts, 8.0 μM pore size, polycarbonate membrane (Corning Incorporate, Corning, NY, USA) were used to perform migration assay. T98G and U87MG cells were grown as indicated above, then harvested by TrypLE^{TM} Express (Invitrogen, Carlsbad, CA, USA) and 10^5 cells were washed three times and then resuspended in 1% FBS containing DMEM medium and seeded in the upper chamber. Lower chamber of the transwell was filled with 600 μl of culture medium containing 10% FBS, 5 μg/ml fibronectin, as an adhesive substrate. Cells were incubated at 37°C for 24 h. The transwell were then removed from the 24-well plates and stained with 0.1% Crystal Violet in 25% methanol. Nonmigrated cells were scraped off the top of the transwell with a cotton swab. % of migrated cells was evaluated by eluting crystal violet with 1% SDS and reading the absorbance at λ 570 nm.

3.12. Cell death quantification. Cells were plated in 96-well plates in triplicate, stimulated and incubated at 37°C in a 5% CO_2 incubator. TRAIL was used at final concentration of 100 ng/ml for 24hr. Temozolomide was use at final concentration of 300 μMol for 48 hrs. Apoptosis was analyzed *via* propidium iodide incorporation in permeabilized cells by flow cytometry. The cells (2×10^5) were washed in PBS and resuspended in 200 μl of a solution containing 0.1% sodium citrate, 0.1% Triton X-100 and 50 μg/ml propidium iodide (Sigma). Following incubation at 4°C for 30 min in the dark, nuclei were analyzed with a Becton

Dickinson FACScan flow cytometer. Cellular debris was excluded from analyses by raising the forward scatter threshold, and the DNA content of the nuclei was registered on a logarithmic scale. The percentage of elements in the hypodiploid region was calculated. Cell viability was evaluated with the CellTiter 96 AQueous One Solution Cell Proliferation Assay (Promega) according to the manufacturer's protocol. Metabolically active cells were detected by adding 20 μL of MTS to each well. After 2 h of incubation, the plates were analyzed in a Multilabel Counter (BioTek).

3.13. Colony Assay. Cells were transfected with miR-scrambled, miR-30b and miR-21 for 24 hrs, then were harvested and 2.4 X 10*4 cells were plated in six well plates. After 24 hr, cells were treated with 50 and 100 ng/ml of superKiller TRAIL for 24 hr. Cells were transferred to 100 mm dishes and let grown for 6 day. After these period the cells were coloured with 01%crystal violet dissolved in methanol 25% solution for 20 min at 4°C. Dishes were washed with water and then let dry on bench.

3.14. Statistical analysis. Continuous variables are expressed as mean values ± SD. One-tailed Student's t test was used to compare values of test and control samples. $P < 0.05$ was considered significant

.

4. Aim I: Identification and characterization of miRNAs involved in glioma tumorigenesis

Results

4.1. miRs expression in glioma cell lines- T98G and U87MG glioma cells have been described as having a different tumorigenic behaviour (Cerchia et al; 2009). In fact, while T98G are not able to grow in nude mice and to form colonies, U87MG, LN18 and LN229 cells form tumours when injected in mice and form colonies in soft agar, even in the absence of serum. We confirmed these data using soft agar and xenograft growth in nude mice (figure 10). In order to investigate the involvement of miR in glioma tumorigenesis, we analyzed miR expression profile in the tumorigenic glioma cell U87MG versus non-tumorigenic T98G cell. The analysis was performed with a microarray chip containing 1150 miR probes, including 326 human and 249 mouse miRs, spotted in duplicates (He et al; 2005). Pairwise significance analysis (PAM) of the microarray indicated that five miR genes were significantly overexpressed in tumorigenic cells with a >2.5-fold change (Table 1). We focus our attention on miR-221 and miR-222, since we and others have already demonstrated that those miRs are frequently overexpressed in a number of human tumours (Pallante et al; 2006, Conti et al; 2009, Pineau et al; 2010).
In order of confirm the array results, we analyzed the levels of miR-222 and -221 in T98G, U87MG, LN18 and LN229 cells with Real-time PCR. Accordingly with microarray data, we found an up-regulation of these two miRs in tumorigenic cells (U87MG, LN18 and LN229) compared to T98G cells (Figure 11A). As expected, the predicted miR-221 and -222 targets, $p27^{kip1}$ and PTEN, were expressed at decreased levels in U87MG cells (Figure 11B) as compared to T98G cells. In order to verify the involvement of these miRs in glioma tumorigenesis we transfected the T98G cell lines with pre-miR-221 and pre-miR-222 and with a scrambled sequence, and U87MG with anti-miR negative control and anti-miR-221 and 222. As shown in figure 11B by soft agar assay we found that in non tumorigenic T98G cell lines overexpressing miR-221 and -222 there was an increase of colony number while in the tumorigenic U87MG overexpressing anti-miR-221 and -222 there was a decrease of colony number.

miR	Intensities of U87MG	Intensities of T98G	Fold change
hsa-miR-221	11150.1	1763.5	6.323
hsa-miR-125b	4697.4	1020.4	4.603
hsa-miR-21	6236.3	1662.4	3.751
hsa-miR-222	16685.8	6014	2.774
hsa-miR-34a	319.1	26.7	11.951

Table 1- All differentially expressed miRs have q <0.01 (false positive rate). T test p<0.05. These miRs were identified by PAM as predictor of glioma cells with the lowest misclassification error.

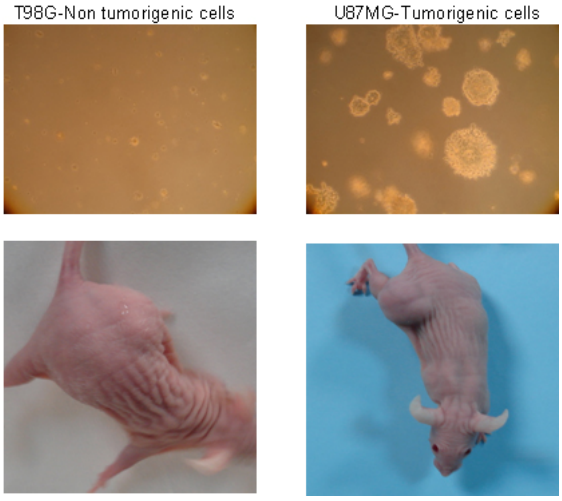

Figure 9- Upper panel. U87MG and T98G were plated in soft agar for two weeks and photographed. Lower panel U87MG and T98G were injected in nude mice and tumors were monitored for 4 weeks.

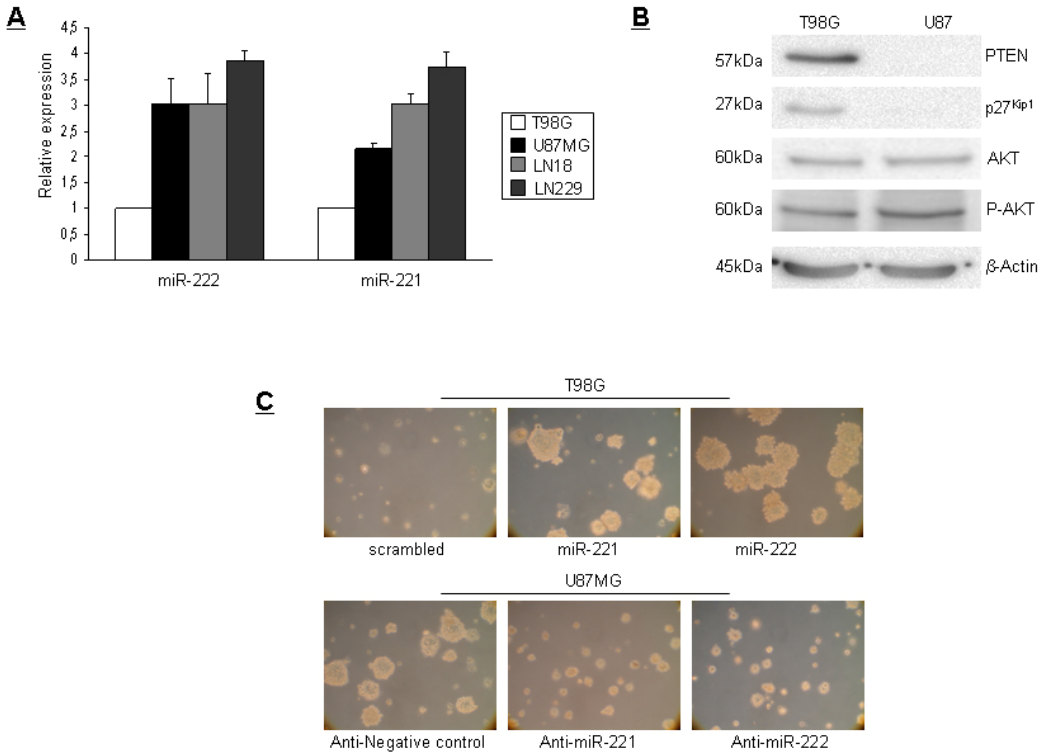

Figure 10- Expression of miR-222 and -221 and their targets in T98G and U87MG glioma cells. (A) Real time PCR of miR-221 and -222 in glioma cells. Representative of at least three independent experiments. **(B)** Western blot analysis of the known miR-221 and -222 targets, PTEN and $p27^{kip1}$. As a consequence of decreased PTEN protein levels, p-AKT levels were increased, although total AKT levels were comparable. β-Actin was used as the loading control. **(C)** Soft agar growth of T98G transfected with pre-miR-221 and 222 or negative control and of U87MG transfected with Anti-miR-221 and 222 and with a negative control.

4.2. Identification of PTPμ as a new target of miR-221 and -222- To find new miR-221 and -222 targets, we used bioinformatics analysis. Comparing the results obtained from the different searches, we found that the protein phosphatase PTPμ was predicted as a target of miR-222 by the miRanda algorithm. RNAhybrid also predicted a possible binding region of miR-221 and -222 in the 3'UTR of PTPμ (Figure 12A). The most widely used approach for experimentally validating miRNA targets is to clone the predicted miRNA-binding sequence downstream of a luciferase reporter construct, and to cotransfect it with the miRNA of interest for luciferase assays. To this end, we cloned the 3'UTR sequence of human PTPμ into the luciferase expressing vector pGL3-control downstream of the luciferase stop codon; Meg01 cells were transiently transfected with this construct in the presence of pre-miR-221 and pre-miR222 or in the presence of a scrambled oligonucleotide acting as a negative control. As reported in Figure 12B, miR-221

and miR-222 significantly reduced luciferase activity compared to the scrambled oligonucleotide. This indicates that miR-221 and -222 bind to the 3'UTR of *ptpm* and impair its mRNA translation. In order to determine that the region was specific for the binding with miR-222 and -221, we generated a deletion mutant (Figure 12C) lacking the binding site, ATGTAGC. The mutant was cloned into the 3'UTR of the luciferase gene and cotransfected with pre-miR-221 and -222 in Meg01 cells. As shown in Figure 12D, miR-221 and -222 did not significantly reduce luciferase activity in the presence of the 3'UTR PTPμ -mut sequence. This result indicates that miR-221 and -222 target PTPμ mRNA at the ATGTAGC sequence.

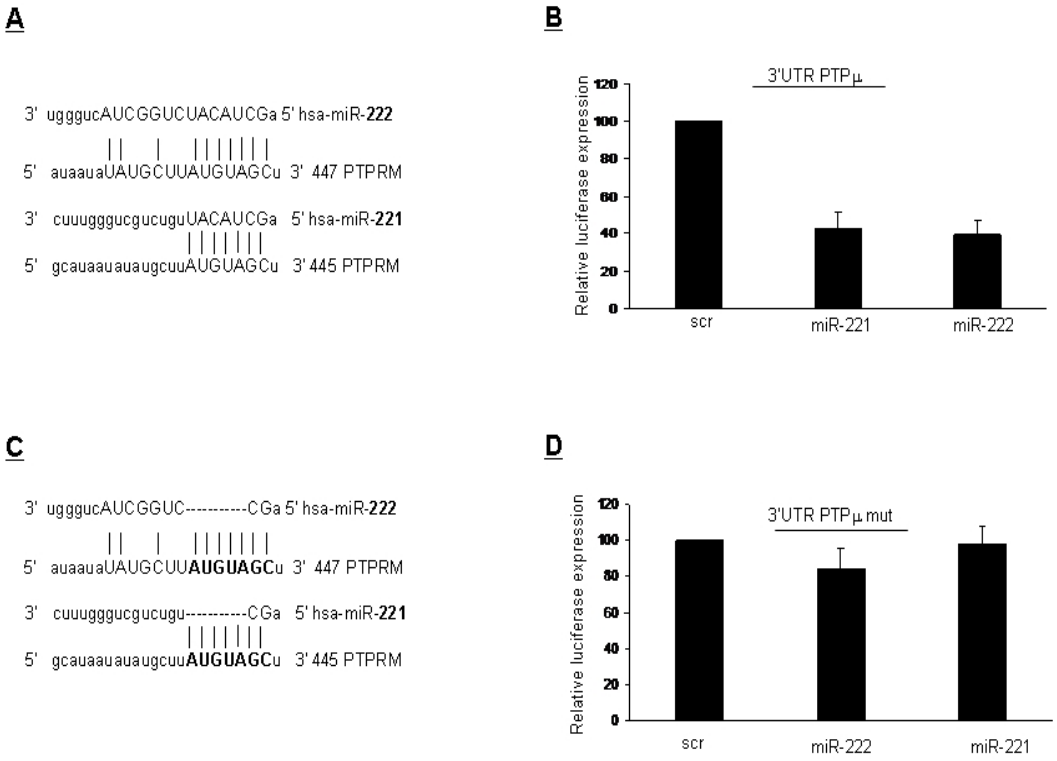

Figure 11- Identification of target sites in the 3'-UTR of PTPμ. Complementary sites for miR-222 and -221 on wild type **(A)** or mutated **(C)** PTPμ 3′UTR. The capital letters identify perfect base matches according to miRanda software. The bold letters identify the deleted regions. For luciferase activity, Meg01 cells were transiently cotransfected with the luciferase reporter containing wild type PTPμ–3′UTR or PTPμ-3′UTR mutant **(D)** in the presence of pre-miR-222, miR-221 or scrambled oligonucleotide. Luciferase activity was evaluated 24 h after transfection as described in Materials and Methods. Representative of at least three independent experiments.

4.3. Expression of PTPμ and miR-222 and -221 in glioma- To assess whether the expression of PTPμ was inversely correlated with miR-221 and -222 in glioma cells, we analyzed the levels of the protein phosphatase in U87MG, LN18, LN229 and T98G cells. We found reduced PTPμ protein (Figure 13A) and mRNA levels (Figure 13B) in U87MG, LN18 and LN229 cells overexpressing miR-221 and -222 compared with T98G. In order to establish a causative link with miRs-222 and -221 and PTPμ, we stably infected T98G cells with a Tween lentiviral construct expressing miR-221 and -222, and then analyzed PTPμ protein and mRNA levels. miR expression in infected cells were monitored by RT-PCR (Figure 13C). We observed decreased PTPμ protein (Figure 13D) and mRNA expression levels (Figure 13E) in miR-222 and -221 stably expressing cells. The same effect was observed in T98G cells transiently transfected with a synthetic pre-miR-222 and miR-221 (Figure 13 G,H). The efficiency of miR expression upon transfection was monitored by RT-PCR (Figure 13F). Consistently with these data, U87-MG cells transfected with the anti-miR-222 and -221 showed an increase of PTPμ protein (Figure 14 A) and RNA levels (Figure 14 B). The efficiency of miR down-regulation upon anti-miR transfection was monitored by RT-PCR (Figure 14 C).

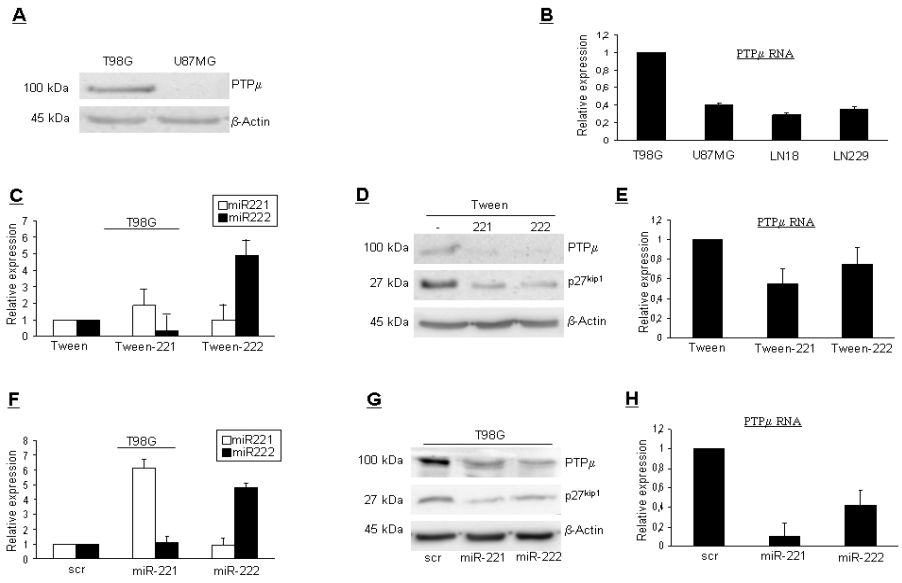

Figure 12- PTPμ and miR-222/221 expression levels are inversely correlated in glioma. PTPμ protein **(A)** and RNA **(B)** expression levels in T98G and U87MG cells. Cell lysates were immunoblotted with anti-PTPμ antibody. To confirm equal loading, the membrane was immunoblotted with anti–β-Actin antibody. Effect of miR transfection on PTPμ expression: miR-222 and -221 constitutive **(C)** or transient **(F)** expression in glioma cells induced a decrease of PTPμ protein **(D, G)** and RNA **(E, H)** expression levels. Relative expressions of mRNA and miR-221 were calculated using the comparative CT methods. Columns, mean of four different experiments; bars, SD.

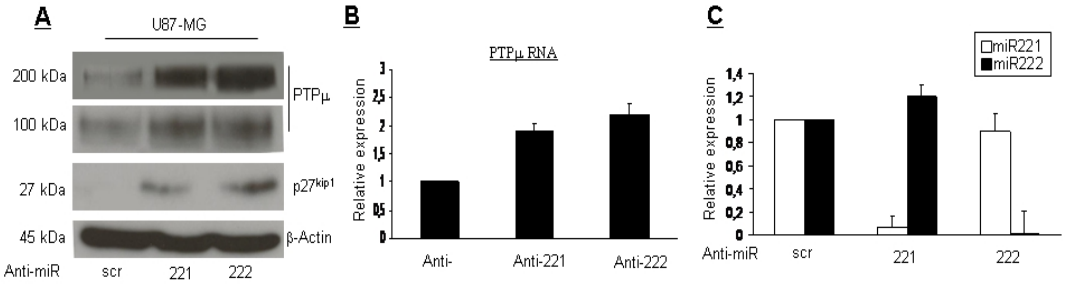

Figure 13- Effects of Anti miR-222 and -221 on PTPμ expression levels in glioma. PTPμ protein **(A)** and RNA **(B)** expression levels in U87MG cells transfected with anti miR-222, -221 or control scrambled (scr). The Anti-miRs were able to increase PTPμ expression levels. **(C)** Anti-miR transfection reduced miR levels as analyzed by Real time PCR. Columns, mean of four different experiments; bars, SD.

4.4. miR-221 and -222 regulates cell motility in glioma cells- We hypothesized that miR-221 and -222 promote cell migration by regulating PTPμ expression. To this end, we analyzed cell motility through a transwell assay in U87MG,LN18. LnN229, T98G parental cells, and T98G transduced with control vector (T98G-tween), or lenti-miR221 and -222 vector (T98G miR-221 and T98G miR-222). As shown in Figure 15A, U87MG, LN18 and LN229 cells have an higher migration rate than T98G. The up-regulation of miR-221/222 in T98G induces an increase of cell motility. The same result was obtained in T98G cells transiently transfected with miR-221/222 (Figure 15B). Conversely, expression of anti-miR-222 was able to reduce cell migration of U87MG (Figure 15B). We also tested the effects of miRs or anti-miR expression on cell adhesion, obtaining the same results (data not shown). Furthermore, transfection of specific PTPμ shRNAi in T98G cells induced a strong reduction of PTP expression levels and at the same time an increase of cell motility while overexpression PTPμ cDNA in U87MG induced a decrease of cell motility (Figure 15C). This result demonstrates strongly that PTPμ protein is able to control cell motility in glioma cells, as reported by other authors (Burgoyne et al; 2009). miRs may target different proteins. In order to demonstrate that migration/adhesion effects observed were carried out by PTPμ, we transfected T98G tween, tween-221 and tween 222 with ectopic PTPμ cDNA lacking the miRNA binding site in its 3'UTR, before assaying migration and adhesion. Levels of transfected PTPμ were analyzed by western blot. Interestingly, transfection of PTPμ in miR-221 and -222 overexpressing U87MG cells was able to overcome the effects of both miRs (Figure 15 C). These rescue experiments proved the causative connection between miR-222, PTPμ and glioma cell motility.

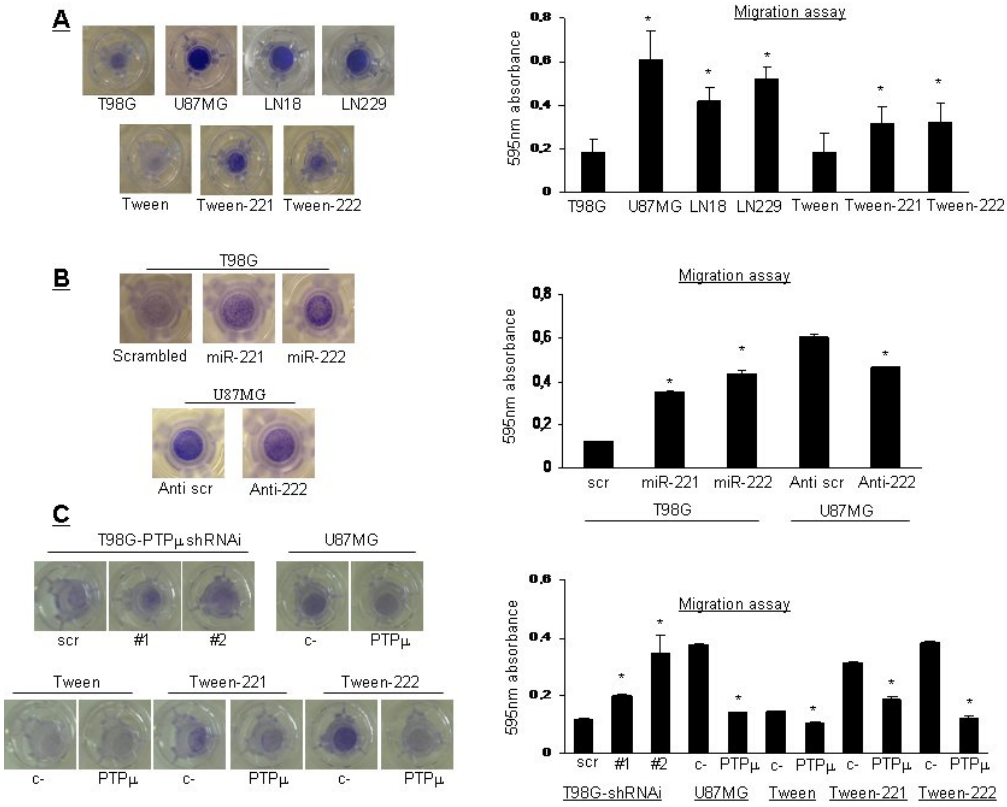

Figure 14- Effects of miR-222 and-221 on cell migration and adhesion. T98G glioma cells showed lower migration compared to U87MG, LN18, LN229 cells (A), whereas T98G cells stably (A) or transiently (B) transduced with miR-222 and -221 exhibited increased migration levels. Transfection of PTPμ cDNA in miR-222 and -221 overexpressing cells was able to rescue the effect of both miRs on invasion (C), whereas T98G transfected with two different PTPshRNAi (#1, #2) exhibited higher migration compared to control scrambled shRNA (shRNAi) (C). Each assay was performed three times in independent experiments (*n*=3). Error bars indicate standard deviation.

4.5. miR-222 and PTPμ mRNA levels in glioma- To evaluate whether PTPμ downregulation in glioma was related to increased miR-222 and -221 levels also in vivo, we analyzed PTPμ and miR-222 -221 expression levels in tumour tissue specimens collected from 18 glioblastoma grade IV patients. As shown in Figure 16, we found an inverse correlation between miR-222 and -221 levels and PTPμ in all glioma samples analyzed. To investigate the inverse relation between miR-221/222 and PTPμ *in vivo*, *in situ* hybridization analysis was performed using 5'-

digoxigenin-labeled LNA (locked nucleic acid) probes on 66 glioma cancers (table 2), followed by immunohistochemical detection of co-expression of PTPμ. As shown in figure 17A, miR-222 was abundantly expressed in cancers and rarely found in normal cells. No co-expression was found with PTPμ. Same result was obtained for miR-221 (data not shown). Importantly, was evident that miR-221/222 were abundantly expressed in the aggressive and metastatic cancers by comparing grade IV glioblastoma with oligodendroglioma, a slowly growing glioma (Figure17). Conversely, PTPμ was highly expressed in oligodendroglioma and normal brain compared to grade IV glioblastoma.

.

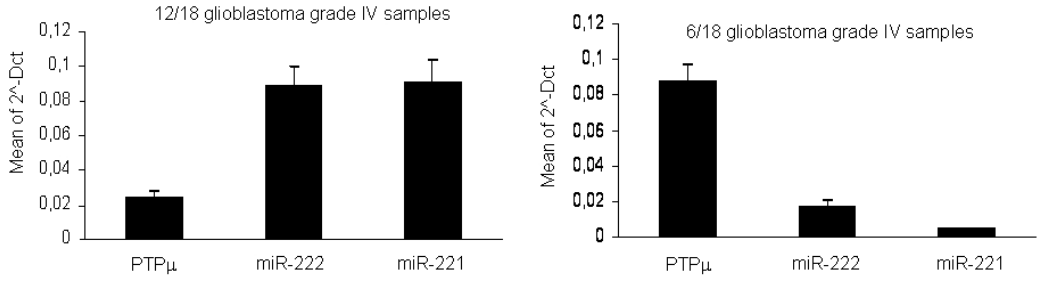

Figure 15 -Correlation of endogenous miR-222 and PTPμ mRNA expression levels in human glioma- Total RNA extracted from tissue specimens collected from 18 high grade glioma-affected individuals was used to analyze miR-222/221 and PTPμ mRNA expression by real-time PCR. In each sample, an inverse correlation between miR-221 and -222 with PTPμ was observed.

	Grade I and II Astrocitomas N=26	**Grade III and IV Glioblastomas N=40**	**Total gliomas N=66**
miR-222 +	13 (50%)	26 (65%)	39 (59%)
PTPμ	9 (34%)	15 (37%)	24 (36%)

Table 2-Results of miR-222 in situ hybridization and PTPμ immunohistochemestry on 66 gliomas (26 Grade I and II, 40 Grade III and IV). N= inicates the number of sample analyzed.

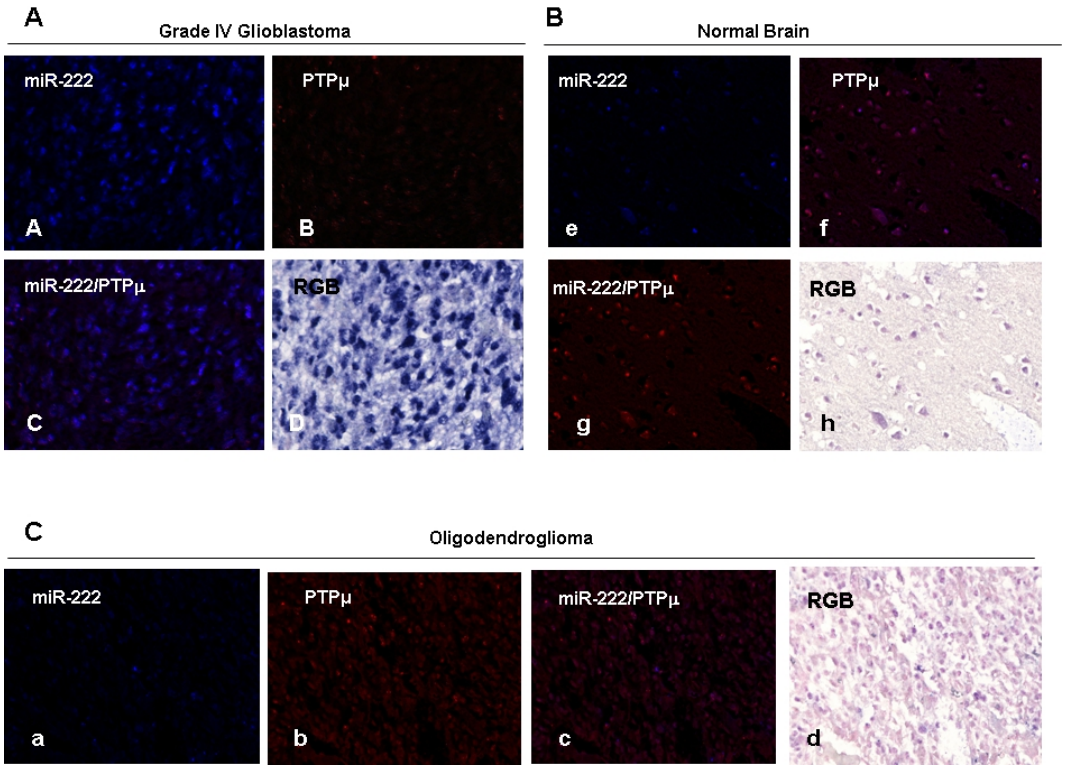

Figure 17- Correlation of miR-222/PTPμ co-expession analyses. (A) 66 glioma cancer tissues on a TMA were analyzed for miR-222 expression by *in situ* hybridization and then for PTPμ, respectively, by immunohistochemistry. Panel A shows miR-222 signal (fluorescent blue) and panel B is the PTPμ signal (fluorescent red) in a grade IV glioblastoma. Panel C shows the mixed signal in which fluorescent yellow is indicative of miR and protein co-expression; note the lack of miR-222 and PTPμ co-expression. Panel D shows the RGB image of the *in situ* hybridization/immunohistochemical reaction shown in panels b-d. **(B)** In the normal brain one sees the miR-222 signal (fluorescent blue) in panel e and the PTPμ image as fluorescent red (panel f). As described in the text, the majority of normal brain were negative for miR-222 (panel e) and positive for PTPμ (panel f). Panel g shows the mixed signal in which fluorescent yellow is indicative of miR and protein co-expression. Panel h shows the RGB image of the *in situ* hybridization/immunohistochemical reaction shown in panels e-g. **(C)** Finally, on 4 oligodendrogliomas, only 1/4 was miR-222+ and 4/4 were PTPμ positive. Panel a shows miR-222 signal (fluorescent blue) and panel b is the PTPμ signal (fluorescent red). Panel c shows the mixed signal in which fluorescent yellow is indicative of miR and protein co-expression; note the lack of miR-222 and PTPμ co-expression. Panel d shows the RGB image of the *in situ* hybridization/immunohistochemical reaction shown in panels b-d.

5. Aim II: identification of miRNAs involved in TRAIL resistance in human glioma

5.1. Selection of TRAIL sensitive vs. TRAIL resistant glioma cell lines- We analyzed TRAIL sensitivity of different human glioma cell lines, as shown in Figure 18. Cells were exposed to TRAIL for 24 hours after which cell death was assessed using an MTT assay or by FACS with annexin V and propidium iodide staining. As shown in Figure 18, we can distinguish two set of cells: TB10, LN229, U251, U87 cells did not display sensitivity when exposed to soluble TRAIL, whereas T98G and LN18 cells underwent to TRAIL-induced cell death.

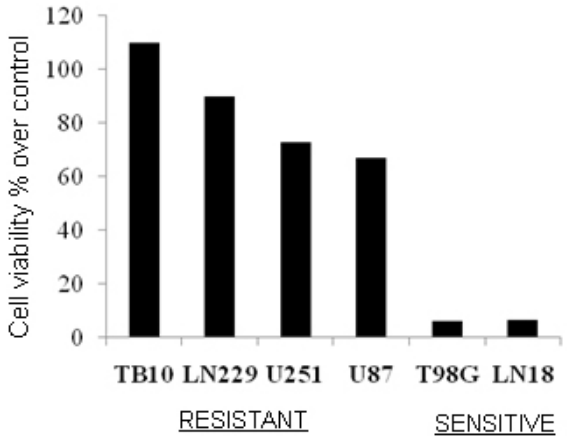

Figure 16- Glioblastoma cell lines TRAIL sensitivity- Glioblastoma cell lines were treated for 24 hrs with superKiller-TRAIL then, cell vitality was assessed with MTT assay.

5.2. miRs expression screening in TRAIL resistant vs. sensitive glioma cell lines- To investigate the involvement of miRs in TRAIL resistance in glioblastoma cell lines, we analyzed the miRs expression profile in TRAIL-resistant versus TRAIL sensitive cells. The analysis was performed with a microarray chip containing 1150 miR probes, including 326 human and 249 mouse miRs, spotted in duplicates, in collaboration with the lab of *Prof. Carlo Croce* **.** Data obtained comparing TB10 and LN229 vs. T98G and LN18 cells, indicated that seven miR genes were significantly overexpressed in resistant glioma cells (TB10 and LN229) with a >1.9-fold change (Table 3). Quantitative Real-Time-polymerase chain reaction (qRT-PCR) validated the microarray analysis.

We tested the all indicated miRs for involvement in TRAIL resistance obtaining significantly results only for miR-30 family and miR-21 that was extensively

investigated.

Unique id	Parametric p-value	FDR	Ratio of geom means
hsa-miR-125b1-A	6.09e-05	0,0209742	3.033
hsa-miR-30b-A	9.14e-05	0,0209742	2,041
hsa-miR-30c-A	0,0001199	0,0209742	2,337
hsa-miR-146b-A	0,0001556	0,0217901	5,972
hsa-miR-181a-5p-A	0,0004698	0,0241983	2,66
hsa-miR-181d-A	0,0004817	0,0241983	3,035
hsa-miR-21-A	0,0032482	0,0741609	1,949

Table 3- All differentially expressed miRs have $q<0.01$ (false positive rate). T test $p<0.05$. These miRs were identified by PAM as predictor of glioma cells with the lowest misclassification error.

5.3. Role of miRs in TRAIL resistance in glioma- In order to test the role of these overexpressed miRs in TRAIL sensitivity in glioma, we transfected T98G TRAIL-sensitive cells with pre-miR-21, -30b, and -30c. TRAIL sensitivity will be evaluated by MTT assay and propidium iodide staining, and colony assay. Data obtained with FACS analysis showed that miR-30b, -30c and -21 transfection induced TRAIL resistance (Figure 19A-B). In order of further evaluate TRAIL sensitivity, we planed to set up colony assays. Cells were transfected with miR-scrambled, miR-30b and miR-21 for 24 hrs, then were harvested and 2.4 X 10*4 cells were plated in six well plates. After 24 hr, cells were treated with 50 and 100 ng/ml of superKiller TRAIL for 24 hr. Cells were let grown for 6 day and then coloured with crystal violet-methanol solution. As shown in Figure 19C cells transfected with miR-30b and miR-21 are more sensitive to TRAIL treatment.

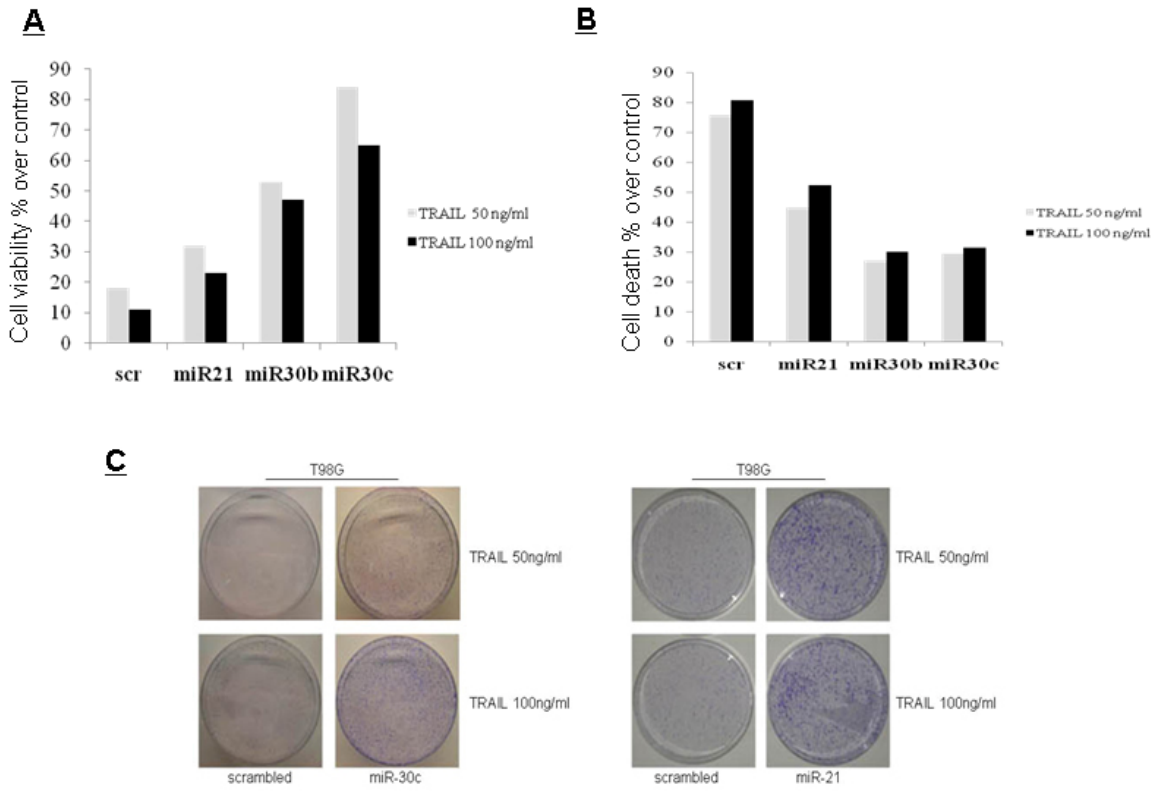

Figure 17-miRs-21 and -30b/c confer TRAIL resistance. (A) T98G cell lines were transfected with miR-21, miR-30b and miR-30c. Cells were then treated with two different concentration of superKiller TRAIL for 24 hrs. Cell viability was assessed with MTT assay and with propidium iodide staining **(B)**. **(C)** Colony assay of T98G cell lines transfected with a scrambled sequence as negative control and with miR-30c or miR-21 and then treated with two different doses of superKiller TRAIL as indicated.

5.4. Identification of cellular targets of miR-30c and miR-21 in glioma cells- A bioinformatics search was used as first attempt using programs available on the web including Pictar, TargetScan, miRanda, and Microcosm target. Comparing the results obtained from the different searches, we found several potential interesting targets of miR-30b, -30c and miR-21 that will be further characterized.
miR-21 targets different tumor suppressor genes in glioblastoma cells such as PTEN (phosphatase and tensin homologue), PDCD4 (programmed cell death 4), TPM1 (Tropomyosin 1) and p53. Although those have been already described as miR-21 targets, their role in TRAIL resistance has not been already described. As shown in Figure 20**,** miR-21 transfection induced a reduction of PTEN, p53 and caspase 3 (already published target) but also p85, the regulatory subunit of PI3K (unpublished target).
We also evaluated the effects of ***miR-30*** on some of the putative targets and found that miR-30 transfection induced a reduction of caspase 3 protein levels (Figure 21)**.** Furthermore we cloned the 3'UTR sequence of caspase 3 into the luciferase

expressing vector pGL3-control downstream of the luciferase stop codon; Meg01 cells were transiently transfected with this construct in the presence of pre-miR-30c or in the presence of a scrambled oligonucleotide acting as a negative control. As shown in Figure miR-21 significantly reduced luciferase activity compared to the scrambled oligonucleotide Figure 22.

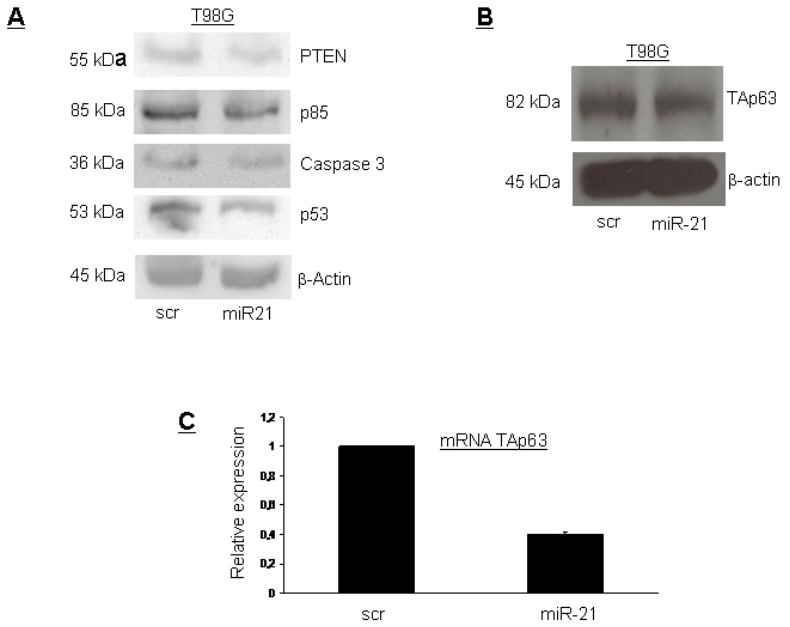

Figure 20- Target identification of miR-21 (A-B) Western blot analysis of cell lysate from T98G transfected with a scrambled sequence as negative control and miR-21. **(C**) Real time PCR of Tap63 mRNA in T98G transfected with a negative control and with miR-21.

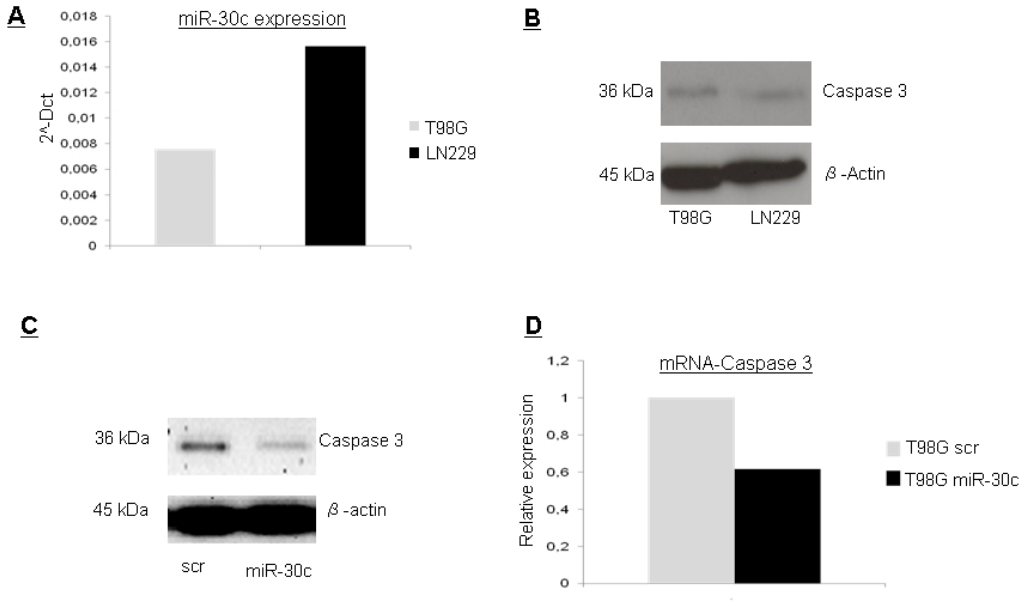

Figure 18-Target identification of miR-30c. (A) Real time PCR of miR-30c expression in T98G and U87MG cell lines. **(B-C)** Western blot analysis of caspase-3 in T98G, LN229 and in T98G transfected with a negative control and with pre-miR-30c. **(D)** Real time PCR of caspase-3 mRNA after miR-30c transfection in T98G cell lines.

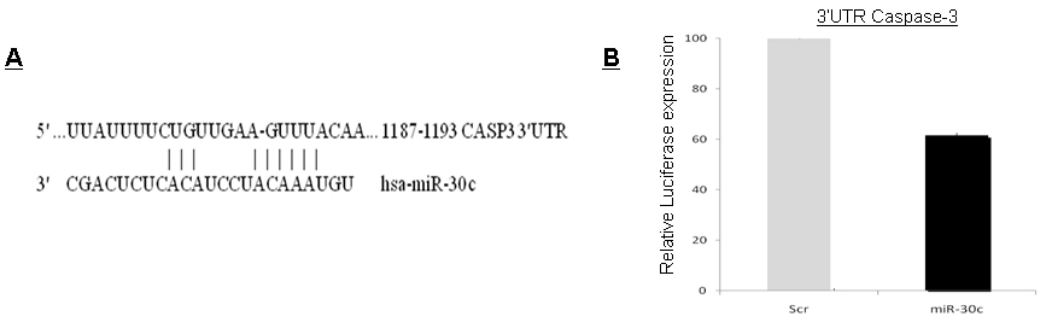

Figure 19-Validation of miR-30c binding to Caspase 3 mRNA. (A) Alignment between miR-30c and 3'UTR Caspase-3 mRNA. **(B)** Luciferase activity of pgl3-3'UTR Caspase -3 vector after MEG01 transfection with pre- miR30-c or negative control.

5.5 Validation of miR-21 and miR-30c mechanisms of action- As reported before miRs may target different proteins. In order to demonstrate that TRAIL resistance observed was carried out by Tap63 and caspase-3 respectively targets of miR-21 and miR-30c, we transfected T98G with ectopic Tap63 and caspase-3 cDNA lacking the miRNA binding site in their 3'UTR and with a control vector or miR-21 (Figure 23A) or miR30 c (Figure 23 B), before TRAIL treatment. Interestingly, transfection of Tap63 and caspase-3 was able to overcome the effects of both miRs (Figure 23A-B). These rescue experiments proved the causative connection between miR-21 and TAp63 and caspase-3 and miR-30c and TRAIL sensitivity.

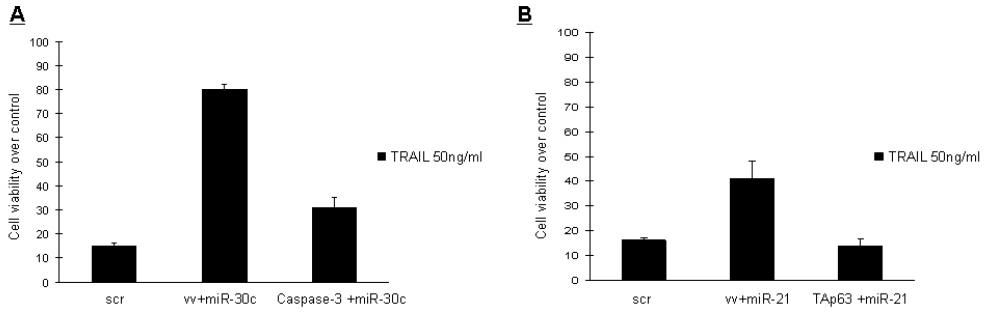

Figure 20-Validation of the involvment of caspase-3 and Tap63. (A-B) Cell viability assay of T98G cells transfected with miR-30c, miR-30c and caspase-3, miR-21, miR-21 and Tap63

6. Aim III- Identification and characterization of miRs involved in glioma response to temolozomide

6.1. Temozolomide sensitivity of human glioma cell lines We analyzed temozolomide sensitivity of human glioma cell lines, T98G and U87MG. Cells were exposed to 300 μMol of temozolomide for 48 hours and cell death was assessed using an MTT assay. As shown in figure 24A, T98G were resistant to temozolomide, whereas U87MG cells were sensitive. To establish a causative effect between temozolomide sensitivity and MGMT expression, we analyzed by western blot the expression of MGMT protein in U87MG and T98G cell lines. As shown in figure 24B, the two cell lines expressed different levels of MGMT protein. We compared through a microarray chip (Liu et al 2004) the miRs expression profile in U87MG cell lines versus T98G cell lines. We found different miRs up regulated in U87MG cell lines and downregulated in T98G and between them we focused our attention on miR-221 and -222. As shown in figure 24C, Real time PCR confirmed the different expression of those miRs in T98G and U87MG. These data indicate that T98G cell lines are more resistant to temozolomide treatment, express higher level of MGMT protein and lower level of miR-221 and -222 if compared to U87MG.

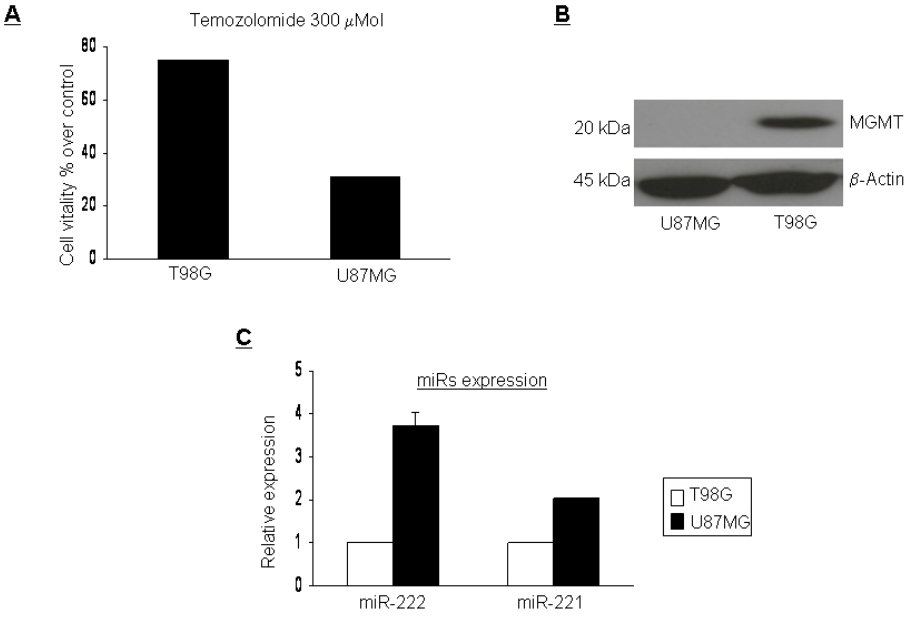

Figure 21-Temozolomide sensitivity and MGMT and MiR-221 and -222 expression in glioma cell lines. (A) Glioma cell lines treatment with 300μMol of temozolomide for 24 hr. Cell viability was valuated with a MTT assay. **(B)** Western blot analysis of MGMT expression in U87MG and T98G. **(C)** Real time expression of miR-221 and -222 expression in T98G and U87MG.

6.2. miR-221 and -222 target MGMT3'UTR. Using bioinformatics analysis available on Web sites and through RNA hybrid alignment we identified a possible binding site of miR-221 and -222 on 3'UTR sequence of MGMT in position 970. To verify if those miRs are capable to bind MGMT 3'UTR we cloned the MGMT 3'UTR downstream the luciferase reporter gene in pGL3 vector. The co-trasfection of miR-221 or -222 and pGL3-MGMT 3'UTR in Meg01 cells induced a decrease of luciferase activity while the co-trasfection of pGL3 vector expressing a mutant MGMT 3'UTR binding site and miRs-221 and -222 didn't induce a significant decrease of luciferase activity. Therefore, the mutated sequence was not able to inhibit the expression of MGMT 3'UTR (figure 25) .

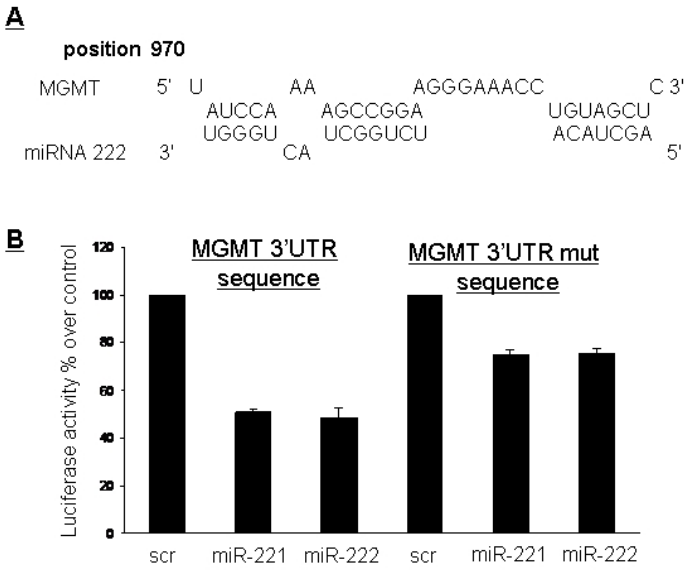

Figure 22- Identification of binding sites of miR-221 and 222 on MGMT 3'UTR. (A) Rna Hybrid prediction analyses of miR-222 and MGMT 3'UTR. **(B)** Luciferase activity of Meg01 cells transiently cotransfected with the luciferase reporter containing wild type MGMT-3′UTR or MGMT-3′UTR mutant in the presence of pre-miR-222, miR-221 or scrambled oligonucleotide. Representative of at least three independent experiments.

6.3. miR-221 and -222 target MGMT protein and mRNA. In order to establish a more causative effect between miR-222 and -221and MGMT, we transfected T98G cells with pre-miR-221 and -222 for 72hr and analyzed MGMT expression levels by western blot and real time PCR. As shown in figure 26A, data confirmed the down-regulation of MGMT protein and the decrease of mRNA upon miRs transfection. On the contrary, the transfection of U87MG with Anti-miR-221 and -222 constructs induced an increase of MGMT protein and mRNA levels (Figure 26B) . The same downregulation of MGMT protein observed in T98G transfected with pre-miRs constructs was observed in T98G stably infected with lentiviral construct encoding for an empty vector (tween) and for miR-221 (tween-221) and miR-222 (Tween-222) (Figure 26C).

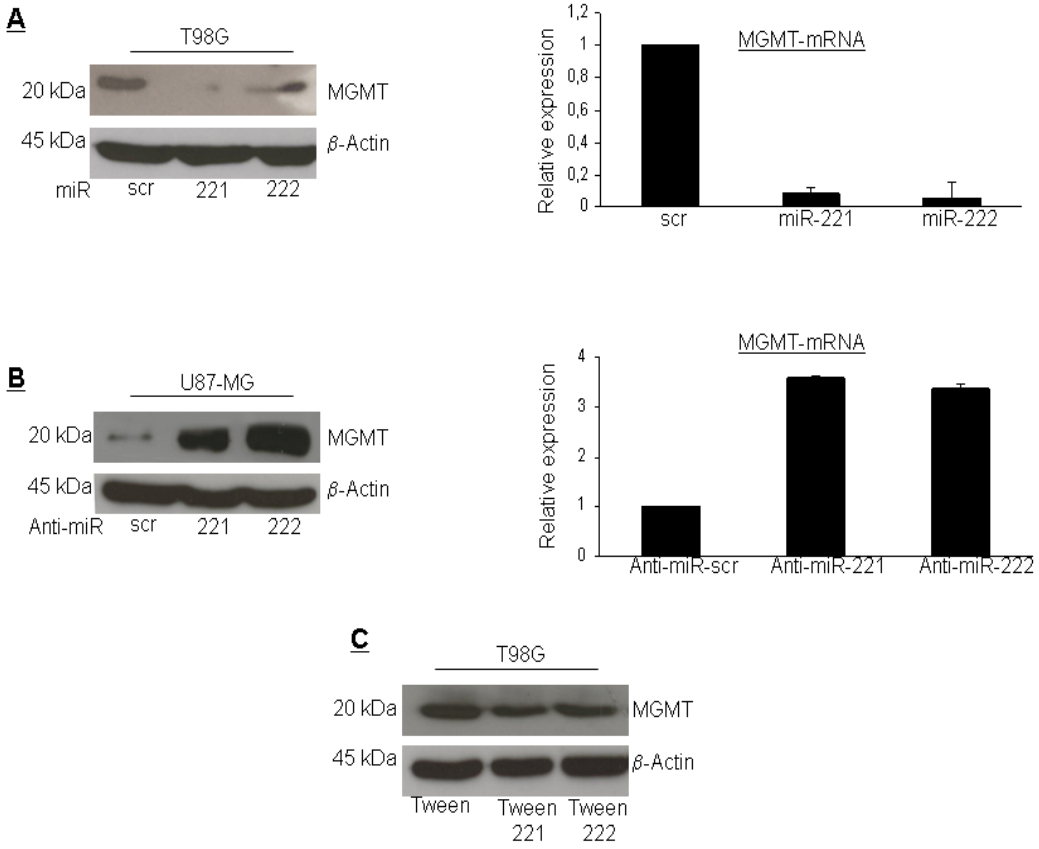

Figure 23- miR-221 and -222 regulate MGMT protein and mRNA levels. (A) Western blot analysis of MGMT protein and Real time PCR of MGMT mRNA extract from T98G transfected with a scrambled sequence or with a pre-miR-221 and -222. **(B)** Western blot analysis of MGMT protein and Real time PCR of MGMT mRNA extract from U87MG transfected with a scrambled sequence or with an Anti-miR-221 and -222. (C) Western blot analysis of MGMT protein level in stably infected T98G cells with lentivirus construct.

6.4. miR-221 and -222 modulate temozolomide sensitivity in glioma cell lines. To verify if miR-221 and -222 have a role in the modulation of temozolomide sensitivity because their effects on MGMT protein and mRNA levels, we studied cell vitality with MTT assay. At first, we characterized cell viability of T98G cells stably expressing miR-221 and miR-222 (T98G tween). As shown in figure 27 A, T98G tween-221 and -222 were more sensitive to treatment with of temozolomide (300 μMol for 48 hrs) compared to non infected cells. When we transfected T98G cells with miR-221 and -222 the effects of temozolomide were even more evident (Figure 27B). This was due to a greater increase of miR expression obtained with transient transfection.

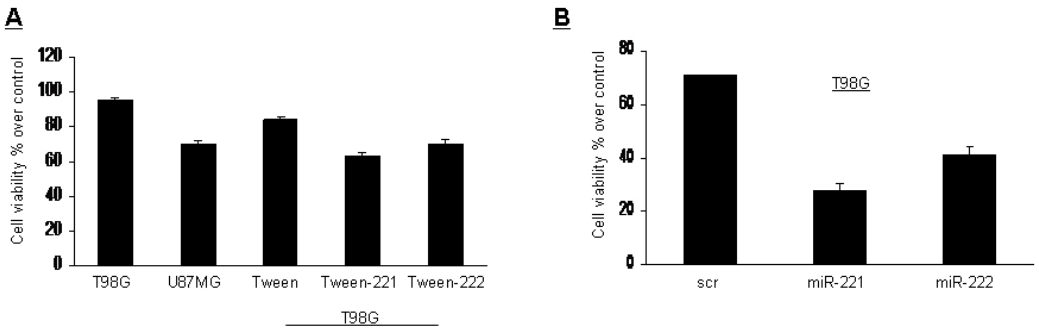

Figure 24- miR-221 and 222 modulate temozolomide sensitivity. (A) T98G, U87MG and T98G stably ex pressing miR-221 and -222 were treated with 300μMol of temozolomide for 48 hrs and the cell viability was assessed by MTT assay. **(B)** Cell viability assay of T98G transiently transfected with miR-221 and -222 and then treated with 300μMol of temozolomide for 48hrs.

6.5. miR-221 and -222 and MGMT mRNA levels in glioma samples. To evaluate whether MGMT downregulation in glioma was related to increased miR-222 and -221 levels also in vivo, we analyzed MGMT and miR-222/ -221 expression levels in tumour tissue specimens collected from 6 glioblastoma grade IV patients. The RNA was extracted by paraffin embed tissue using the Recovery ALL Kit from Ambion. As shown in A and B, we found an inverse correlation between miR-222 and -221 levels and MGMT in all glioma samples analyzed (Figure 28).

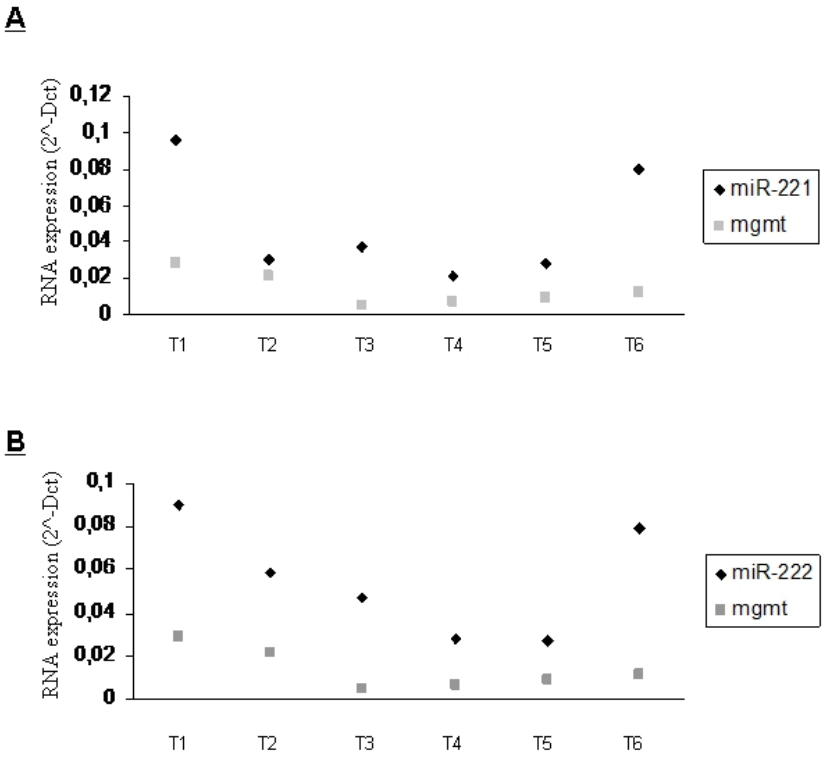

Figure 25-Correlation of endogenous miR-221 and 222 and MGMT mRNA expression levels in human glioma. Total RNA extracted from tissue specimens collected from 6 high grade glioma-affected individuals was used to analyze miR-221 **(A)** and -222 **(B)** and MGMT mRNA expression by real-time PCR. In each sample, an inverse correlation between miR-221 and -222 with MGMT was observed.

7. DISCUSSION AND CONCLUSION

Glioblastoma (GMB) are among the most deadly types of cancer (Tran and Rosenthal; 2010). Advances in standard treatments for this tumour, such as surgery, radiotherapy, and chemotherapy, have not significantly increased patient survival (Huse and Holland; 2010). The lethality of GMB can be attributed to the capacity of the cells to migrate and develop foci throughout the brain (Demuth and Berens; 2004). It is thought that the invasive behaviour of glioblastoma cells is one of the most important causes of poor clinical outcome, enabling tumor cells to actively egress from the main mass and invade the surrounding normal brain where they are out of reach of surgical resection, radiation, and chemotherapy (Giese et al; 2003).

The mechanisms of the spreading phenotype are not well understood so far. It was recently demonstrated that the receptor protein tyrosine phosphatase μ (PTPμ) negatively regulates GMB cell migration (Burgoyne et al; 2009). PTPμ is the prototype of the type IIb subfamily of receptor PTPs (RPTP). In a xenograft mouse model of intracranially injected U87MG cells, PTPμ shRNA was able to induce cell migration and dispersal (Burgoyne et al; 2009). PTPμ may be considered as a "migration suppressor" with regard to the diffuse infiltrative growth pattern observed in human gliomas. It was previously shown that PTPμ protein is downregulated in glioblastoma and that its levels correlated to tumor stage (Burgoyne et al; 2009). In particular, a striking loss of PTPμ protein was observed in highly dispersive GBM compared to less dispersive low-grade astrocytomas and normal brain (Burgoyne et al; 2009). It was recently demonstrated that one mechanism of PTPμ down-regulation in GBM is proteolytic breakdown (Burgoyne et al; 2009).

In this study, we identified a new molecular mechanism of PTPμ downregulation in human glioma, by identifying two related microRNAs that target this phosphatase. In order to identify new signatures of GMB invasiveness, we investigated the microRNA expression profile of tumorigenic U87MG glioma cells compared with non tumorigenic T98G cells. We identified five miR genes significantly overexpressed in tumorigenic cells with a >2.5-fold change. Among the different microRNAs we focused our attention on two highly related miRs, miR-221 and -222. MiR-222 and -221 expression levels in human cancer have been extensively investigated (Garofalo et al; 2008, Garofalo et al; 2009, Visone et al; 2007) and have been frequently found overexpressed in a number of human tumors (Pallante et al; 2006, Conti et al; 2009, Pineau et al; 2010). In GMB tissues and cell lines miR-222 and -221 were found overexpressed (Ciafrè et al; 2005, Conti et al; 2009) and correlated to the stage of the disease. However, the molecular targets of those miRs potentially involved in GBM's invasive behaviour had not been clarified. We provide evidence for the first time that miR-222 and -221 bind to the 3'UTR region of PTPμ and are able to down-regulate PTPμ at RNA and protein levels. By luciferase assay, we also identified the 3'UTR region of the PTP gene that represents the miR binding site.

Because PTPμ has been described to be able to suppress glioma cell migration (Burgoyne et al; 2009), we hypothesized that miR-221 and -222 promote cell migration by down-regulating PTPμ expression. In fact, the analysis of cell motility in T98G cells transduced with miR-221 or -222 demonstrated that up-regulation of those miRs in T98G induced an increase of cell motility. The same result was obtained in T98G cells transiently transfected with either miR-221 or -222. Conversely the expression of anti-miR -222 was able to reduce cell migration of U87MG. Because miRNAs can affect many different proteins, we validated the migration/adhesion effects by co-transfection of miR-222 and ectopic PTPμ lacking the miRNA binding site in its 3'UTR. These rescue experiments proved the causative connection between miR-222/221 PTPμ and migration/invasion.
Moreover, our data show that in specimens of glioma, miR-222 and -221 expressions inversely correlates with that of PTPμ. Therefore, miR-222 and -221 expression levels could predict the aggressive behaviour of glioma.
MicroRNAs are also attractive drug targets since they regulate expression of many proteins in the cell and are differentially expressed in malignant versus normal cells. Recently, multiple studies highlighted the involvement of miR-mediated regulation of protein levels in drug resistance. In this work we highlighted the possible role of different sets of microRNA in TRAIL and temozolomide resistance.
The present study shows that MGMT protein and mRNA are target of miR-221 and 222 and that these two miRs are capable to modulate glioblastoma sensitivity to temozolomide. So far it has been demonstrated that MGMT activity is frequently lost in glioblastoma in the presence of CpG island hypermethylation in the promoter region. Therefore, the methylation status of the MGMT promoter was considered to be indicative of a good outcome in patients with malignant gliomas treated with alkylating agent (Spiegl-Kreinecker et al; 2010). However, in some studies the correlation between MGMT promoter methylation and MGMT expression levels are contradictory. Therefore other possible mechanisms of MGMT modulation should exist. Our study suggests that MGMT may be regulated also by microRNA action in particular by miR-221 and 222. Surprisingly these data could give us a new consideration of miR-221 and 222 function in glioma. These two miRs are usually upregulated in high grade tumours they could be indicative of a good outcome of patients treated with temozolomide also in absence a CpG MGMT promoter non methylated. More association study on patients need to be done do assess clearly this correlation.
Most glioblastomas present resistance to TRAIL, an this resistance may be due to a variety of mechanisms, including high decoy receptor expression, low expression levels of critical mediators of TRAIL signalling, such as caspase-8 and Fas associated death domain, or high expression of inhibitors of apoptosis, such as FLICE-inhibitory protein (cFLIP). Therefore, it's clear that a better comprehension of the mechanisms of TRAIL resistance may represent a powerful instrument to ameliorate glioblastoma patient treatment. Recently several works explored the role of microRNA in TRAIL resistance. We demonstrated that miR-221 and miR-222 regulate death receptor signalling and TRAIL apoptosis sensitivity in non small cell lung cancer and in hepatocarcinoma by modulating

p27kip1, PTEN and TIMP3 expression (Garofalo et al; 2008, Garofalo et al; 2009).
In gliomas, miR-21 was reported to be upregulated , and miR-21 knock-down was associated with increased apoptotic activity. Furthermore, Corsten et al (Corsten et al; 2007), evaluated the combined effects of miR-21 antagonisms and expression in neural precursor cells (NPC) of a secretable variant of the cytototoxic agent TRAIL. They found that pre-treatment of glioma cells with LNA-anti-miR-21 and TRAIL led to synergistic antitumor effect both in vivo and in vitro. Accordingly to this data, we found an upregulation of miR-21 and 30b and 30c in our TRAIL resistance glioblastoma cells, U87MG and LN229. Interestingly, the up regulation of these miRs in TRAIL sensitive cells T98G, induced an increase of cell viability and a decrease of apoptotic cells, underlying a crucial role of miR-21, miR-30b and miR30 c in TRAIL resistance. To clearly understand the role of these miRs in TRAIL resistance we looked for their target through an internet search. Surprisingly we identified caspase-3 as target of miR-30c. Another recent work underlines the crucial role of blocking caspase-3 activity. Infact, a breast cell lines MDA-MB-453 , transfected with 187 individual synthetic miRNAs were screened for probing their behaviour in TRAIL pathway. Thirty four of these miRs led to a differential caspase-3 activation phenotype. Identifying a miR capable to bind and block caspase-3 directly represent a possible strategy to overcame TRAIL resistance.
Corsten and colleagues (Corsten et al; 2007) have not demonstrated a clear correlation between miR-21 targets and TRAIL resistance. In this work we identified as target of miR-21 involved in TRAIL sensitivity the protein TAp-63, one of the two major isoforms of TP63 gene. There are evidences that TAp-63 plays an important role in DNA damage controlling cell cycle and apoptosis in human cancer, although its precise role in tumorigenesis remains to be clarified. TAp-63 shows clear pro-apoptotic activity, mediated both by death receptors (CD95, TNF, TRAIL) and mithocondrial (bax,puma) pathways (Candi et al; 2007). Recently has been demonstrated that Tap63 is induced by a variety of chemotherapeutic agents and that blocking Tap-63 function leads to enhanced chemoresistance (Gressner et al; 2005). All these observation are consistent with our hypothesis of a possible role of miR-21 in regulation of TRAIL sensitivity through the regulation of Tap-63 protein.
In conclusion, miR-based regulation of the numerous molecular pathways involved in gliomagenesis is promising and may provide numerous additional candidates for therapeutic targeting in the near future.

8. Acknowledgments

I am heartily thankful to my supervisor, Momina Condorelli, for her encouragement and guidance. She has supported me throughout my master thesis and my PhD thesis helping me also in solving problems so far away from science. One could not wish for a better and friendlier supervisor.

Drs MariaLaura De Caro del Basso and J. Carlos Martinez-Montero have provided me with all of the human glioblastoma samples covered in this thesis, with consistent quality.

Dr Vittorio de Franciscis and Dr Laura Cerchia for the continuous suggestions.

All my lab buddies. They made lab a convivial place to work. In particular, I would like to thank Ciro Zanca: although he left me alone in my last year of PhD, he continues to support me every day; Michela Garofalo for her help in some experiments and for the continuous suggestions; Monica Brenca, my "first student", we grew up together and spent a lot of nicely hours together; all the other students: Danilo Fiore, Elvira Donnarumma, Stefania Di Costanzo they became my second family. This work was made possible also by them.

Pierlorenzo, known by all as "Professor Pallante", who, in his opinion, has discovered miR-221 and -222 (we leave him to believe it). He sustained me day after day, and brought back the joy in my life. I shall be forever grateful for his love, dedication and persistent confidence in me.

I would like to thank my parents, my grandparents and my twin. They still don't understand and sometimes get angry for the long time that I spent in lab. I don't think they really understood what I do for hours in lab but, in their own way, they encouraged me.

Finally, I would like to thank the Department of Molecular and Cellular Biology and Pathology L. Califano. It has provided the support and equipment I have needed to produce and complete my thesis.

9. REFERENCES

Tran B and Rosenthal MA (2010) Survival comparison between glioblastoma multiforme and other incurable cancers. J Clin Neurosci 17 (4):417-21

Ohgaki H and Kleihues P (2005) Population-Based Studies on Incidence, Survival Rates, and Genetic Alterations in Astrocytic and Oligodendroglial Gliomas. Journal of Neuropathology & Experimental Neurology 64 (6):479-489

Ohgaki H and Kleihues P (2005) Epidemiology and etiology of gliomas. Acta Neuropathologica 109 (1):93-108

Louis D, Ohgaki H, Wiestler O, Cavenee W, Burger P, Jouvet A, Scheithauer B and Kleihues P (2007) The 2007 WHO Classification of Tumours of the Central Nervous System. Acta Neuropathologica 114 (2):97-109

Huse JT and Holland EC (2010) Targeting brain cancer: advances in the molecular pathology of malignant glioma and medulloblastoma. Nat Rev Cancer 10 (5):319-31

Noble M and Mayer-Pröschel M (1997) Growth factors, glia and gliomas. Journal of Neuro-Oncology 35 (3):193-209

Ekstrand AJ, James CD, Cavenee WK, Seliger B, Pettersson RF and Collins VP (1991) Genes for Epidermal Growth Factor Receptor, Transforming Growth Factor Î±, and Epidermal Growth Factor and Their Expression in Human Gliomas in Vivo. Cancer Research 51 (8):2164-2172

Wong AJ, Ruppert JM, Bigner SH, Grzeschik CH, Humphrey PA, Bigner DS and Vogelstein B (1992) Structural alterations of the epidermal growth factor receptor gene in human gliomas. Proceedings of the National Academy of Sciences of the United States of America 89 (7):2965-2969

Hunter T (1995) Protein kinases and phosphatases: The Yin and Yang of protein phosphorylation and signaling. Cell 80 (2):225-236

Sano T, Lin H, Chen X, Langford LA, Koul D, Bondy ML, Hess KR, Myers JN, Hong Y-K, Yung WKA and Steck PA (1999) Differential Expression of MMAC/PTEN in Glioblastoma Multiforme. Cancer Research 59 (8):1820-1824

He J, Allen JR, Collins VP, Allalunis-Turner MJ, Godbout R, Day RS and James CD (1994) CDK4 Amplification Is an Alternative Mechanism to p16 Gene Homozygous Deletion in Glioma Cell Lines. Cancer Research 54 (22):5804-5807

Giese A, Bjerkvig R, Berens ME and Westphal M (2003) Cost of Migration: Invasion of Malignant Gliomas and Implications for Treatment. Journal of Clinical Oncology 21 (8):1624-1636

Sallinen S-L, Sallinen PK, Haapasalo HK, Helin HJ, HelÃ©n PT, Schraml P, Kallioniemi O-P and Kononen J (2000) Identification of Differentially Expressed Genes in Human Gliomas by DNA Microarray and Tissue Chip Techniques. Cancer Research 60 (23):6617-6622

Claes A, Idema A and Wesseling P (2007) Diffuse glioma growth: a guerilla war. Acta Neuropathologica 114 (5):443-458

Dear TN and Kefford RF (1990) Molecular oncogenetics of metastasis. Molecular Aspects of Medicine 11 (4):243-324

Gressens P (2000) Mechanisms and Disturbances of Neuronal Migration. Pediatric Research 48 (6):725-730

Mariani L, McDonough WS, Hoelzinger DB, Beaudry C, Kaczmarek E, Coons SW, Giese A, Moghaddam M, Seiler RW and Berens ME (2001) Identification and Validation of P311 as a Glioblastoma Invasion Gene Using Laser Capture Microdissection. Cancer Research 61 (10):4190-4196

Mori M, Murata Y, Kotani T, Kusakari S, Ohnishi H, Saito Y, Okazawa H, Ishizuka T, Mori M and Matozaki T Promotion of cell spreading and migration by vascular endothelial-protein tyrosine phosphatase (VE-PTP) in cooperation with integrins. Journal of Cellular Physiology 224 (1):195-204

Blanquart C, Karouri S-E and Issad T Protein tyrosine phosphatase-1B and T-cell protein tyrosine phosphatase regulate IGF-2-induced MCF-7 cell migration. Biochemical and Biophysical Research Communications 392 (1):83-88

Hendriks WJAJ, Elson A, Harroch S and Stoker AW (2008) Protein tyrosine phosphatases: functional inferences from mouse models and human diseases. FEBS Journal 275 (5):816-830

Tonks NK (2006) Protein tyrosine phosphatases: from genes, to function, to disease. Nat Rev Mol Cell Biol 7 (11):833-846

Alonso A, Sasin J, Bottini N, Friedberg I, Friedberg I, Osterman A, Godzik A, Hunter T, Dixon J and Mustelin T (2004) Protein Tyrosine Phosphatases in the Human Genome. Cell 117 (6):699-711

Tabernero L, Aricescu AR, Jones EY and Szedlacsek SE (2008) Protein tyrosine phosphatases: structure–function relationships. FEBS Journal 275 (5):867-882

Brady-Kalnay SM, Flint AJ and Tonks NK (1993) Homophilic binding of PTP mu, a receptor-type protein tyrosine phosphatase, can mediate cell-cell aggregation. The Journal of Cell Biology 122 (4):961-972

Gebbink MF, Zondag GC, Wubbolts RW, Beijersbergen RL, van Etten I and Moolenaar WH (1993) Cell-cell adhesion mediated by a receptor-like protein tyrosine phosphatase. Journal of Biological Chemistry 268 (22):16101-16104

Hellberg CB, Burden-Gulley SM, Pietz GE and Brady-Kalnay SM (2002) Expression of the Receptor Protein-tyrosine Phosphatase, PTPÎ¼, Restores E-cadherin-dependent Adhesion in Human Prostate Carcinoma Cells. Journal of Biological Chemistry 277 (13):11165-11173

Burden-Gulley SM and Brady-Kalnay SM (1999) PTPÎ¼ Regulates N-Cadherinâ€“dependent Neurite Outgrowth. The Journal of Cell Biology 144 (6):1323-1336

Burden-Gulley SM, Ensslen SE and Brady-Kalnay SM (2002) Protein Tyrosine Phosphatase-{micro} Differentially Regulates Neurite Outgrowth of Nasal and Temporal Neurons in the Retina. J. Neurosci. 22 (9):3615-3627

Rosdahl JA, Mourton TL and Brady-Kalnay SM (2002) Protein Kinase C [delta] (PKC[delta]) Is Required for Protein Tyrosine Phosphatase [mu] (PTP[mu])-Dependent Neurite Outgrowth. Molecular and Cellular Neuroscience 19 (2):292-306

Burgoyne AM, Palomo JM, Phillips-Mason PJ, Burden-Gulley SM, Major DL, Zaremba A, Robinson S, Sloan AE, Vogelbaum MA, Miller RH and Brady-Kalnay SM (2009) PTPmu suppresses glioma cell migration and dispersal. Neuro Oncol Epub ahead of print

Burgoyne AM, Phillips-Mason PJ, Burden-Gulley SM, Robinson S, Sloan AE, Miller RH and Brady-Kalnay SM (2009) Proteolytic cleavage of protein tyrosine phosphatase mu regulates glioblastoma cell migration. Cancer Res 69 (17):6960-8

Phillips-Mason PJ, Kaur H, Burden-Gulley SM, Craig SE and Brady-Kalnay SM Identification of phospholipase C gamma1 as a protein tyrosine phosphatase mu substrate that regulates cell migration. Journal of Cellular Biochemistry:n/a-n/a

Plowman J, Waud WR, Koutsoukos AD, Rubinstein LV, Moore TD and Grever MR (1994) Preclinical Antitumor Activity of Temozolomide in Mice: Efficacy against Human Brain Tumor Xenografts and Synergism with 1,3-Bis(2-chloroethyl)-1-nitrosourea. Cancer Research 54 (14):3793-3799

Stupp R, Mason WP, van den Bent MJ, Weller M, Fisher B, Taphoorn MJB, Belanger K, Brandes AA, Marosi C, Bogdahn U, Curschmann Jr, Janzer RC, Ludwin SK, Gorlia T, Allgeier A, Lacombe D, Cairncross JG, Eisenhauer E and Mirimanoff RO (2005) Radiotherapy plus Concomitant and Adjuvant Temozolomide for Glioblastoma. New England Journal of Medicine 352 (10):987-996

Agarwala SS and Kirkwood JM (2000) Temozolomide, a novel alkylating agent with activity in the central nervous system, may improve the treatment of advanced metastatic melanoma. Oncologist 5 (2):144-51

Friedman HS, Kerby T and Calvert H (2000) Temozolomide and Treatment of Malignant Glioma. Clinical Cancer Research 6 (7):2585-2597

Stupp R, Mason WP, van den Bent MJ, Weller M, Fisher B, Taphoorn MJ, Belanger K, Brandes AA, Marosi C, Bogdahn U, Curschmann J, Janzer RC, Ludwin SK, Gorlia T, Allgeier A, Lacombe D, Cairncross JG, Eisenhauer E, Mirimanoff RO, Groups EOfRaToCBTaR and Group NCIoCCT (2005) Radiotherapy plus concomitant and adjuvant temozolomide for glioblastoma. N Engl J Med 352 (10):987-96

Kanzawa T, Germano IM, Komata T, Ito H, Kondo Y and Kondo S (2004) Role of autophagy in temozolomide-induced cytotoxicity for malignant glioma cells. Cell Death Differ 11 (4):448-457

Bobola MS, Emond MJ, Blank A, Meade EH, Kolstoe DD, Berger MS, Rostomily RC, Silbergeld DL, Spence AM and Silber JR (2004) Apurinic Endonuclease Activity in Adult Gliomas and Time to Tumor Progression after Alkylating Agent-Based Chemotherapy and after Radiotherapy. Clinical Cancer Research 10 (23):7875-7883

Liu L and Gerson SL (2006) Targeted Modulation of MGMT: Clinical Implications. Clinical Cancer Research 12 (2):328-331

Friedman HS, Keir S, Pegg AE, Houghton PJ, Colvin OM, Moschel RC, Bigner DD and Dolan ME (2002) O6-Benzylguanine-mediated Enhancement of Chemotherapy Molecular Cancer Therapeutics 1 (11):943-948

Esteller M, Risques R-A, Toyota M, Capella G, Moreno V, Peinado MA, Baylin SB and Herman JG (2001) Promoter Hypermethylation of the DNA Repair Gene O6-Methylguanine-DNA Methyltransferase Is Associated with the Presence of G:C to A:T Transition Mutations in p53 in Human Colorectal Tumorigenesis. Cancer Research 61 (12):4689-4692

Hegi ME, Diserens A-C, Gorlia T, Hamou M-F, de Tribolet N, Weller M, Kros JM, Hainfellner JA, Mason W, Mariani L, Bromberg JEC, Hau P, Mirimanoff

RO, Cairncross JG, Janzer RC and Stupp R (2005) MGMT Gene Silencing and Benefit from Temozolomide in Glioblastoma. New England Journal of Medicine 352 (10):997-1003

Schaefer U, Voloshanenko O, Willen D and Walczak H (2007) TRAIL: a multifunctional cytokine. Front Biosci 12 (3813-24)

Hayakawa Y, Screpanti V, Yagita H, Grandien A, Ljunggren H-G, Smyth MJ and Chambers BJ (2004) NK Cell TRAIL Eliminates Immature Dendritic Cells In Vivo and Limits Dendritic Cell Vaccination Efficacy. J Immunol 172 (1):123-129

Janssen EM (2003) CD4 + T cells are required for secondary expansion and memory in CD8 + T lymphocytes. Nature 421:852-856

Walczak H and Krammer PH (2000) The CD95 (APO-1/Fas) and the TRAIL (APO-2L) apoptosis systems. Exp Cell Res 256 (1):58-66

Falschlehner C, Emmerich CH, Gerlach B and Walczak H (2007) TRAIL signalling: Decisions between life and death. Int J Biochem Cell Biol 39 (7-8):1462-75

Garofalo M, Romano G, Quintavalle C, Romano MF, Chiurazzi F, Zanca C and Condorelli G (2007) Selective inhibition of PED protein expression sensitizes B-cell chronic lymphocytic leukaemia cells to TRAIL-induced apoptosis. Int J Cancer 120 (6):1215-22

Zanca C, Garofalo M, Quintavalle C, Romano G, Acunzo M, Ragno P, Montuori N, Incoronato MR, Tornillo L, Baumhoer D, Briguori C, Terracciano L and Condorelli G (2008) PED is overexpressed and mediates TRAIL resistance in human non-small cell lung cancer. J Cell Mol Med [Epub ahead of print]Click here to read

Quintavalle C, Incoronato M, Puca L, Acunzo M, Zanca C, Romano G, Garofalo M, Iaboni M, Croce CM and Condorelli G (2010) c-FLIPL enhances anti-apoptotic Akt functions by modulation of Gsk3[beta] activity. Cell Death Differ

Hanahan D and Folkman J (1996) Patterns and Emerging Mechanisms of the Angiogenic Switch during Tumorigenesis. Cell 86 (3):353-364

Hu B, Guo P, Bar-Joseph I, Imanishi Y, Jarzynka MJ, Bogler O, Mikkelsen T, Hirose T, Nishikawa R and Cheng SY (2007) Neuropilin-1 promotes human glioma progression through potentiating the activity of the HGF//SF autocrine pathway. Oncogene 26 (38):5577-5586

Oliner J, Min H, Leal J, Yu D, Rao S, You E, Tang X, Kim H, Meyer S, Han SJ, Hawkins N, Rosenfeld R, Davy E, Graham K, Jacobsen F, Stevenson S, Ho J,

Chen Q, Hartmann T, Michaels M, Kelley M, Li L, Sitney K, Martin F, Sun J-R, Zhang N, Lu J, Estrada J, Kumar R, Coxon A, Kaufman S, Pretorius J, Scully S, Cattley R, Payton M, Coats S, Nguyen L, Desilva B, Ndifor A, Hayward I, Radinsky R, Boone T and Kendall R (2004) Suppression of angiogenesis and tumor growth by selective inhibition of angiopoietin-2. Cancer cell 6 (5):507-516

Noguera-Troise I, Daly C, Papadopoulos NJ, Coetzee S, Boland P, Gale NW, Chieh Lin H, Yancopoulos GD and Thurston G (2006) Blockade of Dll4 inhibits tumour growth by promoting non-productive angiogenesis. Nature 444 (7122):1032-1037

Pope WB, Lai A, Nghiemphu P, Mischel P and Cloughesy TF (2006) MRI in patients with high-grade gliomas treated with bevacizumab and chemotherapy. Neurology 66 (8):1258-1260

Poulsen HS, Grunnet K, Sorensen M, Olsen P, Hasselbalch B, Nelausen K, Kosteljanetz M and Lassen U (2009) Bevacizumab plus irinotecan in the treatment patients with progressive recurrent malignant brain tumours. Acta Oncologica 48 (1):52-58

Narayana A, Kelly P, Golfinos J, Parker E, Johnson G, Knopp E, Zagzag D, Fischer I, Raza S, Medabalmi P, Eagan P and Gruber ML (2009) Antiangiogenic therapy using bevacizumab in recurrent high-grade glioma: impact on local control and patient survival. Journal of Neurosurgery 110 (1):173-180

Bartel DP (2004) MicroRNAs: genomics, biogenesis, mechanism, and function. Cell 116 (2):281-97

Lee Y, Jeon K, Lee JT, Kim S and Kim VN (2002) MicroRNA maturation: stepwise processing and subcellular localization. EMBO J 21 (17):4663-70

Gregory RI and Shiekhattar R (2005) MicroRNA biogenesis and cancer. Cancer Res 65 (9):3509-12

Lewis BP, Shih Ih, Jones-Rhoades MW, Bartel DP and Burge CB (2003) Prediction of Mammalian MicroRNA Targets. Cell 115 (7):787-798

Kwak PB, Iwasaki S and Tomari Y The microRNA pathway and cancer. Cancer Science 101 (11):2309-2315

Chen JF, Mandel EM, Thomson JM, Wu Q, Callis TE, Hammond SM, Conlon FL and Wang DZ (2006) The role of microRNA-1 and microRNA-133 in skeletal muscle proliferation and differentiation. Nat Genet 38 (2):228-33

Chen CZ, Li L, Lodish HF and Bartel DP (2004) MicroRNAs modulate hematopoietic lineage differentiation. Science 303 (5654):83-6

Naguibneva I, Ameyar-Zazoua M, Polesskaya A, Ait-Si-Ali S, Groisman R, Souidi M, Cuvellier S and Harel-Bellan A (2006) The microRNA miR-181 targets the homeobox protein Hox-A11 during mammalian myoblast differentiation. Nat Cell Biol 8 (3):278-84

Chang J, Nicolas E, Marks D, Sander C, Lerro A, Buendia MA, Xu C, Mason WS, Moloshok T, Bort R, Zaret KS and Taylor JM (2004) miR-122, a mammalian liver-specific microRNA, is processed from hcr mRNA and may downregulate the high affinity cationic amino acid transporter CAT-1. RNA Biol 1 (2):106-13

Esau C, Kang X, Peralta E, Hanson E, Marcusson EG, Ravichandran LV, Sun Y, Koo S, Perera RJ, Jain R, Dean NM, Freier SM, Bennett CF, Lollo B and Griffey R (2004) MicroRNA-143 regulates adipocyte differentiation. J Biol Chem 279 (50):52361-5

Schratt GM, Tuebing F, Nigh EA, Kane CG, Sabatini ME, Kiebler M and Greenberg ME (2006) A brain-specific microRNA regulates dendritic spine development. Nature 439 (7074):283-9

Calin GA, Dumitru CD, Shimizu M, Bichi R, Zupo S, Noch E, Aldler H, Rattan S, Keating M, Rai K, Rassenti L, Kipps T, Negrini M, Bullrich F and Croce CM (2002) Frequent deletions and down-regulation of micro- RNA genes miR15 and miR16 at 13q14 in chronic lymphocytic leukemia. Proc Natl Acad Sci U S A 99 (24):15524-9

Calin GA, Ferracin M, Cimmino A, Di Leva G, Shimizu M, Wojcik SE, Iorio MV, Visone R, Sever NI, Fabbri M, Iuliano R, Palumbo T, Pichiorri F, Roldo C, Garzon R, Sevignani C, Rassenti L, Alder H, Volinia S, Liu CG, Kipps TJ, Negrini M and Croce CM (2005) A MicroRNA signature associated with prognosis and progression in chronic lymphocytic leukemia. N Engl J Med 353 (17):1793-801

Cimmino A, Calin GA, Fabbri M, Iorio MV, Ferracin M, Shimizu M, Wojcik SE, Aqeilan RI, Zupo S, Dono M, Rassenti L, Alder H, Volinia S, Liu CG, Kipps TJ, Negrini M and Croce CM (2005) miR-15 and miR-16 induce apoptosis by targeting BCL2. Proc Natl Acad Sci U S A 102 (39):13944-9

Johnson SM, Grosshans H, Shingara J, Byrom M, Jarvis R, Cheng A, Labourier E, Reinert KL, Brown D and Slack F (2005) RAS is regulated by the let-7 microRNA family. Cell 120 (5):635-47

Costinean S, Zanesi N, Pekarsky Y, Tili E, Volinia S, Heerema N and Croce CM (2006) Pre-B cell proliferation and lymphoblastic leukemia/high-grade lymphoma in EÎ¼-miR155 transgenic mice. Proceedings of the National Academy of Sciences 103 (18):7024-7029

Petrocca F, Vecchione A and Croce CM (2008) Emerging role of miR-106b-25/miR-17-92 clusters in the control of transforming growth factor beta signaling. Cancer Res 68 (20):8198-4

Tavazoie SF, Alarcon C, Oskarsson T, Padua D, Wang Q, Bos PD, Gerald WL and Massague J (2008) Endogenous human microRNAs that suppress breast cancer metastasis. Nature 451 (7175):147-152

Eis PS, Tam W, Sun L, Chadburn A, Li Z, Gomez MF, Lund E and Dahlberg JE (2005) Accumulation of miR-155 and BIC RNA in human B cell lymphomas. Proc Natl Acad Sci U S A 8 (102):10

Kluiver J, Poppema S, de Jong D, Blokzijl T, Harms G, Jacobs S, Kroesen BJ and van den Berg A (2005) BIC and miR-155 are highly expressed in Hodgkin, primary mediastinal and diffuse large B cell lymphomas. J Pathol 207 (2):243-9

Metzler M, Wilda M, Busch K, Viehmann S and Borkhardt A (2004) High expression of precursor microRNA-155/BIC RNA in children with Burkitt lymphoma. Genes, Chromosomes and Cancer 39 (2):167-169

Michael MZ, O' Connor SM, van Holst Pellekaan NG, Young GP and James RJ (2003) Reduced Accumulation of Specific MicroRNAs in Colorectal Neoplasia11Note: Susan M. O' Connor and Nicholas G. van Holst Pellekaan contributed equally to this work. Molecular Cancer Research 1 (12):882-891

Ciafrè SA, Galardi S, Mangiola A, Ferracin M, Liu CG, Sabatino G, Negrini M, Maira G, Croce CM and Farace MG (2005) Extensive modulation of a set of microRNAs in primary glioblastoma. Biochem Biophys Res Commun 334 (4):1351-8

Pallante P, Visone R, Ferracin M, Ferraro A, Berlingieri MT, Troncone G, Chiappetta G, Liu C, Santoro M, Negrini M, Croce CM and Fusco A (2006) MicroRNA deregulation in human thyroid papillary carcinomas. Endocr Relat Cancer 13 (2):497-508

Weber F, Teresi RE, Broelsch CE, Frilling A and Eng C (2006) A Limited Set of Human MicroRNA Is Deregulated in Follicular Thyroid Carcinoma. J Clin Endocrinol Metab 91 (9):3584-3591

He L, Thomson JM, Hemann MT, Hernando-Monge E, Mu D, Goodson S, Powers S, Cordon-Cardo C, Lowe SW, Hannon GJ and Hammond SM (2005) A microRNA polycistron as a potential human oncogene. Nature 435 (7043):828-33

Volinia S, Calin GA, Liu C-G, Ambs S, Cimmino A, Petrocca F, Visone R, Iorio M, Roldo C, Ferracin M, Prueitt RL, Yanaihara N, Lanza G, Scarpa A, Vecchione

A, Negrini M, Harris CC and Croce CM (2006) A microRNA expression signature of human solid tumors defines cancer gene targets. Proceedings of the National Academy of Sciences of the United States of America 103 (7):2257-2261

Bottoni A, Zatelli MC, Ferracin M, Tagliati F, Piccin D, Vignali C, Calin GA, Negrini M, Croce CM and degli Uberti EC (2007) Identification of differentially expressed microRNAs by microarray: A possible role for microRNA genes in pituitary adenomas. Journal of Cellular Physiology 210 (2):370-377

Livak KJ and Schmittgen TD (2001) Analysis of relative gene expression data using real-time quantitative PCR and the 2(-Delta Delta C(T)) Method. Methods 25 (4):402-8

Nuovo G, Lee EJ, Lawler S, Godlewski J and Schmittgen T (2009) In situ detection of mature microRNAs by labeled extension on ultramer templates. Biotechniques 46 (2):115-26

Cerchia L, Esposito CL, Jacobs AH, Tavitian B and de Franciscis V (2009) Differential SELEX in Human Glioma Cell Lines. PLoS ONE 4 (11):e7971

He H, Jazdzewski K, Li W, Liyanarachchi S, Nagy R, Volinia S, Calin GA, Liu CG, Franssila K, Suster S, Kloos RT, Croce CM and de la Chapelle A (2005) The role of microRNA genes in papillary thyroid carcinoma. Proc Natl Acad Sci U S A 102 (52):19075-80

Conti A, Aguennouz M, La Torre D, Tomasello C, Cardali S, Angileri FF, Maio F, Cama A, Germanò A, Vita G and Tomasello F (2009) miR-21 and 221 upregulation and miR-181b downregulation in human grade II-IV astrocytic tumors. J Neurooncol 93 (3):325-32

Pineau P, Volinia S, McJunkin K, Marchio A, Battiston C, Terris B, Mazzaferro V, Lowe SW, Croce CM and Dejean A (2010) miR-221 overexpression contributes to liver tumorigenesis. Proc Natl Acad Sci U S A 107 (1):264-9

Demuth T and Berens ME (2004) Molecular mechanisms of glioma cell migration and invasion. J Neurooncol 70 (2):217-28

Giese A, Bjerkvig R, Berens ME and Westphal M (2003) Cost of migration: invasion of malignant gliomas and implications for treatment. J Clin Oncol 21 (8):1624-36

Garofalo M, Quintavalle C, Di Leva G, Zanca C, Romano G, Taccioli C, Liu CG, Croce CM and Condorelli G (2008) MicroRNA signatures of TRAIL resistance in human non-small cell lung cancer. Oncogene 27 (27):3845-55

Garofalo M, Di Leva G, Romano G, Nuovo G, Suh SS, Ngankeu A, Taccioli C, Pichiorri F, Alder H, Secchiero P, Gasparini P, Gonelli A, Costinean S, Acunzo M, Condorelli G and Croce CM (2009) miR-221&222 regulate TRAIL resistance and enhance tumorigenicity through PTEN and TIMP3 downregulation. Cancer Cell 16 (6):498-509

Visone R, Russo L, Pallante P, De Martino I, Ferraro A, Leone V, Borbone E, Petrocca F, Alder H, Croce CM and Fusco A (2007) MicroRNAs (miR)-221 and miR-222, both overexpressed in human thyroid papillary carcinomas, regulate p27Kip1 protein levels and cell cycle. Endocr Relat Cancer 14 (3):791-8

Spiegl-Kreinecker S, Pirker C, Filipits M, Lötsch D, Buchroithner J, Pichler J, Silye R, Weis S, Micksche M, Fischer J and Berger W (2010) O6-Methylguanine DNA methyltransferase protein expression in tumor cells predicts outcome of temozolomide therapy in glioblastoma patients. Neuro Oncol 12 (1):28-36

Corsten MF, Miranda R, Kasmieh R, Krichevsky AM, Weissleder R and Shah K (2007) MicroRNA-21 knockdown disrupts glioma growth in vivo and displays synergistic cytotoxicity with neural precursor cell delivered S-TRAIL in human gliomas. Cancer Res 67 (19):8994-9000

Candi E, Dinsdale D, Rufini A, Salomoni P, Knight RA, Mueller M, Krammer PH and Melino G (2007) TAp63 and DeltaNp63 in cancer and epidermal development. Cell Cycle 6 (3):274-85

Gressner O, Schilling T, Lorenz K, Schulze Schleithoff E, Koch A, Schulze-Bergkamen H, Lena AM, Candi E, Terrinoni A, Catani MV, Oren M, Melino G, Krammer PH, Stremmel W and Müller M (2005) TAp63alpha induces apoptosis by activating signaling via death receptors and mitochondr**ia**. EMBO J 24 (13):2458-71

Int. J. Cancer: **120,** 1215–1222 (2007)

Selective inhibition of PED protein expression sensitizes B-cell chronic lymphocytic leukaemia cells to TRAIL-induced apoptosis

Michela Garofalo[1], Giulia Romano[1], Cristina Quintavalle[1], Maria Fiammetta Romano[2], Federico Chiurazzi[3], Ciro Zanca[1] and Gerolama Condorelli[1]*

[1]*Department of Cellular and Molecular Biology and Pathology, University of Naples "Federico II," Naples, Italy*
[2]*Dipartimento di Biochimica e Biotecnologie Mediche, Facoltà di Medicina e Chirurgia, Università degli Studi di Napoli "Federico II," Naples, Italy*
[3]*Divisione di Ematologia, Facoltà di Medicina e Chirurgia, Università degli Studi di Napoli, "Federico II," Naples, Italy*

B-cell chronic lymphocytic leukaemia (B-CLL) cells fail to undergo apoptosis. The mechanism underlying this resistance to cell death is still largely unknown. Tumour necrosis factor-related apoptosis-inducing ligand (TRAIL) effectively kills tumour cells but not normal cells, and thus represents an attractive tool for the treatment of cancer. Unfortunately, lymphocytes from B-CLL patients are resistant to TRAIL-mediated apoptosis. Thus, we aimed to study the involvement of PED, a DED-family member with a broad antiapoptotic action, in this resistance. We demonstrate that B lymphocytes obtained from patients with B-CLL express high levels of PED. Treatment of B-CLL cells with specific PED antisense oligonucleotides, a protein synthesis inhibitor or HDAC inhibitors, induced a significant downregulation of PED and sensitized these cells to TRAIL-induced cell death. These findings suggest a direct involvement of PED in resistance to TRAIL-induced apoptosis in B-CLL. It also identifies this DED-family member as a potential therapeutic target for this form of leukaemia.

Key words: apoptosis; death receptors; leukaemia; TRAIL; cancer

B-cell chronic lymphocytic leukaemia (B-CLL) is the most frequent form of leukaemia in Western countries.[1] It is characterized by clonal proliferation and accumulation of long-lived B lymphocytes blocked in the G_0/G_1 phase of the cell cycle in blood, bone marrow, lymph nodes and spleen.[2,3] The accumulation of B lymphocytes in B-CLL is probably consequent to an undefined defect in the apoptotic machinery rather than to an increase in proliferation of leukaemic cells.[4]

Apoptosis is a finely regulated process that involves several molecules and adaptors. The tumour necrosis factor-related apoptosis-inducing ligand (TRAIL) is a member of the tumour necrosis factor family that induces apoptosis by binding to 2 membrane-bound receptors, TRAIL-R1 (DR4) and TRAIL-R2 (DR5).[5] The binding of TRAIL to these receptors results in the recruitment of the adaptor molecule FADD and caspase 8 to the death-inducing signalling complex (DISC), followed by the activation of caspase 8.[6,7] TRAIL induces apoptotic cell death in several tumour-derived cell types but rarely in normal cells.[5,8] Therefore, TRAIL is considered a promising tool for novel therapies. The receptors for TRAIL are constitutively expressed in several tumours, including B-CLL[9,10]; however, in B-CLL, its use is limited due to the frequent resistance of the lymphocytes of these patients to TRAIL-induced cell death.[11]

One of the causes of cell-death resistance could reside in altered expression of apoptosis inhibitory molecules belonging to the DED-containing protein family, such as c-FLIP and PED (also known as PED/PEA-15),[12] which includes procaspase 8, procaspase 10 and FADD.[13] c-FLIP and PED are recruited to the DISC and inhibit the activation of caspase 8. The expression of both proteins is increased in several human malignancies.[13] However, in B-CLL, the expression of c-FLIP is not related to TRAIL resistance[11,14] suggesting that other molecules have a role. We have recently demonstrated that PED is overexpressed in human breast cancer and that its overexpression contributes to resistance to chemotherapeutic drugs.[14] Furthermore, the expression of PED correlates with TRAIL resistance in a human glioma-derived cell line.[15]

In this study, we aimed to investigate the expression of PED in B-CLL and its role in the failure of these tumour cells to undergo TRAIL-induced cell death. We demonstrate that PED protein is upregulated in the lymphocytes from B-CLL patients with respect to those from healthy individuals. Furthermore, PED expression is sensitive to histone deacetylase inhibitors (HDACIs), and specific downregulation of PED expression with antisense oligodeoxynucletides increases sensitivity to TRAIL-induced cell death.

Material and methods

Patient information

We obtained peripheral blood from 40 patients diagnosed with B-CLL as confirmed by clinical, pathological, and flow cytometry criteria.[16] Patient characteristics are reported in Table I. Disease staging is described using the Binet staging system (evaluating enlargement of lymph nodes, the presence of anaemia and/or thrombocytopenia) and the RAI staging system (evaluating the presence of lymphocytosis alone or in combination with lymphadenopathy, spleen or liver enlargement and the presence of anaemia and thrombocytopenia). All the patients analyzed in this study were not on any form of medical treatment.

Isolation of peripheral blood lymphocytes

Peripheral blood lymphocytes were isolated by density gradient centrifugation over Ficoll-Hypaque, as previously reported.[17] Peripheral blood samples were collected in heparin-coated tubes from healthy human blood donors and patients with B-CLL after obtaining informed consent in accordance with the Declaration of Helsinki. PBMCs were isolated by gradient centrifugation with lymphocyte-cell separation medium (Cedarlane Laboratories, Hornby, ON, Canada). T lymphocytes, NK lymphocytes, granulocytes, and monocytes were negatively depleted with immunomagnetic microbeads (MACS microbeads; Miltenyi Biotech, Auburn, CA). The final samples had a purity of more than 90% $CD19^+$ B lymphocytes, as assessed by flow cytometry using specific FITC- or PE-conjugated monoclonal antibodies (MoAbs; Becton Dickinson, San Jose, CA).

Materials, culture conditions and reagents

Cells were grown in a 5% CO_2 atmosphere in RPMI 1640 containing 10% heat-inactivated foetal bovine serum (FBS), 2 mM L-glutamine and 100 U/ml penicillin–streptomycin. Media, sera and

The first two authors contributed equally to this paper.

Grant sponsor: Associazione Italiana Ricerca sul Cancro and the Italian Health Ministry to G.C.; Grant sponsor: MIUR-FIRB; Grant number: RBIN04J4J7; Grant sponsor: MIUR PRINN 04; Grant number: 2004060785_002; Grant sponsor: EU grant EMIL (European Molecular Imaging Laboratories Network); Grant number: Contract No. 503569.

***Correspondence to:** Department of Cellular and Molecular Biology and Pathology, University of Naples "Federico, II", Via Pansini, 5-80131-Naples, Italy. Fax: +39-081-7701016. E-mail: gecondor@unina.it

Received 21 December 2005; Accepted after revision 27 October 2006
DOI 10.1002/ijc.22495
Published online 27 December 2006 in Wiley InterScience (www.interscience.wiley.com).

TABLE I – CLINICAL FEATURES OF PATIENTS

Case number	Sex	WBC (10^6)	Binet	RAI
1	M	28.100	C	IV
2	F	53.200	A	I
3	F	55.500	C	IV
4	F	82.730	B	II
5	F	53.100	C	IV
6	F	33.400	A	I
7	M	72.000	A	I
8	F	35.000	B	I
9	M	42.800	A	I
10	M	85.350	C	IV
11	M	33.500	C	IV
12	M	12.800	A	I
13	M	20.700	B	II
14	F	5.800	A	II
15	F	27.200	A	II
16	F	48.300	B	II
17	M	14.300	A	I
18	M	58.500	C	IV
19	M	82.200	A	II
20	F	43.500	A	I
21	F	22.800	B	II
22	M	9.800	A	I
23	M	13.400	A	I
24	M	12.700	A	I
25	M	31.900	B	II
26	M	26.200	B	II
27	F	19.000	A	II
28	M	9.100	C	IV
29	F	6.000	A	I
30	M	47.700	B	II
31	F	58.260	A	I
32	F	32.410	A	I
33	M	48.430	C	IV
34	F	3.889	A	I
35	M	50.530	A	I
36	F	9.380	C	IV
37	F	68.160	B	II
38	F	25.200	A	I
39	M	68.160	B	II
40	F	25.200	A	I

antibiotics for cell culture were from Life Technologies, (Grand Island, NY). Protein electrophoresis reagents were from Bio-Rad (Richmond, VA) and Western blotting and ECL reagents from Amersham (Aringhton Heights, IL). All other chemicals were from Sigma (St. Louis, MO).

RNA extraction and cDNA amplification

RNA was extracted from samples with Trizol (Invitrogen, Carlsbad, CA) following the manufacturer's protocol, and converted to cDNA using Transcriptor Reverse Transcriptase (Roche Diagnostic, Indianapolis, IN) with random primers (Roche Diagnostic). To detect PED mRNA, 5 μl of the resultant cDNA was added to 50 μl of PCR mixture containing 1× PCR buffer, 2.5 U of Taq DNA polymerase, 1.5 mM $MgCl_2$, 200 μM dNTPs and 20 pmol of each specific primer. The following specific primers were used: PED: (R:5′ GATGTTGTTGGTCAGGTCTTGC-3′; F:5′-GAGCGCTCAGCTCCAGAGG-3′; GAPDH: 5′-TGCCGTCTAGAAAAACCTGC-3′ and 5′-ACCCTGTTGCTGTAGCCAAA-3′ (Primm Srl, Milan, Italy). The PCR cycling conditions were as follows: 1 cycle at 94°C for 2 min and then 25 cycles at 94°C for 40 sec, 60°C for 30 sec and 72°C for 30 sec and a final extension for 7 min at 72°C.

PED antisense oligodeoxynucleotide synthesis and transfection

PED-antisense phosphorothioate oligodeoxynucleotides (ODNs) were obtained from Primm. The sequences of the different ODNs were: A1 (bp 31–50): GCTCAGGGCGCGGGCACTCC; A2 (bp 55–74): GCCATGACGCCTCTGGAGCT; A3 (bp 51–70): TGACGCCTCTGGAGCTGAGC; A4 (bp271–290): TCAGGACGGCGGGAGATCTC; A5 (bp1661–16080): CCCCTCCCACCCCCGCTCTG; A6 (bp 1841–1860): CCAGCAGCCAGCCCTCCCCT. The scrambled control ODN was GGTCCTCCAGCGAGGATTCG. The ODNs were transfected in HeLa cells using the lipofectamine method according to the manufacturer's instructions. For this study, 80% confluent cells grown on p60 dishes were washed and cultured with DMEM without serum or antibiotics, and incubated for 24 hr with the indicated concentrations of ODN plus 15 μl of lipofectamine. Five hours later, an equal volume of DMEM supplemented with 20% FBS was added. The medium was then replaced with DMEM with 10% FBS and cells incubated for an additional 24 hr before being assayed.

Protein isolation and Western blotting

The A3 PED-antisense, scrambled control phosphorothioate ODN (5 μM) or 10 μM cycloheximide (CHX) was added to B-CLL cell cultures for different times (2 days for CHX, 2 and 5 days for ODNs) and PED expression analyzed by Western blot. Briefly, cell pellets were washed twice with cold PBS and resuspended in harvest buffer (30 mM Tris-HCl, pH 7.5, 150 mM NaCl, 10% glycerol, and 0.1% Triton X-100) containing Proteinase Inhibitor Cocktail (Roche Diagnostic). Solubilized proteins were incubated for 30 min on ice. After centrifugation at 10,000*g* for 30 min at 4°C, supernatants were collected. Fifty micrograms of sample extracts were resolved on 12% SDS-polyacrylamide gels using a mini-gel apparatus (Bio-Rad) and transferred to Hybond-C extra nitrocellulose (Amersham Pharmacia Biotech, Piscataway, NJ). Membranes were blocked for 1 hr with 5% nonfat dry milk in TBS containing 0.05% Tween-20 and incubated for 2 hr with the specified antibodies. The following antibodies were used: anti-PED serum as previously described,[18] anti-β-actin (Sigma), anti-c-FLIP (Alexis), anti-bcl2 (sc-509) and anti-Bak (sc-832) were from Santa Cruz, anticytochrome *c* and anti-Bax were from BD Pharmingen, anti-TRAIL receptors antibodies from ProSci (Poway, CA).

Washed membranes were then incubated for 45 min with HRP-conjugated anti-rabbit or anti-mouse secondary antibodies (Amersham Pharmacia Biotech) and visualized using chemiluminescence detection (Amersham Pharmacia Biotech). To measure cytochrome *c* released from the mitochondria into the cytosol, cells were lysed with ice-cold lysis buffer (25 mM Tris-HCl and 5 mM $MgCl_2$ pH 7.4). Supernatant was collected and analyzed by Western blot with an antibody against cytochrome *c*. β-Actin was used as a loading control.

Cell death quantification and flow cytometry

Apoptosis was analyzed *via* propidium iodide incorporation in permeabilized cells by flow cytometry. The cells (5×10^5) were washed in PBS and resuspended in 500 μl of a solution containing 0.1% sodium citrate, 0.1% Triton X-100 and 50 μg/ml propidium iodide (Sigma). Following incubation at 4°C for 30 min in the dark, nuclei were analyzed with a Becton Dickinson FACScan flow cytometer. Cellular debris was excluded from analyses by raising the forward scatter threshold, and the DNA content of the nuclei was registered on a logarithmic scale. The percentage of elements in the hypodiploid region was calculated. Alternatively, we measured cell viability with the CellTiter 96® AQueous One Solution Cell Proliferation Assay (Promega, Madison, WI), according to the manufacturer's protocol. Cells were plated in 96-well plates in triplicates, stimulated and incubated at 37°C in a 5% CO_2 incubator. Metabolically active cells were detected by adding 20 μl of MTS to each well. After 2 hr of incubation, the plates were analyzed on a Multilabel Counter (Bio-Rad).

Flow cytometry for surface receptors

To measure cell surface expression of TRAIL receptors, cells were collected and washed twice in PBS. One million cells were incubated with PE-conjugated purified monoclonal antibodies against TRAIL receptors (R&D system) or with mouse isotype control phycoerythrin-conjugated IgG_{2b}, on ice for 1 hr. After

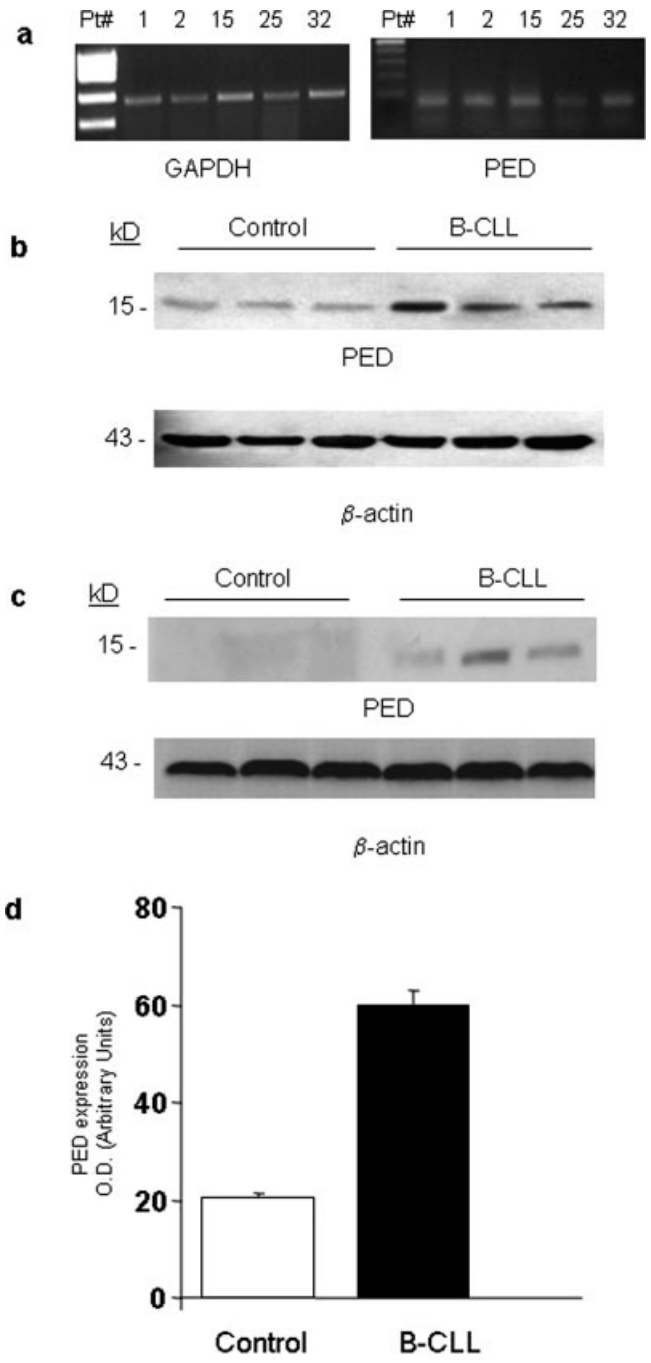

Figure 1 – PED expression in human lymphocytes. (*a*) RNA was extracted from primary lymphocytes and was subjected to RT-PCR analysis with PED-specific primers. GAPDH was used as the control. A representative experiment is shown. In this experiment we loaded samples from patients 1, 2, 15, 25 and 32. (*b* and *c*) PED expression was analyzed by Western blotting in total lymphocytes (*b*) or in purified $CD19^+$ B cells (*c*) from different patients and controls. Loading was assessed on the same membrane with an anti-β-actin antibody. A representative experiment is shown. (*d*) Densitometric analysis of PED expression levels in lymphocytes from 20 patients and 8 unaffected individuals. We represent average PED expression level after normalization to β-actin.

incubation, cells were washed once with 3 ml PBS, centrifuged, resuspended in 1 ml of PBS and the relative level of surface antigens assessed by FACS analysis (FACSsort; Becton Dickinson).

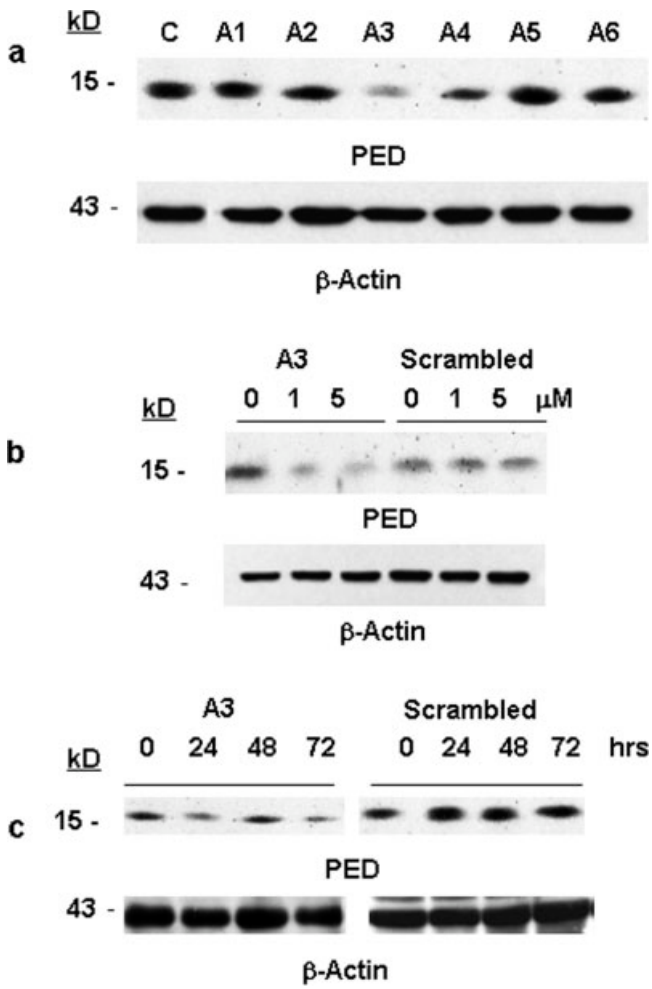

Figure 2 – Effects of antisense oligodeoxynucleotides on PED expression. (*a*) HeLa cells were transfected with different PED antisense ODNs (A1–A6), as described in the Material and Methods section. The level of PED was analyzed by Western blotting. ODN A3 and A4 induced ~80% and 40% reductions in PED levels, respectively. (*b*) HeLa cells were transfected with PED antisense ODN A3 or with control scrambled ODN at different concentrations. Twenty-four hours after transfection, cells were harvested and PED expression analyzed by Western blotting. A representative experiment is shown. (*c*) HeLa cells were transfected with PED antisense ODN A3 or with control scrambled ODN for different lengths of time after which cells were harvested and PED expression analyzed by Western blotting. Loading was assessed on the same membrane with an anti-β-actin antibody.

Effects of HDAC inhibitors

The HDAC inhibitors, valproic acid (VPA, 1 mM) or tricostatin A (TSA, 100 ng/ml), were added to B-CLL cell cultures for 12 hr and protein expression analyzed by Western blotting as described. The effects of these compounds on cell viability were assayed with the CellTiter 96 AQueous One Solution Cell Proliferation Assay.

Statistical analysis

Unpaired Student's *t*-test was performed to determine differences between mean values for continuous variables. Probability values <0.05 were considered significant. Data were analysed with SPSS for Windows, release 10.0 (SPSS, Chicago, IL).

Results

PED mRNA and protein expression in B-CLL cells

We assessed PED expression in primary lymphocytes obtained from B-CLL patients (clinical profiles shown in Table I) and

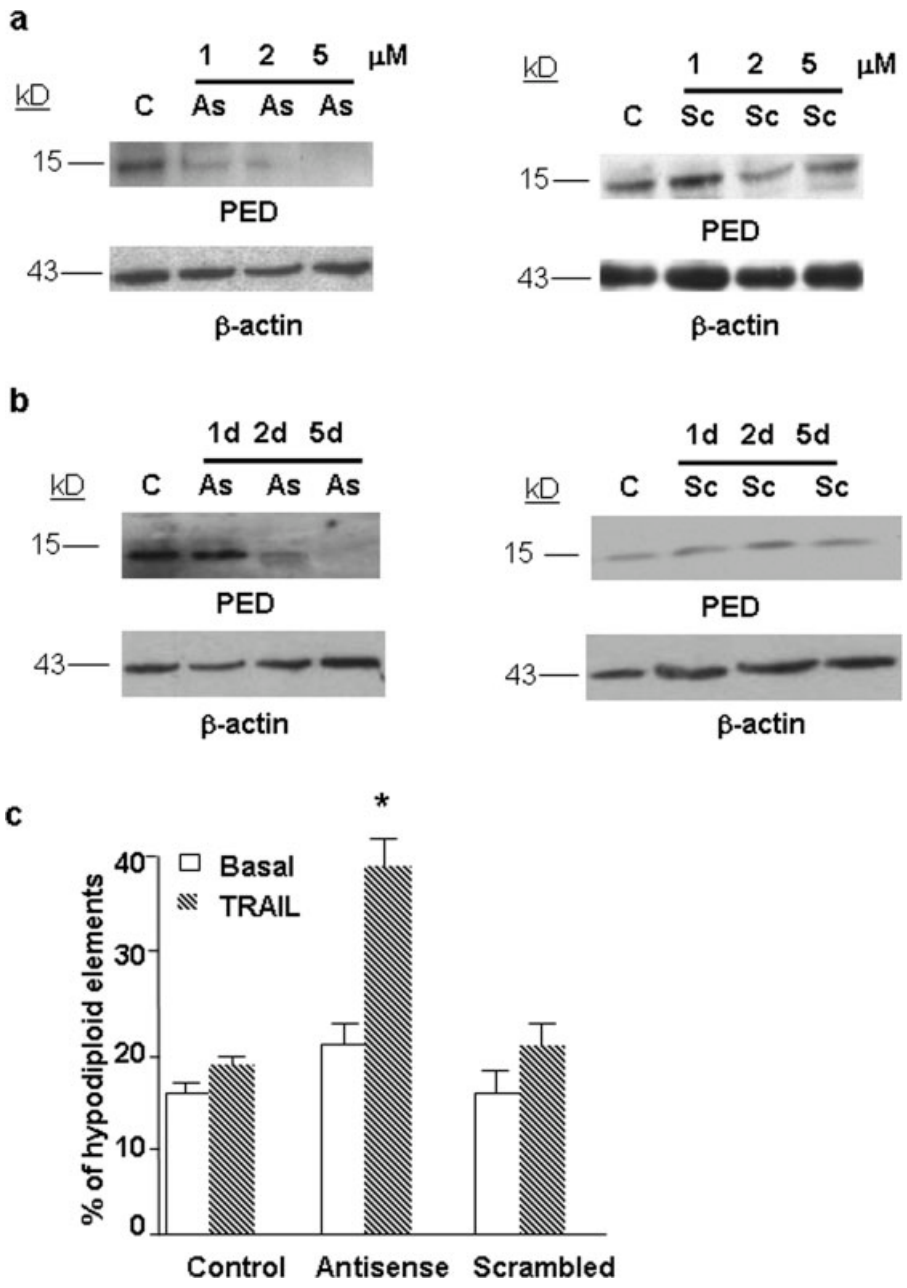

FIGURE 3 – Downregulation of PED in B lymphocytes obtained from B-CLL patients increases sensitivity to TRAIL-induced cell death. (*a*) B-CLL cells were incubated for 48 hr with 1, 2 or 5 μM antisense ODN (As) or with scrambled ODN (Sc) or (*b*) 1, 2 or 5 days with 5 μM antisense ODN (As) or with scrambled ODN (Sc). The cells were then harvested and PED expression analyzed by Western blotting. Loading was assessed on the same blot with an anti-β-actin antibody. Western blot analysis shows that the antisense ODN induced PED down regulation (left panels) whereas scrambled ODN produced no effects (right panels). We performed similar experiments with lymphocytes from 4 patients and show only representative data from one. (*c*) Percentage of hypodiploid nuclei assessed by FACS analysis in nontransfected B-CLL cells (control) and in cells treated with PED antisense or scrambled ODN for 24 hr in the absence (basal) or presence (TRAIL) of 200 ng TRAIL/ml for an additional 24 hr. The data were obtained from 4 independent experiments using cells from different patients. $^*p < 0.05$.

healthy individuals. PED mRNA was detected in lymphocytes of patients with B-CLL (Fig. 1*a*). Furthermore, PED protein expression was greater in lymphocytes from B-CLL patients than in those from healthy individuals: this was true when analyzing total peripheral lymphocytes (Figs. 1*b* and 1*d*) or purified $CD19^+$ B lymphocytes (Fig. 1*c*).

Effects of PED downregulation on TRAIL sensitivity

Primary cultures of lymphocytes from B-CLL patients are resistant to TRAIL-induced cell death.[10] Since in several tumour cell lines PED has an inhibitory action towards death-receptor ligands and chemotherapeutics,[12,14] we addressed whether the upregulation of PED found in B-CLL patients plays a role in the defective TRAIL sensitivity of leukaemic cells.

To this aim, we used an antisense ODN-based approach to downmodulate PED expression. Antisense-ODN has been successfully utilized in B-cell chronic leukaemia.[19–21] First, we evaluated the efficacy of the antisense ODNs designed on 6 different regions of PED in the coding or in the 3′ and 5′ nontranslated regions. HeLa cells are particularly useful for this type of experiment because they express high endogenous levels of PED and are easily transfected. As shown in Figure 2*a*, ODNs named A1, A2, A5 and A6 produced no relevant effects on PED expression. Differently, ODN A3 and A4 induced ~80% and 40% reductions in the level of PED, respectively, while a scrambled negative control for ODN A3 (ODN A3Sc) had no effect (Figs. 2*b* and 2*c*). Dose–response experiments revealed that in HeLa cells, ODN A3 was effective in reducing PED expression at a concentration as low as 1 μM (Fig. 2*b*). On the contrary, ODN A3Sc produced no effect even at a concentration of 5 μM. Time–course experiments revealed that ODN A3 was effective as soon as 24 hr, whereas its control, ODN A3Sc, had no effect even after 72 hr of incubation (Fig. 2*c*).

Next, we tested the effect of PED-ODN on primary B cells from leukaemic patients. Similarly to HeLa cells, in B-CLL derived lymphocytes ODN A3 was effective at concentrations ranging from 2 to 5 μM (Fig. 3*a*), reaching >90% reduction in PED after 48 hr.

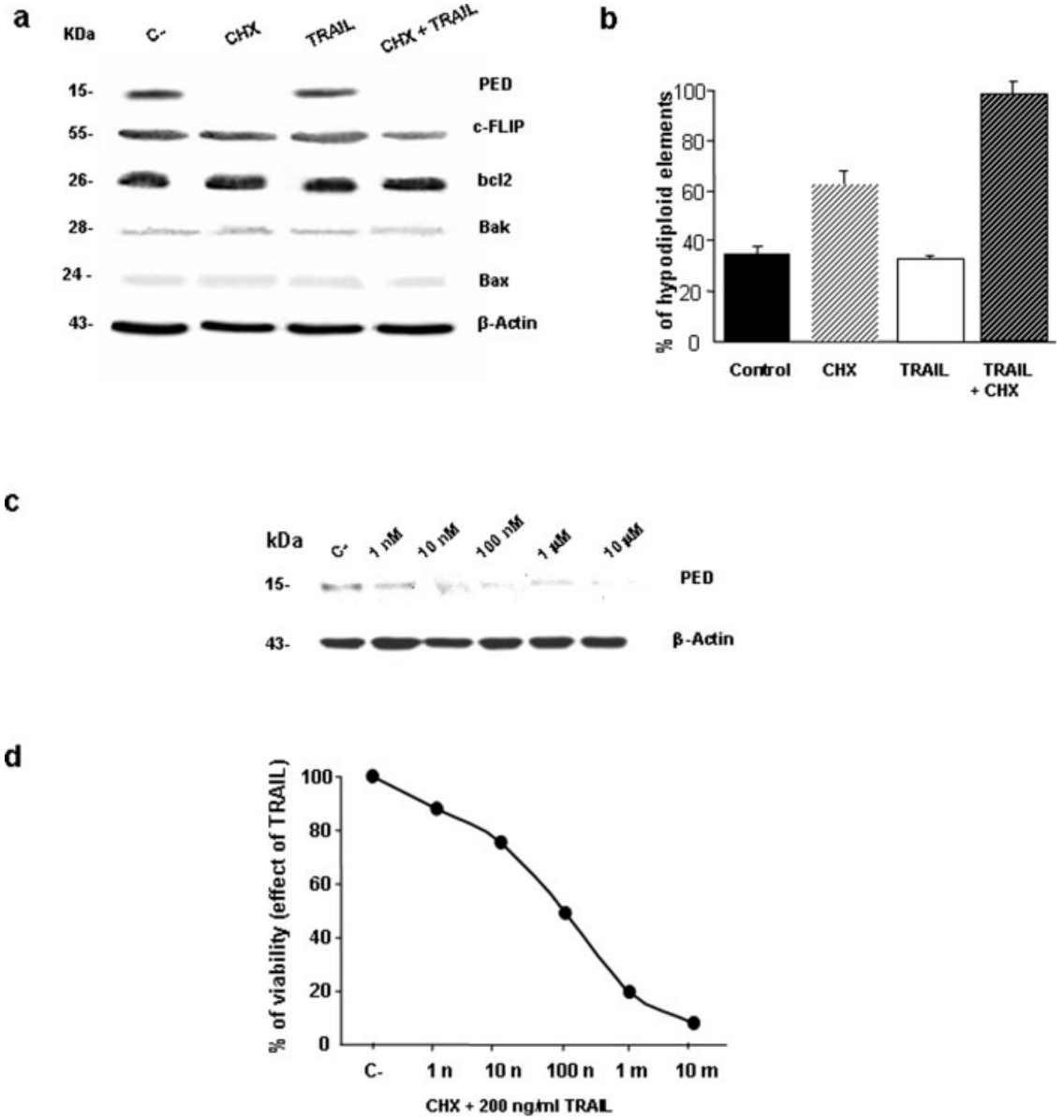

FIGURE 4 – Effects of cycloheximide (CHX) on PED expression and TRAIL sensitivity. (*a*) BCLL cells were incubated with 10 μM CHX in the presence or absence of TRAIL (200 ng/ml) for 24 hr. Western blot analysis of B-CLL cells shows that CHX induced PED downregulation, whereas bcl2, bax, Bak and c-FLIP protein levels were unaffected. Loading was assessed on the same blot with an anti-β-actin antibody. (*b*) Percentage of hypodiploid nuclei assessed by FACS analysis in B-CLL cells with or without treatment with CHX, TRAIL alone or in combination, for 24 hr. Data were obtained from 4 independent experiments using cells from different patients. $*p < 0.05$; (*c*) CHX dose–response of PED expression. B-CLL cells were incubated with different amounts of CHX, as indicated, for 24 hr, and PED then analyzed by Western blot. (*d*) CHX dose–response of TRAIL-induced cell death. B-CLL cells were incubated with different amounts of CHX, as indicated, for 24 hr. TRAIL (200 ng/ml) was added for 16 hr, and cell viability assessed with the CellTiter Proliferation Assay. There is a direct correlation between the quantity of CHX and sensitivity to TRAIL.

ODN A3Sc had no effect even after 5 days of continuous incubation at 5 μM (Fig. 3*b*). The viability of the cells, as assessed with the CellTiter Proliferation Assay, did not change after incubation with ODNs (data not shown).

We then determined the involvement of PED in the TRAIL-resistant phenotype of lymphocytes from B-CLL patients. B-CLL cells were transfected with ODN, and apoptosis evaluated with flow cytometry by measuring hypodiploidy. As shown in Figure 3*c*, in the absence of TRAIL, B-CLL cells displayed a basal level of 16% hypodiploid elements. A similar percentage was measured in cells transfected with ODN A3Sc. Incubation of nontransfected or ODN A3Sc-transfected B-CLL cells with TRAIL did not produce an increment in the percentage of hypodiploid nuclei, reflecting the described low sensitivity of these cells to TRAIL. However, treatment with PED-specific antisense ODN A3 increased the percentage of hypodiploid nuclei to 22% in the absence of TRAIL, indicating that PED down-modulation had determined a slight increase of basal apoptosis. Moreover, ODN A3 sensitized these cells sufficiently to make them responsive to TRAIL-induced cell death, as demonstrated by the increase in hypodiploidy.

Downregulation of PED expression with CHX

CHX has been reported to enhance and restore sensitivity to death receptor-induced apoptosis, presumably by reducing the expression

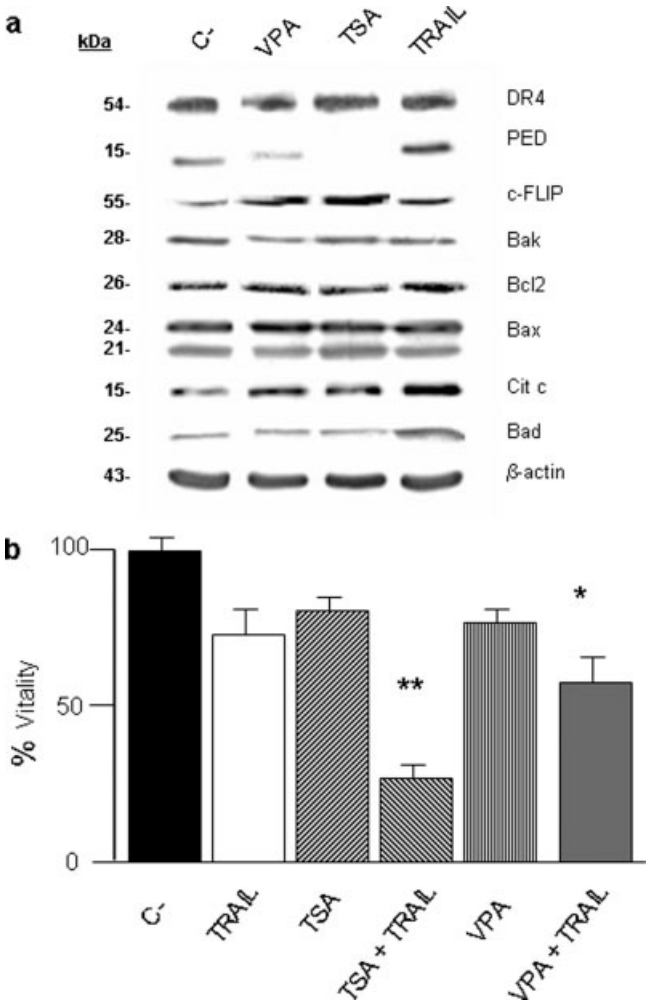

FIGURE 5 – Effects of HDACIs on PED expression and TRAIL sensitivity. (*a*) B-CLL cells were preincubated for 24 hr with HDACIs, either 1 mM valproic acid (VPA) or 100 ng/ml tricostatin A (TSA) as indicated, and then with 200 ng/ml TRAIL for an additional 16 hr. Western blot analysis shows that TSA and VPA induced PED downregulation whereas TRAIL did not. c-FLIP, bcl2, Bax, Bak, TRAIL receptors (DR4) protein levels were unaffected by HDAC inhibitors. Cytochrome *c* release, evaluated as described in the Material and Methods section, did not change after HDACI treatment. Loading was assessed with β-actin. (*b*) Viability after treatment with TRAIL. B-CLL cells were preincubated for 24 hr with 1 mM VPA or 100 ng/ml TSA, and then with 200 ng/ml TRAIL for an additional 16 hr. Metabolically active cells were detected by the addition of 20 µl MTS to each well. After 5 hr of incubation, the plates were analyzed with the CellTiter 96® AQueous One Solution Cell Proliferation Assay. Data were obtained from 4 independent experiments using cells from different patients and expressed as % viable cells. $*p < 0.05$; $**p < 0.001$.

of antiapoptotic proteins.[22] We thus evaluated the effects of CHX on the expression of different apoptosis signalling molecules in B-CLL cells (Fig. 4*a*). PED levels were found clearly reduced after treatment with CHX, while the expression of several Bcl-2 family members (bcl2, Bak, Bax) and c-FLIP were unaffected. PED expression was not restored by concomitant treatment with TRAIL, indicating that TRAIL-induced pathways are not involved in the regulation of PED protein level. These data are in accordance with results obtained in human glioma cells where we found that PED, but not c-FLIP, was reduced in the presence of CHX.[15] Therefore, this inhibiting action on PED expression may be critical for CHX-induced sensitization of tumour cells. We next investigated the effects of CHX on the sensitivity to TRAIL in primary B-CLL cell cultures. As shown in Fig. 4*b*, TRAIL-induced cell death was significantly enhanced in the presence of CHX, reaching 98% hypodiploid nuclei compared with 36% in the absence of CHX. To strengthen this observation, we evaluated the dose–response effect of CHX on PED expression and sensitivity to TRAIL. We found that the level of PED was correlated to CHX dose (Fig. 4*c*), and coherently, that sensitivity to TRAIL increased with increasing quantities of CHX (Fig. 4*d*).

Effects of HDAC inhibitors on PED expression and TRAIL sensitivity

Recently, several inhibitors of histone deacetylase have entered clinical trials.[23,24] HDACIs exert their antitumour effects through the ability to induce growth arrest, differentiation and apoptosis. Recent reports demonstrate that HDACIs sensitize resistant cells of patients with B-CLL to TRAIL-induced apoptosis by facilitating increased formation of the TRAIL DISC.[25] We therefore tested the effects of VPA and TSA on PED expression and TRAIL sensitivity in primary B-CLL lymphocytes. PED expression was clearly reduced in lymphocytes from B-CLL patients after incubation with HDACIs (Fig. 5*a*). The effects of HDACI on cell death were not related to c-FLIP, to different components of the mitochondrial pathway, or to alteration of surface TRAIL DR4 or DR5 receptors, analyzed either by Western blot or by FACS, since their expression was not affected by these drugs (Figs. 5*a* and 6). Pretreatment with either HDACI determined an increase in TRAIL-induced cell death (Fig. 5*b*). Interestingly, TSA induced complete silencing of PED, and the addition of TRAIL in this setting had a stronger apoptotic effect than with VPA, thus further supporting the correlation between PED levels and resistance to TRAIL.

Discussion

B-CLL is presently an incurable malignancy due to accumulation of monoclonal B cells that develop resistance to conventional anticancer agents. Thus, identification and evaluation of novel agents for the treatment of refractory B-CLL are important and challenging tasks. TRAIL is an attractive therapeutic tool for B-CLL and other malignancies because it induces cell death in several tumour-derived cell types but rarely in normal cells. However, many reports have demonstrated the resistance of malignant B cells to death receptor-induced apoptosis. This study was designed to investigate the molecular determinants responsible for the prolonged survival and accumulation of leukaemic cells in patients with B-CLL. To this end, we analyzed the role of the DED-containing protein PED, in TRAIL resistance in B-CLL. PED is a molecule that plays a crucial role in regulating apoptosis signals in different cell types. We addressed the question of whether PED expression may contribute to cell death resistance. For this purpose, we used the antisense ODN approach. Antisense ODNs targeted to specific genes have shown considerable potential as therapeutic agents. Antisense therapy uses single-stranded synthetic ODNs that are either unmodified or have been chemically modified to regulate gene expression at the translational step. The specificity of target gene binding and consequent inhibition of individual gene products make antisense compounds an attractive new class of drugs for clinical applications.[26] Moreover, chemical modification of the phosphorothioate backbone increases resistance to nuclease digestion and prolongs half-lives within tissues.

Antisense therapy has been proved to be particularly useful in chronic leukaemia. Previous studies have described that the combination of Bcl-2 antisense ODNs with conventional chemotherapeutic drugs elicit an enhanced therapeutic effect in B-CLL.[27] In the present study, we have identified a specific ODN sequence that inhibits PED expression in HeLa cells and in B lymphocytes. Furthermore, we describe that in primary cultures of lymphocytes from leukaemia, specific inhibition of PED with ODN augments both spontaneous and TRAIL-induced cell death. The levels of

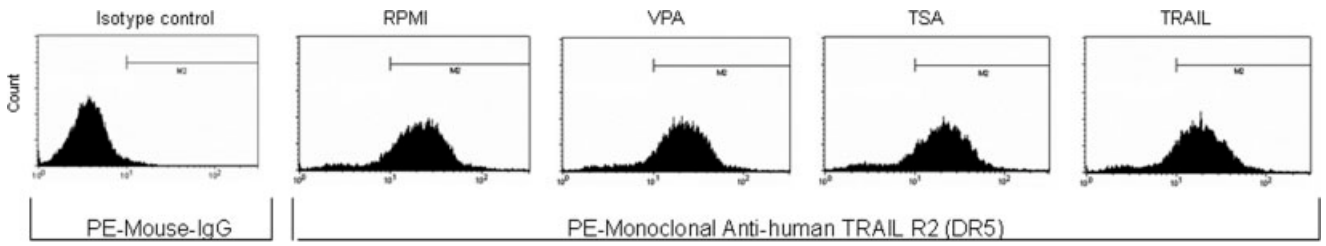

FIGURE 6 – Flow cytometry analysis of TRAIL receptor expression on $CD19^+$ B cells. Receptor expression was detected by single-colour flow cytometry performed on freshly isolated B-CLL cells, treated as described in Figure 5. Cells (1×10^6) were stained with monoclonal antibody phycoerythrin-conjugated anti-human TRAIL-R2 (DR5), TRAIL-R1 (DR4), TRAIL-R3 (dcy1) or TRAIL-R4 (dcy2), or with phycoerythrin-conjugated mouse IgG_{2b} isotype control. Surface expression of DR5 TRAIL receptors was unaffected by HDAC inhibitors. Same results were obtained with DR-4 (data not shown). No detectable expression of TRAIL-R3 or TRAIL-R4 was observed, in agreement with other studies.[9,10]

PED correlate with TRAIL resistance also in other malignancies such as human glioma[15] and nonsmall cell lung cancer (NSCLC) (Condorelli *et al*., submitted). In NSCLC, the involvement of PED in the refractoriness to TRAIL-induced cell death was investigated by silencing PED expression in TRAIL-resistant and high PED-expressing NSCLC cells, with a PED siRNA. Transfection with PED-siRNA induced a significant downregulation of PED and sensitized these cells to TRAIL-induced cell death. Thus, PED may represent a target against TRAIL-induced cell death resistance in several forms of malignancies. Further studies are in progress in our lab to investigate the potential use of specific PED ODNs in enhancing the therapeutic effects of different chemotherapeutic drugs in B-CLL.

HDACIs have been used in cancer therapy for their potential to inhibit proliferation and survival of tumour cells. It has been reported that they cause not only cell cycle arrest and differentiation but also apoptosis. Recent reports demonstrate that HDAC inhibitors sensitize resistant primary cells from patients with B-CLL to TRAIL-induced apoptosis by facilitating increased formation of the TRAIL DISC.[25] Here, we describe that the treatment with 2 different HDACIs, VPA and TSA, induced a reduction in PED levels and a concomitant increase of cell death. Interestingly, both HDACIs used in our experimental system did not induce a reduction of c-FLIP levels. Previous reports have shown that HDACIs induce downregulation of c-FLIP in some cell types,[28] but the effects of HDACIs on c-FLIP downregulation in chronic leukaemia is controversial. In agreement with our data, other authors[29,30] did not find any change in c-FLIP expression upon treatment with VPA, SAHA, sodium butyrate or depsipeptide. Thus, data from these authors do not support a role for c-FLIP in the sensitization of B-CLL lymphocytes to cell death. Aron *et al*.[31] reported that depsipeptide was able to induce a reduction of c-FLIP levels in B-CLL, although not in all patients. Further studies are needed to understand these discrepancies. However, in our work, we demonstrate that CHX increased sensitivity to TRAIL through the downregulation of PED and not c-FLIP. These data further support a prominent role for PED rather than c-FLIP in the insensitivity of B-CLL to TRAIL. Furthermore, our results revealed that cytochrome *c* release was not increased upon HDACI treatment and that the amount of different bcl2 family members was not affected.

Taken together these results indicate that PED exerts an antiapoptotic effect in B-CLL cells, probably by interfering with TRAIL-DISC signalling. Indeed, PED downregulation restores sensitivity to TRAIL in B-CLL. Thus, modulation of PED levels could represent an important tool for improving TRAIL sensitivity in different types of transformed cells.

Acknowledgements

We wish to thank Dr. Vittorio de Franciscis for suggestions and constructive criticism, Mr. Michael Latronico for paper revision, Mr. Paolo Bruni for technical assistance with $CD19^+$ isolation and Prof. Silvestro Formisano for continuous support.

References

1. Rozman C, Montserrat E. Chronic lymphocytic leukemia. N Engl J Med 1995;333:1052–7.
2. Cheson BD, Bennett JM, Grever M, Kay N, Keating MJ, O'Brien S, Rai RK. National Cancer Institute-sponsored Working Group guidelines for chronic lymphocytic leukemia: revised guidelines for diagnosis and treatment. Blood 1996;87:4990–7.
3. Hamblin TJ, Oscier DG. Chronic lymphocytic leukaemia: the nature of the leukaemic cell. Blood Rev 1997;11:119–28.
4. Caligaris-Cappio F, Ferrarini M. B cells and their fate in health and disease. Immunol Today 1996;17:206–8.
5. Walczak H, Miller RE, Ariail K, Gliniak B, Griffith TS, Kubin M, Chin W, Jones J, Woodward A, Le T, Smith C, Smolak P, et al. Tumoricidal activity of tumor necrosis factor-related apoptosis-inducing ligand in vivo. Nat Med 1999;5:157–63.
6. Griffith TS, Lynch DH. TRAIL: a molecule with multiple receptor and control mechanisms. Curr Opin Immunol 1998;10:559–63.
7. Sprick MR, Weigand MA, Rieser E, Rauch CT, Juo P, Blenis J, Krammer PH. FADD/MORT1 and caspase-8 are recruited to TRAIL receptors 1 and 2 and are essential for apoptosis mediated by TRAIL receptor 2. Immunity 2000;12:599–609.
8. Kang J, Kisenge RR, Toyoda H, Tanaka S, Bu J, Azuma E, Komaday Y. Chemical sensitization and regulation of TRAIL-induced apoptosis in a panel of B-lymphocytic leukaemia cell lines. Br J Haematol 2003;123:921–32.
9. Secchiero P, Tiribelli M, Barbarotto E, Celeghini C, Michelutti A, Masolini P, Fanin R, Zauli G. Aberrant expression of TRAIL in B chronic lymphocytic leukemia (B-CLL) cells. J Cell Physiol 2005;205:246–52.
10. MacFarlane M, Harper N, Snowden RT, Dyer MJ, Barnett JA, Pringle GA, Cohen GM. Mechanism of resistance to TRAIL-induced apoptosis in primary B-cell chronic lymphocytic leukemia. Oncogene 2002;21:6809–18.
11. MacFarlane M, Inoue S, Kohlhaas SL, Majid A, Harper N, Kennedy DB, Dyer MJ, Cohen GM. Chronic lymphocytic leukemic cells in exhibit apoptotic signaling via TRAIL-R1. Cell Death Differ 2005;12:773–82.
12. Condorelli G, Vigliotta G, Cafieri A, Trencia A, Andalò P, Oriente F, Miele C, Caruso M, Formisano P, Beguinot F. PED/PEA-15: an anti-apoptotic molecule that regulates FAS/TNFR1-induced apoptosis. Oncogene 1999;18:4409–15.
13. Xiao C, Yang BF, Asadi N, Beguinot F, Hao C. Tumor necrosis factor-related apoptosis-inducing ligand-induced death-inducing signaling complex and its modulation by c-FLIP and PED/PEA-15 in glioma cells. J Biol Chem 2002;277:25020–5.
14. Stassi G, Garofalo M, Zerilli M, Ricci-Vitiani L, Zanca C, Todaro M, Aragona F, Limite G, Petrella G, Condorelli G. PED mediates AKT-dependent chemoresistance in human breast cancer cells. Cancer Res 2005;65:6668–75.
15. Hao C, Beguinot F, Condorelli G, Trencia A, Van Meir EG, Yong VW, Parney IF, Roa WH, Petruk KC. Induction and intracellular regulation of tumor necrosis factor related apoptosis-inducing ligand (TRAIL) mediated apotosis in human malignant glioma cells. Cancer Res 2001;61:1162–70.

16. Contri A, Brunati AM, Trentin L, Cabrelle A, Miorin M, Cesaro L, Pinna LA, Zambello R, Semenzato G, Donella-Deana A. Chronic lymphocytic leukemia B cells contain anomalous Lyn tyrosine kinase, a putative contribution to defective apoptosis. J Clin Invest 2005; 115:369–78.
17. Yang MH, Lin SJ. Effect of two-round ficoll-hypaque density gradient centrifugation on lymphocyte subsets and natural killer activity of umbilical cord blood mononuclear cells. Pediatr Hematol Oncol 2001;18:57–63.
18. Condorelli G, Vigliotta G, Iavarone C, Caruso M, Tocchetti CG, Andreozzi F, Cafieri A, Tecce MF, Formisano P, Beguinot L, Beguinot F. PED/PEA-15 gene controls glucose transport and is overexpressed in type 2 diabetes mellitus. EMBO J 1998;17:3858–66.
19. Konopleva M, Tari AM, Estrov Z, Harris D, Xie Z, Zhao S, Lopez-Berestein G, Andreff M. Liposomal Bcl-2 antisense oligonucleotides enhance proliferation, sensitize acute myeloid leukemia to cytosine-arabinoside, and induce apoptosis independent of other antiapoptotic proteins. Blood 2000;95:3929–38.
20. Romano MF, Avellino R, Petrella A, Bisogni R, Romano S, Venuta S. Rapamycin inhibits doxorubicin-induced NF-κB/Rel nuclear activity and enhances the apoptosis of melanoma cells. Eur J Cancer 2004; 40:2829–36.
21. Aichberger KJ, Mayerhofer M, Krauth MT, Skvara H, Florian S, Sonneck K, Akgul C, Derdak S, Pickl WF, Wacheck V, Selzer E, Monia BP, et al. Identification of mcl-1 as a BCR/ABL-dependent target in chronic myeloid leukemia (CML): evidence for cooperative antileukemic effects of imatinib and mcl-1 antisense oligonucleotides. Blood 2005;105:3303–11.
22. Enari M, Hase A, Nagata S. Apoptosis by a cytosolic extract from Fas-activated cells. EMBO J 1995;14:5201–8.
23. Johnstone RW, Licht JD. Histone deacetylase inhibitors in cancer therapy: is transcription the primary target? Cancer Cell 2003;4:13–18.
24. Marks PA, Richon VM, Miller T, Kelly WK. Histone deacetylase inhibitors. Adv Cancer Res 2004;91:137–68.
25. Inoue S, MacFarlane M, Harper N, Wheat LM, Dyer MJ, Cohen GM. Histone deacetylase inhibitors potentiate TNF-related apoptosis-inducing ligand (TRAIL)-induced apoptosis in lymphoid malignancies. Cell Death Differ 2004;S193–S206.
26. Qiang Hu, Bally MB, Madden TD. Subcellular trafficking of antisense oligonucleotides and down-regulation of *bcl-2* gene expression in human melanoma cells using a fusogenic liposome delivery system. Nucleic Acids Res 2002;30:3632–41.
27. Pepper C, Thomas A, Hoy T, Cotter F, Bentley P. Antisense-mediated suppression of Bcl-2 highlights hits pivotal role in failed apoptosis in B-cell chronic lymphocytic leukaemia. Br J Haematol 1999;107:661–5.
28. Watanabe K, Okamoto K, Yonehara S. Sensitization of osteosarcoma cells to death receptor-mediated apoptosis by HDAC inhibitors through downregulation of cellular FLIP. Cell Death Differ 2005;12:10–18.
29. Inoue H, Shiraki K, Murata K, Sugimoto K, Kawakita T, Yamaguchi Y, Saitou Y, Enokimura N, Yamamoto N, Yamanaka Y, Nakano T. Adenoviral-mediated transfer of *p53* gene enhances TRAIL-induced apoptosis in human hepatocellular carcinoma cells. Int J Mol Med 2004;14:271–5.
30. Rosato RR, Almenara JA, Dai Y, Grant S. Simultaneous activation of the intrinsic and extrinsic pathways by histone deacetylase (HDAC) inhibitors and tumor necrosis factor-related apoptosis-inducing ligand (TRAIL) synergistically induces mitochondrial damage and apoptosis in human leukemia cells. Mol Cancer Ther 2003;2:1273–84.
31. Aron JL, Parthun MR, Marcucci G, Kitada S, Mone AP, Davis ME, Shen T, Murphy T, Wickham J, Kanakry C, Lucas DM, Reed JC, et al. Depsipeptide (FR901228) induces histone acetylation and inhibition of histone deacetylase in chronic lymphocytic leukemia cells concurrent with activation of caspase 8-mediated apoptosis and down-regulation of c-FLIP protein. Blood 2003;102:652–8.

J. Cell. Mol. Med. Vol 12, No 6A, 2008 pp. 2416-2426

PED is overexpressed and mediates TRAIL resistance in human non-small cell lung cancer

Ciro Zanca [a, #], Michela Garofalo [a, #], Cristina Quintavalle [a], Giulia Romano [a, c], Mario Acunzo [a], Pia Ragno [b], Nunzia Montuori [a], Mariarosaria Incoronato [c], Luigi Tornillo [d], Daniel Baumhoer [d], Carlo Briguori [e], Luigi Terracciano [d], Gerolama Condorelli [a, *]

[a] Department of Cellular and Molecular Biology and Pathology, 'Federico II' University of Naples, Naples, Italy & Istituto di Endocrinologia ed Oncologia Sperimentale, C.N.R., IEOS, Naples, Italy
[b] Dipartimento di Chimica, Università degli Studi di Salerno, Salerno, Italy
[c] Fondazione SDN, Naples, Italy
[d] Institute of Pathology, University of Basel, Basel, Switzerland
[e] Clinica Mediterranea, Naples, Italy

Received: September 3, 2007; Accepted: February 12, 2008

Abstract

PED (phosphoprotein enriched in diabetes) is a death-effector domain (DED) family member with a broad anti-apoptotic action. PED inhibits the assembly of the death-inducing signalling complex (DISC) of death receptors following stimulation. Recently, we reported that the expression of PED is increased in breast cancer cells and determines the refractoriness of these cells to anticancer therapy. In the present study, we focused on the role of PED in non-small cell lung cancer (NSCLC), a tumour frequently characterized by evasion of apoptosis and drug resistance. Immunohistochemical analysis of a tissue microarray, containing 160 lung cancer samples, indicated that PED was strongly expressed in different lung tumour types. Western blotting performed with specimens from NSCLC-affected patients showed that PED was strongly up-regulated (>6 fold) in the areas of tumour compared to adjacent normal tissue. Furthermore, PED expression levels in NSCLC cell lines correlated with their resistance to tumour necrosis factor related apoptosis-inducing ligand (TRAIL)-induced cell death. The involvement of PED in the refractoriness to TRAIL-induced cell death was investigated by silencing PED expression in TRAIL-resistant NSCLC cells with small interfering (si) RNAs: transfection with PED siRNA, but not with cFLIP siRNA, sensitized cells to TRAIL-induced cell death. In conclusion, PED is specifically overexpressed in lung tumour tissue and contributes to TRAIL resistance.

Keywords: lung cancer • apoptosis • AKT

Introduction

Lung cancer is the leading cause of cancer-related mortality in western countries [1]. The late stage at diagnosis in many patients, and the high rate of relapse for those initially diagnosed in earlier stages, contribute to its lethality. Non-small cell lung cancer (NSCLC) is the most common type of lung cancer, accounting for approximately 80% of cases [2]. One of the most important issues that affects survival rate, is resistance to therapeutic drugs. Only 20–30% of treated NSCLC patients have clinical evidence of a response. Therefore, the development of new therapeutic strategies is necessary for the treatment of this type of tumour.

Apo2L/TNF-related apoptosis-inducing ligand (TRAIL) is a relatively new member of the tumour necrosis factor (TNF) ligand family, which induces apoptosis in a variety of cancers. Four cognate receptors have been identified: the death receptors, TRAIL-R1/DR4 and TRAIL-R2/DR5; and the decoy receptors, TRAIL-R3/DcR1 and TRAIL-R4/DcR2 [3]. The decoy receptors have been proposed to competitively inhibit TRAIL-induced apoptosis by acting as non-functional receptors. All four TRAIL receptors are

[#]These authors contributed equally to this work.
*Correspondence to: Prof. Gerolama CONDORELLI,
Dipartimento di Biologia e Patologia Cellulare e Molecolare & Facoltà di Scienze Biotecnologiche,
Università degli Studi di Napoli 'Federico II',
Via Pansini, 5, 80131 Naples, Italy.
Tel.: +39 081 7464416
Fax: +39 081 7701016
E-mail: gecondor@unina.it

doi:10.1111/j.1582-4934.2008.00283.x

highly expressed in a wide variety of normal cells, but the expression of decoy receptors is substantially limited in tumour cells [4, 5].

Treatment with TRAIL induces programmed cell death in a wide range of transformed cells, both *in vitro* and *in vivo*, without producing significant effects in normal cells [6, 7]. This unique property makes TRAIL an attractive candidate for cancer therapy. However, a significant proportion of cancer cell lines is resistant to TRAIL-induced apoptosis [8]. Apoptotic signalling could be opposed by enhanced expression of intracellular molecules acting at multiple levels [9, 10]. Among these molecules is PED (phosphoprotein enriched in diabetes) (known also as PED/PEA-15), a death-effector domain (DED) family member of 15 kD involved in cell growth and metabolism [9, 11, 12]. PED inhibits the formation of a functional death-inducing signalling complex (DISC) and the activation of caspase 8, which take place following treatment with different apoptotic cytokines including CD95/FasL, TNF-α and TRAIL [9, 13–16]. The anti-apoptotic action of PED is accomplished, at least in part, through its DED domain, which acts as a competitive inhibitor for pro-apoptotic molecules during the assembly of the DISC [9, 15]. PED is overexpressed in a number of different tumours, including human glioma [13], squamous carcinoma [17], breast cancer [18] and B-cell lymphocytic leukaemia [19]. We recently reported that human breast cancer cells express high levels of PED and that AKT/PKB activity regulates PED protein levels [18, 19]. Furthermore, high PED expression levels determine resistance of breast cancer cells to chemotherapy-induced cell death.

In this study, we focused on the involvement of PED in determining the 'TRAIL-resistant phenotype' in NSCLC. We analysed PED expression in specimens from 27 NSCLC-affected patients and in a large human tissue microarray containing 160 lung tumour samples. The effect of silencing PED expression in NSCLC cell lines was also investigated.

Methods

Materials

Media, sera and antibiotics for cell culture were from Life Technologies, Inc. (Grand Island, NY, USA). Protein electrophoresis reagents were from Bio-Rad (Richmond, VA, USA), and Western blotting and ECL reagents were from Amersham (Aringhton Heights, IL, USA). All other chemicals were from Sigma (St. Louis, MO, USA) unless otherwise stated. The following primary antibodies were used: anti-PED antibody [11]; anti-β-actin antibody (Ab-1, mouse IgM, Oncogene, Darmstadt, Germany); anti-caspase 8 antibody (1C12, Cell Signaling Technology, Inc., Danvers, MA, USA), anti-caspase 3 antibody (Abcam, Cambridge, USA); anti-caspase 10 antibody (StressGene, Victoria, BC Canada); anti-cFLIP (NF6) antibody (Alexis, Lausen, Switzerland); anti-FADD antibody (BD Transduction Laboratories, San Jose, CA, USA); anti-TRAIL receptor antibodies (R&D Systems, Minneapolis, MN, USA) and anti PARP antibody (SC7150 Santa Cruz Biotechnology, Inc., Santa Cruz, CA, USA).

Cell culture

Human CALU-1 and A459 NSCLC cell lines were grown in DMEM; H460 and A549 cell lines were grown in RPMI. Media were supplemented with 10% heat-inactivated FBS, 2 mM L-glutamine and 100 U/ml penicillin-streptomycin.

Protein isolation and Western blotting

Lung tissue specimens (neoplastic and adjacent normal tissue) were collected during surgical intervention on 27 patients affected with lung tumour, in accordance with the ethical standards of the institutional responsible committee on human experimentation. The clinical and pathological characterization (including tumor, node, metastasis (TNM) staging) of these patients, which were not receiving medical treatment at the time of the operation, is shown in Table 1. The collected samples were homogenized in 1 ml PBS (0.14M NaCl, 2.7 mM KCl, 8 mM Na_2HPO_4, 1.5 mM KH_2PO_4) containing 1% Triton X-100 and proteinase inhibitor cocktail, with a tissue homogenator. Cultured cells were pelleted, washed twice with cold PBS and lysed in the same harvest buffer. Solubilized proteins were incubated for 30 min. on ice, and after centrifugation at $10,000 \times g$ for 30 min. at 4°C, supernatants were collected. Fifty micrograms of sample extract were resolved on 12% SDS-polyacrylamide gels using a mini-gel apparatus and transferred to Hybond-C extra nitrocellulose. Membranes were blocked for 1 hr with 5% non-fat dry milk in Tris Buffered Saline (TBS) containing 0.05% Tween-20, incubated for 2 hrs with primary antibody, washed and incubated with secondary antibody, and visualized by chemiluminescence.

Cell death and cell proliferation quantification

Cells were plated in 96-well plates in triplicate and incubated at 37°C in a 5% CO_2 incubator. To induce apoptosis, Superkiller TRAIL (Alexis Biochemicals) was used for 24 hrs at 10 ng/ml. Cell viability was evaluated with the CellTiter 96® AQ_{ueous} One Solution Cell Proliferation Assay (Promega, Madison, WI, USA), according to the manufacturer's protocol. Metabolically active cells were detected by adding 20 μl of MTS to each well. After 2 hrs of incubation, the plates were analysed in a Multilabel Counter (Bio-Rad). Apoptosis was also assessed using annexin V-FITC Apoptosis Detection Kits followed by flow cytometric analysis. Cells were seeded at 1.8×10^6 cells per 100-mm dish, grown overnight in 10% Fetal Bovine Serum (FBS)/RPMI, washed with PBS, then treated for 24 hrs with 200 ng TRAIL. Following incubation, cells were washed with cold PBS and removed from the plates by very mild trypsinization conditions (0.01% trypsin/ethylenediaminetetraacetic acid). The resuspended cells were washed with cold PBS and stained with FITC-conjugated annexin V antibody and propidium iodide according to the instructions provided by the manufacturer (Roche Applied Science, Indianapolis, IN, USA). Cells (50,000 per sample) were then subjected to flow cytometric analysis. Propidium iodide staining and flow cytometry analysis were done as described [19].

Flow cytometry

The relative level of surface TRAIL receptors was assessed by FACS analysis. To this end, 1 million cells were collected and washed twice in PBS, incubated with PE-conjugated purified monoclonal antibodies against

Table 1 Clinical features of the patients

P #	Sex	Age	Histology	TNM
1	M	49	ADENO	T1N0MX
2	M	61	ADENO	T2N2MX
3	M	68	ADENO	T3N0MX
4	M	64	ADENO	T1N0MX
5	M	63	ADENO	T2N1MX
6	M	55	ADENO	T2N2MX
7	M	56	ADENO	T2N0MX
8	M	56	SQUAM	T1N1MX
9	M	63	ADENO	T3N2MX
10	M	66	ADENO	T1N1MX
11	M	77	ADENO	T1N0MX
12	M	69	SQUAM	T2N0MX
13	M	61	SQUAM	T2N0MX
14	F	52	ADENO	T2N0MX
15	M	57	ADENO	T2N2M1
16	M	80	SQUAM	T2N0MX
17	M	63	ADENO	T1N2MX
18	M	55	ADENO	T1N2MX
19	M	63	SQUAM	T2N0MX
20	M	67	SQUAM	T1N0MX
21	M	63	SQUAM	T1N0MX
22	M	70	SQUAM	T3N0MX
23	M	68	SQUAM	T1N0MX
24	M	55	ADENO	T1N0MX
25	M	64	ADENO	T1N0MX
26	M	69	SQUAM	T2N0MX
27	M	68	ADENO	T1N0MX

Age (years), sex and TNM (tumour, node, metastasis) staging [30] of patients (P) are reported. All patients were smokers. Histology of the tumours indicated that most were adenocarcinoma (ADENO) and the remaining squamous cell carcinomas (SQUAM).

TRAIL receptors or with mouse isotype control phycoerythrin IgG2b for 1 hr on ice, and then washed once with 3 ml PBS. After centrifugation, the cell pellet was resuspended in 1 ml PBS and analysed with a FACSsort (Becton Dickinson, Franklin Lakes, NJ, USA).

Small interfering (si) RNAs

The Dharmacon siDesign Center software program was used to design a duplex siRNA targeting PED mRNA (siPED). This duplex consisted of a 21 nt double-stranded RNA, comprised 19 base pairs with two T, 3' overhanging ends, synthesized by Invitrogen (Invitrogen Corporation, Carlsbad, CA, USA) (UCACUAUGGUGGUUGACUATT). c-FLIP siRNA was purchased from Santa Cruz Biotechnology, Inc. (sc-35388). siCONTROL Non-Targeting siRNA Pool #2 (D-001206-14-05) was from Dhamarcon (Lafayette, CO, USA) and comprised four siCONTROL non-targeting siRNAs. Each individual siRNA within this pool was characterized by genome-wide microarray analysis and found to have minimal off-target signatures.

Transfection experiments

CALU-1 or H460 cells were cultured to 80% confluence in p60 plates. Control, PED or cFLIP siRNA (100 nM), PED or c-FLIP siRNA were transiently transfected in cells kept in antibiotic-free, serum-containing medium, using LIPOFECTAMINE 2000, according to the manufacturer's instructions. Cells were incubated with siRNAs for the indicated times. PED protein levels were up-regulated where indicated by transfecting cells with 5 μg of pcDNA3-Myc PED [12].

Tissue microarray construction and immunohistochemistry

Cylinders of 0.6-mm diameter were punched from donor blocks in areas identified as neoplastic after analysis of haematoxylin and eosin stained sections. The tissue cylinders were inserted into a recipient paraffin block using a precision instrument (Beecher Instruments, Sun Prairie, WI, USA) [20]. Standard indirect staining procedures were used for immunohistochemistry (ABC-Elite-Kit, Vector Laboratories, Burlingame, CA, USA). After heat-induced pre-treatment (in citrate buffer, pH 6, water bath at 90°C for 30 min.) for antigen retrieval, a rabbit polyclonal anti-PED antibody [11] was applied for 2 hrs at a dilution of 1:5000 at 37°C. The slides were then incubated with the secondary, biotinylated antibody. Osmium-enhanced diaminobenzidine was used as the chromogen. Counterstaining was carried out with Harris' haematoxylin. Only fresh cut sections were stained to minimize the influence of slide ageing and maximize repeatability and reproducibility of the experiment. For negative controls, the primary antibody was omitted; as positive control, normal tissue with known PED positivity was used. For each sample, percentage of positive tumour cells and staining intensity (0, faint, moderate or intense) were recorded. A case was graded: (*i*) negative, if no cells were stained; (*ii*) weakly positive (mild), if up to 33% of cells were stained; (*iii*) moderately positive if 34–66% of cells were stained or (*iv*) strongly positive if 67–100% of cells were positive. Staining intensity was not used for correlation with clinical findings, as it can vary depending on the manner of tissue fixation. The slides were all evaluated in 1 day by an experienced pathologist (DB).

Results

PED expression in NSCLC tissue

Specimens were collected from 27 NSCLC-affected patients (clinical features are summarized in Table 1) and processed for Western blotting. PED was increased in the tumour tissue of all the patients

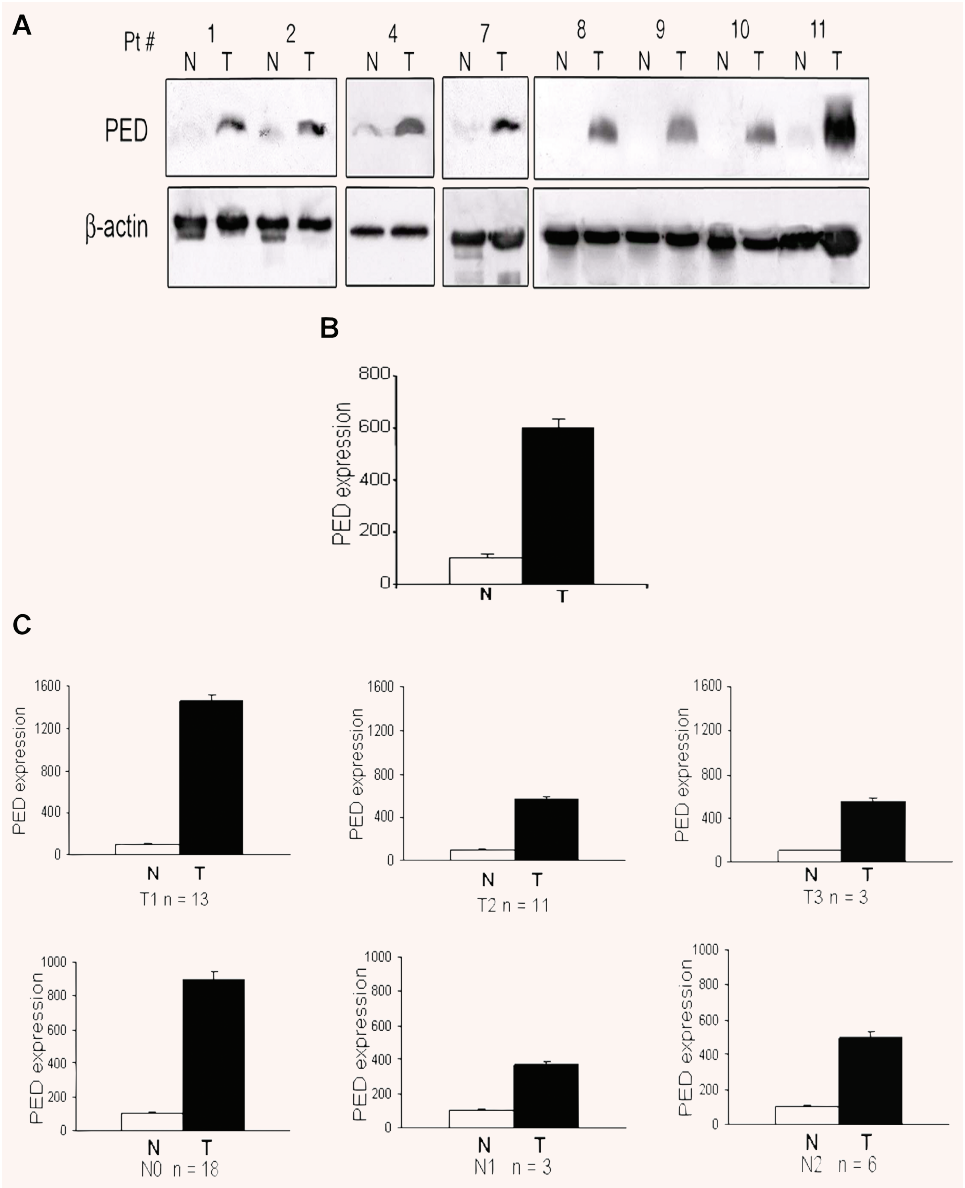

Fig. 1 PED expression is increased in human lung cancer. (**A**) Western blots showing expression of PED in tumour (T) and adjacent normal (N) lung tissue from some of the 27 NSCLC-affected patients (Pt). β-Actin was used for the loading control. (**B**) Graph of densitometric analysis. Mean ± SD PED expression of all the tumour samples (T) normalized to β-actin and expressed as percentage respect to the adjacent normal tissue (N). PED was >6-fold higher in cancer tissue compared to normal areas. (**C**) PED expression during T1, T2, T3 and N0, N1 and N2 stages of the disease. PED expression is greater during the initial stages (T1 and N0) of the disease compared with the T2 and N1 lesions.

analysed and only rarely expressed in the adjacent normal tissue (Fig. 1A). The mean PED expression level was sixfold higher in the transformed areas compared to normal tissue (Fig. 1B). Furthermore, analysis of TNM staging revealed that the expression of PED was greater during the initial stages of the disease (T1 and N0) than in T2 and N1 lesions (Fig. 1C). We also analysed PED expression on a tissue microarray constructed from 160 different histological lung cancer samples. As shown in Table 2, PED expression was considered high in the majority of cases and in all the types of lung tumour present, with only 4% of the tumours analysed resulting negative for PED staining. Immunohistochemical analysis of PED expression is depicted in Fig. 2 where it is possible to evaluate the different PED staining intensity. Part (A) represents an example of PED negative staining; part (B), of mild; part (C) of moderate and part (D) of strong PED staining. The majority of samples showed strong staining for PED.

PED expression correlates with resistance to TRAIL in NSCLC cell lines

PED is a DED-containing protein that inhibits the formation of a functional DISC following treatment with different apoptotic stimuli, including TRAIL, in several cell types [9, 15, 21]. We therefore, investigated whether PED expression correlated with resistance to TRAIL in different NSCLC cell lines. As shown in Fig. 3A, PED is

Table 2 PED expression analysed in the lung cancer tissue microarray

Histological type	PED expression				Total
	Negative	sssMild	Moderate	Strong	
Adenocarcinoma	1 (2.3%)	8 (18.6%)	10 (23.2%)	24 (55.8%)	43
Large cell carcinoma	1 (2.4%)	2 (4.8%)	15 (36.5%)	23 (56.1%)	41
Small cell carcinoma	2 (6.6%)	5 (16.6%)	7 (23.3%)	16 (53.3%)	30
Squamous cell carcinoma	2 (4.3%)	11 (23.9%)	13 (28.2%)	20 (43.4%)	46

Top number indicates number of cases present in the tissue microarray; the bottom number indicates its relative percentage. PED expression was graded: negative: no staining; mild: 0–33% positively staining cells; moderate: 34–66% positively staining cells and strong: 67–100% positively staining cells.

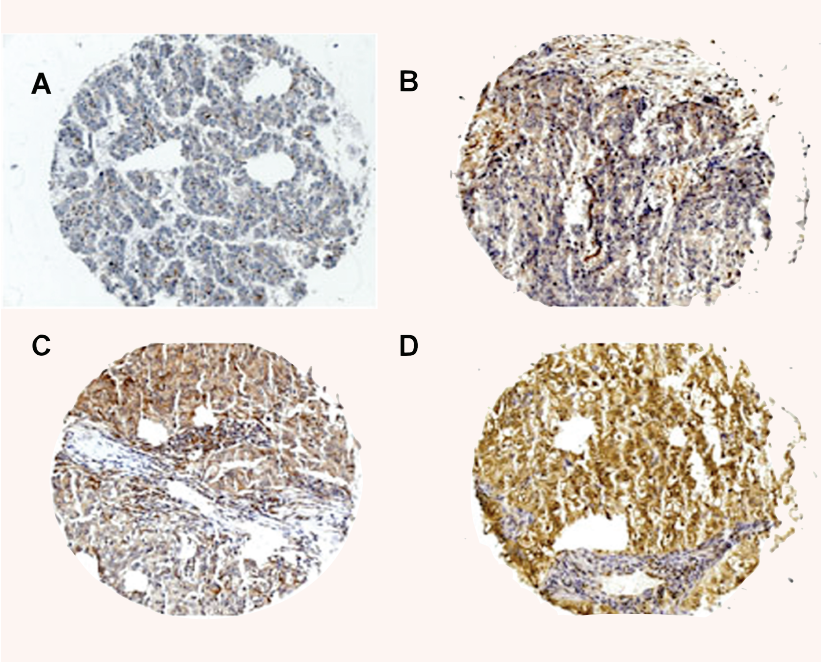

Fig. 2 PED expression levels in NSCLC cancer samples. Immunohistochemical analysis of paraffin-embedded NSCLC sections labelled with anti-PED antibody (1:5000) and revealed by secondary, biotinylated antibody. (**A**) Negative; (**B**) mild; (**C**) moderate and (**D**) strong staining.

expressed at higher levels in CALU-1 cells compared to H460 cells. Intermediate levels of expression were observed in A459 and A549 cells. When exposed to TRAIL, H460 cells underwent TRAIL-induced cell death, whereas CALU-1 cells were completely resistant (Fig. 3B and C). A459 and A549 cells exhibited intermediate sensitivities to TRAIL (Fig. 3B and C). Therefore, PED expression levels correlated with TRAIL resistance in the NSCLC cell lines analysed. We also studied several components of the extrinsic cell death signalling pathway. As shown in Fig. 3A, the expression of these TRAIL signalling molecules was comparable in the four cell lines, although c-FLIP expression was slightly lower in H460 cells.

TRAIL resistance in NSCLC cells does not depend on the expression of TRAIL receptors

TRAIL resistance could be correlated with different expression levels of TRAIL receptors. To exclude this possibility, we investigated the cell surface expression of all four TRAIL receptor subtypes in CALU-1 and H460 cells. As shown in Fig. 4, expression of functional and decoy TRAIL receptors was comparable in the two cell lines.

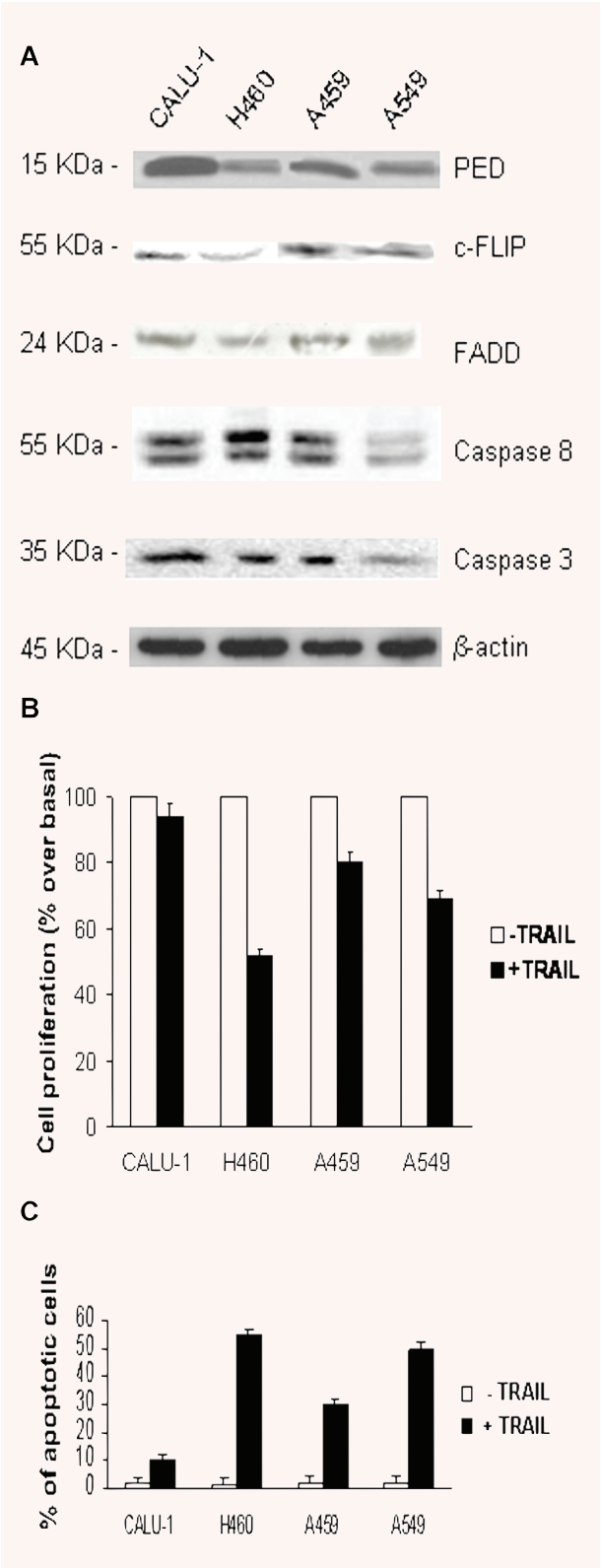

Effect of the down-regulation of PED and c-FLIP on insensitivity to TRAIL in CALU-1 cells

To better clarify the role of PED in TRAIL resistance in lung cancer cells, we transfected CALU-1 cells with PED siRNA. PED siRNA specificity was tested in CALU-1 cells by the co-transfection of PED siRNA with Myc-tagged PED cDNA [12]. The PED siRNA duplex suppressed both endogenous (15 kD) and exogenous (23 kD) PED expression, whereas a control siRNA was not effective in reducing PED protein levels (Fig. 5A). This silencing effect was evident at 48 hrs and more marked at 72 hrs. We found that also other in cell lines (HeLa, Human embryonic kidney 293) PED siRNA was able to knock-down PED expression (data not shown). Transfected cells were then exposed to TRAIL. As expected, siRNA-mediated knock-down of PED was responsible for sensitization of CALU-1 cells to TRAIL-induced cell death (Fig. 5B). Interestingly, comparable results were obtained when we knocked-down PED expression in A459 and A549 cells (Fig. 5B).

The treatment of CALU-1 cells with a specific c-FLIP$_L$ siRNA down-regulated c-FLIP$_L$ expression but did not increase sensitivity to TRAIL-induced cell death (Fig. 5C). These data further confirm that PED protects lung cancer cells from TRAIL-induced apoptosis, and that inhibiting PED expression results in increased TRAIL sensitivity.

Effects of silencing PED on caspase activation in CALU-1 cells

We then examined the activation of caspase 8 and PARP upon exposure to TRAIL in CALU-1 cells treated with PED siRNA. As shown in Fig. 6A, TRAIL-induced caspase 8 and PARP activation was greater in CALU-1 cells following PED siRNA transfection.

Effect of increasing PED expression on TRAIL sensitivity in H460 cells

To further evaluate the role of PED in apoptosis resistance, TRAIL-sensitive H460 cells were transfected with PED cDNA to up-regulate

Fig. 3 PED expression correlates with TRAIL resistance in NSCLC cell lines. (**A**) Fifty micrograms of total cell extract from CALU-1, H460, A459 and A549 cells were analysed by Western blotting for the expression of PED and other TRAIL signalling molecules. β-Actin was used as the loading control. Representative blots are shown. (**B**) Viability after treatment with TRAIL. Cells were incubated with superkiller TRAIL (10 ng/ml) for 24 hrs and viability evaluated as described in the methods section. Mean ± SD of three independent experiments in triplicate. (**C**) Annexin V and propidium iodide staining of NSCLC cells after TRAIL treatment. Mean ± SD of four independent experiments in duplicate.

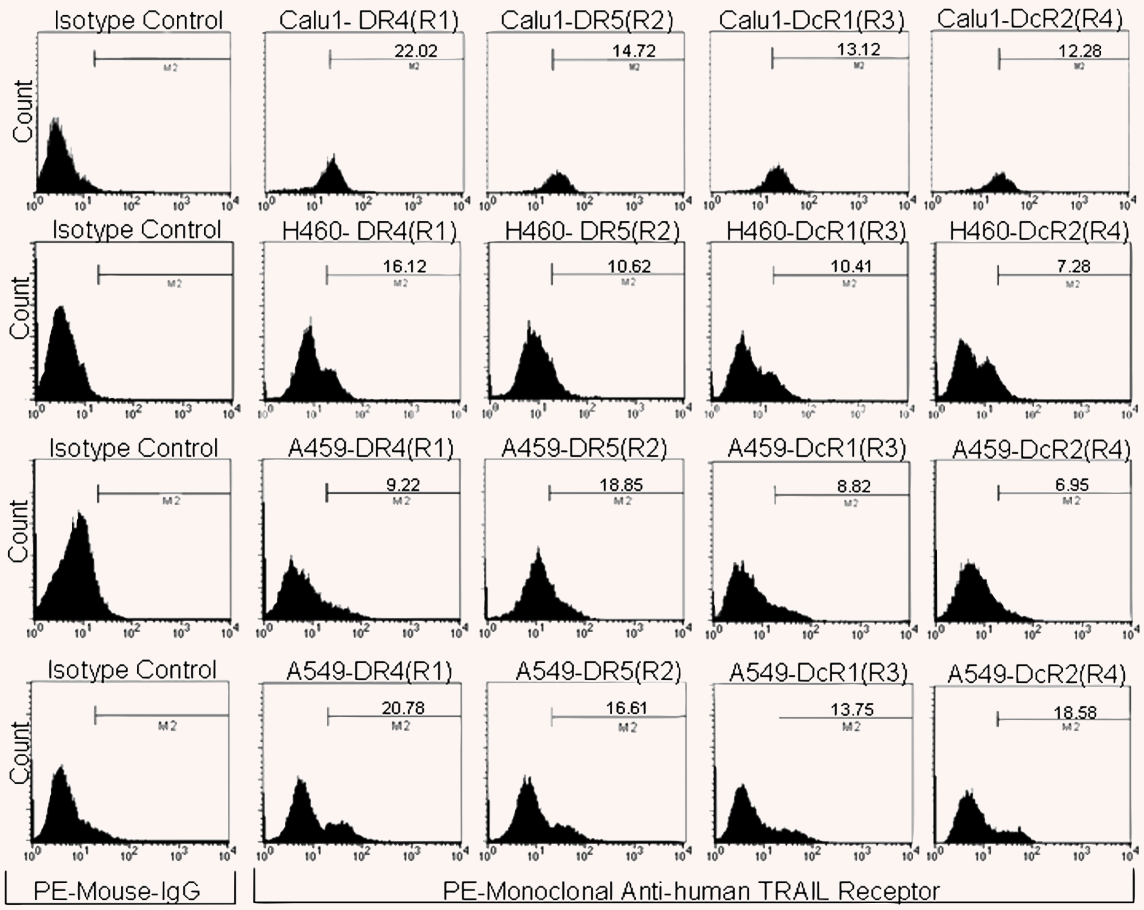

Fig. 4 Surface expression of TRAIL receptors does not differ in TRAIL-resistant and TRAIL-sensitive cells. Surface expression of the four TRAIL receptor isotopes (R1, R2, R3 and R4) was analysed by flow cytometry with specific PE-conjugated antibodies. Isotype-matched antibodies were used as control for unspecific binding. Receptor expression levels were comparable in CALU-1 and H460 cells.

PED protein levels and then analysed for their susceptibility to TRAIL-induced cell death. Increasing the expression of PED in these cells (Fig. 6C) rendered them resistant to TRAIL, as assessed by Western blotting for caspase 8 and PARP (Fig. 6B) or by a cell viability assay (Fig. 6D).

Discussion

Increased expression of DED family members with anti-apoptotic functions, such as PED, represents a possible mechanism by which tumour cells escape apoptosis. PED acts primarily by preventing the interaction between the adaptor molecule, FADD, and procaspase-8 [9, 15]. We have reported that PED inhibits the anti-apoptotic signal of death receptors in many different cell types, including breast carcinoma and glioma [9, 13–16], in which it is overexpressed. Lung tumours are among the most aggressive types of cancer and are frequently resistant to drug-induced cell death [1]. Eighty percentage of lung cancers are of the NSCLC type. Advances in standard treatment for this tumour, such as surgery, radiotherapy and chemotherapy, have not significantly increased patient survival. Thus, novel treatment strategies are urgently needed to improve the clinical management of this serious disease. Recent studies have demonstrated that targeting TNF superfamily death receptors is a promising strategy for the treatment of cancer [22]. Apoptosis-based anti-cancer therapies are designed to achieve tumour eradication through the

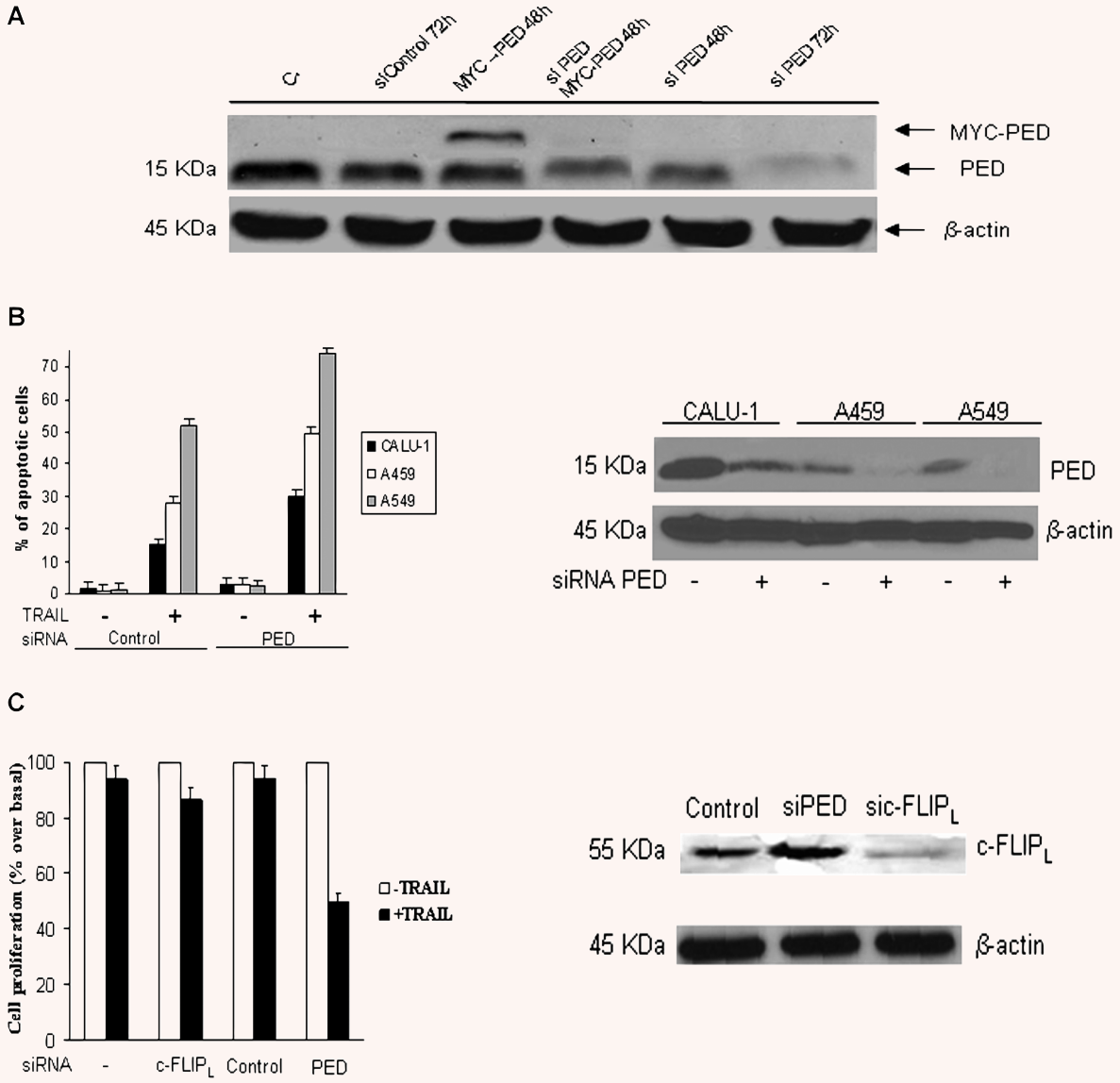

Fig. 5 Down-regulation of PED restores TRAIL sensitivity in CALU-1 cells. (**A**) PED siRNA or a control oligo were transiently transfected in CALU-1 cells in the presence or absence of PED-Myc cDNA. Cells were incubated for 48 or 72 hrs and analysed by Western blotting. The PED siRNA duplex suppressed both exogenous and endogenous PED expression, whereas control siRNA had no effects. (**B**) PED siRNA effects in A459 and A549 cells. PEDsi RNA, transfected in NSCLC cells was able to reduce PED expression levels (right panel) and induce an increase in TRAIL sensitivity (left panel), as assessed by flow cytometry. Mean ± SD of two independent experiments in duplicate. (**C**) c-FLIP$_L$ siRNA or PED siRNA were transfected as described in Methods. Cells were analysed for c-FLIP expression after 72 hrs incubation. c-FLIP$_L$ siRNA but not PED siRNA was able to reduce c-FLIP$_L$ expression Effects of silencing PED and c-FLIP$_L$ on TRAIL-induced cell death: CALU-1 cells were transfected with siRNA for PED, c-FLIP$_L$ or control for 48 hrs, after which cells were trypsinized, plated in 96-well plates in triplicate and further incubated with superkiller TRAIL for 24 hrs. Metabolically active cells were then detected as indicated in the Methods. Mean ± SD of four independent experiments in duplicate. Down-regulation of PED, but not cFLIP$_L$, was responsible for increased sensitivity of CALU-1 cells to TRAIL-mediated cell death.

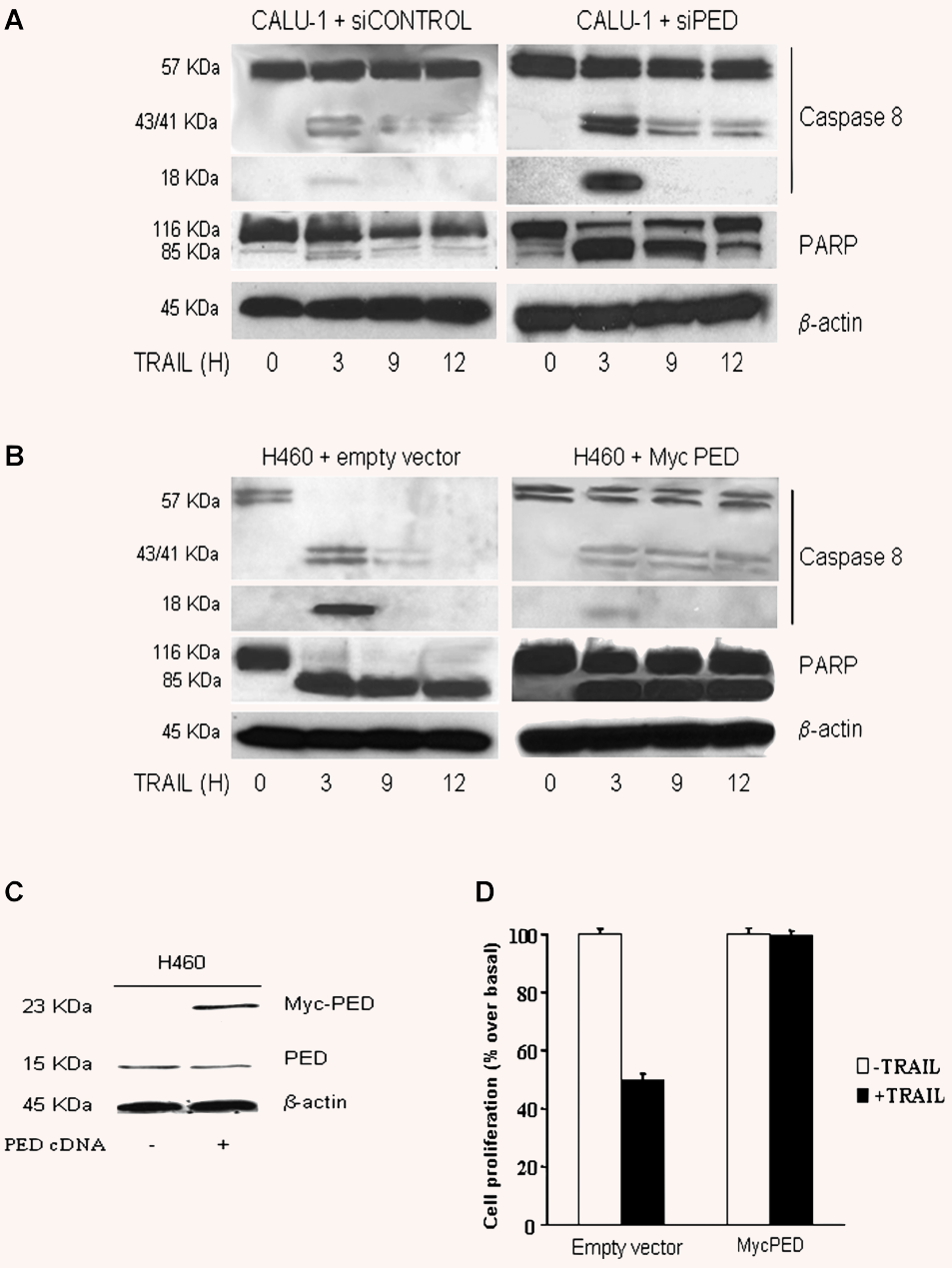

Fig. 6 Effects of PED on caspase activation. (**A**) CALU-1 cells were transfected with PED or control siRNA for 72 hrs and then treated with superkiller TRAIL for the indicated times. Lysates were examined by Western blotting with anti-caspase 8 or anti-PARP antibodies. Cleavage of caspase 8 and PARP was detected at a greater amount in CALU-1 cells transfected with PED siRNA. β-Actin was used as the loading control. (**B**) PED cDNA (PED-Myc) was transiently transfected in H460 cells and cells were analysed for caspase 8 and PARP activation as previously described or for or for cell viability (**D**) as indicated. (**C**) Western blot analysis of PED expression revealed that transfection increased PED expression levels in H460 cells. β-Actin was used as the loading control. Representative blots are shown.

use of death-inducing molecules capable of activating the apoptotic program selectively in neoplastic cells. Due to its specific toxicity for transformed cells, recombinant forms of TRAIL are among the most promising apoptosis-based anti-tumour agents [7, 23–25]. In fact, a number of biotech and pharmaceutical companies developed recombinant TRAIL/Apo2L as well as humanized agonistic mAb targeting TRAIL-R1 or TRAIL-R2 that are currently being evaluated in phase I and phase II clinical trails [7]. However, in a number of patients, tumour cells evade death signals generated by drugs through the activation of effective anti-apoptotic mechanisms [26–28]. In the present report, we demonstrate that PED is overexpressed in lung cancer tissue obtained from 27 NSCLC-affected patients. Interestingly, TNM staging revealed that PED expression is greater during the first phase of the disease (T1) than in T2 lesions. The analysis of PED expression in pre-malignant lesions, such as metaplastic bronchial lesions, could shed light on the role of PED in tumour initiation, progression and invasiveness. This study shows that PED regulates the susceptibility to TRAIL-induced death in lung cancer cells. In fact, although the levels of PED differ significantly in CALU-1 (TRAIL-insensitive) and H460 (TRAIL-sensitive) cells, the levels of the other signalling components (such as TRAIL receptors caspases, and FADD) were comparable. Modulation of the sensitivity to TRAIL by PED was confirmed by down regulating PED expression with PED siRNA: when transfected, the otherwise TRAIL-insensitive CALU-1 cells became susceptible to this cytotoxic cytokine. Moreover, PED overexpression in H460 cells was able to change their phenotype from TRAIL-sensitive to TRAIL insensitive.

Because resistance of different tumours may be mediated by diverse survival mechanisms, we investigated the role of c-FLIP in TRAIL resistance by down-regulation of c-FLIP expression with a specific siRNA. As already observed in other tumour types such as glioma [13] and B-cell chronic leukaemia [19], the effects of PED are prevalent over those mediated by c-FLIP for sensitivity to TRAIL. Thus, it is possible that c-FLIP and PED contribute differently, depending to the cell type or tumour type to induce resistance to TRAIL. Our data thus demonstrate that PED plays a major role in TRAIL resistance in NSCLC. Although PED expression was completely and specifically inhibited by the transfection with PED siRNA duplex, TRAIL sensitivity was not fully recovered. These results suggest that it is likely that there might be alternative mechanisms for TRAIL resistance. We have recently addressed this point by a microRNAs screening of TRAIL resistance in NSCLC and found several new microRNAs and targets involved in TRAIL resistance (Garofalo *et al.*, in press).

Mice that are genetically deficient in the TRAIL gene, exhibit increased susceptibility to experimental and spontaneous tumours [29], suggesting an important role of endogenous TRAIL in tumour surveillance. Thus, the overexpression of a gene involved in resistance to TRAIL could be important for responsiveness to chemotherapy. Because expression levels of PED are a focal point for the regulation of apoptosis, PED represents a key target for treatment of cancer.

Acknowledgements

This work was partially supported by funds from: Associazione Italiana Ricerca sul Cancro, AIRC (G.C.), MIUR-FIRB (RBIN04J4J7), and EU grant EMIL (European Molecular Imaging Laboratories Network) contract no. 503569. M.A. is a recipient of the FIRC fellowship. G.R. is a recipient of the Fondazione SDN fellowship. C.Q. is a recipient of the Clinica Mediterranea-Federico II Training programme. We wish to thank Michael Latronico for paper revision.

References

1. **Parker SL, Tong T, Bolden S, Wingo PA.** Cancer statistics. *CA Cancer J Clin.* 1997; 47: 5–27.
2. **Travis WD, Travis LB, Devessa SS.** Lung Cancer. *Cancer.* 1995; 75: 191–202.
3. **Marsters SA, Sheridan JP, Pitti RM, Huang A, Skubatch M, Baldwin D, Yuan J, Gurney A, Goddard AD, Godowski P,Ashkenazi A.** A novel receptor for Apo2L/TRAIL contains a truncated death domain. *Curr Biol.* 1997; 7: 1003–6.
4. **Pan G, Ni J, Wei F, Yu G, Gentz R, Dixit VM.** An antagonist decoy receptor and a death domain-containing receptor for TRAIL. *Science.* 1997; 277: 815–8.
5. **Sheridan JP, Marsters SA, Pitti RM, Gurney A, Skubatch M, Baldwin D, Ramakrishnan L, Gray CL, Baker K, Wood WI, Goddard AD, Godowski P, Ashkenazi A.** Control of TRAIL-induced apoptosis by a family of signaling and decoy receptors. *Science.* 1997; 277: 818–21.
6. **Falschlehner C, Emmerich CH, Gerlach B, Walczak H**. TRAIL signalling: decisions between life and death. *Int J Biochem Cell Biol.* 2007; 39: 1462–75.
7. **Schaefer U, Voloshanenko O, Willen D, Walczak H.** TRAIL: a multifunctional cytokine. *Front Biosci.* 2007; 12: 3813–24.
8. **Zhang L, Fang B.** Mechanisms of resistance to TRAIL-induced apoptosis in cancer. *Cancer Gene Ther.* 2005; 12: 228–37.
9. **Condorelli G, Vigliotta G, Cafieri A, Trencia A, Andalo P, Oriente F, Miele C, Caruso M, Formisano P, Beguinot F.** PED/PEA-15: an anti-apoptotic molecule that regulates FAS/TNFR1-induced apoptosis. *Oncogene.* 1999; 18: 4409–15.
10. **Reed JC.** Apoptosis-targeted therapies for cancer. *Cancer Cell.* 2003; 3: 17–22.
11. **Condorelli G, Vigliotta G, Iavarone C, Caruso M, Tocchetti CG, Andreozzi F, Cafieri A, Tecce MF, Formisano P, Beguinot L, Beguinot F.** PED/PEA-15 gene controls glucose transport and is overexpressed in type 2 diabetes mellitus. *EMBO J.* 1998; 17: 3858–66.
12. **Condorelli G, Trencia A, Vigliotta G, Perfetti A, Goglia U, Cassese A, Musti AM, Miele C, Santopietro S, Formisano P, Beguinot F.** Multiple members of the

mitogen-activated protein kinase family are necessary for PED/PEA-15 anti-apoptotic function. *J Biol Chem.* 2002; 277: 11013–8.

13. **Hao C, Beguinot F, Condorelli G, Trencia A, Van Meir EG, Yong VW, Parney IF, Roa WH, Petruk KC.** Induction and intracellular regulation of tumor necrosis factor-related apoptosis-inducing ligand (TRAIL) mediated apotosis in human malignant glioma cells. *Cancer Res.* 2001; 61: 1162–70.
14. **Kitsberg D, Formstecher E, Fauquet M, Kubes M, Cordier J, Canton B, Pan G, Rolli M, Glowinski J, Chneiweiss H.** Knock-out of the neural death effector domain protein PEA-15 demonstrates that its expression protects astrocytes from TNFalpha-induced apoptosis. *J Neurosci.* 1999; 19: 8244–51.
15. **Xiao C, Yang BF, Asadi N, Beguinot F, Hao C.** Tumor necrosis factor-related apoptosis-inducing ligand-induced death-inducing signaling complex and its modulation by c-FLIP and PED/PEA-15 in glioma cells. *J Biol Chem.* 2002; 277: 25020–5.
16. **Ricci-Vitiani L, Pedini F, Mollinari C, Condorelli G, Bonci D, Bez A, Colombo A, Parati E, Peschle C, De Maria R.** Absence of caspase 8 and high expression of PED protect primitive neural cells from cell death. *J Exp Med.* 2004; 200: 1257–66.
17. **Dong G, Loukinova E, Chen Z, Gangi L, Chanturita TI, Liu ET, Van Waes C.** Molecular profiling of transformed and metastatic murine squamous carcinoma cells by differential display and cDNA microarray reveals altered expression of multiple genes related to growth, apoptosis, angiogenesis, and the NF-kappaB signal pathway. *Cancer Res.* 2001; 61: 4797–808.
18. **Stassi G, Garofalo M, Zerilli M, Ricci-Vitiani L, Zanca C, Todaro M, Aragona F, Limite G, Petrella G, Condorelli G.** PED mediates AKT-dependent chemoresistance in human breast cancer cells. *Cancer Res.* 2005; 65: 6668–75.
19. **Garofalo M, Romano G, Quintavalle C, Romano MF, Chiurazzi F, Zanca C, Condorelli G.** Selective inhibition of PED protein expression sensitizes B-cell chronic lymphocytic leukaemia cells to TRAIL-induced apoptosis. *Int J Cancer.* 2007; 120: 1215–22.
20. **Kononen J, Bubendorf L, Kallioniemi A, Barlund M, Schraml P, Leighton S, Torhorst J, Mihatsch MJ, Sauter G, Kallioniemi OP.** Tissue microarrays for high-throughput molecular profiling of tumor specimens. *Nat Med.* 1998; 4: 844–7.
21. **Trencia A, Perfetti A, Cassese A, Vigliotta G, Miele C, Oriente F, Santopietro S, Giacco F, Condorelli G, Formisano P, Beguinot F.** Protein kinase B/Akt binds and phosphorylates PED/PEA-15, stabilizing its antiapoptotic action. *Mol Cell Biol.* 2003; 23: 4511–21.
22. **Tamada K, Chen L.** Renewed interest in cancer immunotherapy with the tumor necrosis factor superfamily molecules. *Cancer Immunol Immunother.* 2006; 55: 355–62.
23. **Carlo-Stella C, Lavazza C, Locatelli A, Viganò L, Gianni AM, Gianni L.** Targeting TRAIL agonistic receptors for cancer therapy. *Clin Cancer Res.* 2007; 13: 2313–7.
24. **Cretney E, Takeda K, Smyth MJ.** Cancer: novel therapeutic strategies that exploit the TNF-related apoptosis-inducing ligand (TRAIL)/TRAIL receptor pathway. *Int J Biochem Cell Biol.* 2007; 39: 280–6.
25. **Lee JY, Huerta-Yepez S, Vega M, Baritaki S, Spandidos DA, Bonavida B.** The NO TRAIL to YES TRAIL in cancer therapy *Int J Oncol.* 2007; 31: 685–91.
26. **Brown JM, Attardi LD.** The role of apoptosis in cancer development and treatment response. *Nat Rev Cancer.* 2005; 5: 231–7.
27. **Kaufmann SH, Vaux DL.** Alterations in the apoptotic machinery and their potential role in anticancer drug resistance. *Oncogene.* 2003; 22: 7414–30.
28. **Ghobrial IM, Witzig TE, Adjei AA.** Targeting apoptosis pathways in cancer therapy. *CA Cancer J Clin.* 2005; 55: 178–94.
29. **Cretney E, Takeda K, Yagita H, Glaccum M, Peschon JJ, Smyth MJ.** Increased susceptibility to tumor initiation and metastasis in TNF-related apoptosis-inducing ligand-deficient mice. *J Immunol.* 2002; 168: 1356–61.
30. **Kang J, Kisenge RR, Toyoda H, Tanaka S, Bu J, Azuma E, Komada Y.** Chemical sensitization and regulation of TRAIL-induced apoptosis in a panel of B-lymphocytic leukaemia cell lines. *Br J Haematol.* 2003; 123: 921–32.

Oncogene (2008), 1–11

www.nature.com/onc

ORIGINAL ARTICLE

MicroRNA signatures of TRAIL resistance in human non-small cell lung cancer

M Garofalo[1,2,3], C Quintavalle[1,2], G Di Leva[3], C Zanca[1,2], G Romano[1,2], C Taccioli[3], CG Liu[3], CM Croce[3] and G Condorelli[1,2,4]

[1]Department of Cellular and Molecular Biology and Pathology, University of Naples Federico II, Naples, Italy; [2]Istituto di Endocrinologia ed Oncologia Sperimentale, CNR, IEOS, Naples, Italy; [3]Department of Molecular Virology, Immunology and Medical Genetics, Human Cancer Genetics Program, Comprehensive Cancer Center, The Ohio State University, Columbus, OH, USA and [4]Facoltà di Scienze Biotecnologiche, University of Naples Federico II, Naples, Italy

To define novel pathways that regulate susceptibility to tumor necrosis factor (TNF)-related apoptosis-inducing ligand (TRAIL) in non-small cell lung cancer (NSCLC), we have performed genome-wide expression profiling of microRNAs (miRs). We show that in TRAIL-resistant NSCLC cells, levels of different miRs are increased, and in particular, miR-221 and -222. We demonstrate that these miRs impair TRAIL-dependent apoptosis by inhibiting the expression of key functional proteins. Indeed, transfection with anti-miR-221 and -222 rendered CALU-1-resistant cells sensitive to TRAIL. Conversely, H460-sensitive cells treated with -221 and -222 pre-miRs become resistant to TRAIL. miR-221 and -222 target the 3′-UTR of Kit and $p27^{kip1}$ mRNAs, but interfere with TRAIL signaling mainly through $p27^{kip1}$. In conclusion, we show that high expression levels of miR-221 and -222 are needed to maintain the TRAIL-resistant phenotype, thus making these miRs as promising therapeutic targets or diagnostic tool for TRAIL resistance in NSCLC.
Oncogene advance online publication, 4 February 2008; doi:10.1038/onc.2008.6

Keywords: microRNA; non-small cell lung cancer; apoptosis

Introduction

MicroRNAs (miRs) are a small noncoding family of 19–25 nt RNAs that play an important role in the negative regulation of gene expression by base-pairing to complementary sites on the target mRNAs (Calin and Croce, 2006). Currently $\geqslant$460 miRs have been identified in humans and other eukaryotic species (miR registry, www.sanger.ac.uk/Software/Rfam/mirna/index.shtml). The expression pattern of miRs is often developmentally regulated and/or tissue specific, although some miRs are steadily expressed in the whole organism (Liu *et al*., 2004; Sempere *et al*., 2004). In lower species, miRs are involved in a variety of basic processes, for example, cell proliferation and apoptosis (Xu *et al*., 2004; Cheng *et al*., 2005), neuronal development (Smirnova *et al*., 2005), fat metabolism (Xu *et al*., 2003) and stress response (Dresios *et al*., 2005). In some studies, key target mRNAs have been identified but relatively little is known about the functional role of miRNAs in mammalian species. We do know, however, that miR-181 is involved in the control of lymphopoiesis (Chen *et al*., 2004), miR-375 regulates insulin secretion by targeting myotrophin mRNA (Poy *et al*., 2004), and the miR-let7 family may play a role in oncogenesis via RAS oncogene mRNAs (Johnson *et al*., 2005). miR-15a and miR-16-1 are deleted or downregulated in the majority of chronic lymphocytic leukemia (Calin *et al*., 2005). Functional studies indicated that miR-221 and -222 inhibit normal erythropoiesis and erythroleukemic cell growth at least in part via Kit receptor downmodulation (Felli *et al*., 2005), and their ectopic overexpression directly results in $p27^{kip1}$ downregulation in aggressive prostate carcinoma (Galardi *et al*., 2007). Lung tumors are among the most deadly types of cancer. Advances in standard treatments for this tumor, such as surgery, radiotherapy and chemotherapy, have not significantly increased patient survival. One of the most important issues that affects survival rate is resistance to therapeutic drugs. Only 20–30% of treated non-small cell lung cancer (NSCLC) patients have clinical evidence of a response. Therefore, the development of new therapeutic strategies is necessary for the treatment of this type of cancer. The Apo2L/tumor necrosis factor (TNF)-α-related apoptosis-inducing ligand (TRAIL) is a relatively new member of the TNF family known to induce apoptosis in a variety of cancers (Schaefer *et al*., 2007). TRAIL can bind to five receptors, of which four are located at the cell surface: TRAIL-R1 (DR4), TRAIL-R2 (DR5), TRAIL-R3 (DcR1) and TRAIL-R4 (DcR2). Only two of these receptors, R1 and R2, contain a functional cytoplasmic death domain motif and are capable of delivering the apoptotic signal of

Correspondence: Professor G Condorelli, Dipartimento di Biologia e Patologia Cellulare e Molecolare and Facoltà di Scienze Biotecnologiche, Università degli Studi di Napoli Federico II, Via Pansini 5, Naples 80131, Italy.
E-mail: gecondor@unina.it
Received 13 November 2007; revised 21 December 2007; accepted 4 January 2008

TRAIL by association of the death domain with the Fas-associated death domain protein (FADD), containing the death effector domain, which is involved in the activation of caspase 8 (Falschlehner *et al*., 2007). The other two receptors, DcR1 and DcR2, are 'decoy receptors' and lack the ability to initiate the apoptotic cascade. Treatment with TRAIL induces programmed cell death in a wide range of transformed cells, both *in vitro* and *in vivo*, without producing significant effects in normal cells (Falschlehner *et al*., 2007; Schaefer *et al*., 2007). However, a significant proportion of human cancer cells are resistant to TRAIL-induced apoptosis, and the mechanism of sensitization seems to differ among cell types. Different studies relate resistance to TRAIL-induced cell death to downstream factors. It has been shown that downregulation of PED or cellular FLICE-like inhibitory protein (c-Flip) can sensitize cells to TRAIL-induced apoptosis (Fulda *et al*., 2000; Garofalo *et al*., 2007). However, the mechanism of TRAIL resistance is still largely unknown.

In this study, to identify novel mechanisms implicated in TRAIL resistance, we performed a genome-wide expression profiling of miRs in four different cell lines. We found that miR-221 and -222 are markedly upregulated in TRAIL-resistant, and downregulated in TRAIL-sensitive, NSCLC cells. Our experiments indicate that miR-221 and -222 modulate TRAIL sensitivity in lung cancer cells mainly by modulating $p27^{kip1}$ expression and TRAIL-induced caspase machinery.

Results

The cytotoxic effects of TRAIL in human non-small cell lung cancer

We analysed TRAIL sensitivity of different human NSCLC cell lines: A459, A549, CALU-1 and H460. Cells were exposed to TRAIL for 24 and 48 h (Figure 1a) after which cell death was assessed using a 3-(4,5-dimethylthiazol-2-yl)-2,5-diphenyltetrazolium bromide (MTT) assay or by fluorescence-activated cell sorting (FACS) with annexin V and propidium iodide staining (data not shown). As shown in Figure 1a, H460 cells underwent TRAIL-induced cell death whereas CALU-1 cells did not display sensitivity when exposed to soluble TRAIL; A459 and A549 cells showed an intermediate sensitivity. A possible mechanism of the differential sensitivity of the tested cells to TRAIL-induced apoptosis could be due to the variability of the cell surface levels of the death receptors resulting in increased apoptotic signaling in the sensitive cells. However, functional TRAIL receptor isoforms (TRAIL-R1 and -R2) analysed by western blot (Figure 1b) or FACS analysis (data not shown) revealed comparable levels of expression in TRAIL-sensitive compared to TRAIL-resistant cells. Furthermore, although H460 cells express low levels of DcR1, the expression of DcR2 receptor is greater compared to CALU-1. Therefore, the expression of the decoy receptors within the two cell lines is balanced.

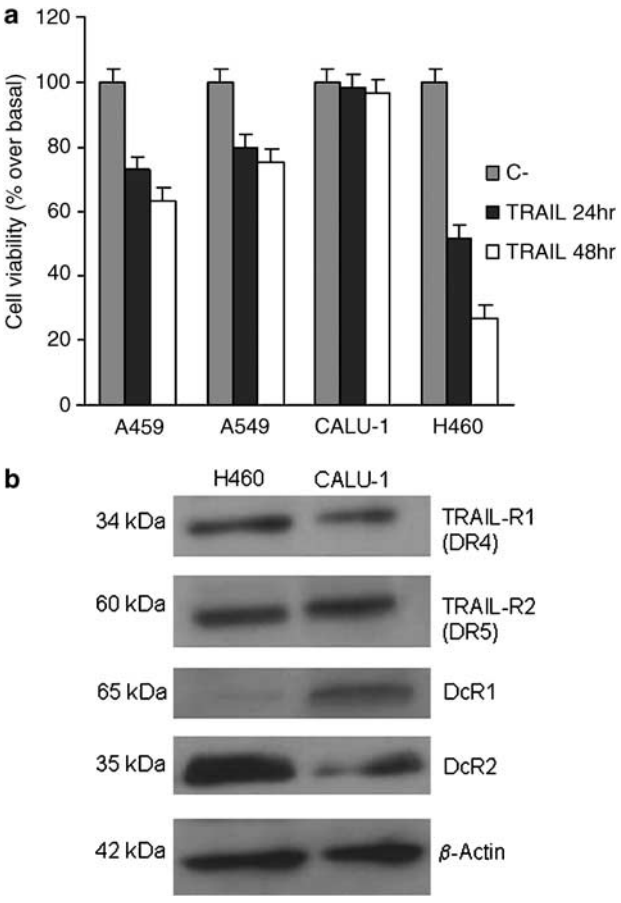

Figure 1 Sensitivity of non-small cell lung cancer (NSCLC) to tumor necrosis factor (TNF)-related apoptosis-inducing ligand (TRAIL)-inducing apoptosis. (**a**) NSCLC cells were incubated with Super-Killer-TRAIL (400 ng ml^{-1}) for 24 and 48 h and viability was evaluated as described in 'Experimental procedures' section. Mean ± s.d. of four independent experiments repeated in triplicate. H460 cells were more sensitive to TRAIL-induced apoptosis compared to CALU-1. A459 and A549 exhibited an intermediate sensitivity. (**b**) TRAIL receptors expression in CALU-1 and H460 cells. Total extract (50 μg) was loaded onto 10% SDS–polyacrylamide gels (PAGE). The membrane was blotted with anti-TRAIL-R1/DR4, TRAIL/DR5 (1 μg ml^{-1}) and DcR1 and DcR2 antibodies (0.5 μg ml^{-1}). Loading control was obtained with anti-β-actin antibody (1:5000).

miRs expression screening in TRAIL-resistant versus -sensitive NSCLC cell lines

To investigate the involvement of miRs in TRAIL resistance, we analysed the miRs expression profile in TRAIL-resistant (CALU-1) and semi-resistant NSCLC cell lines (A459 and A549) versus TRAIL-sensitive cell line (H460). The analysis was performed with a microarray chip containing 1150 miR probes, including 326 human and 249 mouse miRs, spotted in duplicates (Liu *et al*., 2004). Pair-wise significance analysis (PAM) of the microarray indicated that five miR genes were significantly overexpressed in resistant NSCLC cells with a >1.5-fold change (Figure 2). These miRs were miR-222, -100, -221, -125b and -15b (Table 1). Three of these miRs, miR-222, -221 and -100, showed dramatic overexpression with 5- to 8-fold higher levels in resistant

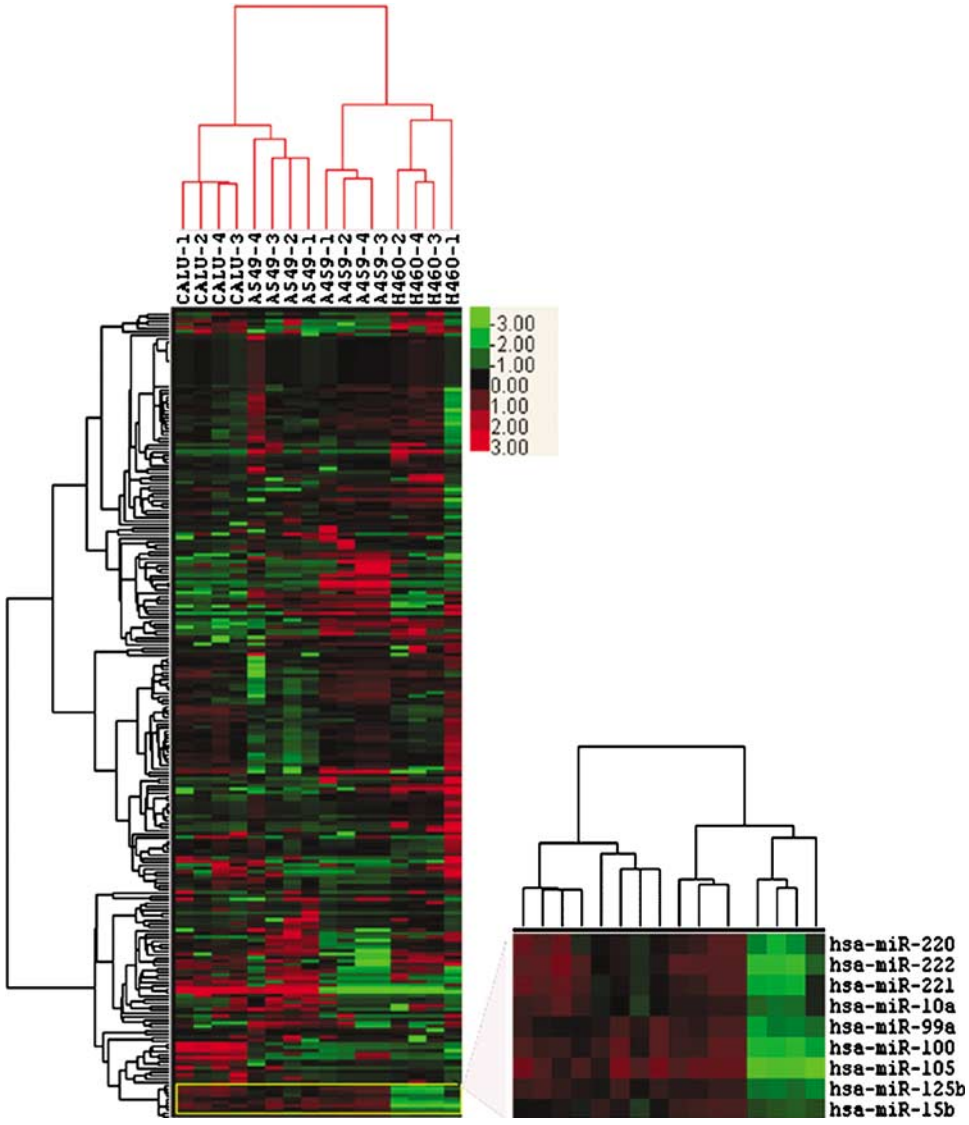

Figure 2 MicroRNA (miR) expression signature in resistant versus sensitive non-small cell lung cancer (NSCLC) cells. Fold changes (resistant versus sensitive) of the miRs present in NSCLC cells. The tree displays the $\log_2$ transformation of the average fold changes. Arrays were mean centered and normalized by using Gene Cluster 2.0. Average linkage clustering was performed by using uncensored correlation metric.

Table 1 Up- and downregulated miRs in TRAIL-resistant NSCLC cells

miRNAs	Chromosomal location	*Fold change*
has-miR-222	Xp11.3	8.6
has-miR-100	3q 26.1	8.3
has-miR-221	Xp11.3	5.9
has-miR-125b	11q23-24	5.4
has-miR-15b	3q26.1	3.6
hasmiR96	7q32.2	0.5
has-miR-9	1q23.1	0.072

All differentially expressed miRs have $Q<0.01$ (false-positive rate). *t*-Test, $P<0.05$. These miRs were identified by PAM as predictor of NSCLC with the lowest misclassification error. All the miRs, except miR-9 and -96, are upregulated in the TRAIL-resistant cells compared to the TRAIL-sensitive one.

NSCLC cells compared to the sensitive NSCLC cells. Downregulation occurred for only two miRs, miR-9 and -96 (Table 1). To validate the microarray analysis, we performed quantitative real-time-polymerase chain reaction (qRT-PCR) of the most overexpressed miRs (miR-222, -100, -221, -125b) and of the downregulated miR-9 in NSCLC cells. The analysis confirmed the results obtained by the microarray (Figure 3a). The expression of miR-222 in NSCLC cells was also confirmed with Northern blot (Figure 3b).

Role of miR-221 and -222 in TRAIL resistance in NSCLC

To test the role of these overexpressed miRs in TRAIL sensitivity in lung cancer, we transfected H460 TRAIL-sensitive cells with pre-miR-221 and -222. Increased expression of these miRs upon transfection was confirmed by real-time PCR (data not shown). Overexpression of miR-221 and -222 in H460 cells made these cells more resistant to TRAIL-induced cell death by about 40%, as assessed by MTT assay (Figure 4a).

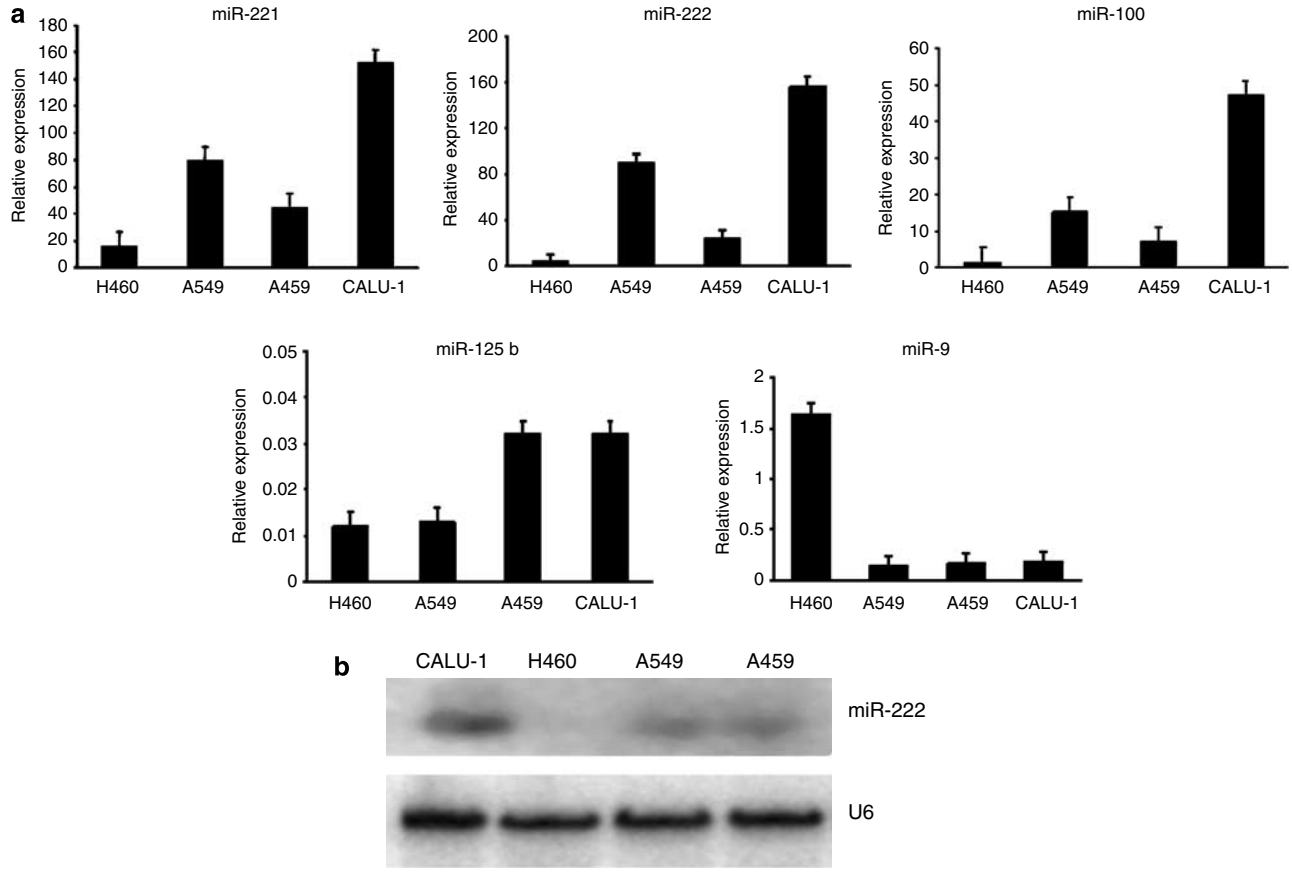

Figure 3 MicroRNAs (miRs) down- and upregulated in tumor necrosis factor (TNF)-related apoptosis-inducing ligand (TRAIL)-resistant or -sensitive non-small cell lung cancer (NSCLC) cells. (**a**) Real-time PCR of the most promising miR targets obtained with microarray screening was performed by extracting RNA from the different NSCLC cells, as described in 'Experimental procedures' section. Total 5 μg of RNA in 10 μl PCR reaction was used. TaqMan ΔC_T values were converted into absolute copy numbers using a standard curve from synthetic lin-4 miRNA. Data are expressed as the relative expression of the different miRs, compared to 18S rRNA. miRs 222, 100, 221, 125b were markedly upmodulated in resistant but not in sensitive cell cultures, while miR-9 was markedly downmodulated. (**b**) Northern blot analysis of miR-222 expression. RNA (10 μg) was loaded onto a precast 15% denaturing polyacrylamide gel (Bio-Rad). RNA was then electrophoretically transferred to BrightStar blotting membranes and membrane incubated with labeled miR-222 probe. miR-222 was strongly upregulated in TRAIL-resistant CALU-1 cells.

The same results were obtained by annexin V–fluorescein isothiocyanate (FITC) staining (Figure 4b). Interestingly, pre-miR-100 also increased TRAIL sensitivity, while pre-miR-125b and control miR overexpression did not produce any effect (data not shown). We also tested the effects of miRs 221 and 222 on the activation of caspase 8, 3 and poly-(ADP-ribose)polymerase (PARP). Interestingly, while in H460 cells, TRAIL induced the activation of caspase cascade, as assessed by the appearance of the cleaved fragment, the co-incubation of TRAIL with pre-miRs 221 or 222 induced a reduction of TRAIL-mediated cell death machinery activation (Figure 4c). We also tested the effect of miR-221 and -222 on the expression of some of TRAIL signaling molecules. Interestingly, Mcl-1 and FADD were upregulated, suggesting an indirect effect of those miRs. TRAIL receptors expression was not affected by miR-221 and -222 upmodulation (Figure 4e).

Anti-miR inhibitors are sequence-specific nucleotides that specifically target and knock down individual miR molecules. We transfected CALU-1 TRAIL-resistant cells with anti-miR inhibitors -221 and -222 and then assessed TRAIL sensitivity. The levels of miR-221 and -222, assessed by real time (RT)–PCR, were reduced (data not shown). Interestingly, the inhibition of miR-221 and -222 expression with the specific anti-miR inhibitor was able to change the insensitive TRAIL phenotype to a sensitive one (Figure 5a). A scrambled nonspecific anti-miR did not produce any effect. TRAIL receptors expression was not affected by miR-221 and -222 downmodulation (Figure 5b).

p27^{kip1} and Kit expression in NSCLC

We analysed the predicted targets of the three most significantly overexpressed miRNAs (miR-222, -100 and -221) in TRAIL-resistant cells. In this study, we focused on miR-221 and -222, which are located close to each other on the short arm of the X chromosome. The concordant expression pattern in NSCLC suggested shared regulatory mechanisms for the expression of these two clustered miRs. They are upregulated in

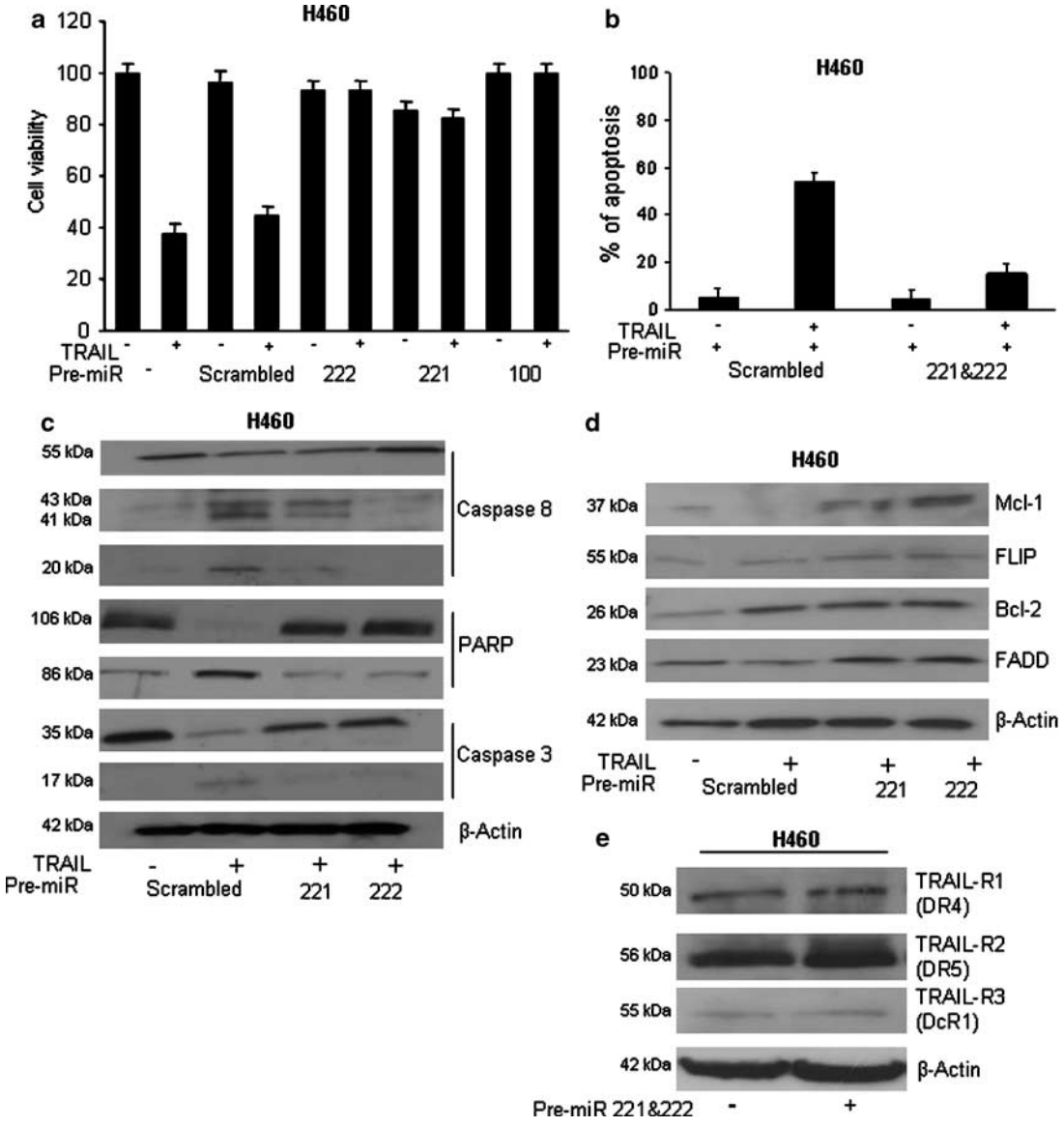

Figure 4 MicroRNA (miR)-222 transfection induced tumor necrosis factor (TNF)-related apoptosis-inducing ligand (TRAIL) resistance in H460 cells. Cell death effects of miRs: cells were transfected either with control-scrambled miR or with 100 nmol of pre-miR-221, -222 or -100. Twenty-four hours after transfection, cells were spitted into 96-well plates and treated with 400 ng ml^{-1} of Super-Killer TRAIL for 24 h. Apoptosis was evaluated either with CellTiter Assay (**a**), or with annexin V staining (**b**). The same cells were also assessed for caspase activation and expression of TRAIL signaling molecules by western blot (**c**–**e**). Total extract (80 μg) was loaded onto 10% SDS–polyacrylamide gels (PAGE). The membrane was blotted with the different antibodies as indicated. Loading control was obtained using anti-β-actin antibody. MiR-221 and -222 overexpression induced TRAIL resistance in H460 cells.

TRAIL-resistant NSCLC cells and may promote TRAIL resistance by blocking expression of key functional proteins. Different studies have demonstrated that both the proto-oncogene Kit and the tumor suppressor p27^{kip1} are miR-221 and -222 targets (Felli *et al*., 2005; He *et al*., 2005; Poliseno *et al*., 2006; le Sage *et al*., 2007). We thus investigated Kit and p27^{kip1} expression in NSCLC cells. Western blotting of NSCLC cells with a monoclonal anti-Kit antibody revealed two bands of ~140 and 120 kDa, corresponding to the mature fully and the partially glycosylated Kit isoforms (Tamborini *et al*., 2004; Figure 6a). Interestingly, Kit protein was markedly upregulated in sensitive, and downregulated in resistant, NSCLC cells. FACS analysis, used for quantitative determination of cell surface Kit-receptor expression (Figure 6b), confirmed the western blot results. Next, we analysed p27^{kip1} expression in NSCLC cells. Interestingly, as for Kit, western blot analysis showed that p27^{kip1} is clearly detectable in H460 cells, is reduced in A459 and A549 cells, and completely absent in CALU-1 cells (Figure 6a). Kit and p27^{kip1} were both targets of miR-221 and -222 in human NSCLC cells since their expression was modulated in CALU-1 cells upon anti-miR-222 transfection or in H460 cells treated with pre-miR-221 and -222 (Figure 6c). Furthermore, p27^{kip1} was downregulated in

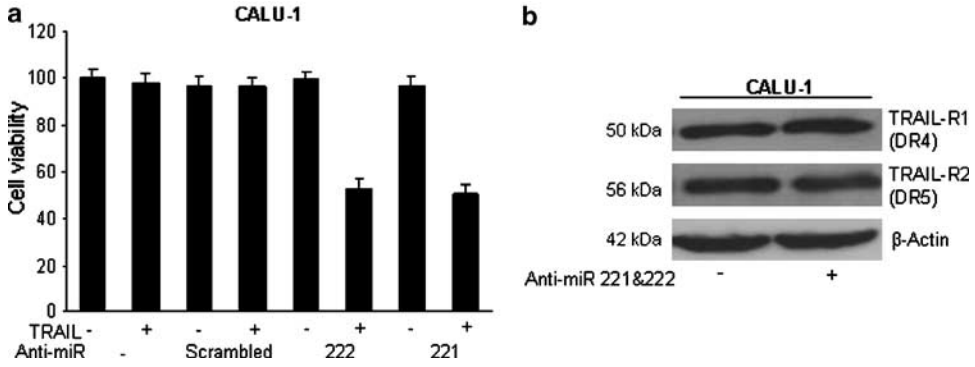

Figure 5 Effects of anti-microRNAs (miRs) on cell death. (**a**) CALU-1 cells were transfected with 100 nM of anti-miRs 222, 221 or a scrambled control. Twenty-four hours after transfection, cells were split into 96–well plates and treated with 400 ng ml^{-1} of Super-Killer tumor necrosis factor (TNF)-related apoptosis-inducing ligand (TRAIL) for 24 h, and cell viability was assessed as previously described. Downregulation of miRs 221 and 222 in CALU-1 cells increased TRAIL sensitivity. (**b**) The same cells extract were also assessed for expression of TRAIL receptors R1 and R2 by western blot. Loading control was obtained using anti-β-actin antibody.

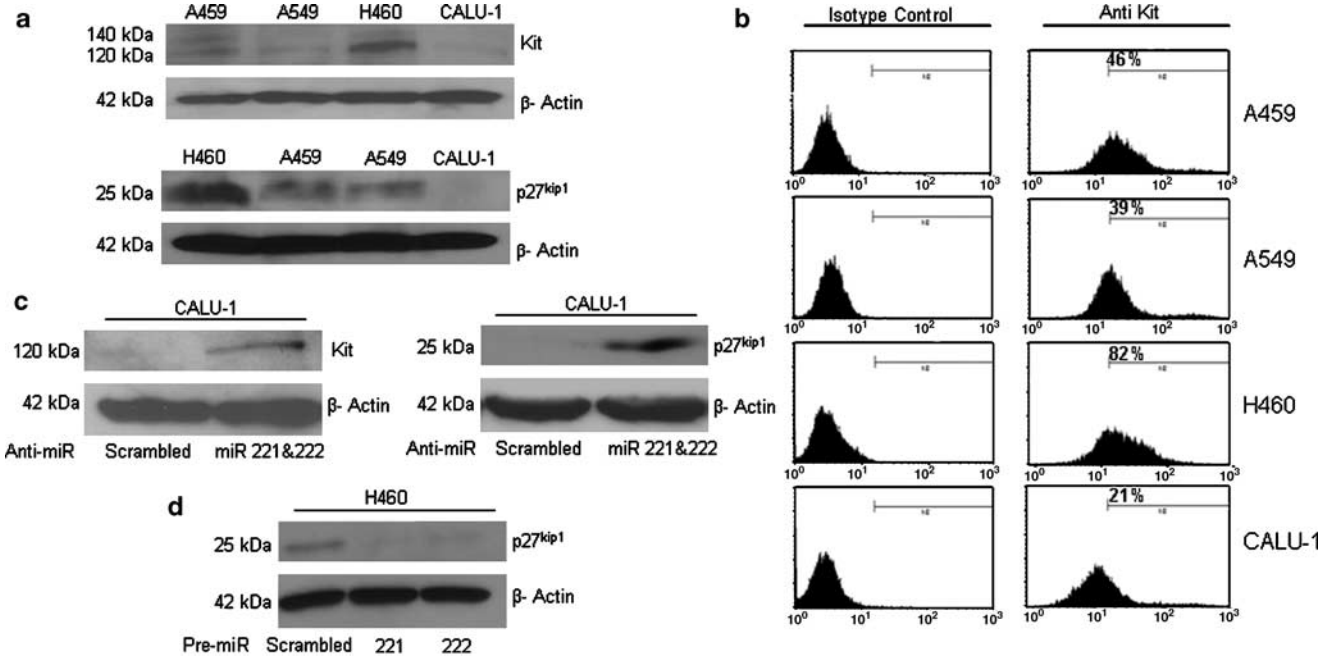

Figure 6 Kit and p27^{kip1} expression in non-small cell lung cancer (NSCLC) cells. (**a**) Proteins from CALU-1, A459, A549 and H460 cells were extracted with radioimmuno precipitation assay (RIPA) buffer. Sample extract (50 μg) was resolved on 7.5% SDS–polyacrylamide gels (PAGE) and transferred to Hybond-C nitrocellulose. Membranes were incubated with anti-Kit primary antibody (0.2 μg ml^{-1}) or anti-p27 antibody. (**b**) Fluorescence-activated cell sorting (FACS) analysis of cell surface Kit expression. Cells were stained with primary antihuman h-SCFR affinity-purified goat immunoglobulin G (IgG; 1 μg ml^{-1}) or mouse mAb 002 (isotype control) followed by 10 μl of secondary antibody, Fluorescein-conjugated goat F(ab')2, as described in 'Experimental procedures' section. Surface and total Kit expression was higher in the H460 cells. (**c**) CALU-1 cells were transfected with 100 nmol of anti-microRNAs (miR)-221 and -222 for 48 h. Total extract (50 μg) was loaded onto 7.5–12% SDS–PAGE. The membrane was blotted with anti-Kit (0.2 μg ml^{-1}) or anti-p27^{kip1} (1 μg ml^{-1}) antibody. Loading control was obtained with anti-β-actin antibody (1:5000). Anti-miR-221 and -222 were able to increase Kit and p27^{kip1} expression. (**d**) p27^{kip1} expression upon miR-222 and -221. Cells were transfected with either scrambled or miR-221 and -222 and p27^{kip1} expression was assessed by western blot. miR-222 and -221 were able to downregulate p27^{kip1} expression.

H460 cells transfected with premiR-221 and -222 (Figure 6d). A gene expression profiling in TRAIL-resistant and -sensitive NSCLC cells, using oligonucleotide microarrays, confirmed the down-regulation of Kit and p27^{kip1} in CALU-1-resistant NSCLC cells (data not shown).

Role of the miR-221 and -222 targets, p27^{kip1} and Kit, on TRAIL-mediated apoptosis in NSCLC

To investigate whether p27^{kip1} or Kit were involved in TRAIL resistance, we silenced these genes with specific siRNAs and then evaluated TRAIL sensitivity. Specific anti-Kit or anti-p27^{kip1} siRNAs induced a reduction of

endogenous expression of Kit or p27^{kip1} proteins by about 70% (Figures 7a and d). To evaluate the role of p27^{kip1} and Kit in these cells, we measured survival after treatment with TRAIL. Surprisingly, anti-p27^{kip1} siRNA transfection increased H460 cell resistance to TRAIL as assessed by annexin V staining (Figure 7b) or PARP and caspase 8 activation (Figure 7c); on the contrary anti-Kit siRNA transfection (Figure 7e).

Discussion

Apoptosis-based anticancer therapies are designed to achieve tumor eradication through the use of death-inducing molecules capable of activating the apoptotic program selectively in neoplastic cells. Owing to its specific toxicity for malignant cells, recombinant forms of TRAIL are among the most promising apoptosis-based antitumor agents (Walczak *et al*., 1999; Walczak and Krammer, 2000). Therapy based on the use of agonistic TRAIL receptor antibodies is now in phase 2 clinical trial in different kinds of cancer, included NSCLC (Koschny *et al*., 2007). However, in a number of patients, tumor cells evade death signals generated by drugs through the activation of effective antiapoptotic mechanisms (Brown and Attardi, 2005; Ghobrial *et al*., 2005). The aim of the present study was to identify specific signatures as potential therapeutic targets for the TRAIL-resistant phenotype in non-small cell lung cancer (NSCLC).

For this purpose, we analysed miRs expression profile in TRAIL-resistant (CALU-1) and semi-resistant NSCLC cell lines (A459 and A549) versus a TRAIL-sensitive cell line (H460). We identified five miRs

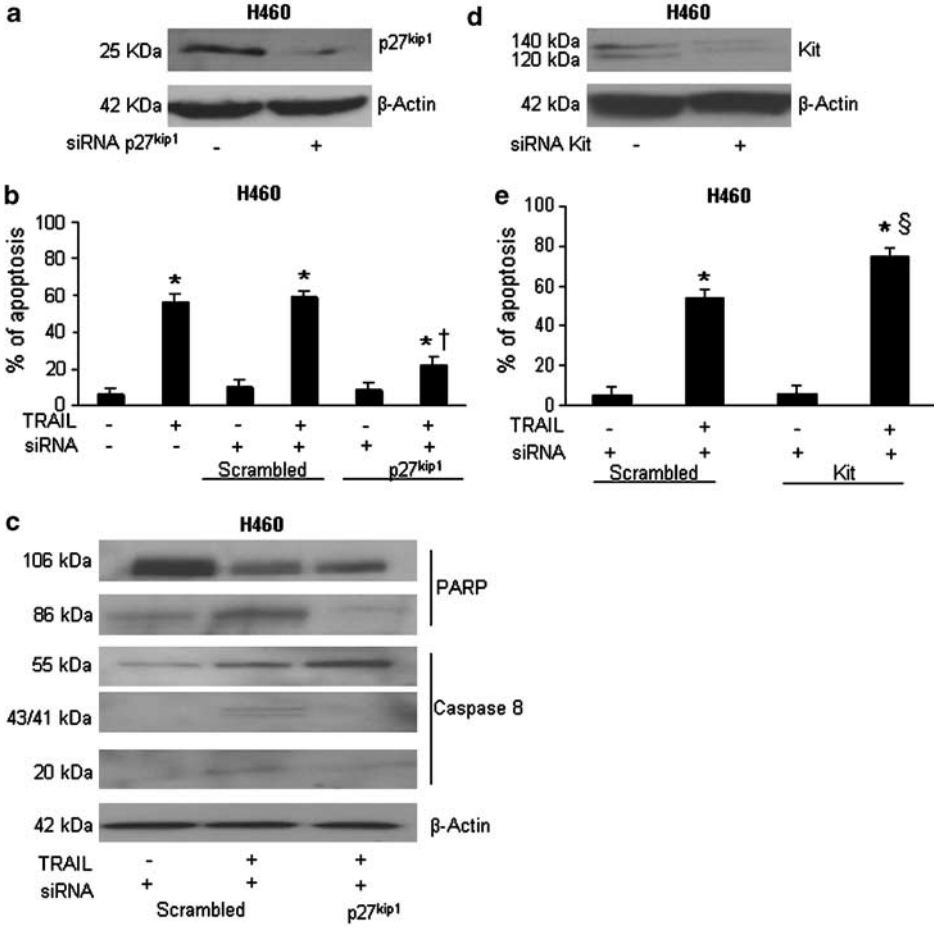

Figure 7 Effect of p27^{kip1} and Kit inhibition on tumor necrosis factor (TNF)-related apoptosis-inducing ligand (TRAIL) resistance in human non-small cell lung cancer (NSCLC) cells. (**a**) H460 cells were cultured to 80% confluence and transiently transfected with anti-p27^{kip1} siRNA, a pool of four target-specific 20–25 nt siRNAs designed to knock down p27 gene expression. Total cell extract (50 μg) was loaded onto 12% SDS–polyacrylamide gels (PAGE). Anti-p27 siRNA induced a marked downregulation of p27 expression in H460 cells. (**b**, **c**) Interfering with p27 expression increased TRAIL resistance in H460 cells, as assessed by annexin V (**b**) or poly-(ADP-ribose) polymerase (PARP) and caspase 8 activation (**c**). Mean ± s.d. of four independent experiments in duplicate. $^{*}P<0.005$ (± TRAIL); $^{\dagger}P<0.001$ (Scrambled + TRAIL) versus (si-p27 + TRAIL). (**d**) H460 cells were transiently transfected with siKit RNA and analysed by western blot. Anti-Kit siRNA induced a marked downregulation of Kit expression in H460 cells. (**e**) Annexin V staining of apoptotic cells upon 24 h of TRAIL incubation. Inhibition of Kit did not induce a significant increment in TRAIL sensitivity. Mean ± s.d. of three independent experiments in duplicate. $^{*}P<0.005$. The Student's *t*-test was used as statistical method. $^{*}P<0.005$ (Scrambled ± TRAIL) versus (siKit ± TRAIL). $^{\S}P>0.05$ (Scrambled + TRAIL versus siKit + TRAIL).

upregulated in the resistant cell lines (miR-222, -100, -221, -125b and -15b) and between these we further analysed four of them with the highest fold change (miR-222, -100, -221 and -125b). This pattern was specific for NSCLC cells since we did not find the same pattern in breast cancer cells analysed with the same array (data not shown).

Forced overexpression of the miR-222, -100 and -221, but not of miR-125b, in the sensitive H460 cells increased resistance to TRAIL in these cells, thus indicating that repression of their target proteins is implicated in causing TRAIL resistance. Kept together, our results show that the sensitivity of a cancer cell to a defined external signal is dictated by the expression of a small number of miRs.

Further, to support the involvement of miR-mediated regulation of protein levels in TRAIL resistance, we investigated the potential protein targets of miRs identified in our screening. We focused on the two highly related miRs, miR-221 and -222, that recognize several predicted target genes involved in intracellular signaling (and cell death), and thus good candidate regulators of cell response to TRAIL.

Recent reports revealed that the receptor tyrosine kinase Kit and the cyclin-dependent kinase (cdk) inhibitor, $p27^{kip1}$, are both miR-221 and -222 functional targets (Felli *et al*., 2005; He *et al*., 2005; Poliseno *et al*., 2006; le Sage *et al*., 2007). Here we demonstrate that silencing of $p27^{kip1}$, but not of Kit, increases TRAIL resistance. This result well supports the implication of miR-221 and -222 in determining the resistant/sensitive phenotype in NSCLC cells, and indicates $p27^{kip1}$ among target proteins that contribute to maintain cell sensitivity to TRAIL-induced cell death. Taken together these results indicate that even though miR-221 and -222 regulate the levels of both $p27^{kip1}$ and Kit proteins, their effects on TRAIL sensitivity are mainly mediated by $p27^{kip1}$. However, it seems plausible that silencing of other additional targets of miR-221 and -222 contributes to TRAIL resistance in NSCLC cells. miR-221- and -222-mediated downregulation of $p27^{kip1}$ has been implicated in maintaining a more aggressive cancer phenotype, thus indicating $p27^{kip1}$ as *bona fide* tumor suppressor (Galardi *et al*., 2007). $p27^{kip1}$ is a member of cdk inhibitory proteins with putative tumor suppressor functions (Sherr and Roberts, 1999). More recently, $p27^{kip1}$ has been described to play different roles depending on the cell type context and on its cytosolic or nuclear cellular localization (Blain *et al*., 2003; Coqueret, 2003). The functions of $p27^{kip1}$ in the apoptotic process remain unclear. Adenovirus-mediated transient overexpression of $p27^{kip1}$ was demonstrated to induce apoptosis in transfected cell (Craig *et al*., 1997; Katayose *et al*., 1997). Other reports describe p27 as antiapoptotic gene (St Croix *et al*., 1996; Eymin *et al*., 1999). Therefore, this suggests that the survival effects of $p27^{kip1}$ are cell-type specific and may be mediated by p27 effects on anti-apoptotic protein expression (Eymin *et al*., 1999; Woltman *et al*., 2003). Whether similar molecular mechanisms underlie the increase in TRAIL resistance upon silencing of $p27^{kip1}$ remains to be further investigated.

The role of miRs in the regulation of TRAIL signaling has been described, although not in lung cancer. Mott *et al*. (2007) described that miR-29b is able to regulate Mcl1-1 protein and thus TRAIL-mediated cytotoxicity in cholangiocarcinoma cell lines. Corsten *et al*. (2007) demonstrated that the combined effect of miR-21 antagonism and soluble TRAIL delivery in glioma cells leads to increase in caspase activity and cell death in glioma cells. More recently, Ovcharenko *et al*. (2007) described a genome-scale miRs and RNAi screen in breast cancer cells. They found a number of different miRs that target TRAIL signaling molecules. Interestingly, they have also found an interrelationship between cell cycle regulation and apoptosis signal transduction pathways.

In conclusion, our results demonstrate that the intracellular levels of few miRs may modulate sensitivity of NSCLC cells to a death receptor ligand with important implications in the design of new therapeutic agents.

Experimental procedures

Materials

Media, sera and antibiotics for cell culture were from Life Technologies, Inc. (Grand Island, NY, USA). Protein electrophoresis reagents were from Bio-Rad Laboratories (Richmond, VA, USA) and western blotting and ECL reagents from GE Healthcare (Piscataway, NJ, USA). All other chemicals were from Sigma (St Louis, MO, USA).

Cell culture

Human CALU-1 and A549 NSCLC cell lines were grown in Dulbecco's modified Eagle's medium containing 10% heat-inactivated fetal bovine serum (FBS) and with 2 mM L-glutamine and 100 U ml^{-1} penicillin–streptomycin. H460 and A459 cell lines were grown in RPMI containing 10% heat-inactivated FBS and with 2 mM L-glutamine and 100 U ml^{-1} penicillin–streptomycin.

Western blotting

Total proteins from CALU-1, A459, A549 and H460 cells were extracted with radioimmunoprecipitation assay (RIPA) buffer (0.15 mM NaCl, 0.05 mM Tris-HCl, pH 7.5, 1% Triton, 0.1% SDS, 0.1% sodium deoxycholate and 1% Nonidet P40). Sample extract (50 μg) was resolved on 7.5–12% SDS–polyacrylamide gels (PAGE) using a mini-gel apparatus (Bio-Rad Laboratories) and transferred to Hybond-C extra nitrocellulose. Membranes were blocked for 1 h with 5% nonfat dry milk in Tris-buffered saline containing 0.05% Tween 20, incubated for 2 h with primary antibody, washed and incubated with secondary antibody, and visualized by chemiluminescence. The following primary antibodies were used: Kit (R&D System, Minneapolis, MN, USA), and a secondary anti-goat immunoglobulin G (IgG) antibody peroxidase conjugate (Chemicon, Pittsburg, PA, USA); anti-TRAIL-R1,

-R2, -R3 and -R4 (Santa Cruz Inc., Santa Cruz, CA, USA), anti-$p27^{kip1}$ (Santa Cruz Inc), anti-caspase 8 (Cell Signaling, Danvers, MA, USA), anti-caspase 3 and anti-PARP (Santa Cruz Inc), anti-β-actin antibody (Sigma), anti-Mcl-1, anti-Bcl2,FADD (Santa Cruz), anti-FLIP (Alexis Biochemicals, Lausen, Switzerland). Expression levels were analysed with Scion Image.

FACS analysis

For flow cytometry analysis of cell surface Kit, cells were stained with primary antihuman h-SCFR affinity-purified goat IgG or mouse mAb 002 (isotype control, both from R&D Systems), followed by secondary antibody, Fluorescein-conjugated goat F(ab')2 (R&D Systems).

Cell death and cell proliferation quantification

Cells were plated in 96-well plates in triplicate and incubated at 37 °C in a 5% CO_2 incubator. Super-Killer TRAIL (Alexis Biochemicals) was used for 24–48 h at 400 ng ml^{-1}. Cell viability was evaluated with the CellTiter 96 AQueous One Solution Cell Proliferation Assay (Promega, Madison, WI, USA), according to the manufacturer's protocol. Metabolically active cells were detected by adding 20 µl of MTT to each well. After 2 h of incubation, the plates were analysed in a Multilabel Counter (Bio-Rad Laboratories). Apoptosis was assessed using annexin V–FITC apoptosis detection kits followed by flow cytometric analysis. Cells were seeded at 1.8×10^6 cells per 100 mm dish, grown overnight in 10% FBS/RPMI, washed with phosphate-buffered saline (PBS) and then treated for 24 h with 200 ng TRAIL. Following incubation, cells were washed with cold PBS and removed from the plates by trypsinization. The resuspended cells were washed with cold PBS and stained with FITC-conjugated annexin V antibody according to the manufacturer's instructions (Roche Applied Science, Indianapolis, IN, USA). Cells (50 000 per sample) were then subjected to flow cytometric analysis. Flow cytometry analyses were done as described (Garofalo *et al*., 2007). The fraction of H460 cells treated with TRAIL was taken as the apoptotic cell population. The percentage of apoptosis indicated was corrected for background levels found in the corresponding untreated controls.

RNA extraction and Northern blotting

Total RNA was extracted with TRIzol solution (Invitrogen, Carlsbad, CA, USA) and the integrity of RNA was assessed with an Agilent BioAnalizer 2100 (Agilent, Palo Alto, CA, USA). Northern blotting was performed as described (Calin *et al*., 2002). Total RNA (10 µg) from cell lines was loaded onto a precast 15% denaturing polyacrylamide gel (Bio-Rad). The RNA was then electrophoretically transferred to BrightStar blotting membranes (Ambion, Austin, TX, USA). The oligonucleotides used as probes were the complementary sequences of the mature miRNA (miRNA registry): miR-221, 5′-GAAACCCAGCAGACAATGTAGCT-3′; miR-222, 5′-GAGACCCAGTAGCCAGATGTAGCT-3′. miR probes were end-labeled with [γ-^{32}P]-ATP by T4 polynucleotide kinase (USB, Cleveland, OH, USA). Prehybridization and hybridization were carried out in Ultrahyb Oligo solution (Ambion) containing 10^6 c.p.m. per ml probes overnight at 37 °C. The most stringent wash was with 2 × SSC and 1% SDS at 37 °C. For reuse, blots were stripped by boiling and reprobed. As a loading control U6 rRNA was used. The image of Northern hybridization signals was produced by using Stormscanner and ImageQuant TL softwares (Molecular Dynamics, Sunnyvale, CA, USA).

miRNA microarray experiments

Total RNA (5 µg) from each sample was reverse transcribed using biotin end-labeled random octamer oligonucleotide primer. Hybridization of biotin-labeled complementary DNA was performed on a new Ohio State University custom miRNA microarray chip (OSU_CCC version 3.0), which contains 1150 miRNA probes, including 326 human and 249 mouse miRNA genes, spotted in duplicates. The hybridized chips were washed and processed to detect biotin-containing transcripts by streptavidin–Alexa647 conjugate and scanned on an Axon 4000B microarray scanner (Axon Instruments, Sunnyvale, CA, USA).

Raw data were normalized and analysed in Genespring 7.2 software (zcomSilicon Genetics, Redwood City, CA, USA). Expression data were median centered by using both the Genespring normalization option and the global median normalization of the Bioconductor package (www.bioconductor.org) with similar results. Statistical comparisons were done by using the Genespring ANOVA tool, Predictive Analysis of Microarray and the Significance Analysis of Microarray softwares (http://www-stat.stanford.edu/~tibs/SAM/index.html).

Real-time PCR

Real-time PCR was performed using a standard TaqMan PCR Kit protocol on a 7900HT Sequence Detection System (P/N 4329002, Applied Biosystems, Austin, TX, USA). The 10 µl PCR reaction included 0.67 µl RT product, 1 µl TaqMan Universal PCR Master Mix (P/N 4324018, Applied Biosystems), 0.2 mM TaqMan probe, 1.5 mM forward primer and 0.7 mM reverse primer. The reactions were incubated in a 96-well plate at 95 °C for 10 min, followed by 40 cycles of 95 °C for 15 s and 60 °C for 1 min. All reactions were run in triplicate. The threshold cycle (C_T) is defined as the fractional cycle number at which the fluorescence passes the fixed threshold. The comparative C_T method for relative quantization of gene expression (User Bulletin no. 2, Applied Biosystems) was used to determine miRNA expression levels. The y axis represents the $2^{(-\Delta C_T)}$, or the relative expression of the different miRs. miRs expression was calculated relative to 18S rRNA and multiplied by 10^4. Experiments were carried out in triplicate for each data point, and data analysis was performed by using software (Bio-Rad).

Transfection of Pre-miRs and anti-miR miRNA inhibitors in NSCLC cells

TRAIL-sensitive cell lines (H460) were cultured to 80% confluence in p60 plates with a serum-free medium without antibiotics and then transfected with 100 nmol of pre-miR-221 and -222 oligonucleotides or negative control for 48 h (Ambion). CALU-1 cells were cultured to 80% confluence in p60 plates with a serum-free medium without antibiotics. Total 100 nmol of 221 and 222 anti-miR inhibitors (Ambion) were transiently transfected in cells using Lipofectamine 2000 according to manufacturer's instructions. Cells were incubated in the presence of the specific anti-miR inhibitors and negative control (a random sequence anti-miR molecule) for 48 h. Subsequently, TRAIL-induced cell death was analysed as previously described.

Anti-p27^{kip1} siRNA transfection in NSCLC

H460 cells were cultured to 80% confluence and transiently transfected using Lipofectamine 2000 with anti-p27^{kip1} siRNA (Santa Cruz), a pool of four target-specific 20–25 nt siRNAs designed to knock down gene expression. p27^{kip1} siRNA (20 nmol) was transfected with 6 μl transfection reagent, as described in the manufacturer's protocol.

Statistical analysis

Continuous variables are expressed as mean values ± standard deviation (s.d.). The Student's *t*-test was used to determine the role of miRs, anti-miRs, Kit or p27 expression on NSCLC cells apoptosis. $P<0.05$ was considered significant.

Acknowledgements

This work was partially supported by funds from Associazione Italiana Ricerca sul Cancro, AIRC (GC), MIUR-FIRB (RBIN04J4J7), EU grant EMIL (European Molecular Imaging Laboratories Network) contract No. 503569. CQ is a recipient of Clinica Mediterranea Training program. GR is the recipient of SDN fellowship. We thank Dr Vittorio de Franciscis, Michael Latronico and Stefan Costinean for revision of this paper.

References

Blain SW, Scher HI, Cordon-Cardo C, Koff A. (2003). p27 as a target for cancer therapeutics. *Cancer Cell* **3**: 111–115.

Brown JM, Attardi LD. (2005). The role of apoptosis in cancer development and treatment response. *Nat Rev Cancer* **5**: 231–237.

Calin GA, Croce CM. (2006). MicroRNA signatures in human cancers. *Nat Rev Cancer* **6**: 857–866.

Calin GA, Dumitru CD, Shimizu M, Bichi R, Zupo S, Noch E *et al*. (2002). Frequent deletions and down-regulation of micro-RNA genes miR15 and miR16 at 13q14 in chronic lymphocytic leukemia. *Proc Natl Acad Sci USA* **99**: 15524–15529.

Calin GA, Ferracin M, Cimmino A, Di Leva G, Shimizu M, Wojcik SE *et al*. (2005). A microRNA signature associated with prognosis and progression in chronic lymphocytic leukemia. *N Engl J Med* **353**: 1793–1801.

Chen CZ, Li L, Lodish HF, Bartel DP. (2004). MicroRNAs modulate hematopoietic lineage differentiation. *Science* **303**: 83–86.

Cheng AM, Byrom MW, Shelton J, Ford LP. (2005). Antisense inhibition of human miRNAs and indications for an involvement of miRNA in cell growth and apoptosis. *Nucleic Acids Res* **33**: 1290–1297.

Coqueret O. (2003). New roles for p21 and p27 cell-cycle inhibitors: a function for each cell compartment? *Trends Cell Biol* **13**: 65–70.

Corsten MF, Miranda R, Kasmieh R, Krichevsky AM, Weissleder R, Shah K. (2007). MicroRNA-21 knockdown disrupts glioma growth *in vivo* and displays synergistic cytotoxicity with neural precursor cell delivered S-TRAIL in human gliomas. *Cancer Res* **67**: 8994–9000.

Craig C, Wersto R, Kim M, Ohri E, Li Z, Katayose D *et al*. (1997). A recombinant adenovirus expressing p27^{kip1} induces cell cycle arrest and loss of cyclin-Cdk activity in human breast cancer cells. *Oncogene* **14**: 2283–2289.

Dresios J, Aschrafi A, Owens GC, Vanderklish PW, Edelman GM, Mauro VP. (2005). Cold stress-induced protein Rbm3 binds 60S ribosomal subunits, alters microRNA levels, and enhances global protein synthesis. *Proc Natl Acad Sci USA* **102**: 1865–1870.

Eymin B, Sordet O, Droin N, Munsch B, Haugg M, Van de Craen M *et al*. (1999). Caspase-induced proteolysis of the cyclin-dependent kinase inhibitor p27^{kip1} mediates its anti-apoptotic activity. *Oncogene* **18**: 4839–4847.

Falschlehner C, Emmerich CH, Gerlach B, Walczak H. (2007). TRAIL signalling: decisions between life and death. *Int J Biochem Cell Biol* **39**: 1462–1475.

Felli N, Fontana L, Pelosi E, Botta R, Bonci D, Facchiano F *et al*. (2005). MicroRNAs 221 and 222 inhibit normal erythropoiesis and erythroleukemic cell growth via kit receptor down-modulation. *Proc Natl Acad Sci USA* **102**: 18081–18086.

Fulda S, Meyer E, Debatin KM. (2000). Metabolic inhibitors sensitize for CD95 (APO-1/Fas)-induced apoptosis by down-regulating Fas-associated death domain-like interleukin 1-converting enzyme inhibitory protein expression. *Cancer Res* **60**: 3947–3956.

Galardi S, Mercatelli N, Giorda E, Massalini S, Frajese GV, Ciafrè SA *et al*. (2007). miR-221 and miR-222 expression affects the proliferation potential of human prostate carcinoma cell lines by targeting p27^{kip1}. *J Biol Chem* **282**: 23716–23724.

Garofalo M, Romano G, Quintavalle C, Romano MF, Chiurazzi F, Zanca C *et al*. (2007). Selective inhibition of PED protein expression sensitizes B-cell chronic lymphocytic leukaemia cells to TRAIL-induced apoptosis. *Int J Cancer* **120**: 1215–1222.

Ghobrial IM, Witzig TE, Adjei AA. (2005). Targeting apoptosis pathways in cancer therapy. *CA Cancer J Clin* **55**: 178–194.

He H, Jazdzewski K, Li W, Liyanarachchi S, Nagy R, Volinia S *et al*. (2005). The role of microRNA genes in papillary thyroid carcinoma. *Proc Natl Acad Sci USA* **102**: 19075–19080.

Johnson SM, Grosshans H, Shingara J, Byrom M, Jarvis R, Cheng A *et al*. (2005). RAS is regulated by the let-7 microRNA family. *Cell* **120**: 635–647.

Katayose Y, Kim M, Rakkar AN, Li Z, Cowan KH, Seth P. (1997). Promoting apoptosis: a novel activity associated with the cyclin-dependent kinase inhibitor p27. *Cancer Res* **57**: 5441–5445.

Koschny R, Walczak H, Ganten TM. (2007). The promise of TRAIL-potential and risks of a novel anticancer therapy. *J Mol Med* **85**: 923–935.

le Sage C, Nagel R, Egan DA, Schrier M, Mesman E, Mangiola A *et al*. (2007). Regulation of the p27(^{kip1}) tumor suppressor by miR-221 and miR-222 promotes cancer cell proliferation. *EMBO J* **26**: 3699–3708.

Liu CG, Calin GA, Meloon B, Gamliel N, Sevignani C, Ferracin M *et al*. (2004). An oligonucleotide microchip for genome-wide microRNA profiling in human and mouse tissues. *Proc Natl Acad Sci USA* **101**: 9740–9744.

Mott JL, Kobayashi S, Bronk SF, Gores GJ. (2007). mir-29 regulates Mcl-1 protein expression and apoptosis. *Oncogene* **26**: 6133–6140.

Ovcharenko D, Kelnar K, Johnson C, Leng N, Brown D. (2007). Genome-scale microRNA and small interfering RNA screens identify small RNA modulators of TRAIL-induced apoptosis pathway. *Cancer Res* **67**: 10782–10788.

Poliseno L, Tuccoli A, Mariani L, Evangelista M, Citti L, Woods K *et al*. (2006). MicroRNAs modulate the angiogenic properties of HUVECs. *Blood* **108**: 3068–3071.

Poy MN, Eliasson L, Krutzfeldt J, Kuwajima S, Ma X, Macdonald PE *et al*. (2004). A pancreatic islet-specific microRNA regulates insulin secretion. *Nature* **432**: 226–230.

Schaefer U, Voloshanenko O, Willen D, Walczak H. (2007). TRAIL: a multifunctional cytokine. *Front Biosci* **12**: 3813–3824.

Sempere LF, Freemantle S, Pitha-Rowe I, Moss E, Dmitrovsky E, Ambros V. (2004). Expression profiling of mammalian microRNAs uncovers a subset of brain-expressed microRNAs with possible roles in murine and human neuronal differentiation. *Genome Biol* **5**: R13.

Sherr CJ, Roberts JM. (1999). CDK inhibitors: positive and negative regulators of G_1-phase progression. *Genes Dev* **13**: 1501–1512.

Smirnova L, Grafe A, Seiler A, Schumacher S, Nitsch R, Wulczyn FG. (2005). Regulation of miRNA expression during neural cell specification. *Eur J Neurosci* **21**: 1469–1477.

St Croix B, Flørenes VA, Rak JW, Flanagan M, Bhattacharya N, Slingerland JM *et al*. (1996). Impact of the cyclin-dependent kinase inhibitor $p27^{kip1}$ on resistance of tumor cells to anticancer agents. *Nat Med* **2**: 1204–1210.

Tamborini E, Bonadiman L, Negri T, Greco A, Staurengo S, Bidoli P *et al*. (2004). Detection of overexpressed and phosphorylated wild-type kit receptor in surgical specimens of small cell lung cancer. *Clin Cancer Res* **10**: 8214–8219.

Walczak H, Krammer PH. (2000). The CD95 (APO-1/Fas) and the TRAIL (APO-2L) apoptosis systems. *Exp Cell Res* **256**: 58–66.

Walczak H, Miller RE, Ariail K, Gliniak B, Griffith TS, Kubin M *et al*. (1999). Tumoricidal activity of tumor necrosis factor-related apoptosis-inducing ligand *in vivo*. *Nat Med* **5**: 157–163.

Woltman AM, van der Kooij SW, Coffer PJ, Offringa R, Daha MR, van Kooten C. (2003). Rapamycin specifically interferes with GM-CSF signaling in human dendritic cells, leading to apoptosis via increased $p27^{kip1}$ expression. *Blood* **101**: 1439–1445.

Xu P, Guo M, Hay BA. (2004). MicroRNAs and the regulation of cell death. *Trends Genet* **20**: 617–624.

Xu P, Vernooy SY, Guo M, Hay BA. (2003). The *Drosophila* microRNA Mir-14 suppresses cell death and is required for normal fat metabolism. *Curr Biol* **13**: 790–795.

OPEN ACCESS Freely available online

PLoS one

Akt Regulates Drug-Induced Cell Death through Bcl-w Downregulation

Michela Garofalo[1,2☯], Cristina Quintavalle[1,3☯], Ciro Zanca[1], Assunta De Rienzo[5], Giulia Romano[4], Mario Acunzo[1,3], Loredana Puca[1], Mariarosaria Incoronato[4], Carlo M. Croce[2], Gerolama Condorelli[1,3,6]*

1 Department of Cellular and Molecular Biology and Pathology, "Federico II" University of Naples, Naples, Italy, **2** Department of Molecular Virology, Immunology and Medical Genetics, Human Cancer Genetics Program, Comprehensive Cancer Center, The Ohio State University, Columbus, Ohio, United States of America, **3** IEOS, CNR, Naples, Italy, **4** Fondazione SDN, Naples, Italy, **5** IRGS, Biogem s.c.ar.l., Ariano Irpino (AV), Italy, **6** Facoltà di Scienze Biotecnologiche, "Federico II" University of Naples, Naples, Italy

Abstract

Akt is a serine threonine kinase with a major role in transducing survival signals and regulating proteins involved in apoptosis. To find new interactors of Akt involved in cell survival, we performed a two-hybrid screening in yeast using human full-length Akt c-DNA as bait and a murine c-DNA library as prey. Among the 80 clones obtained, two were identified as Bcl-w. Bcl-w is a member of the Bcl-2 family that is essential for the regulation of cellular survival, and that is up-regulated in different human tumors, such as gastric and colorectal carcinomas. Direct interaction of Bcl-w with Akt was confirmed by immunoprecipitation assays. Subsequently, we addressed the function of this interaction: by interfering with the activity or amount of Akt, we have demonstrated that Akt modulates the amount of Bcl-w protein. We have found that inhibition of Akt activity may promote apoptosis through the downregulation of Bcl-w protein and the consequential reduction in interaction of Bcl-w with pro-apoptotic members of the Bcl-2 family. Our data provide evidence that Bcl-w is a new member of the Akt pathway and that Akt may induce anti-apoptotic signals at least in part through the regulation of the amount and activity of Bcl-w.

Citation: Garofalo M, Quintavalle C, Zanca C, De Rienzo A, Romano G, et al. (2008) Akt Regulates Drug-Induced Cell Death through Bcl-w Downregulation. PLoS ONE 3(12): e4070. doi:10.1371/journal.pone.0004070

Editor: Neil Hotchin, University of Birmingham, United Kingdom

Received June 10, 2008; **Accepted** November 22, 2008; **Published** December 30, 2008

Funding: This work was partially supported by funds from: Associazione Italiana Ricerca sul Cancro, AIRC (G.C.), MIUR-FIRB (RBIN04J4J7), EU grant EMIL (European Molecular Imaging Laboratories Network) contract No 503569. The funders had no role in study design, data collection and analysis, decision to publish, or preparation of the manuscript. C.Q. is a recipient of Clinica Mediterranea- Federico II FiXO Training program. G.R. is recipient of Fondazione SDN fellowship. We wish to thank Dr. Vittorio de Franciscis and Michael Latronico for paper revision, and Maria Fiammetta Romano and Simona Romano for their help with FACS analysis.

Competing Interests: The authors have declared that no competing interests exist.

* E-mail: gecondor@unina.it

☯ These authors contributed equally to this work.

Introduction

Akt is a serine–threonine kinase downstream of PTEN/PI3K, involved in cellular survival pathways [1,2]. In mammalian cells, the three Akt family members, Akt1/PKBα, Akt2/PKBβ, and Akt3/PKBγ are encoded by three different genes [3,4]. They are ubiquitously expressed, although their levels are variable, depending upon the tissue type and pathological/physiological state. Increased expression or activation of Akt has been described as a frequent phenomena in human cancer [1,5,6]. Akt has been demonstrated to phosphorylate a number of proteins involved in apoptotic signaling cascades, including the Bcl-2 family member BAD [7], pro-caspase 9 [4], the forkhead transcription factors, FKHR and FKHRL1 [8,9], and p21 cipWAF1. Phosphorylation of these proteins prevents apoptosis through several mechanisms [10]. Apoptosis, or programmed cell death, is an evolutionarily conserved mechanism of elimination of unwanted cells [11]. Apoptosis is triggered via two principal signaling pathways [12]. The extrinsic pathway is activated by the engagement of death receptors on the cell surface [13]. The other pathway is triggered by various intracellular and extracellular stresses, such as growth–factor withdrawal, hypoxia, DNA damage, and anticancer therapy [13,14]. Intrinsic-pathway induced-apoptosis is generally regulated by the fine balance of Bcl-2 family proteins in a cell- and tissue-specific manner [11]. Apoptosis is believed to be the major mechanism responsible for chemotherapy-induced cell death in cancer. However, tumor cells often retain the ability to evade drug-induced death signals because of the activation of anti-apoptotic mechanisms [15–17]. Understanding these evading mechanisms is a first step needed for the design of rational anticancer therapy. Therefore, we decided to address the role of Akt in apoptosis resistance in human cancer by finding new partners involved in resistance to cell death. To this end, we performed a two hybrid screening in yeast using human full-length Akt c-DNA as bait and a murine c-DNA library as prey. Among the possible interactors of Akt, we decided to focus on Bcl-w, a member of the Bcl-2 family. Biochemical experiments confirmed the interaction of Akt with Bcl-w. Further, we demonstrate that Akt modulates the half-life of Bcl-w. We also found that Bcl-w is a substrate of Akt and, more importantly, that Akt regulates its anti-apoptotic activity and interaction with some of the pro-apoptotic members of the Bcl-2 family.

Methods

Materials

Media, sera, and antibiotics for cell culture were from Life Technologies, Inc. (Grand Island, NY, USA). Protein electropho-

resis reagents were from Bio-Rad (Richmond, VA, USA), and Western blotting and ECL reagents were from GE Healthcare. All other chemicals were from Sigma (St. Louis, MO, USA).

Plasmids

Plasmids pEF FLAG(hs) Bcl-w , pEF EE Bax, pEF EE Bik, pEF EE Bad cDNAs were kindly provided by Elisabeth Cory and David Huang laboratories (Victoria, Australia). Akt wild type (HA-Akt, cDNA), Akt E40 K (constitutively active Akt cDNA, HA-Akt-D+) and Akt K179M (dominant negative Akt cDNA, HA-Akt-D-) were a kind gift of Prof. G.L. Condorelli (University of Rome "La Sapienza").

Cell culture

Human HeLa and HEK-293 cell lines were grown in DMEM containing 10% heat-inactivated FBS and with 2 mM L-glutamine and 100 U/ml penicillin-streptomycin.

Yeast Two-hybrid System

All experiments were performed in the yeast reporter MaV203. The cDNA library was synthesized from rat FRTL-5 cell poly(A)$^+$ RNA plasmid by Life Technologies and cloned into the pPC86GAL4AD vector, and was kindly provided by Prof. Roberto Di Lauro (Naples, Italy). Screening of the library was performed essentially following instructions for the ProQuest two-hybrid system (Life Technologies) and has been previously described [18]. The GAL4 DNA-binding domain/hAkt fusion was obtained from Dr. Alfonso Bellacosa (Fox Chase Cancer Centre, Philadelphia, Pennsylvania, USA). Subsequently, yeast pLEx4-Akt plasmid was transformed with the pPC86AD-cDNA library and plated onto plates lacking histidine in the presence of 3AT (aminotriazole; 10 mM). Approximately 1.2×10^6 individual clones were plated, and about 200 grew on the selective medium. Resistant colonies were grown on a master plate and then replica-plated onto selection plates to determine their ability to induce three independent reporters (*HIS3*, *URA3*, and *lacZ*). Eighty independent clones were isolated after this first screening. DNA was isolated from each positive clone and sequenced to identify the inserts. Independent pPC86AD clones were retransformed into yeast and tested for interaction with a fresh Akt clone.

Generation of Bcl-w deletion mutants

We generated by PCR two deletion mutants of Bcl-w cDNA, using as template the plasmid pEF FLAG Bcl-w: the following primers were used for the bclw-BH4 mutant, which included only the N-terminal BH4 domain (45 aa): BH4-For-HINDIII:cccaagctt-atggactacaaagacgatgacgataaag and BH4-Rev-Xba1: gctcta-gaggcttggtgcagcgggtc; the following primers were used for CT-Bcl-w, which included the remaining coding sequence of 97aa: CT-For-HINDIII: cccaagcttcccagcagctgacccgct and CT-Rev-Xba1: gctctagatcacttgctagcaaaaaaggccc.

Temperature cycles were the following: 95°C 1 minute; 95°C 50 seconds, 60°C 50 seconds, 68°C 7 minutes for 35 cycles; 68°C 2 minutes. The amplified sequences were cloned in p3X-Flag-CMV previously linearized with the restriction enzymes HINDIII and XbaI.

Generation of stable transfectants

HeLa cells were transfected with 4 μg of Flag-Bcl-w cDNA using lipofectamine 2000 according to the manufacturer's protocol (InVitrogen, Carlsbad, CA). After 48 hr of transfection, cells were selected using a medium containing 10% FBS, 2 mMol L-glutammine, 100 U/ml pen/strep, and 3.75 μg/ml of puromicine. After 15 days the clones were isolated and maintained in culture with 2.5 μg/ml of puromicine. Twenty colonies were isolated and tested through western blot to verify the expression of the construct.

Western blotting

Total protein from HeLa and HEK 293 cells was extracted with RIPA buffer (0.15 mM NaCl, 0.05 mM Tris-HCl, pH 7.5, 1% Triton, 0.1% SDS, 0.1% sodium deoxycolate and 1% Nonidet P40). Fifty μg of sample extract were resolved on 7.5–12% SDS-polyacrylamide gels using a mini-gel apparatus (Bio-Rad Laboratories, Richmond, CA) and transferred to Hybond-C extra nitrocellulose. Membranes were blocked for 1 hr with 5% non-fat dry milk in TBS containing 0.05% Tween-20, incubated over night with primary antibody, washed and incubated with secondary antibody, and visualized by chemiluminescence. The following primary antibodies were used: Anti Flag M2 and anti-β-actin antibody from Sigma (St. Louis, MO, USA), anti HA and anti EE from Covance (Berkeley,CA USA); anti Bcl-w from Abcam (Cambridge, MA); anti-Akt, -Phospho Akt substrate, -phospho ser473 Akt from Cell signalling (Danvers, MA USA); anti-Bcl2, -BAD, -BIK and -BAX from Santa Cruz, Inc (Santa Cruz, CA USA), caspase -9 and -3 from Cell Signaling (Danvers, MA USA), and PARP antibodies from Santa Cruz (Santa Cruz, CA USA).

Phosphorylation experiments

In order to study Bcl-w phosphorylation in intact cells, 293 cells were transiently transfected with different Akt cDNAs constructs as indicated. After 24 h, the cells were rinsed with 150 mM NaCl and incubated in serum-free culture medium for 16 h at 37°C. Insulin (final concentration, 100 nM) or 20% serum was then added, and the cells were rapidly rinsed with ice-cold saline followed by solubilization with 0.5 ml of RIPA buffer per dish for 1 hr at 4°C. Lysates were centrifuged at 5,000×g for 20 min, and solubilized proteins were precipitated with the indicated antibodies, separated by SDS-PAGE, and revealed by western blot with the anti-Akt substrate antibody that recognizes all the phosphorylated Akt substrates (Cell Signaling, Danvers, MA USA). Phospho-(Ser/Thr) Akt Substrate Antibody preferentially recognizes peptides and proteins containing phospho-Ser/Thr preceded by Lys/Arg at positions −5 and −3. Some cross-reactivity has been described for peptides that contain phospho-Ser/Thr preceded by Arg/Lys at positions −3 and −2, thus recognizing also a low-stringency Akt kinase motif.

Immunoprecipitation

Cells were cultured at a final concentration of 90% in p100 plates. The cells were harvested with RIPA Buffer on a shaker for 30 minutes. 1 mg of total extract was immunoprecipitated using the indicated antibodies (5 μg/ml Anti-FLAG, 2 μg/ml Anti-HA, 3 μg/ml anti-Akt, 5 μg/ml anti-Bcl-w, 3 μg/ml anti-EE), for 16 hrs on shaker. Then, A/G beads (Santa Cruz, Santa Cruz, CA USA) were added for two hrs. The beads were washed for three times with washing buffer (50 mM Tris Hcl pH 7.5, 150 mM NaCl, 0.1% Triton, 10% glycerol), and then 20 μl of sample buffer was added; the samples were boiled at 100°C for 5 minutes and then the supernatants resolved by SDS-PAGE.

Cytosol/mitochondria separation

Cells were grown in p100 plates and the mitochondrial and cytoplasmic fractions isolated using the Mitochondria/Cytosol Fractionation Kit (Biovision San Francisco, CA USA) according to the manufacturer's protocol.

Akt Kinase Assay

Akt activity was assayed in vitro as previously reported [19]. Briefly, HEK-293 cells were transfected with 4 μg of Flag-Bcl-w cDNA. 1 mg of total cell extract was immunoprecipitated using an anti-FLAG antibody (Sigma) and A/G beads (SantaCruz, Santa Cruz, CA USA) for 18 hr. The beads were incubated in a kinase reaction mixture containing 20 mM HEPES [pH 7.2], 1 mM $MgCl_2$, 10 mM $MnCl_2$,1 mM dithiothreitol, 5 mM ATP, 0.2 mM EGTA, 1 mM protein kinase inhibitor, 10 μCi of [γ–^{32}P]ATP, and 2 μg of rAkt (Cell signaling, Danvers, MA USA) for 30 minutes at room temperature. The samples were boiled at 100°C for 5 minutes, centrifuged and the supernatant loaded on a 12.5% maxi protean gel (BioRad, Richmond VA, USA). The gel was run overnight and then visualized by autoradiography.

Cell death and cell proliferation quantification

Cells were plated in 96-well plates in triplicate and incubated at 37°C in a 5%CO_2 incubator. Different chemotherapics (30 mg/ml cisplatin, 10 mg/ml epirubicin) were added for 24 hrs to the medium. Cell viability was evaluated with the CellTiter 96® Aqueous One Solution Cell Proliferation Assay (Promega, Madison, WI), according to the manufacturer's protocol. Metabolically active cells were detected by adding 20 μl of MTT to each well. After 2 h of incubation, the plates were analyzed in a Multilabel Counter (Bio-Rad, Richmond, VA, USA). Apoptosis was assessed using PI (propidium iodide)-FITC staining followed by flow cytometric analysis. Cells were seeded at 1.8×10^6 cells per 100 mm dish, grown overnight in 10% FBS/DMEM, washed with PBS, then treated for 24 hours with chemotherapics. Following incubation, cells were washed with cold PBS and removed from the plates by mild trypsinization. The resuspended cells were washed with cold PBS and stained with PI-FITC staining according to the instructions provided by the manufacturer (Roche Applied Science, Indianapolis, IN). Cells (50,000 per sample) were then subjected to flow cytometric analysis. Flow cytometry analysis were done as described [20]. The percentage of apoptosis indicated was corrected for background levels found in the corresponding untreated controls.

siRNA transfection

HeLa cells were cultured to 80% confluence and transiently transfected using LIPOFECTAMINE 2000 with 100 nM anti-Akt

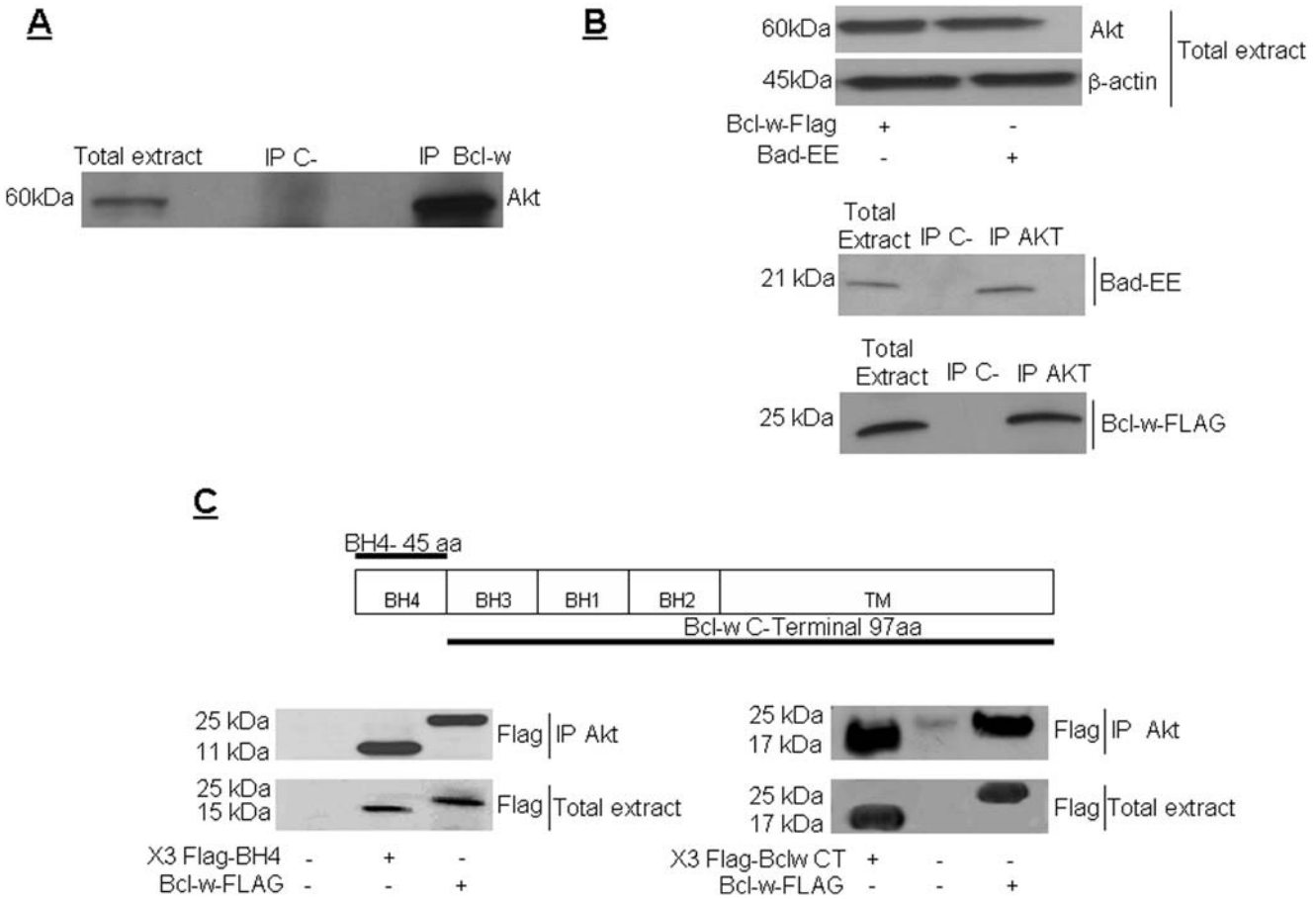

Figure 1. Akt interacts with Bcl-w. (A) Co-immunoprecipitation of endogenous Akt with Bcl-w. Wt HeLa cells were lysed and 1 mg of protein extract immunoprecipitated using an anti-Bcl-w antibody. Immunoprecipitates and total lysates (50 μg) were separated on 12%SDS polyacrilamide gel and blotted with an anti-Akt antibody. As negative control, proteins were incubated with beads without antibody **(B)** Co-immunoprecipitation of transfected Akt with FLAG-Bcl-w or EE-BAD. HEK-293 cells were tansfected with 2 μg of HA-Akt and 2 μg of FLAG-Bcl-w or EE-BAD cDNAs, as indicated. After 48 hr, cells were lysed, and 1 mg of protein extract was immunoprecipitated using an anti-HA antibody. Immunoprecipitates were subsequently blotted with anti-HA, anti-Flag or anti-EE antibodies, as indicated. **(C)** HEK-293 cells were transfected with 2 μg of either wt-Bcl-w cDNA or the deletion mutants, Bcl-w/BH4 or Bcl-w/CT, as indicated. Protein extracts were immunoprecipitated using an anti-Akt antibody. Immunoprecipitates and total lysates were resolved on 12%SDS-PAGE and transferred to Hybond-C nitrocellulose. Membranes were incubated with an anti-FLAG antibody. Both deletion mutants, Bclw/BH4 and Bclw/CT, immunoprecipitated with Akt.
doi:10.1371/journal.pone.0004070.g001

siRNA (Dharmacon, Lafayette, CO USA), a pool of 4 target-specific 20–25 nt siRNAs, or 150 nM anti-Bcl-w si-RNA (InVitrogen, Carlsbad, CA) with 6 µl transfection reagent, as described in the manufacturer's protocol.

Results

Akt interacts with Bcl-w

To find new interactors of Akt, we performed a yeast two-hybrid screening with human full-length Akt c-DNA sequence as bait and a murine c-DNA thyroid library as prey. Among the 100 clones obtained, two were identified as Bcl-w, covering its full coding sequence. To confirm the interaction between Akt and Bcl-w, we immunoprecipitated proteins from untreated, Akt-transfected, and Bcl-w-transfected cells with an anti-Bcl-w antibody. We found that Akt co-immunoprecipitates with Bcl-w in extracts from untransfected and transfected cells (Figure 1A and 1B). The extent of Akt binding with Bcl-w was comparable to that with its substrate, Bad (Figure 1B).

Bcl-w contains four Bcl-2 homology (BH) domains and a transmembrane (TM) fragment at the C-terminal region, important for its insertion into the mitochondrial outer membrane. We verified whether these regions are important for the interaction with Akt. For this, HA-Akt cDNA was transfected together with one of two Bcl-w domain-region cDNAs obtained by PCR and fused to the FLAG epitope: these were the BH4 domain (45 aa) of Bcl-w, located at the N-terminus, and the remaining portion of the protein (97aa). Extracts were immunoprecipitated with an anti-Flag antibody and blotted with an anti-HA antibody. We found that Akt interacts with both Bcl-w deletion mutants, indicating that Akt may interact with Bcl-w at multiple sites (Figure 1C).

Role of Akt activation on Akt/Bcl-w interaction

To find whether the activity of Akt influences its interaction with Bcl-w, HeLa cells were transfected either with wild type Akt (Akt wt) cDNA or with one of two mutants: an HA-tagged kinase dead-Akt construct (Akt D−) with dominant negative functions, and a constitutively active Akt construct (Akt D+). Protein extracts were immunoprecipitated with a monoclonal anti-HA antibody and then blotted with an anti-FLAG antibody. We found that Bcl-w interacts with wild type Akt and more efficiently with the activated kinase, but not with the kinase-dead Akt (Figure 2A).

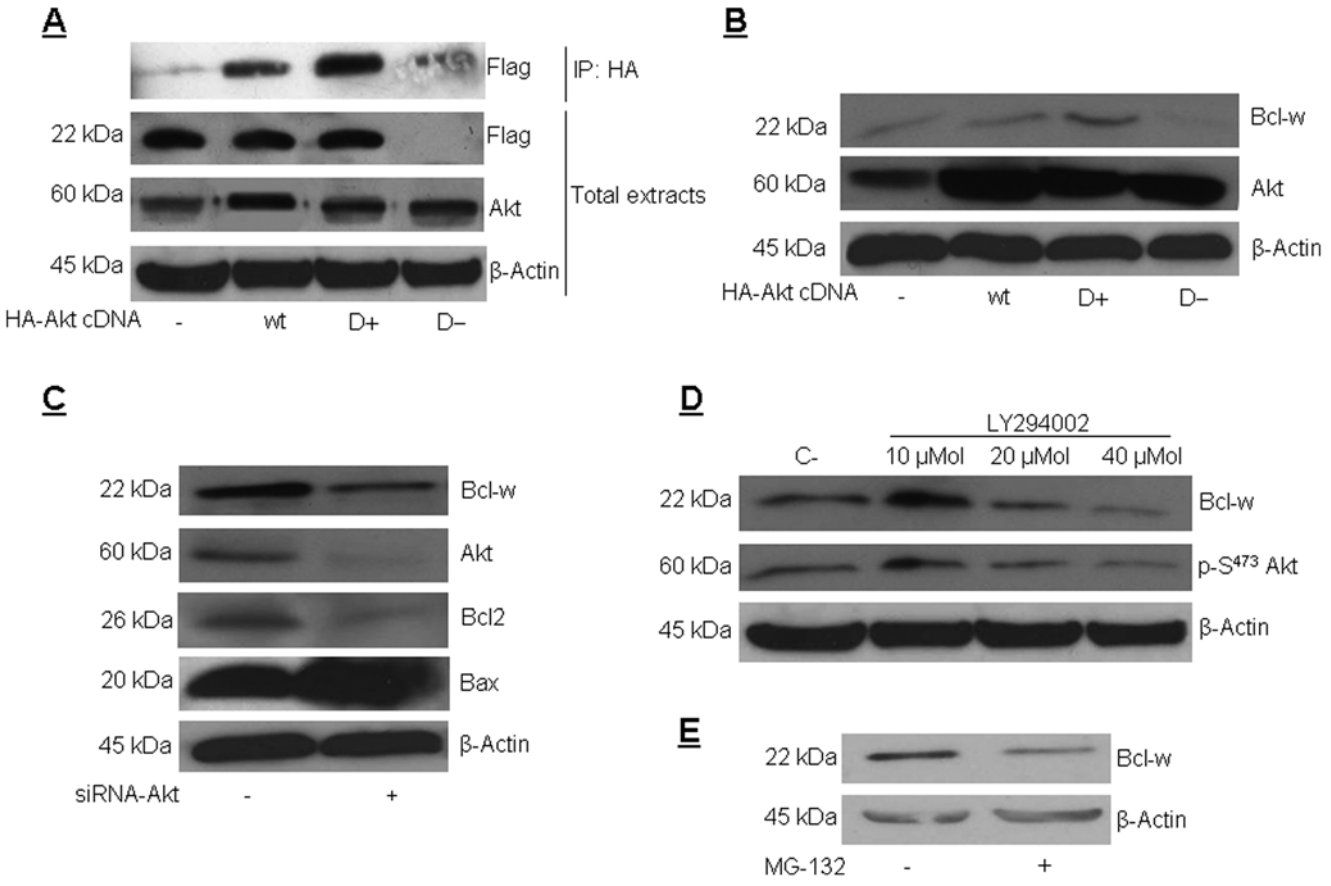

Figure 2. Akt activity regulates Bcl-w expression. (A) HeLa cells were transfected with 2 µg of HA-Akt wt, Akt D+, or HA-Akt D− cDNA and 2 µg Flag-Bcl-w for 48 hrs. Protein extracts were immunoprecipitated with an anti-HA monoclonal antibody. Immunoprecipitates were resolved on 12% SDS-PAGE and transferred to Hybond-C nitrocellulose. Membranes were incubated with anti-Flag antibody (0.2 µg/ml). 50 µg of total sample extracts were also analyzed by western blot using the indicated antibodies. Loading control was obtained using anti-β actin antibody. **(B)** HeLa cells were transfected with 4 µg of HA-Akt wt, HA-Akt D+, or HA-Akt D− cDNA for 48 hrs. Protein extracts were blotted with anti-Bcl-w antibody in order to detect endogenous levels of Bcl-w. Loading control was obtained with anti-β actin antibody. **(C)** Cells were transfected with 100 nM of siAkt-RNA for 48 hrs. Cellular proteins were solubilized and analyzed by western blot using the indicated antibodies. **(D)** HeLa cells were treated with 10, 20 or 40 µM of LY294002 for 24 hrs. Protein extracts were analyzed by western blot using the indicated antibodies. Loading control was obtained using anti-β actin antibody. **(E)** Bcl-w HeLa cells were treated with 10 µM of MG-132 for 8 hrs. 40 µg of protein extracts were analyzed by western blot with anti-Bcl-w antibodies. Loading control was obtained using anti-β actin antibody.
doi:10.1371/journal.pone.0004070.g002

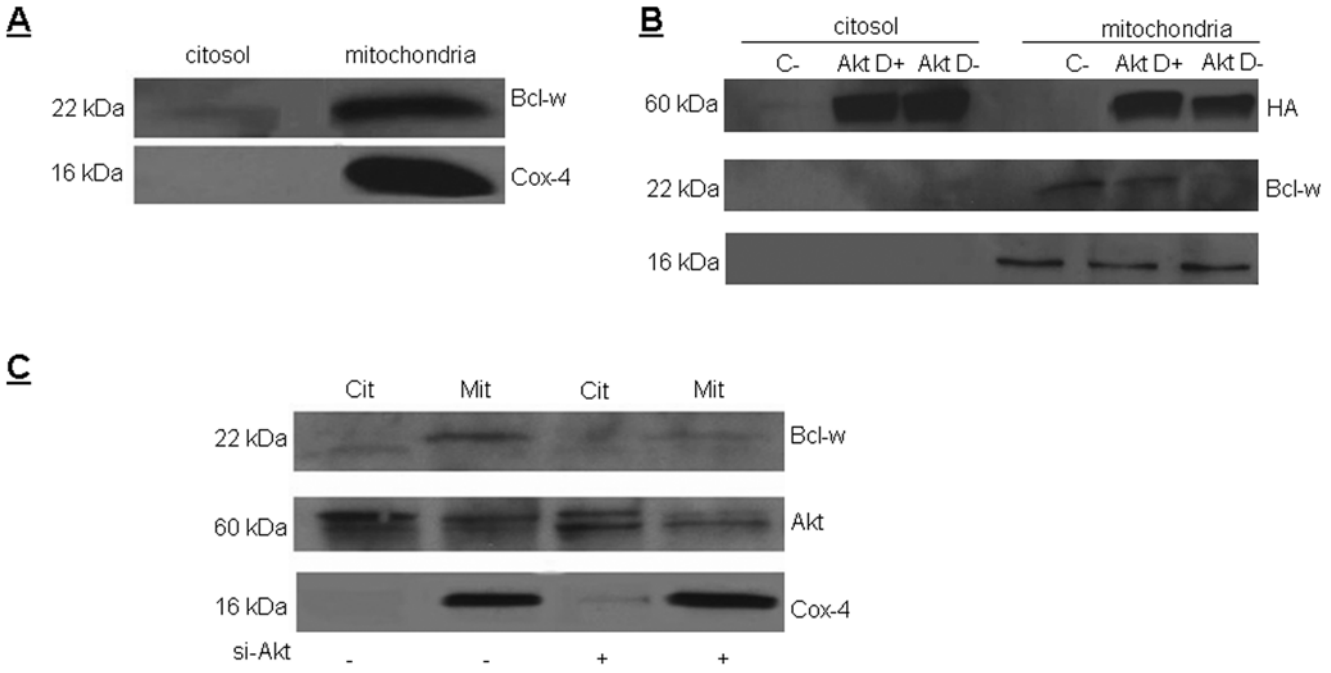

Figure 3. Akt controls Bcl-w localization. (A) HeLa cells were subjected to fractionated separation of mitochondrial/cytosolic proteins using a mitochondria/cytosol fractionation kit (Biovision). Protein extracts were loaded onto 15% SDS polyacrilamide gel, and analyzed by western blot by anti-Bcl-w antibody. As a control of the mitochondrial fraction, an anti-cox4 antibody was used. **(B)** HeLa cells were transfected with 2 μg of HA-Akt WT, D+, or D− for 48 hrs. Cells were subjected to mitochondria/cytosol separation as above. Protein extracts were analyzed by western blot using anti-Bcl-w, anti-Akt, or anti-cox4 antibodies. **(C)** Cells were transfected with 100 nM of siAkt-RNA for 48 hrs. Cytosol and mitochondria were isolated as described in the methods and analyzed by western blot using the indicated antibodies.
doi:10.1371/journal.pone.0004070.g003

Akt regulates Bcl-w expression

When we transfected cells with Akt D−, we noticed a fall in the expression of Bcl-w (Figure 2A). Therefore, lack of interaction between Bcl-w and the kinase-dead Akt could have been due to reduced expression of Bcl-w rather than to poor interaction with Akt D−. To address this issue, we inhibited Akt in three different ways: by interfering with its endogenous function; by treating cells with Akt-siRNA; and by inhibiting the PI3K/Akt pathway with a specific drug. In order to interfere with endogenous Akt activity, we transfected cells with the previously described Akt mutant cDNAs (Akt wt, Akt D+, and Akt D−). We found that Bcl-w was reduced after transfection with inactive Akt, whereas Bcl-w expression increased upon transfection with Akt D+ (Figure 2B). In order to knock down endogenous Akt, HeLa cells were transfected with a pool of Akt siRNAs. We found that endogenous Akt expression, analyzed by Western blot, was reduced by >80% after 48 hrs. This reduction in Akt expression was followed by a drastic reduction in the level of Bcl-w. Moreover, the expression of the anti-apoptotic protein, Bcl-2, but not of the pro-apoptotic protein, Bax, was also reduced (Figure 2C). Finally, incubation of HeLa cells with 10, 20 or 40 μM of LY294002, a specific inhibitor of the PI3K pathway, resulted in reduced amount of Bcl-w protein (Figure 2D). All these results provide evidence that the kinase activity of Akt regulates the expression of Bcl-w.

To gain insight on the mechanism of Akt-mediated Bcl-w regulation, we treated Bcl-w/HeLa cells with the proteasome inhibitor, MG-132, for 8 hrs and then analyzed Bcl-w levels by western blot (Figure 2E). The inhibition of the proteasome did not result in an increase in Bcl-w expression, suggesting that the ubiquitin pathway is not directly involved in the regulation of Bcl-w by Akt.

Role of Akt in Bcl-w subcellular localization

Bcl-w is an anti-apoptotic protein weakly linked to the outer mitochondrial membrane [21]. To verify its intracellular localization, extracts of HeLa cells were fractionated to isolate mitochondria from the cytosol. We found that Bcl-w is present mainly in mitochondrial protein extracts (Figure 3A). To clarify the role of Akt in determining Bcl-w cellular localization, HeLa cells were transfected with Akt wt, Akt D+, or Akt D− cDNAs before fractional separation. We found that the presence of the kinase-dead Akt mutant reduced the amount of Bcl-w linked to the mitochondrial fraction and induced only a slight increase in the cytosolic one (Figure 3B). Similar results were obtained in cells transfected with Akt siRNA (Figure 3C). Thus, Akt acts mainly on Bcl-w expression.

Akt phosphorylates Bcl-w

Akt is a serine threonine kinase that phosphorylates different pro- and anti-apoptotic proteins. Thus, in vitro and in vivo phosphorylation assays were performed to uncover whether Bcl-w is a substrate of Akt. For in vitro assays, cells were transfected with Flag-Bcl-w and the extracts obtained immunoprecipitated using a monoclonal anti-Flag antibody. Immunoprecipitates were incubated with a constitutively active Akt recombinant protein in the presence of $\gamma P^{32}ATP$. We found that Akt phosphorylates Bcl-w in vitro, although not with the same efficiency as histone H2B (Figure 4A).

To study the effects of Akt kinase activity on Bcl-w phosphorylation in intact cells, we generated HeLa cells that stably expressed Flag-Bcl-w (HeLa/Bcl-w). HeLa/Bcl-w cells were stimulated with insulin or 10% serum for 15 min, and protein extracts then immunoprecipitated using an anti-Flag antibody and

blotted with an anti-phospho (Ser/Thr) Akt substrate antibody that recognizes the Akt substrate motif. We found that the phosphorylated band corresponding to Bcl-w immunoprecipitates upon stimulation with serum or insulin. These results taken together provide evidence that Bcl-w may be a substrate of Akt both in vitro and in intact cells (Figure 4B).

In turn, to investigate whether Bcl-w overexpression regulates Akt kinase activity, HEK293 cells were co-transfected with Flag-Bcl-w and HA-tagged Gsk3β, one of the main Akt substrates. 48 hours after transfection, the cells were stimulated with insulin for 10 min, cellular extracts immunoprecipitated with an anti-HA antibody, and then immunoblotted with an antibody that recognizes the phosphorylated form of Gsk3β. We did not find a change in the extent of Gsk3β phosphorylation by overexpressing Bcl-w (Figure 4C). Therefore, Bcl-w binds to Akt and is a direct substrate of Akt; however, this binding does not alter the activity of Akt on other substrates.

Role of Bcl-w/Akt interaction on cell death

Given that Bcl-w is an anti-apoptotic member of the Bcl-2-family, we investigated the role of Akt activity on this function. We first analyzed the effect of Bcl-w overexpression in preventing apoptosis induced by two different chemotherapics, i.e. cisplatin and epirubicin, in HeLa/Bcl-w compared to parental untransfected HeLa cells. Cells were treated with 30 μg/ml cisplatin or with 10 μg/ml epirubicin for 24 hr. Cell death was assessed with a cell viability assay, with propidium iodide staining followed by FACS analysis, or by caspase 9, −3, and PARP activation. We found that HeLa/Bcl-w cells were 80–90% resistant to cell death induced by the chemotherapics. This was confirmed by analysis of the activation state of the intrinsic apoptotic pathway (caspase 9, −3, and PARP) (Figure 5A).

To test the role of Akt activity on the antiapoptotic function of Bcl-w, we repeated the above experiments in Bcl-w/HeLa cells transfected for 48 hr either with Akt D− cDNA or with Akt siRNAs. We found that the inhibition of Akt kinase activity or protein quantity resulted in a strong activation of the downstream effector PARP (Figure 5 b, left panel), that is partially reflected as reduction of pro-survival effect of Bcl-w (∼20%) (Figure 5B). Thus, Akt activity mediates the anti-apoptotic function at least in part by regulating the intracellular levels of Bcl-w. Given that inhibiting Akt results in a reduction of Bcl-w levels, these results suggest that Akt may contribute to Bcl-w protective effects mainly by regulating its intracellular levels.

To further confirm this, we down-regulated Bcl-w expression with two specific Bcl-w-siRNAs, and analyzed the effects of Bcl-w down-regulation on chemotherapy-induced cell death. We found that 72 hrs of incubation with Bcl-w siRNAs drastically reduced Bcl-w protein (Figure 6 A) although to different extents (siRNA61 was more effective than siRNA62). The assessment of cell viability

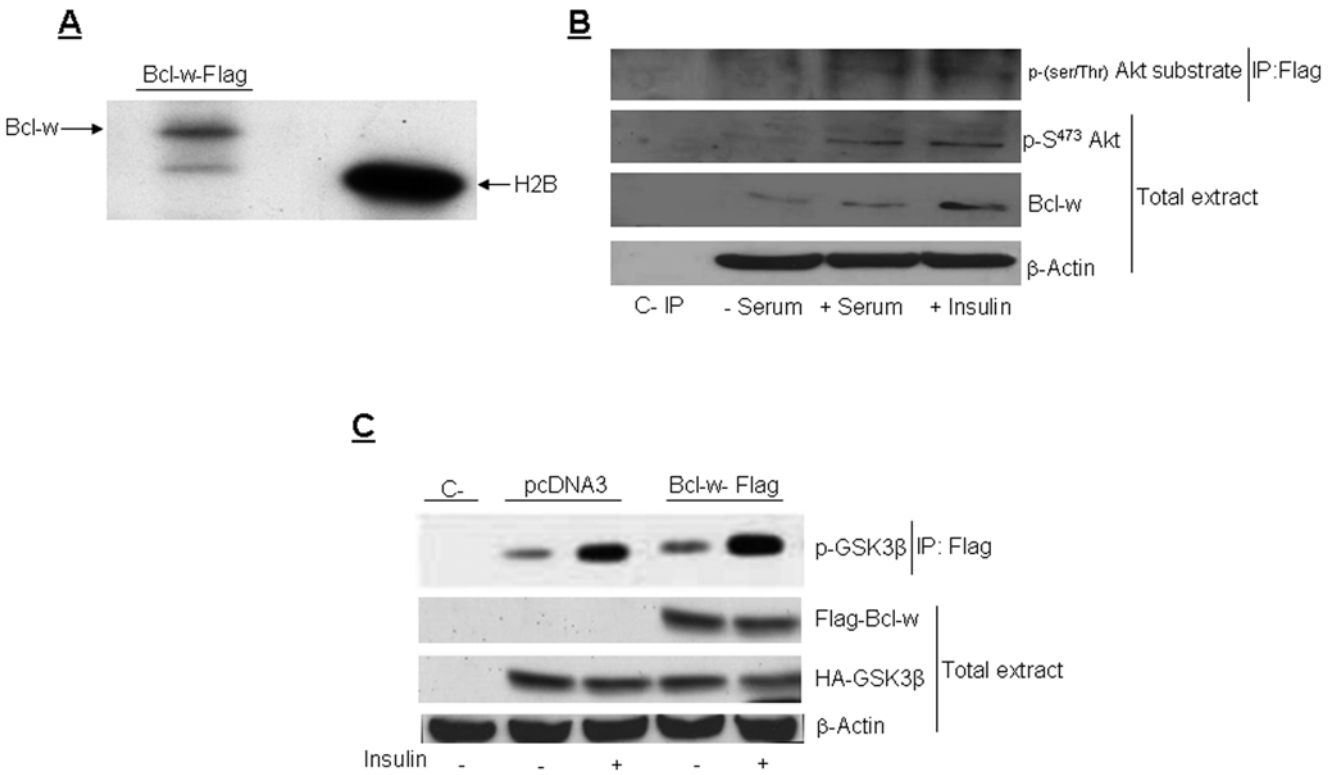

Figure 4. Akt phosphorylates Bcl-w in vitro and in vivo. (A) HeLa cells were transfected with 2 μg of DNA of Flag Bcl-w, solubilized, and 1 mg of protein extract was immunoprecipitated with an anti-M2 Flag antibody. Immunoprecipitates were incubated with recombinant constitutive active Akt (rAkt), and in vitro kinase assay was conducted as described in the methods. Samples were loaded onto 2.5% SDS-PAGE and analyzed by autoradiography. As positive control we used Histone2B (H2B). **(B)** HeLa Bcl-w stable expressing clones were serum starved for 18 hrs and then stimulated with 100 nM insulin or with 20% serum for 15 min as indicated. Cells were solubilized and immunoprecipitated with an anti-M2 Flag antibody. Immunoprecipitates were loaded onto SDS-PAGE and blotted with an anti-phospho Akt substrate antibody that recognizes all the phosphorylated Akt substrates. Total extracts were analyzed by western blot using the indicated antibodies. **(C)** HeLa cells were transfected with 2 μg of pcDNA3 empty vector or 2 μg of HA-GSK3β, and 2 μg of Flag-Bcl-w for 48 hrs. Cells were stimulated with 100 nM insulin for 15 min, solubilized, immunoprecipitated using an anti-HA antibody, and analyzed by western blot using an anti-phospho-Gsk3 antibody. Total extracts were analyzed by western blot using the indicated antibodies. Bcl-w overexpression does not affect Akt activity.
doi:10.1371/journal.pone.0004070.g004

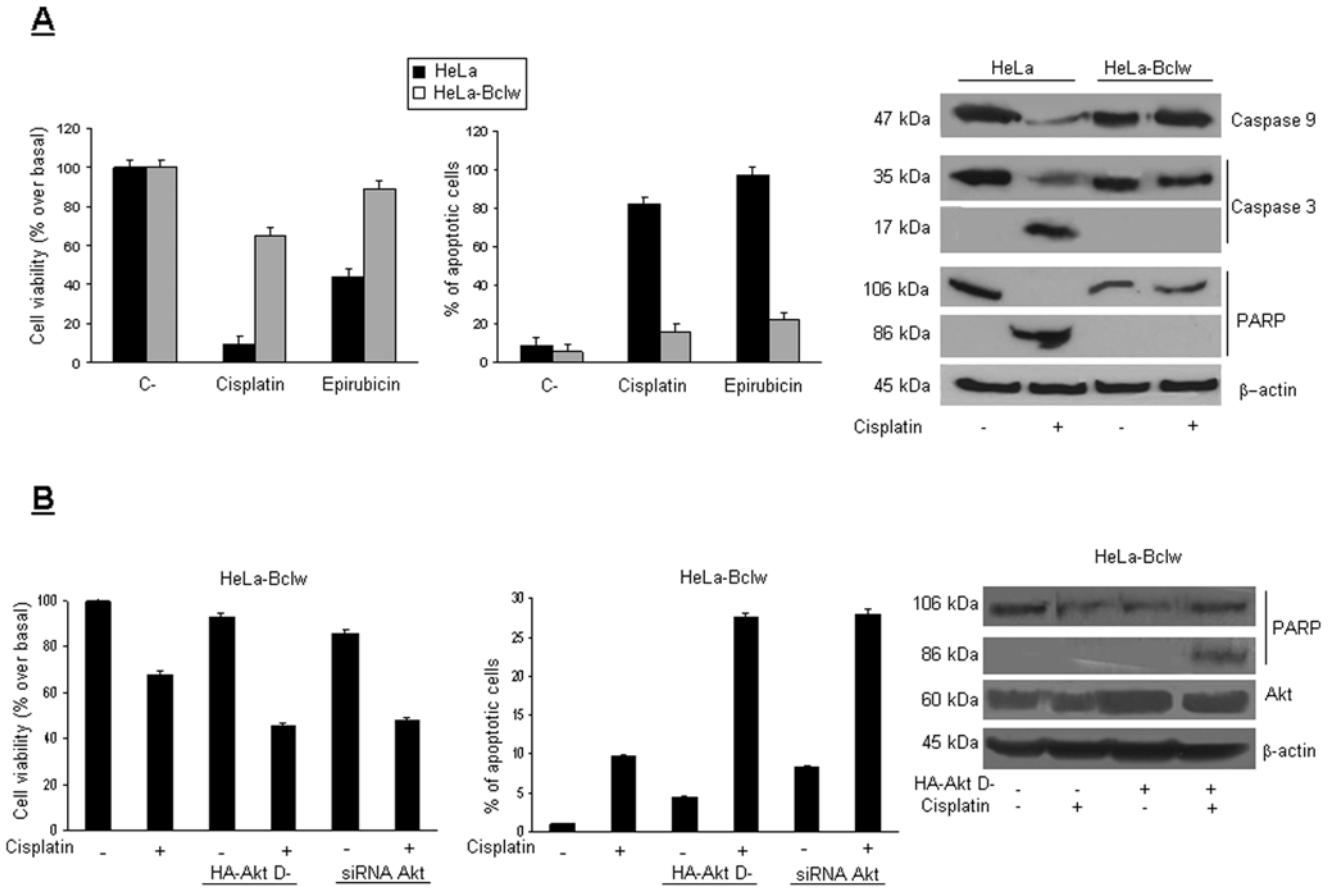

Figure 5. Akt regulates the anti-apoptotic function of Bcl-w. (A) HeLa control cells and HeLa cells stably expressing Flag-Bcl-w were plated in 96 well plates in triplicate and treated with 30 μg/ml of cisplatin or 10 μg/ml of epirubicin for 24 hr. Apoptosis was analyzed by Cell Vitality assay, by propidium iodide staining and FACS analysis, or by western blot for caspase cascade activation with anti-caspase-3, -9, and PARP antibodies. Loading control was obtained with anti β-actin. **(B)** HeLa-Flag Bcl-w cells were transfected with 4 μg of HA-Akt D− cDNA or with 100 nM of siAkt-RNA for 48 hrs and then treated with 30 μg/ml of cisplatin for 24 hr. Cell death was then analyzed as described above. Total lysates were analyzed by western blot using an anti-PARP antibody. Loading control was obtained with an anti-β-actin antibody. Inactivation of Akt activity resulted in a reduction in the protective effect of Bcl-w on cell death.
doi:10.1371/journal.pone.0004070.g005

(Figure 6B) and of apoptotic cells (Figure 6C) provided evidence that the effect of cell death induced by chemotherapics was proportional to the expression of Bcl-w. Furthermore, by reducing Bcl-w level, we obtained the same ~20% increase in cell death that we observed in HeLa cells treated with Akt siRNA. Thus, the reduction in Bcl-w expression secondary to Akt inactivation contributes to the resistance of cancer cells to chemotherapy-induced cell death.

Akt regulates Bcl-w interaction with Bcl-2 family members

The intrinsic apoptotic pathway is regulated by the net interactions of pro- and anti-apoptotic Bcl-2 members [22]. To evaluate the effect of Akt activity on the interaction of Bcl-w with the pro-apoptotic Bcl-2 members, we set up co-immunoprecipitation experiments with Bcl-w and Bad, Bik, or Bax in cells overexpressing the dominant negative Akt cDNA. We found that Akt inactivation resulted in a drastic reduction of Bcl-w interaction with the pro-apoptotic proteins (Figure 7). This further confirms the stimulatory role of Akt activity on Bcl-w anti-apoptotic function.

Discussion

Apoptosis is believed to be the major mechanism of chemotherapy-induced cell death in cancer [23,24]. Unfortunately, many tumour cells evade drug-induced death signals [25]. Akt is an important survival-signaling molecule, whose function is frequently found altered in human cancer [5,26]. Therefore, we decided to address the role of Akt in apoptosis resistance in human cancer by finding new partners of Akt by two hybrid screening in yeast. Among the interactors of Akt that we found, we focused on Bcl-w, a pro-survival member of the Bcl-2 protein family [27,28] that has received less attention compared to its other family members. By genetic and biochemical methods, we have demonstrated here that Akt interacts with the N- and C-terminal sequences of the Bcl-w protein, and phosphorylates Bcl-w both in vitro and in the intact cell. The analysis of the Bcl-w sequence did not reveal a canonical Akt phosphorylation motif [29]. However, there is evidence that Akt may phosphorylate cellular substrates at the level of a partially conserved sequence motif [29]. Bcl-w posses at least 6 serine/threonines that are included in "degenerated" Akt phosphorylation sites. By site-directed mutagenesis, we mutated two of these sites (ser 62 and ser 83) substituting the serine with an alanine (data

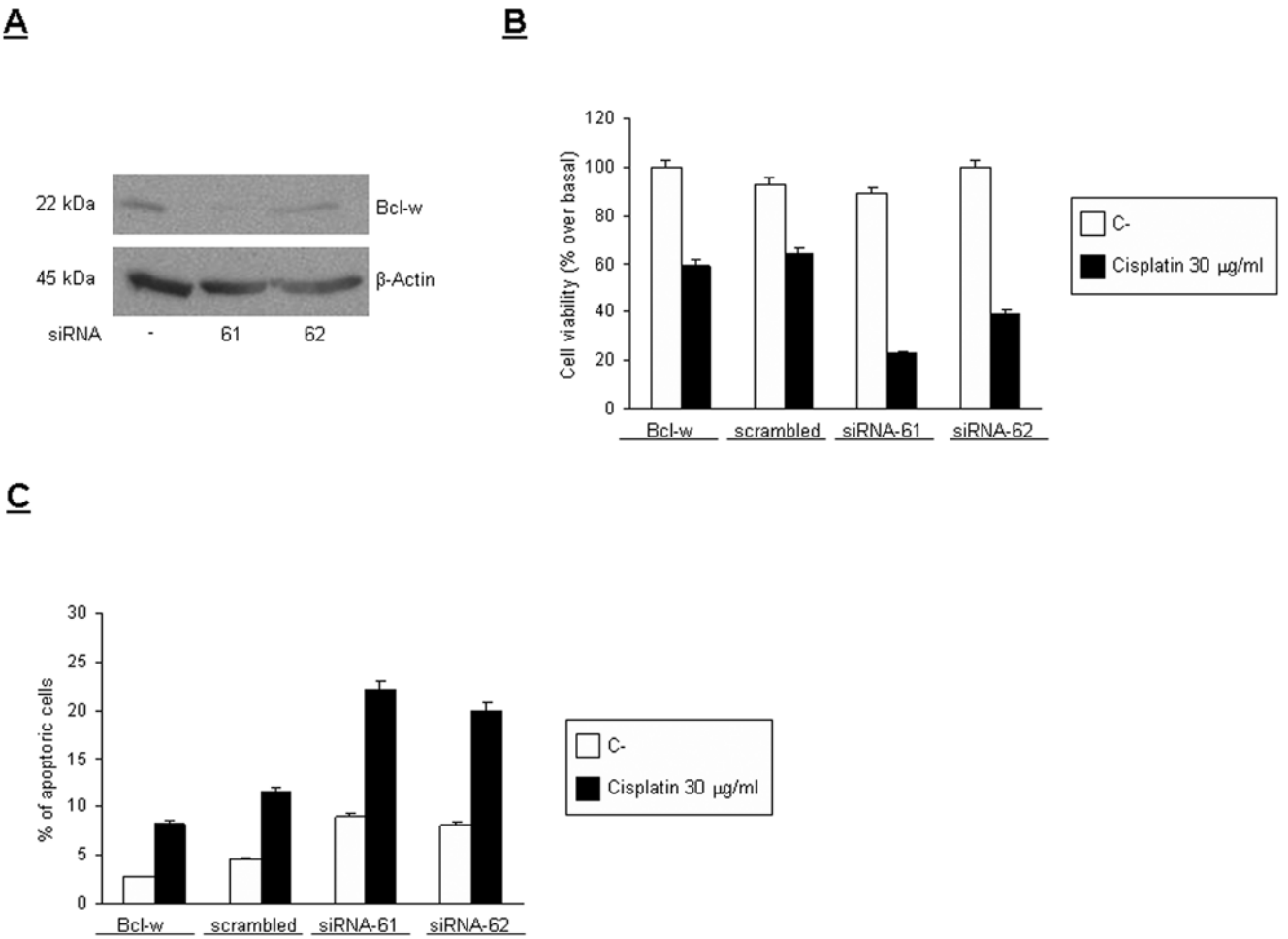

Figure 6. Effects of Bcl-w si RNA on cell death. (A) Cells were transfected with 150 nM of siBcl-w-RNAs for 72 hrs. Total lysates were analyzed by western blot using anti-Bcl-w antibodies. Loading control was obtained with an anti-β-actin antibody. **(B, C)** Cells were transfected with 150 nM of siBcl-w-RNAs for 48 hrs. Then, the cells were splitted into 96 wells and then treated with 30 μg/ml of cisplatin for 24 hr. Cell death was then analyzed with MTT **(B)** or propidium iodide staining and FACS analysis **(C)**. Bcl-w down-regulation induces an increase of cell death.
doi:10.1371/journal.pone.0004070.g006

not shown). These mutations did not result in a change of Bcl-w phosphorylation state, so the hypothetical Akt phosphorylation site must be located elsewhere. We are now addressing this issue.

We have also demonstrated here that interfering with the activity or amount of Akt reduces the quantity of Bcl-w protein; oppositely, transfection of a dominant active Akt mutant increased the content of Bcl-w in cells.

Akt-mediated Bcl-w down-regulation was observed to occur also in glioma (data not shown). Thus, Akt affects Bcl-w function in various cell types at least in part by regulating its expression. The mechanisms underlying this are not clear, but the regulation of Bcl-w protein levels is unlikely mediated by the ubiquitin-proteasome pathway, as evidenced by the negative result obtained with a proteasome inhibitor. Furthermore, Akt inhibition did not produce an effect on Bcl-w mRNA, as evaluated by Real Time PCR (data not shown). Other possible Akt-mediated regulatory effects on RNA or protein stability are under investigation in our laboratory.

Several studies have suggested that Akt may regulate the balance between pro- and anti-apoptotic signals, at least in part by regulating the cellular localization of Bcl-2 family members [30,31]. Thus, in this study we have analyzed the effect of Akt activation on the subcellular localization of Bcl-w. We found Bcl-w predominantly associated with the mitochondrial fraction, as previously described also by O'Reilly et al. [32]. The presence of the kinase-dead Akt mutant reduced the amount of Bcl-w linked to this fraction, but it did not increase Bcl-w in the cytosol; we obtained similar results with cells transfected with Akt siRNA. Thus, via binding and phosphorylating Bcl-w, Akt may control Bcl-w activity mainly through the regulation of Bcl-w protein expression. We are conducting experiments with Bcl-w phosphorylation mutants to formally prove this conclusion.

Moreover, with the intent to clarify the role of Akt-mediated regulation of Bcl-w on its anti-apoptotic functions, we established a Bcl-w overexpressing cell line. These cells exhibit a significant decrease of chemotherapy-mediated cell death. When we evaluated the effects of decreasing Akt activity on survival in Bcl-w/HeLa cells, we found a ~20% increase in cell death. However, when we analyzed cell death by western blot of PARP activation, the active PARP fragment was present exclusively in Bcl-w/HeLa cells incubated with Akt D− cDNA. Thus, even though the differences that we observe with FACS analysis and cell vitality are of small entity, the end point, that is cell death evaluated as PARP activation, is reached only in Bcl-w cells where Akt has been inactivated.

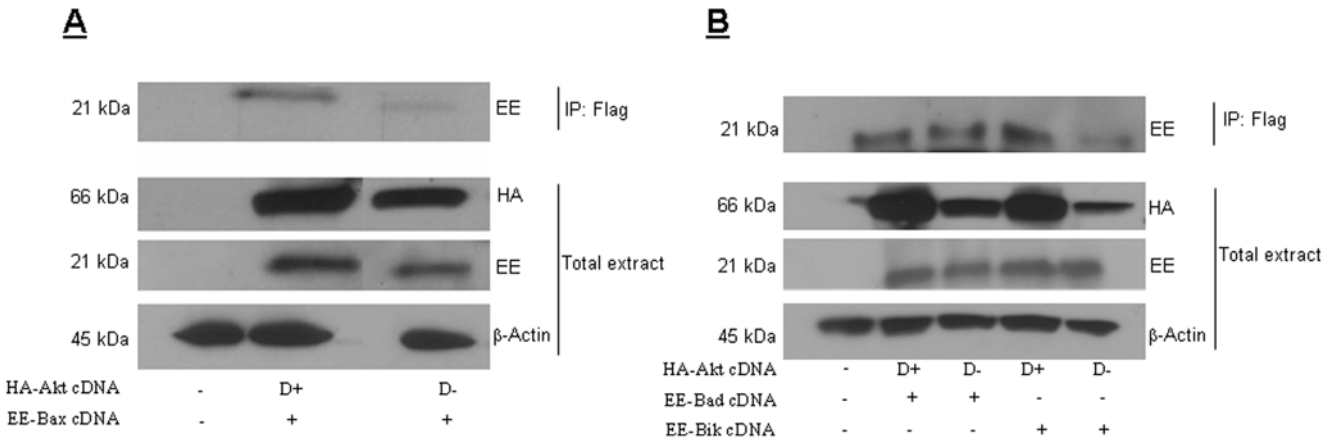

Figure 7. (A) Akt activity regulates Bcl-w interaction with Bcl-2 family members. Flag-Bcl-w/HeLa cells were transfected with 2 μg of either HA-Akt D+ or HA-Akt D− cDNA, and 2 μg of EE-Bax cDNA for 48 hr. Cells were harvested and 1 mg of total lysate immunoprecipitated using an anti-Flag antibody. The immunoprecipitates were then blotted with an anti-EE antibody. Total protein was normalized using anti-EE, -HA or -β-actin antibodies, as indicated. **(B)** Flag Bcl-w/HeLa cells were transfected with 2 μg of HA-Akt D+ or HA-Akt D− cDNA, and 2 μg of either EE-Bad or EE-Bik cDNA, as indicated, for 48 hr. Cells were harvested and 1 mg of total lysate immunoprecipitated using anti-Flag antibody. The immunoprecipitates were then blotted with an anti-EE antibody. Total protein was normalized using anti-EE, -HA or -β-actin antibodies, as indicated. Inactivation of Akt induced a reduction of Bcl-w interaction with the pro-apoptotic Bcl-2 members.
doi:10.1371/journal.pone.0004070.g007

On the other hand, our data provide evidence that Bcl-w is not the only defense mechanism of the cell toward chemotherapy-induced apoptosis, and many other Bcl-2 family members may mediate anti-apoptotic signals. Therefore, downregulation of Akt may result in a pronounced efficacy in cancer cells were Bcl-w predominates over the other Bcl-2 family members [33–35].

When appropriate stimuli are present, homodimerization of pro-apoptotic members of the Bcl-2 family activates the intrinsic apoptotic cascade. Bcl-w interacts with pro-apoptotic members of the Bcl-2 family, such as Bad, Bax, and Bik, blocking the formation of the homodimers and, thus, the activation of the apoptotic cascade. Events that inhibit the formation of these Bcl-w/pro-apoptotic Bcl-2 member complexes may lead to the activation of apoptosis [36]. We show here that Bcl-w/Bax, Bcl-w/Bad, and Bcl-w/Bik interactions were drastically reduced in cells overexpressing dominant-inactive Akt cDNA, indicating that Akt activity is necessary for these interactions. Therefore, Akt may regulate the anti-apoptotic function of Bcl-w, reducing its amount in the cell and, thus, impairing the balance of homo- and heterodimer formation upon apoptotic stimuli.

Bcl-w can be up-regulated in tumors such as gastric and colorectal cancer [33–35]. Interestingly, the PI3k-Akt pathway is involved in the progression and chemoresistance of these types of cancer [37–39]. Therefore, increased Akt activity can be speculated to promote survival and anti-apoptotic signaling in cancer cells at least in part through increasing Bcl-w levels. Recently, Bcl-w was reported to promote gastric cancer cell invasion, by inducing matrix metalloproteinase-2 expression [34]. Bcl-w is up-regulated also through pathways besides the Akt one: Tran et al. demonstrated that Bcl-w can be up-regulated via the NFkB pathway activated by TWEAK (tumor necrosis factor-like weak inducer of apoptosis) through stimulation of its receptor, Fn14; moreover, the TWEAK-Fn14 pathway can induce survival of glioma cells, at least in part by up-regulating the quantity of Bcl-w protein [40]. In addition, Yao et al. reported that up-regulation of Bcl-w protein mediates the neuroprotective effect of estrogens [41]. Therefore, Bcl-w participates in a number of different systems that regulate survival and anti-apoptotic pathways.

The results that we have presented here provide the first evidence that Akt interacts with, and regulates the levels of, Bcl-w, moving the balance of the Bcl-2 family toward anti-apoptotic members. Enhancement of this Akt/Bcl-w anti-apoptotic pathway can be speculated as one mechanism responsible for the reduced sensitivity to apoptosis of cancer cells that are resistant to chemotherapy-induced cell death. This finding may be of importance in optimizing a strategy for the treatment of cancers, such as gastric and colon adenocarcinoma, in which Bcl-w has been found to be increased.

Author Contributions

Conceived and designed the experiments: MG GC. Performed the experiments: MG CQ CZ ADR GR MA LP MI. Contributed reagents/materials/analysis tools: CC. Wrote the paper: GC.

References

1. Manning BD, Cantley LC (2007) AKT/PKB signaling: navigating downstream. Cell 129: 1261–1274.
2. Song G, Ouyang G, Bao S (2005) The activation of Akt/PKB signaling pathway and cell survival. J Cell Mol Med 9: 59–71.
3. Bellacosa A, Franke TF, Gonzalez-Portal ME, Datta K, Taguchi T, et al. (1993) Structure, expression and chromosomal mapping of c-akt: relationship to v-akt and its implications. Oncogene 8: 745–754.
4. Datta SR, Brunet A, Greenberg ME (1999) Cellular survival: a play in three Akts. Genes Dev 13: 2905–2927.
5. Yoeli-Lerner M, Toker A (2006) Akt/PKB signaling in cancer: a function in cell motility and invasion. Cell Cycle 5: 603–605.
6. Toker A, Yoeli-Lerner M (2006) Akt signaling and cancer: surviving but not moving on. Cancer Res 66: 3963–3966.
7. Datta SR, Dudek H, Tao X, Masters S, Fu H, et al. (1997) Akt phosphorylation of BAD couples survival signals to the cell-intrinsic death machinery. Cell 91: 231–241.
8. Tang ED, Nuñez G, Barr FG, Guan KL (1999) Negative regulation of the forkhead transcription factor FKHR by Akt. J Biol Chem 274: 16741–16746.
9. Kops GJ, de Ruiter ND, De Vries-Smits AM, Powell DR, Bos JL, et al. (1999) Direct control of the Forkhead transcription factor AFX by protein kinase B. Nature 398: 630–634.
10. Blume-Jensen P, Hunter T (2001) Oncogenic kinase signalling. Nature 411: 355–365.
11. Danial NN, Korsmeyer SJ (2004) Cell death: critical control points. Cell 116: 205–219.
12. Hengartner MO (2000) The biochemistry of apoptosis. Nature 407: 770–776.

13. Okada H, Mak TW (2004) Pathways of apoptotic and non-apoptotic death in tumour cells. Nat Rev Cancer 4: 592–603.
14. Ghobrial IM, Witzig TE, Adjei AA (2005) Targeting apoptosis pathways in cancer therapy. CA Cancer J Clin 55: 178–194.
15. Reed JC (2003) Apoptosis-targeted therapies for cancer. Cancer Cell 3: 17–22.
16. Kelley SK, Ashkenazi A (2004) Targeting death receptors in cancer with Apo2L/TRAIL. Curr Opin Pharmacol 4: 333–339.
17. Longley DB, Johnston PG (2005) Molecular mechanisms of drug resistance. J Pathol 205: 275–292.
18. Missero C, Pirro MT, Simeone S, Pischetola M, Di Lauro R (2001) The DNA glycosylase T:G mismatch-specific thymine DNA glycosylase represses thyroid transcription factor-1-activated transcription. J Biol Chem 276: 33569–33575.
19. Dudek H, Datta SR, Franke TF, Birnbaum MJ, Yao R, et al. (1997) Regulation of neuronal survival by the serine-threonine protein kinase Akt. Cell 275: 661–665.
20. Garofalo M, Romano G, Quintavalle C, Romano MF, Chiurazzi F, et al. (2007) Selective inhibition of PED protein expression sensitizes B-cell chronic lymphocytic leukaemia cells to TRAIL-induced apoptosis. Int J Cancer 120: 1215–1222.
21. Kaufmann T, Schinzel A, Borner C (2004) Bcl-w(edding) with mitochondria. Trends Cell Biol 14: 8–12.
22. Strasser A, O'Connor L, Dixit VM (2000) Apoptosis signaling. Annu Rev Biochem 69.
23. Johnstone RW, Ruefli AA, Lowe SW (2002) Apoptosis: a link between cancer genetics and chemotherapy. Cell 108: 153–164.
24. Houghton JA (1999) Apoptosis and drug response. Curr Opin Oncol 11: 475–481.
25. Igney FH, Krammer PH (2002) Death and anti-death: tumour resistance to apoptosis. Nat Rev Cancer 2: 277–288.
26. Plas DR, Thompson CB (2005) Akt-dependent transformation: there is more to growth than just surviving. Oncogene 24: 7435–7442.
27. Russell LD, Warren J, Debeljuk L, Richardson LL, Mahar PL, et al. (2001) Spermatogenesis in Bclw-deficient mice. Biol Reprod 65: 318–332.
28. Gibson L, Holmgreen SP, Huang DC, Bernard O, Copeland NG, et al. (1996) bcl-w, a novel member of the bcl-2 family, promotes cell survival. Oncogene 13: 665–675.
29. Trencia A, Perfetti A, Cassese A, Vigliotta G, Miele C, et al. (2003) Protein kinase B/Akt binds and phosphorylates PED/PEA-15, stabilizing its antiapoptotic action. Mol Cell Biol 23: 4511–4521.
30. Franke TF, Hornik CP, Segev L, Shostak GA, Sugimoto C (2003) PI3K/Akt and apoptosis: size matters. Oncogene 22: 8983–8998.
31. Zha J, Harada H, Yang E, Jockel J, Korsmeyer SJ (1996) Serine phosphorylation of death agonist BAD in response to survival factor results in binding to 14-3-3 not BCL-X(L). Cell 87: 619–628.
32. O'Reilly LA, Print C, Hausmann G, Moriishi K, Cory S, et al. (2001) Tissue expression and subcellular localization of the pro-survival molecule Bcl-w. Cell Death Differ 8: 486–494.
33. Wilson JW, Nostro MC, Balzi M, Faraoni P, Cianchi F, et al. (2000) Bcl-w expression in colorectal adenocarcinoma. Br J Cancer 82: 178–185.
34. Bae IH, Park MJ, Yoon SH, Kang SW, Lee SS, et al. (2006) Bcl-w promotes gastric cancer cell invasion by inducing matrix metalloproteinase-2 expression via phosphoinositide 3-kinase, Akt, and Sp1. Cancer Res 66: 4991–4995.
35. Lee HW, Lee SS, Lee SJ, Um HD (2003) Bcl-w is expressed in a majority of infiltrative gastric adenocarcinomas and suppresses the cancer cell death by blocking stress-activated protein kinase/c-Jun NH2-terminal kinase activation. Cancer Res 63: 1093–1100.
36. Yan W, Samson M, Jégou B, Toppari J (2000) Bcl-w forms complexes with Bax and Bak, and elevated ratios of Bax/Bcl-w and Bak/Bcl-w correspond to spermatogonial and spermatocyte apoptosis in the testis. Mol Endocrinol 14: 682–699.
37. Han Z, Wu K, Shen H, Li C, Han S, et al. (2008) Akt1/protein Kinase Balpha is Involved in Gastric Cancer Progression and Cell Proliferation. Dig Dis Sci Epub ahead of print.
38. Yu HG, Ai YW, Yu LL, Zhou XD, Liu J, et al. (2008) Phosphoinositide 3-kinase/Akt pathway plays an important role in chemoresistance of gastric cancer cells against etoposide and doxorubicin induced cell death. Int J Cancer 122: 433–443.
39. Michl P, Downward J (2005) Mechanisms of disease: PI3K/AKT signaling in gastrointestinal cancers. Z Gastroenterol 43: 1133–1139.
40. Tran NL, McDonough WS, Savitch BA, Sawyer TF, Winkles JA, et al. (2005) The tumor necrosis factor-like weak inducer of apoptosis (TWEAK)-fibroblast growth factor-inducible 14 (Fn14) signaling system regulates glioma cell survival via NFkappaB pathway activation and BCL-XL/BCL-W expression. J Biol Chem 280: 3483–3492.
41. Yao M, Nguyen TV, Pike CJ (2007) Estrogen regulates Bcl-w and Bim expression: role in protection against beta-amyloid peptide-induced neuronal death. J Neurosci 27: 1422–1433.

Published Online First on April 13, 2010 as 10.1158/0008-5472.CAN-09-3341

Therapeutics, Targets, and Chemical Biology

Cancer Research

miR-212 Increases Tumor Necrosis Factor–Related Apoptosis-Inducing Ligand Sensitivity in Non–Small Cell Lung Cancer by Targeting the Antiapoptotic Protein PED

Mariarosaria Incoronato[1], Michela Garofalo[5], Loredana Urso[1], Giulia Romano[1], Cristina Quintavalle[2], Ciro Zanca[2], Margherita Iaboni[2], Gerald Nuovo[5], Carlo Maria Croce[5], and Gerolama Condorelli[2,3,4]

Abstract

PED/PEA-15 (PED) is a death effector domain family member of 15 kDa with a broad antiapoptotic function found overexpressed in a number of different human tumors, including lung cancer. To date, the mechanisms that regulate PED expression are unknown. Therefore, we address this point by the identification of microRNAs that in non–small cell lung cancer (NSCLC) modulate PED levels. In this work, we identify miR-212 as a negative regulator of PED expression. We also show that ectopic expression of this miR increases tumor necrosis factor–related apoptosis-inducing ligand (TRAIL)–induced cell death in NSCLC cells. In contrast, inhibition of endogenous miR-212 by use of antago-miR results in increase of PED protein expression and resistance to TRAIL treatment. Besides, in NSCLC, we show both *in vitro* and *in vivo* that PED and miR-212 expressions are inversely correlated, that is, PED is upregulated and miR-212 is rarely expressed. In conclusion, these findings suggest that miR-212 should be considered as a tumor suppressor because it negatively regulates the antiapoptotic protein PED and regulates TRAIL sensitivity. *Cancer Res; 70(9); OF1–9. ©2010 AACR.*

Introduction

Lung cancer is one of the most common causes of cancer-related deaths worldwide. About 80% of all lung cancers are of the non–small cell lung carcinoma (NSCLC) type, which is divided in to three subtypes: squamous cell carcinoma (25–30%), adenocarcinoma (40%), and large-cell carcinoma (10–15%; ref. 1). Because of their resistance to therapeutic drugs, standard treatment of these tumors has only a 20% to 30% positive clinical response. Therefore, to develop new therapeutic strategies to improve therapy for NSCLC is important in understanding the molecular mechanisms involved in cell death resistance.

Apoptosis is the predominant mechanism by which cancer cells die in response to cytotoxic drugs. Resistance to drug treatment is due to deregulation of apoptosis-related proteins. Among these proteins is PED/PEA-15, a death effector domain (DED) family member of 15 kDa having a variety of effects on cell growth and metabolism (2–4). PED/PEA-15 was found overexpressed in a number of different human tumors, including gliomas, squamous carcinoma, thyroid, breast, lung cancer, and B-cell chronic lymphocytic leukemia (5–9). PED/PEA-15 has a broad antiapoptotic action, being able to inhibit both the intrinsic and the extrinsic apoptotic pathways. Inhibition of the extrinsic pathway is accomplished through its DED, which likely acts as a competitive inhibitor for proapoptotic molecules during the assembly of the death-inducing signaling complex (3, 6). Recently, regulation of PED/PEA-15 phosphorylation by PTEN was shown to play a key role in determining whether a cell dies by type I or type II Fas-induced apoptosis (10). We recently showed that in NSCLC, PED/PEA-15 overexpression is responsible for a tumor necrosis factor–related apoptosis-inducing ligand (TRAIL)–resistant phenotype (9). Furthermore, PED is upregulated in breast cancer where it induces resistance to chemotherapeutic treatment (8, 9). To date, although PED/PEA-15 is overexpressed in a number of different cancer types, the mechanisms that regulate its expression are unknown.

An important mechanism of protein expression regulation involves microRNAs (miRNA). These molecules are evolutionarily conserved, endogenous noncoding RNAs of about 22 nucleotides (nt) in length that function at the posttranscriptional level (11). In animals, single-stranded miRNAs bind with specific mRNAs through sequences that are partially complementary to the 3′ untranslated region (UTR) of the target mRNA (12). miRNAs are involved in numerous cellular processes including development, differentiation, proliferation, apoptosis, and response to stress (13, 14). To date, more than 600 human miRNAs have been experimentally identified and estimated to

Authors' Affiliations: [1]Fondazione IRCCS SDN, Naples, Italy; [2]Dipartimento di Biologia e Patologia Cellulare e Molecolare and [3]Facoltà di Scienze Biotecnologiche, "Federico II" University of Naples; [4]Istituto di Endocrinologia e Oncologia Sperimentale, Consiglio Nazionale delle Ricerche, Naples, Italy; and [5]Department of Molecular Virology, Immunology and Medical Genetics, Human Cancer Genetics Program, Comprehensive Cancer Center, The Ohio State University, Columbus, Ohio

Note: Supplementary data for this article are available at Cancer Research Online (http://cancerres.aacrjournals.org/).

M. Garofalo and L. Urso contributed equally to this work.

Corresponding Author: Gerolama Condorelli, Dipartimento di Biologia e Patologia Cellulare e Molecolare, Via Pansini, 5, 80131 Naples, Italy. Phone: 39-081-746-4416; Fax: 39-081-746-3308; E-mail: gecondor@unina.it.

doi: 10.1158/0008-5472.CAN-09-3341

regulate more than one third of cellular mRNAs. Interestingly, numerous oncogenes and tumor suppressor genes are regulated by miRNAs. With the advent of miRNA expression profiling, significant effort is being made to correlate miRNA expression with tumor prognosis (15, 16). To date, a number of downregulated miRNAs found in lung cancer correlate with patient survival (17, 18) and with therapeutic response (19).

In this article, we identify a miRNA that regulates PED/PEA-15 expression. Our data indicate that miR-212 negatively modulates PED/PEA-15 expression and sensitizes non–small cell lung cancer (NSCLC) cells to TRAIL-induced apoptosis. Moreover, we report that NSCLC-affected lung tissue overexpressing PED/PEA-15 protein has a concordant downregulation of miR-212.

Materials and Methods

Cell culture and transfection. Calu-1 (NSCLC) cells were grown in DMEM; H460 cells were grown in RPMI. Media were supplemented with 10% heat-inactivated fetal bovine serum (FBS), 2 mmol/L L-glutamine, and 100 units/mL penicillin/streptomycin. For transient transfection, cells at 50% confluency were transfected using Lipofectamine 2000 (Invitrogen) with 100 nmol/L (final) of pre-miR-212, pre-miR-34a, pre-miR-124a, scrambled, or antisense miR-212 (Applied Biosystems). Transfections were done with Lipofectamine 2000 according to the manufacturer's instructions (Invitrogen). Meg01 cells (human, chronic myelogenous leukemia cells) were grown in RPMI 1640 + 2 mmol/L glutamine + 10% FBS.

Lung cancer samples. A total of 18 snap-frozen normal and malignant lung tissues (12 men and 6 women; median age, 70.0 y; range, 55–82 y) were collected at the Ohio State University Medical Center (Columbus, OH).

Protein isolation and Western blotting. Cells were washed twice in ice-cold PBS and lysed in JS buffer [50 mmol/L HEPES (pH 7.5) containing 150 mmol/L NaCl, 1% glycerol, 1% Triton X100, 1.5 mmol/L $MgCl_2$, 5 mmol/L EGTA, 1 mmol/L Na_3VO_4, and 1× protease inhibitor cocktail]. Protein concentration was determined by the Bradford assay (Bio-Rad) using bovine serum albumin as the standard, and equal amounts of proteins were analyzed by SDS-PAGE (12.5% acrylamide). Gels were electroblotted onto polyvinylidene difluoride membranes (Millipore). For immunoblot experiments, membranes were blocked for 1 h with 5% nonfat dry milk in TBS containing 0.1% Tween 20 and incubated at 4°C overnight with primary antibody. Detection was done with peroxidase-conjugated secondary antibodies using the enhanced chemiluminescence system (Amersham-Pharmacia Biosciences). Primary antibodies used were anti-PED (3), anti–caspase-8 (Cell Signaling), and anti–β-actin (Sigma).

Cell death quantification. Calu-1 cells were transfected with pre-miR-212 or control for 48 h. Cells were then trypsinized, plated in 96-well plates in triplicate, and further incubated with 10 or 25 ng/mL superkiller TRAIL (Alexis Biochemicals) for 24 h. Cell viability was evaluated with the CellTiter 96 AQueous One Solution Cell Proliferation Assay (Promega) according to the manufacturer's protocol. Metabolically active cells were detected by adding 20 μL of MTS to each well. After 2 h of incubation, the plates were analyzed in a Multilabel Counter (BioTek).

Cell death assessment by Annexin V staining. Calu1 cells were transfected with 100 nmol/L miR scrambled and with 100 nmol/L miR-212. After 48 h, cells were treated with 10 or 25 ng/mL of TRAIL for 24 h, harvested, washed twice with cold PBS, and stained with Annexin V-FITC Apoptosis Detection Kit 1 (BD Pharmingen). Briefly, cells were resuspended in 100 μL of 1× binding buffer and 5 μL of Annexin V and then incubated for 15 min at room temperature. Apoptotic cells were analyzed by flow cytometry.

RNA extraction and real-time PCR. Total RNAs (miRNA and mRNA) were extracted using miRNeasy Mini Kit (Qiagen) according to the manufacturer's protocol. Reverse transcription of total miRNA and mRNA was done starting from equal amounts of total RNA/sample (1 μg) using miScript Reverse Transcription Kit (Qiagen). For cultured cells, quantitative analyses of PED, glyceraldehyde-3-phosphate dehydrogenase (as an internal reference), miR-212, and RNU5A (as an internal reference) were done by real-time PCR using specific primers (Qiagen), miScript SYBR Green PCR Kit (Qiagen), and QuantiTect SYBR Green PCR Kit (Qiagen), respectively. The reaction for detection of mRNAs was done as follows: 95°C for 15 min, 40 cycles of 94°C for 15 s, 55°C for 30 s, and 72°C for 30 s. The reaction for detection of miRNAs was done as follows: 95°C for 15 min, 40 cycles of 94°C for 15 s, 55°C for 30 s, and 70°C for 30 s. To analyze PED and miR-212 expression in lung tissue specimens (neoplastic and normal tissue), real-time PCR was done using a standard TaqMan PCR Kit protocol on an Applied Biosystems7900HT Sequence Detection System (Applied Biosystems). The reactions were incubated at 95°C for 10 min, followed by 40 cycles of 95°C for 15 s and 60°C for 1 min.

All reactions were run in triplicate. The threshold cycle (CT) is defined as the fractional cycle number at which the fluorescence passes the fixed threshold. For relative quantitation, the $2^{(-\Delta CT)}$ method was used as previously described (20). Experiments were carried out in triplicate for each data point, and data analysis was done by using Bio-Rad IQ software.

Luciferase assay. The 3′UTR of the human *PED* gene was PCR amplified using the PED primers 5′-tctagaaaggcaaagagaccactcaaccccca-3′ (forward) and 5′-tctagaatgttcttcaccaaggagagagggaaggtt-3′ (reverse) and cloned downstream of the Renilla luciferase stop codon in pGL3 control vector (Promega), giving rise to pcDNA/PED-clone1 (3). This construct was used to generate, by inverse PCR, the p3′-UTRmut-PED plasmid (primers: PED-mut1, FW 5′-tgtttgtactcctgtgctgtcctgagtaccagc-3′, RW 5′-gctggtactcaggacagcacaggagtacaaaca-3′; PED-mut2, FW 5′-agttgttcctactcagcactctaaacctagggagg-3′, RW 5′-cctccctaggtttagagtgctgagtaggaacaact-3′). MeG01 cells were cotransfected with 1 μg of p3′UTR-PED and with p3′ UTRmut-PED plasmid and 1 μg of the Renilla luciferase expression construct pRL-TK (Promega) with Lipofectamine 2000 (Invitrogen). Cells were harvested 24 h posttransfection and assayed with Dual Luciferase Assay (Promega) according to the manufacturer's instructions. Three independent experiments were done in triplicate.

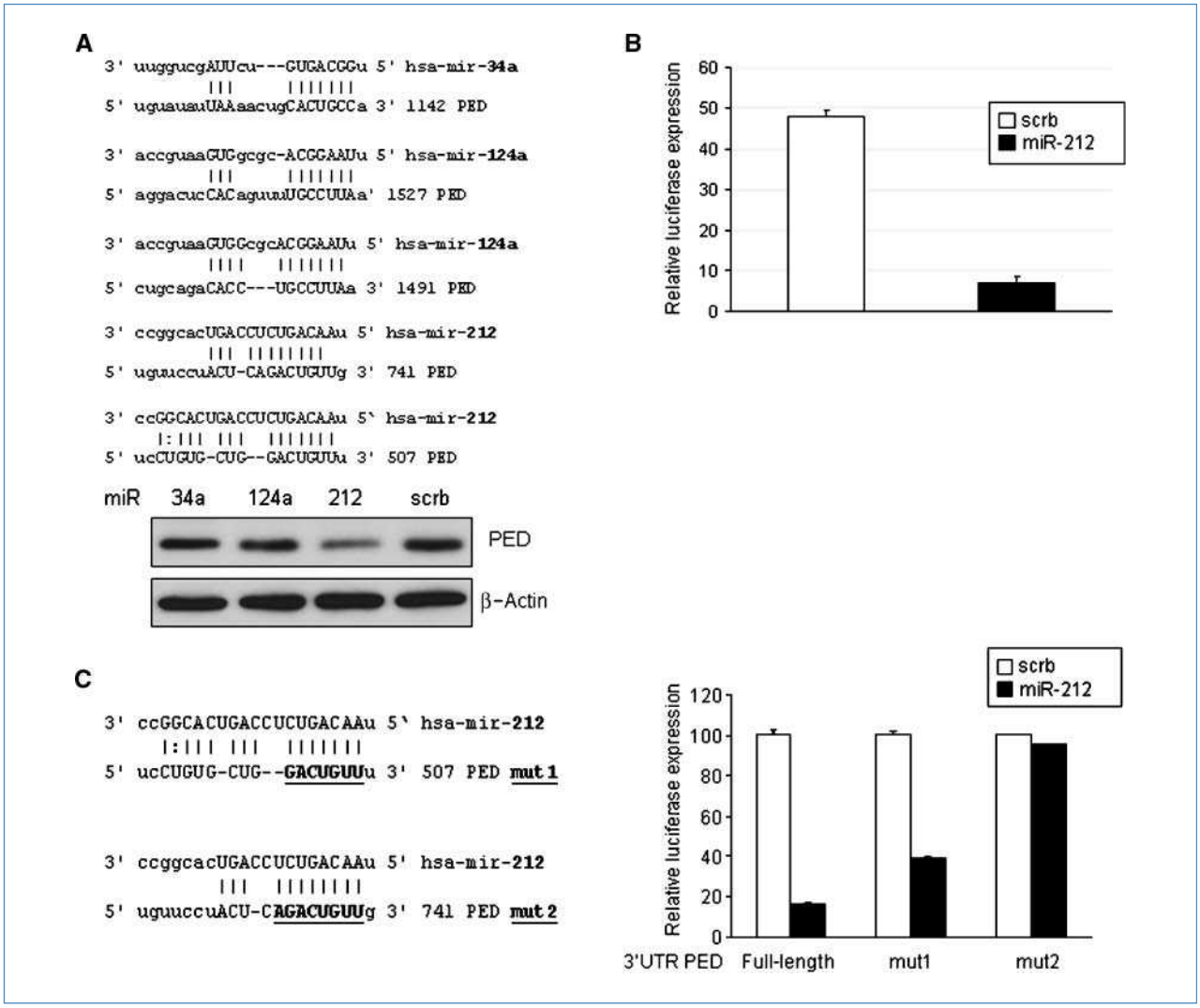

Figure 1. PED expression is regulated by miR-212. A, top, complementary sites on *PED* 3′UTR for miR-34a, miR-124a, and miR-212. The capital letters identify perfect base matches according to the Pictar, TargetScan, miRanda, and miRBase softwares (bottom). Western blot analysis of cellular extracts of Calu-1 cells transfected for 72 h with pre-miR-34a, pre-miR-124a, pre-miR-212, or a scrambled oligonucleotide (scrb). Cell lysates were immunobloted with anti-PED antibody. To confirm equal loading, the membrane was probed with anti–β-actin antibody as indicated. B, Meg01 cells were transiently cotransfected with the luciferase reporter containing *PED* 3′UTR and pre-miR-212 or scrambled oligonucleotide. C, left, complementary sites for miR-212 on *PED* 3′UTR. The bold letters identify the deletion regions of mutants (mut) 1 and 2, respectively. Right, Meg01 cells were transiently transfected with the luciferase reporter containing full-length *PED* 3′UTR, mut1, or mut2 in the presence of pre-miR-212 or scrb. C and D, luciferase activity was evaluated 24 h after transfection as described in Materials and Methods. Representative of at least three independent experiments.

miRNA locked nucleic acid* in situ *hybridization of formalin-fixed, paraffin-embedded tissue section. *In situ* hybridization was carried out on deparaffinized human lung and liver tissues using previously published protocol (21), which includes a digestion in pepsin (1.3 mg/mL) for 30 min. The sequence of the probes containing the six dispersed locked nucleic acid (LNA) modified bases with digoxigenin conjugated to the 5′ end was miR-212-(5′) UAACAGUCUCCAGUCACGGCC. The probe cocktail and tissue miRNA were codenatured at 60°C for 5 min, followed by hybridization at 37°C overnight and a low stringency wash in 0.2× SSC and 2% bovine serum albumin at 4°C for 10 min. The probe-target complex was seen due to the action of alkaline phosphatase on the chromogen nitroblue tetrazolium and bromochloroindolyl phosphate. Negative controls included the use of a probe, which should yield a negative result in such tissues. No counterstain was used to facilitate colabeling for PED protein. After *in situ* hybridization for the miRNAs, as previously described (21), the slides were analyzed for immunohistochemistry using the optimal conditions for PED (1:800, cell conditioning for 30 min). For the immunohistochemistry, we used the Ultrasensitive Universal Fast Red system from Ventana Medical Systems. We used normal lung tissues as controls for these proteins. The percentage of tumor cells expressing PED and miR-212 was then analyzed with emphasis on colocalization of the respective targets (miR-212 and either PED).

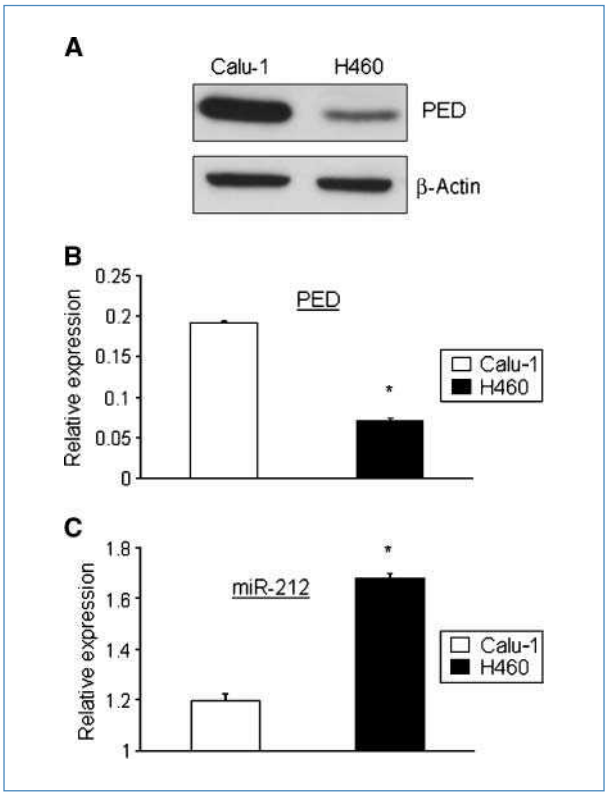

Figure 2. PED and miR-212 expression levels are inversely correlated in NSCLC. A, cell lysates from Calu-1 and H460 cells were immunoblotted with anti-PED antibody. To confirm equal loading, the membrane was immunoblotted with anti–β-actin antibody. Blots are representative of at least four independent experiments. B and C, total RNA (mRNAs and miRNAs) was extracted from Calu-1 and H460 cells and 1 μg was reverse transcribed and amplified as described in Materials and Methods. Relative expressions of PED mRNA (B) and miR-212 (C) were calculated using the comparative CT methods. Columns, mean of four different experiments; bars, SD. *, $P < 0.05$, Student's t test. There is an inverse correlation between PED and miR-212 expressions in NSCLC.

Statistical analysis. Continuous variables are expressed as mean values ± SD. One-tailed Student's t test was used to compare values of test and control samples. $P < 0.05$ was considered significant.

Results

Identification of miRNA involved in PED regulation. To identify miRNAs that specifically target PED (PED/PEA-15), we used bioinformatic analyses available on the web, including Pictar, TargetScan, miRanda, and miRBase. Comparing the results obtained from the different searches, we found that miR-34a, miR-124a, and miR-212 consistently showed the highest score of probability for targeting PED 3′UTR. PED 3′UTR contains two potential binding sites for miR-212 at nt 507 and nt 741, one for miR-34a at nt 1142, and two for miR-124a at nt 1491 and nt 1527 (Fig. 1A, top).

To asses whether exogenous expression of the selected miRNAs induced PED downregulation, we used Calu-1 cells, which express high PED levels (9). To this end, Calu-1 cells were transiently transfected with 100 nmol/L of the indicated pre-miRNAs for 72 hours, and PED expression levels then identified by Western blot analysis (Fig. 1A, bottom). As shown, miR-212 induced the greatest decrease in PED protein.

The most widely used approach for experimentally validating miRNA targets is to clone the predicted miRNA-binding sequence downstream of a luciferase reporter construct and to cotransfect it with the miRNA of interest. To this end, we cloned the 3′UTR sequence of human PED into the luciferase expressing vector pGL3-control downstream of the luciferase stop codon; Meg01 cell lines were transiently transfected with this construct in the presence of pre-miR-212 or a scrambled oligonucleotide acting as a negative control. As reported in Fig. 1B, miR-212 significantly reduced luciferase activity compared with the scrambled oligonucleotide. This indicates that miR-212 binds to the 3′UTR of *Ped* and impairs PED mRNA translation.

As reported above, miR-212 targets two regions of the 3′ UTR of PED mRNA (Fig. 1A). To determine which of the two regions is implicated in the binding with miR-212, we generated two deletion mutants (Fig. 1C, left): mut1, lacking the first binding site, GACTGTT (top); and mut2, lacking the second binding site, AGACTGTT (bottom). The two mutants were cloned into the 3′UTR of the luciferase gene and co-transfected with pre-miR-212 into the Meg01 cell line. As shown in Fig. 1C (right), miR-212 did not significantly reduce luciferase activity in the presence of the mut2 sequence. This result indicates that miR-212 targets PED mRNA at the AGACUGUU sequence.

miR-212 modulates PED mRNA levels. To asses whether PED upregulation in lung cancer cells was due to decreasing expression of miR-212, we analyzed in Calu-1 and H460 cells, expressing different amounts of PED protein (Fig. 2A), the levels of miR-212 and PED mRNA by real-time PCR. As shown in Fig. 2B and C, an inverse correlation between PED mRNA and miR-212 levels was found.

It is known that miRNAs regulate gene expression either by direct cleavage of the targeted mRNAs or by inhibiting translation (22). To determine whether the binding of miR-212 to PED 3′UTR results in mRNA degradation, Calu-1 cells were transfected for 48 or 72 hours with pre-miR-212, and PED expression was then evaluated by real-time PCR and Western blot. As shown in Fig. 3A, exogenous expression of miR-212 induced a marked reduction of PED mRNA (top) as well as PED protein (middle) levels. The efficiency of miR-212 transfection was evaluated by reverse transcription-PCR (RT-PCR; bottom). Next, to assess whether miR-212 plays a physiologic role in controlling PED expression, we treated H460 cells, which express high levels of miR-212, with a specific antago-miR-212. As shown in Fig. 3B, increased expression of PED mRNA (top) and PED protein (middle) was evident already at 48 hours of antago-miRNA transfection. The efficiency of antago-miR-212 transfection was evaluated by RT-PCR of the endogenous miRNA (bottom). Taken together, the results show that in lung cancer cells, PED and miR-212 expressions are inversely correlated and that miR-212 regulates PED expression.

miR-212 and PED mRNA levels in NSCLC tissue. To evaluate whether PED upregulation in lung cancer is related to decreased miR-212 levels also *in vivo*, we analyzed PED and miR-212 expression levels in tissue specimens collected from 18 patients (14 NSCLC-affected individuals and 4 with normal lung tissue). As shown in Fig. 4, in normal lung samples, the levels of miR-212 were high whereas PED was expressed at low levels. On the contrary, in the majority of lung cancer samples, miR-212 was expressed at low levels and PED was overexpressed.

To corroborate these findings, *in situ* hybridization analysis was done, using 5′-dig-labeled LNA probes, on NSCLC and normal lung tissues, followed by immunohistochemistry for PED (Fig. 5). MiR-212 and PED expressions were inversely related in NSCLC and the adjacent normal lung tissues. Lung cancer cells showed high expression of PED and rarely expressed miR-212 (Fig. 5A–C), whereas the adjacent nonmalignant lung expressed miR-212 abundantly and rarely showed detectable PED signal (Fig. 5A–C). Costaining of PED and miR-212 showed that the two labelings did not overlap (Fig. 5C-c), showing that PED and miR-212 were not expressed in the same cell. *In situ* hybridization was done for 110 samples. The majority of cancer cells were positive for PED (84%). Seventy-three percent of the samples were negative for miR-212. When we analyzed for double staining, we found that 60% (65 of 110 patients) of the cells were PED positive/miR-212 negative (PED^+/miR^-), 24% (26 of 110 patients) were PED^+/miR^+, 3.6% (4 of 110 patients) were PED^-/miR^+, and 13% (15 of 110 patients) were PED^-/miR^-. These results further support our above finding that the upregulation of PED in lung cancer is dependent on decreased miR-212 levels.

MiR-212 increases TRAIL-induced cell death in NSCLC cells. We have previously shown that a TRAIL-resistant phenotype in NSCLC is related to overexpression of PED (9). The observation that miR-212 targets PED suggests that ectopic expression of this miRNA should increase sensitivity to TRAIL. To this aim, we transfected Calu-1 cells with pre-miR-212, and caspase-8 activation was then evaluated following treatment with TRAIL (Fig. 6A). As shown, PED expression decreased in the presence of exogenous miR-212, and caspase-8 activation

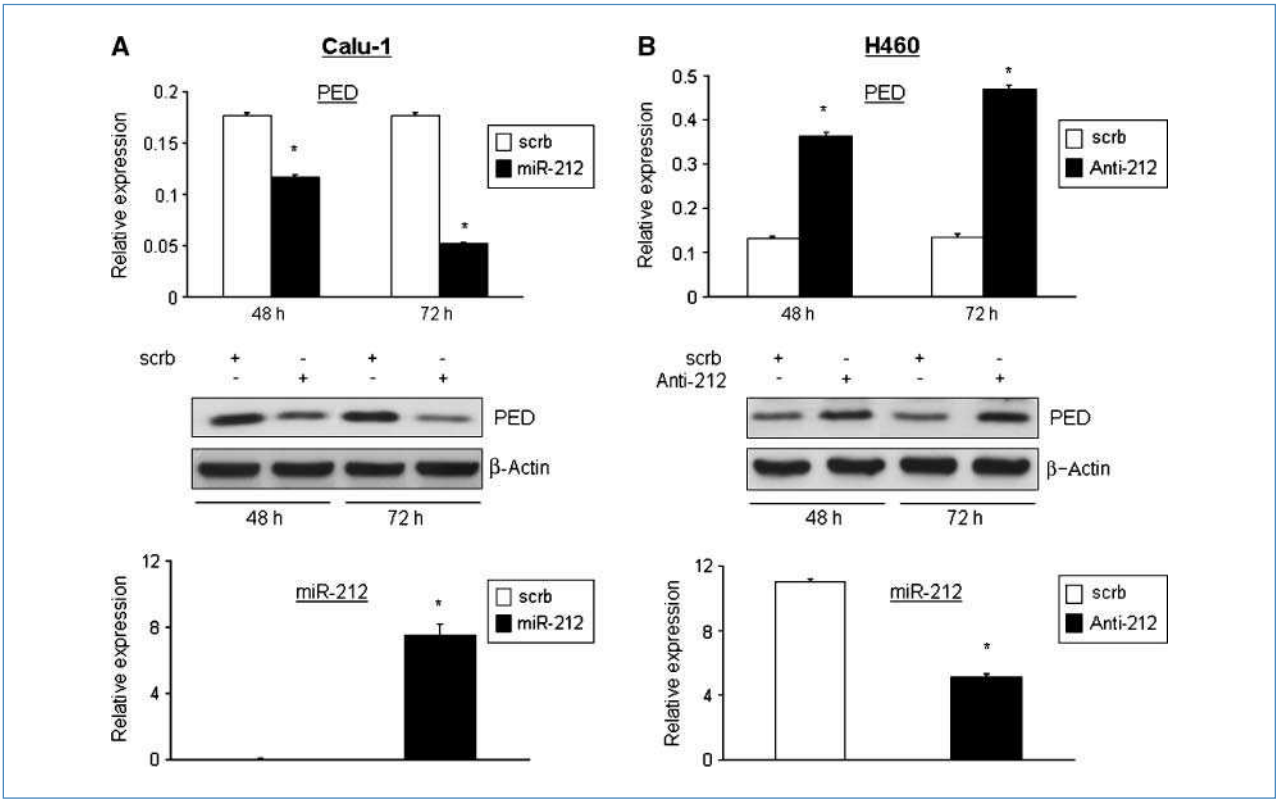

Figure 3. miR-212 regulates PED expression levels. A, top, Calu-1 cells were transfected for 48 and 72 h with pre-miR-212 or scrb. After transfection, total RNA was extracted and 1 μg was reverse transcribed and amplified as described in Materials and Methods. As shown, PED mRNA was downregulated by miR-212 transfection. Middle, cell lysates from Calu-1 cells were collected after 48 and 72 h from pre-miR-212 or scrb transfections and immunoblotted with anti-PED antibody. To confirm equal loading, the membrane was immunoblotted with anti–β-actin antibody. As shown, decreasing amount of PED protein was evident in the presence of exogenous pre-miR-212 (bottom). Relative expression of ectopic miR-212 after the transfection was evaluated. B, top, H460 cells were transfected for 48 and 72 h with antago-miR-212 (anti-212) or scrb. After transfection, total RNA was extracted and 1 μg was reverse transcribed and amplified as described in Materials and Methods. As shown, an increasing amount of PED mRNA was evident in the presence of exogenous anti-212 (middle). Cell lysates from H460 cells were collected after 48 and 72 h from anti-212 or scrb transfections and immunoblotted with anti-PED antibody. To confirm equal loading, the membrane was immunoblotted with anti–β-actin antibody. As shown, an increasing amount of PED protein was evident in the presence of exogenous anti-212 (bottom). Relative expression of endogenous miR-212 after the antago-miR-212 transfection was evaluated. Blots are representative of at least four independent experiments. Columns, mean of four different experiments; bars, SD. *, $P < 0.05$, Student's *t* test.

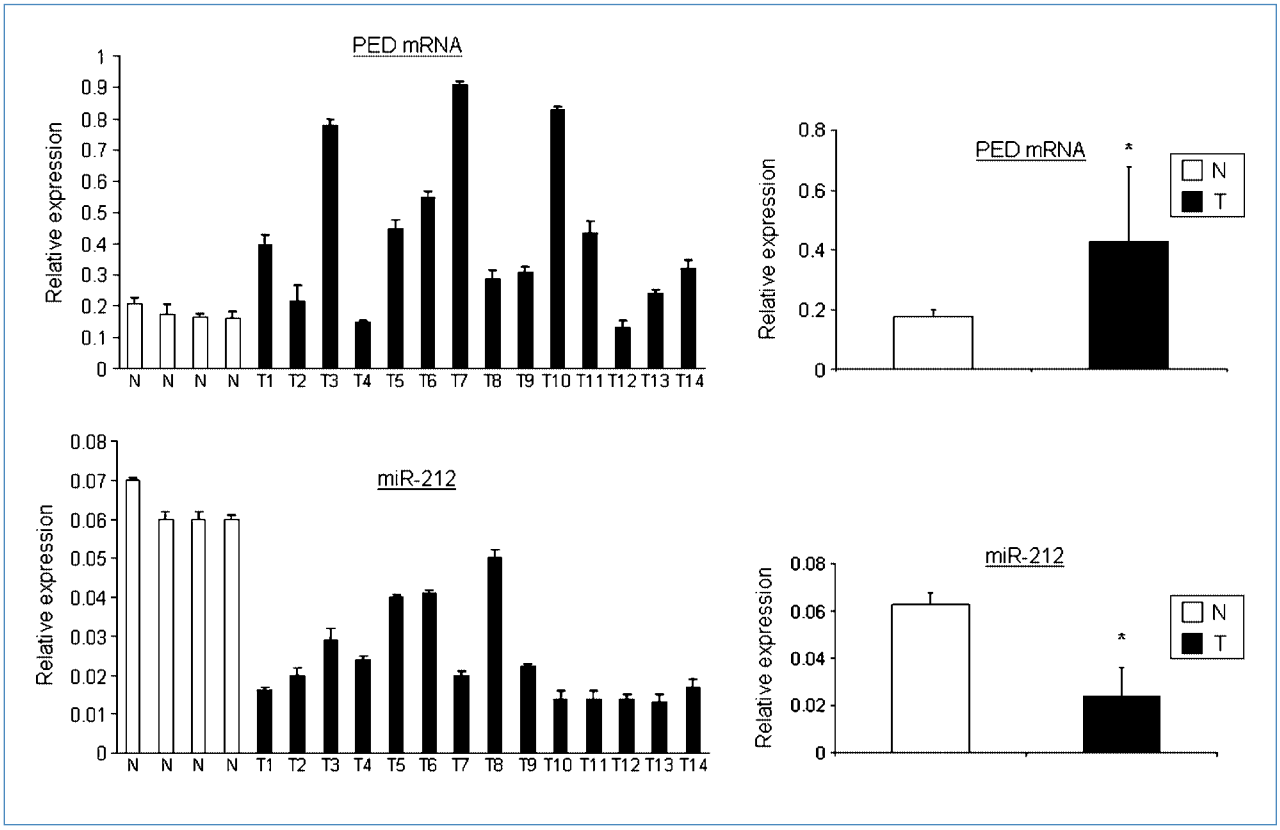

Figure 4. Correlation of endogenous miR-212 and PED mRNA expression levels in human lung cancer. Left, total RNA extracted from tissue specimens collected from 14 NSCLC-affected individuals and 4 control individuals was used to analyze miR-212 and PED mRNA expression by real-time PCR (right). Average of control versus tumor samples. Columns, mean PED or miR-212 expression of all the tumor samples (T) and normal tissue (N); bars, SD. *, $P < 0.05$, *t* test. As shown, there is an inverse correlation between miR-212 and PED mRNA expression levels. The normal lung RNA expressed high miR-212 and low PED mRNA levels; all the tumors analyzed expressed high PED mRNA and very low miR-212 levels.

was evident 2 hours after TRAIL treatment (compare lane 5 with lane 6 and lane 7 with lane 8). To further confirm this result, we analyzed TRAIL-induced cell death in the presence of exogenous pre-miR-212 with a cell viability assay (Supplementary Fig. S1A) and Annexin V apoptosis assay (Fig. 6B and Supplementary Fig. S1B for representative dot blot). By time course and dose/response analysis (data not shown), we found that to better appreciate a difference in cell viability, low concentrations of TRAIL were needed. To this end, Calu-1 cells were transfected for 48 hours with pre-miR-212, then stimulated with 10 and 25 ng/mL of TRAIL for 24 hours, and cell death was evaluated. As shown in Fig. 6B, transfection of miR-212 increased TRAIL-induced cell death up to 3-fold that of Calu-1 cells. Thus, PED downregulation induced by miR-212 increases sensitivity to TRAIL in lung cancer cells.

To further evaluate the role of miR-212 in apoptosis sensitivity, TRAIL-sensitive H460 cells were transfected with antagomiR-212 to decrease endogenous miR-212 and then analyzed for their susceptibility to TRAIL-induced cell death. As shown in Fig. 6C, antago-miR treatment increased PED protein and rendered H460 cells more resistant to TRAIL. To confirm that PED is an important target of miR-212 for regulation of apoptosis, Calu-1 cells were transfected with pre-miR-212 in the presence or in the absence of PED-myc cDNA that lacks 3′UTR. As shown in Fig. 6D, ectopic expression of miR-212 and PED-myc cDNA restores the apoptotic resistance, assessed as caspase-8 activation. To confirm this result, we analyzed TRAIL-induced cell death in the presence of exogenous pre-miR-212 and PED-myc with a cell viability assay, obtaining the same results (Supplementary Fig. S1C). Taken together, these results indicate that miR-212 increases TRAIL sensitivity by targeting the antiapoptotic protein PED.

Discussion

The resistance of tumors to current chemotherapeutic protocols remains a major problem in cancer therapy. Defects in the apoptotic program may contribute to treatment resistance and tumor progression and may be caused by deregulated expression of antiapoptotic molecules. Better knowledge of tumor biology is providing the opportunity to treat lung cancer with a new class of anticancer drugs. PED is overexpressed in lung cancer, as well as in other human tumors including gliomas, squamous carcinoma, breast cancer, and thyroid cancer, and its overexpression is related to resistance to chemotherapy and TRAIL-induced cell death (4–9). Furthermore, we recently showed that PED is upregulated and induces resistance to TRAIL in NSCLC (9). Even so, the

molecular mechanisms of deregulation of PED expression in cancer cells are still unknown. We therefore have set out to identify possible miRNAs able to regulate PED expression in human lung cancer.

Here, we found that in lung cancer cells, miR-212 was able to target PED 3′UTR and decrease its levels, thus suggesting that by maintaining PED levels low, miR-212 action may contribute to tumor suppression.

Over the past few years, several miRs have been implicated in various human cancers. Both losses and gains of miR function have been shown to contribute to cancer development through a range of mechanisms (23, 24).

More often in various human tumors has been observed an overexpression of miRs, and several of these miRs function as oncogenes. When downregulated, miRNAs are considered tumor suppressor because they usually prevent tumor development by negatively inhibiting molecules involved in apoptosis resistance.

Different studies show that lung adenocarcinoma has a miR expression signature that greatly adapts to the use of clinical data in predicting an individual's survival. Low expression of let-7a and high expression of miR-155 are linked to unfavorable clinical outcome in lung cancer (17). The miR-34 cluster (miR-34a, miR-34b, miR-34c) is repressed in cancers and miR-34c is involved in p53 tumor suppression in many cancers, including lung cancer (25, 26). Bandi et al. (27) identified miR-15a and miR-16 as frequently deleted in NSCLC, implying an increase of cell cycle. Furthermore, Nasser et al. (28) showed that miR-1 was downregulated in lung cancer and was related to increased migration and motility of lung cancer cells.

Using real-time RT-PCR, Yu et al. (29) analyzed miR expression in 112 different NSCLC patients. They found that two miRs acted as antitumoral genes (miR-221 and let-7a) and three miRs were risky for NSCLC (miR-137, miR-372, and miR-182). Liu et al. (30) found that miR-34c, miR-145, and miR-142-5p were suppressed in transgenic lung cancers as well as human normal versus malignant lung tissues.

MiR-212 expression levels in human cancer have not been extensively investigated thus far. Recently, miR-212 downregulation has been found to be involved in lung cancer response to chemotherapy, in particular to docetaxel (31). The molecular targets responsible to this resistance have not been identified thus far, but it would be interesting to speculate that PED may participate in this process.

Our data show that in sample specimens from lung cancer, miR-212 expression is low compared with normal samples. Interestingly, miR-212 expression inversely correlates with PED expression and with response to TRAIL treatment. Therefore, miR-212 expression could predict therapeutic response to TRAIL in lung cancer.

The mechanisms of miR-212 downregulation in human cancer are not clear at the moment. miR-212 is located on human chromosome 17, in a region that is frequently lost

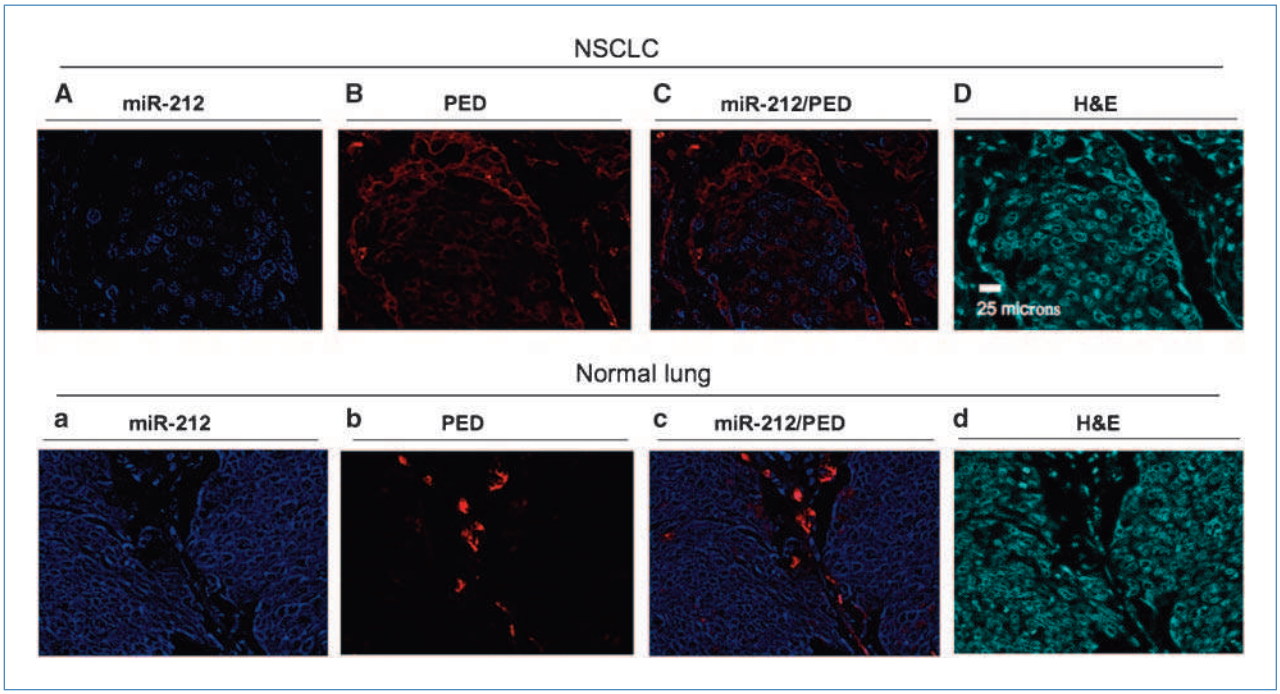

Figure 5. Immunohistochemistry and *in situ* hybridization of lung carcinoma and normal tissue samples. MiR-212 (blue; A-a) and PED (red; B-b) expressions were inversely related in lung cancer and the adjacent normal lung tissues (C-c shows colocalization expression of PED and miR-212). Top, PED (B) and miR-212 (A) expressions were confined mostly to cancer cells. However, note that cancer cells express PED and do not express miR-212 and vice versa (C). Bottom, a nest of cancer cells expressing only miR-212 (a). Note that PED expression (b) is confined to the benign stromal cells that are found in the desmoplastic tissue surrounding the cancer cells nest. Bar, 25 μm. The magnification is the same for all images. D-d, H&E. One hundred ten lung carcinoma and normal samples were analyzed. As described in the text, the majority of cancer cells were positive for PED and negative for miR-212. In the cases of lung carcinoma where both miR-212 and PED expressions were noted, cancer cells expressing PED were distinct from those expressing miR-212.

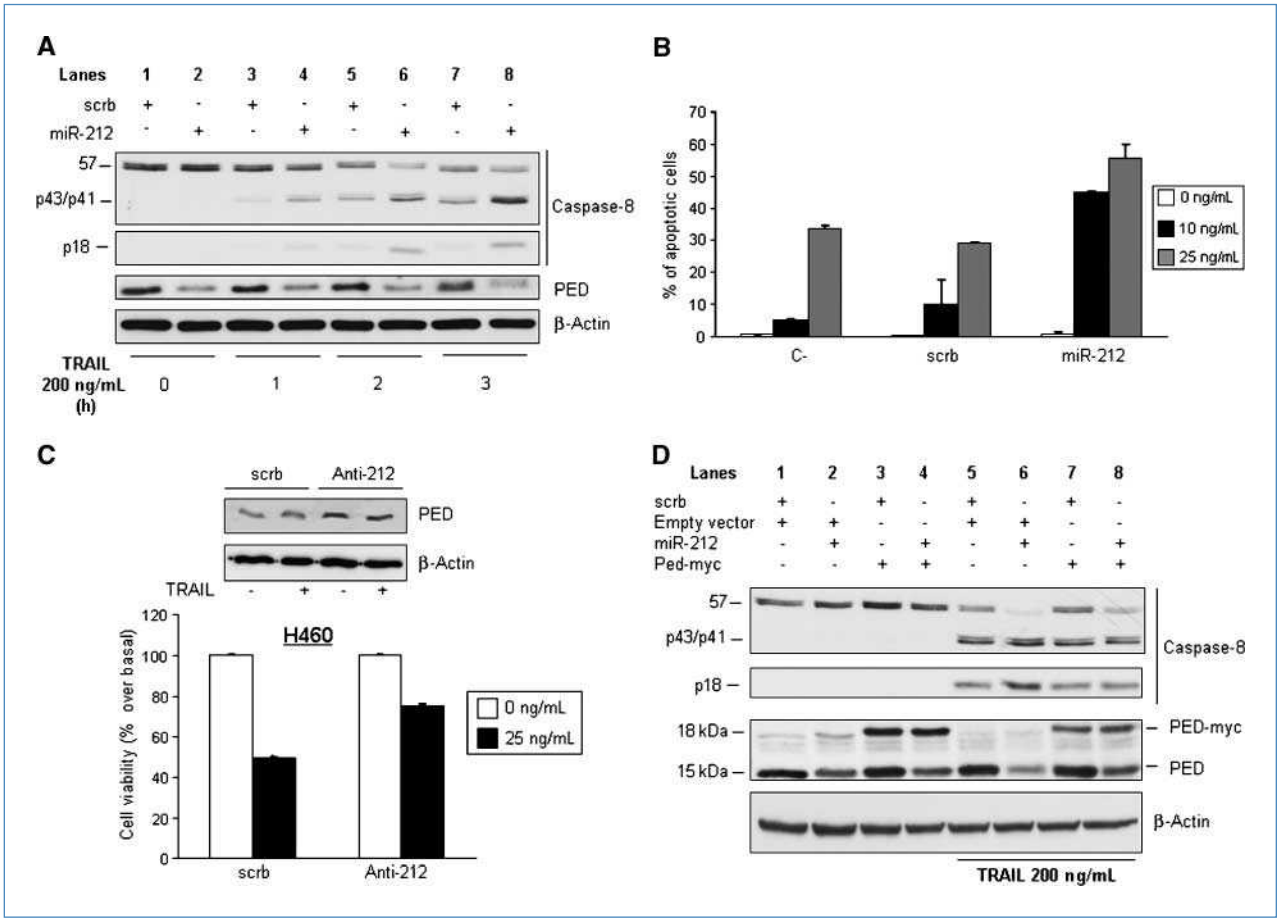

Figure 6. miR-212 transfection induces TRAIL sensitivity. A, Calu-1 cells were transfected either with pre-miR-212 or with scrb. After 72 h, cells were treated with 200 ng/mL Super-Killer TRAIL for the indicated times. Lysates were analyzed by Western blotting with anti–caspase-8 and anti-PED antibodies. Cleavage of caspase-8 was more evident in Calu-1 cells transfected with miR-212 compared with scrb. β-Actin antibody was used as loading control. B, Calu-1 cells were transfected either with pre-miR-212 or with scrb for 48 h. Then, the cells were incubated with 10 or 25 ng/mL of Super-Killer TRAIL for 24 h. Apoptosis was evaluated with Annexin V staining. Columns, mean of four independent experiments in triplicate; bars, SD. Downregulation of PED by miR-212 was responsible for increased sensitivity of Calu-1 cells to TRAIL-mediated cell death. C, H460 cells were transfected either with anti-212 or with scrb for 48 h, then the cells were incubated with 25 ng/mL Super-Killer TRAIL for 24 h. Top, upregulation of PED expression after antago-miR transfection was evaluated by Western blotting using anti-PED antibody. β-Actin antibody was used as loading control. Bottom, cell viability was evaluated by CellTiter Assay. Columns, mean of four independent experiments in triplicate; bars, SD. D, Calu-1 cells were transfected with miR-212 in the presence or absence of PED-myc recombinant protein. After 72 h, cells were treated with 200 ng/mL Super-Killer TRAIL for 3 h and caspase-8 activation was analyzed by Western blotting with anti–caspase-8 antibodies. Cleavage of caspase-8 was more evident in Calu-1 cells transfected with miR-212 in the absence of PED-myc recombinant protein. Expressions of PED-myc (18 kDa) and endogenous PED (15 kDa) were evaluated with anti-PED antibody. β-Actin antibody was used as loading control.

in different human cancers (32), and this may represent a mechanism to explain its low expression.

The silencing of miR in cancer can be caused not only by deletions and mutations but also by epigenetic changes. Altered patterns of epigenetic modifications, in particular the methylation of CpG islands in the promoter regions of some miRs, have been described (33). The miR-212 promoter region is possibly rich in CpG islands. Experiments are under way in our lab to clarify whether methylation may be a mechanism involved in the regulation of miR-212 expression levels.

In summary, miRs are potential antineoplasitc agents. Perhaps combination therapy with different miRs will be needed to confer desired antitumorigenic effects. It will be critical to discern which miRs are overexpressed in lung cancer and which need to be inactivated to inhibit lung carcinogenesis. Conceivably, these miRs or their derivates would become agents to treat or chemoprevent lung cancer.

Disclosure of Potential Conflicts of Interest

No potential conflicts of interest were disclosed.

Acknowledgments

We thank Dr. Vittorio de Franciscis and Michael Latronico for paper revision, and Maria Fiammetta Romano and Simona Romano for their help with FACS experiments.

Grant Support

Associazione Italiana Ricerca sul Cancro (G. Condorelli), Ministero dell'Istruzione, dell'Università e della Ricerca-Fondo per gli Investimenti della Ricerca di Base grant RBIN04J4J7, EU grant EMIL (European Molecular Imaging Laboratories Network) contract no. 503569, and Fondazione SDN.

The costs of publication of this article were defrayed in part by the payment of page charges. This article must therefore be hereby marked *advertisement* in accordance with 18 U.S.C. Section 1734 solely to indicate this fact.

Received 09/10/2009; revised 01/12/2010; accepted 02/02/2010; published OnlineFirst 04/13/2010.

References

1. Travis WD. Pathology of lung cancer. Clin Chest Med 2002;23:65–81.
2. Condorelli G, Vigliotta G, Cafieri A, et al. PED/PEA-15: an anti-apoptotic molecule that regulates FAS/TNFR1-induced apoptosis. Oncogene 1999;18:4409–15.
3. Condorelli G, Vigliotta G, Iavarone C, et al. PED/PEA-15 gene controls glucose transport and is overexpressed in type 2 diabetes mellitus. EMBO J 1998;17:3858–66.
4. Renault F, Formstecher E, Callebaut I, Junier MP, Chneiweiss H. The multifunctional protein PEA-15 is involved in the control of apoptosis and cell cycle in astrocytes. Biochem Pharmacol 2003;66:1581–8.
5. Xiao C, Yang BF, Asadi N, Beguinot F, Hao C. Tumor necrosis factor-related apoptosis-inducing ligand-induced death-inducing signaling complex and its modulation by c-FLIP and PED/PEA-15 in glioma cells. J Biol Chem 2002;277:25020–5.
6. Kitsberg D, Formstecher E, Fauquet M, et al. Knock-out of the neural death effector domain protein PEA-15 demonstrates that its expression protects astrocytes from TNFα-induced apoptosis. J Neurosci 1999;19:8244–51.
7. Garofalo M, Romano G, Quintavalle C, et al. Selective inhibition of PED protein expression sensitizes B-cell chronic lymphocytic leukaemia cells to TRAIL-induced apoptosis. Int J Cancer 2007;120:1215–22.
8. Stassi G, Garofalo M, Zerilli M, et al. PED mediates AKT-dependent chemoresistance in human breast cancer cells. Cancer Res 2005;65:6668–75.
9. Zanca C, Garofalo M, Quintavalle C, et al. PED mediates TRAIL resistance in human non small cell lung cancer. J Cell Mol Med 2008;12:2416–26.
10. He L, Hannon GJ. MicroRNAs: small RNAs with a big role in gene regulation. Nat Rev Genet 2004;5:522–31.
11. Lagos-Quintana M, Rauhut R, Lendeckel W, Tuschl T. Identification of novel genes coding for small expressed RNAs. Science 2001;294:853–8.
12. Lim LP, Lau NC, Garrett-Engele P, et al. Microarray analysis shows that some microRNAs down-regulate large numbers of target mRNAs. Nature 2005;433:769–73.
13. Chen CZ, Li L, Lodish HF, Bartel DP. MicroRNAs modulate hematopoietic lineage differentiation. Science 2004;303:83–6.
14. Cheng AM, Byrom MW, Shelton J, Ford LP. Antisense inhibition of human miRNAs and indications for an involvement of miRNA in cell growth and apoptosis. Nucleic Acids Res 2005;33:1290–7.
15. Calin GA, Croce CM. MicroRNA-cancer connection: the beginning of a new tale. Cancer Res 2006;66:7390–4.
16. Calin GA, Croce CM. MicroRNA signatures in human cancers. Nat Rev Cancer 2006;6:857–66.
17. Yanaihara N, Caplen N, Bowman E, et al. Unique microRNA molecular profiles in lung cancer diagnosis and prognosis. Cancer Cell 2006;9:189–98.
18. Takamizawa J, Konishi H, Yanagisawa K, et al. Reduced expression of the let-7 microRNAs in human lung cancers in association with shortened postoperative survival. Cancer Res 2004;64:3753–6.
19. Garofalo M, Quintavalle C, Di Leva G, et al. MicroRNA signatures of TRAIL resistance in human non-small cell lung cancer. Oncogene 2008;27:3845–55.
20. Livak KJ, Schmittgen TD. Analysis of relative gene expression data using real-time quantitative PCR and the 2(−ΔΔC(T)) method. Methods 2001;25:402–8.
21. Nuovo G, Lee EJ, Lawler S, Godlewski J, Schmittgen T. *In situ* detection of mature microRNAs by labeled extension on ultramer templates. Biotechniques 2009;46:115–26.
22. Robins H, Press WH. Human microRNAs target a functionally distinct population of genes with AT-rich 3′ UTRs. Proc Natl Acad Sci U S A 2005;102:15557–62.
23. Croce CM. Causes and consequences of microRNA dysregulation in cancer. Nat Rev Cancer 2009;10:704–14.
24. Garofalo M, Condorelli GL, Croce CM, Condorelli G. MicroRNAs as regulators of death receptors signaling. Cell Death Differ 2009, Epub ahead of print.
25. He H, Jazdzewski K, Li W, et al. The role of microRNA genes in papillary thyroid carcinoma. Proc Natl Acad Sci U S A 2005;102:19075–80.
26. Bommer GT, Gerin I, Feng Y, et al. p53-mediated activation of miRNA34 candidate tumor-suppressor genes. Curr Biol 2007;17:1298–307.
27. Bandi N, Zbinden S, Gugger M, et al. miR-15a and miR-16 are implicated in cell cycle regulation in a Rb-dependent manner and are frequently deleted or downregulated in non-small cell lung cancer. Cancer Res 2009;69:5553–9.
28. Nasser MW, Datta J, Nuovo G, et al. Down-regulation of micro-RNA-1 (miR-1) in lung cancer. Suppression of tumorigenic property of lung cancer cells and their sensitization to doxorubicin-induced apoptosis by miR-1. J Biol Chem 2008;283:33394–405.
29. Yu SL, Chen HY, Chang GC, et al. MicroRNA signature predicts survival and relapse in lung cancer. Cancer Cell 2008;13:48–57.
30. Liu X, Sempere LF, Galimberti F, et al. Uncovering growth-suppressive MicroRNAs in lung cancer. Clin Cancer Res 2009;15:1177–83.
31. Rui W, Bing F, Hai-Zhu S, Wei D, Long-Bang C. Identification of microRNA profiles in docetaxel-resistant human non-small cell lung carcinoma cells (SPC-A1). J Cell Mol Med 2009, Epub ahead of print.
32. Konishi H, Sugiyama M, Mizuno K, et al. Detailed characterization of a homozygously deleted region corresponding to a candidate tumor suppressor locus at distal 17p13.3 in human lung cancer. Oncogene 2003;221892–905.
33. Peacock JW, Palmer J, Fink D, et al. PTEN loss promotes mitochondrially dependent type II Fas-induced apoptosis via PEA-15. Mol Cell Biol 2009;29:1222–34.

Cell Death and Differentiation (2010) 17, 1908–1916

www.nature.com/cdd

c-FLIP$_L$ enhances anti-apoptotic Akt functions by modulation of Gsk3β activity

C Quintavalle[1], M Incoronato[2], L Puca[1], M Acunzo[1], C Zanca[1], G Romano[2], M Garofalo[1,3], M Iaboni[1], CM Croce[3] and G Condorelli*[,1,4,5]

Akt is a serine–threonine kinase that has an important role in transducing survival signals. Akt also regulates a number of proteins involved in the apoptotic process. To find new Akt interactors, we performed a two-hybrid screening in yeast using full-length Akt cDNA as bait and a human cDNA heart library as prey. Among 200 clones obtained, two of them were identified as coding for the c-FLIP$_L$ protein. c-FLIP$_L$ is an endogenous inhibitor of death receptor-induced apoptosis through the caspase-8 pathway. Using co-immunoprecipitation experiments of either transfected or endogenous proteins, we confirmed the interaction between Akt and c-FLIP$_L$. Furthermore, we observed that c-FLIP$_L$ overexpression interferes with Gsk3-β phosphorylation levels. Moreover, through its effects on Gsk3β, c-FLIP$_L$ overexpression in cancer cells induced resistance to tumor necrosis factor-related apoptosis-inducing ligand (TRAIL). This effect was mediated by the regulation of p27^{Kip1} and caspase-3 expression. These results indicate the existence of a new mechanism of resistance to TRAIL in cancer cells, and unexpected functions of c-FLIP$_L$.
Cell Death and Differentiation (2010) **17,** 1908–1916; doi:10.1038/cdd.2010.65; published online 28 May 2010

Apoptosis, or programmed cell death, is an evolutionarily conserved mechanism of elimination of unwanted cells. This endogenous death machinery is triggered via two principal signaling pathways.[1] The extrinsic pathway is activated by the engagement of death receptors on the cell surface. The binding of ligands, such as Fas, tumor necrosis factor (TNF), or TNF-related apoptosis-inducing ligand (TRAIL) to cognate death receptors (DRs) induces the formation of the death-induced signaling complex (DISC). This DISC complex in turn recruits caspase-8 and promotes the cascade of procaspase activation.[2] The intrinsic pathway is triggered by various intracellular and extracellular stresses, signals of which converge mainly to the mitochondria.[2,3] The balance between pro- and anti-apoptotic members of apoptosis is crucial for the regulation of survival and cell death. Aberrant resistance to apoptosis may lead to the development of cancer.

Cellular FLICE-inhibitory protein (c-FLIP) is a death effector domain (DED)-containing family member that inhibits one of the most proximal steps of DR-mediated apoptosis. Two isoforms of c-FLIP are commonly detected in human cells: a long form (c-FLIP$_L$) and a short form (c-FLIP$_S$). c-FLIP$_L$, a 55-kDa protein, contains two DEDs and a caspase-like domain, whereas c-FLIP$_S$, a 26-kDa protein consists only of two DEDs.[4] Both isoforms are recruited to the DISC, prevent procaspase-8 activation and block DR-mediated apoptosis, although through different mechanisms.[5,6] c-FLIP$_L$ is over-expressed in a number of different tumors and its over-expression is related to TRAIL resistance.[7,8] Beside cell death, c-FLIP$_L$ might also regulate other DR-mediated signals that may be important for tumor-promoting functions, such as proliferation, migration, inflammation or metastasis.[9–11] The activation of the transcription factor NF-κB, the PKB/Akt pathway and mitogen-activated protein kinases (MAPKs), such as c-Jun N-terminal kinase (JNK), extracellular signal-regulated kinase (ERK) and p38, has been demonstrated to be a consequence of DR triggering.[9] Akt is a serine–threonine kinase that regulates the expression and the function of a number of proteins involved in the apoptotic process.[12] Akt interaction or phosphorylation of different signaling molecules may regulate their function by different mechanisms, including increased protein stability, cellular localization or binding to a different cellular partner. Akt interacts with a number of proteins involved in apoptotic signaling cascades, including BAD,[13] caspase-9,[14] the Forkhead transcription factor FOXO3[15] and Bcl-w.[16] The interaction of Akt with one of these proteins prevents apoptosis through several different mechanisms.[13] One major Akt substrate is the serine–theronine kinase Gsk3.[17] Originally studied for its role in glycogen metabolism and insulin action, Gsk3, present in the cells in two isoforms, Gsk3α and Gsk3β, has subsequently been shown to have central functions in many cellular processes, including transcription, cell cycle division, cell fate determination and stem cell maintenance, as well as in apoptosis.[17,18] Gsk3 is constitutively active in resting cells, and is functionally inactivated after phosphorylation in response to different stimuli.

[1]Department of Cellular and Molecular Biology and Pathology, 'Federico II' University of Naples, Naples, Italy; [2]Fondazione SDN, Naples, Italy; [3]Department of Molecular Virology, Immunology and Medical Genetics, Human Cancer Genetics Program, Comprehensive Cancer Centre, The Ohio State University, Columbus, OH, USA; [4]IEOS, CNR, Naples, Italy and [5]Facoltà di Scienze Biotecnologiche, 'Federico II' University of Naples, Naples, Italy
*Corresponding author: G Condorelli, Dipartimento di Biologia e Patologia Cellulare e Molecolare & Facoltà di Scienze Biotecnologiche, Università degli Studi di Napoli "Federico II", Via Pansini, 5. 80131 Naples, Italy. Tel: +39 081 7464416; Fax: +39 081 7463308; E-mail: gecondor@unina.it
Keywords: apoptosis; AKT; Bcl-2 family
Abbreviations: TRAIL, TNF-Related Apoptosis Inducing Ligand; DISC, Death-induced signaling complex; TNF, Tumor necrosis factor; DR, Death receptors; c-FLIP, Cellular FLICE-inhibitory protein; DED, Death Effector Domain; MAPK, mitogen-activated protein kinases; JNK, cJun N-terminal kinase; Akt D-, kinase-dead Akt; Akt D+, constitutively active Akt; ERK, extracellular signal-regulated kinase; cIAP-1, cellular inhibitor of apoptosis protein-1; NSCLC, non small cell lung cancer
Received 28.4.09; revised 15.3.10; accepted 15.4.10; Edited by M Piacentini; published online 28.5.10

In this study, we set out to find and investigate new possible partners of Akt that may participate in the regulation of the apoptosis pathway. In this study, we provide evidence that Akt directly interacts with c-FLIP$_L$. Furthermore, we demonstrate that c-FLIP$_L$ modulates the activation of Gsk3β. We also provide evidence that this interaction is important for the regulation of TRAIL sensitivity, through the regulation of p27 and caspase-3 levels.

Results

Akt interacts with c-FLIP$_L$. To find new Akt interactors, we performed a yeast two-hybrid screening. We used the full-length human Akt cDNA sequence as bait and a human cDNA heart library as prey. Among the 200 clones obtained, two were identified to code for the anti-apoptotic protein, c-FLIP$_L$. To prove the interaction between Akt and c-FLIP$_L$, we performed immunoprecipitation experiments on endogenous proteins and on protein extracts from cells transfected with Akt and c-FLIP$_L$ cDNAs. We were able to confirm the Akt–c-FLIP$_L$ interaction in extracts from transfected cells (Figure 1a), and in endogenous proteins from different cell lines (Figure 1b). To verify whether Akt activity has a role in Akt–c-FLIP$_L$ interaction, HeLa cells were transfected with either wild-type Akt cDNA or with two different Akt mutants: kinase-dead Akt (Akt D) and constitutively active Akt (Akt D+). Protein extracts were

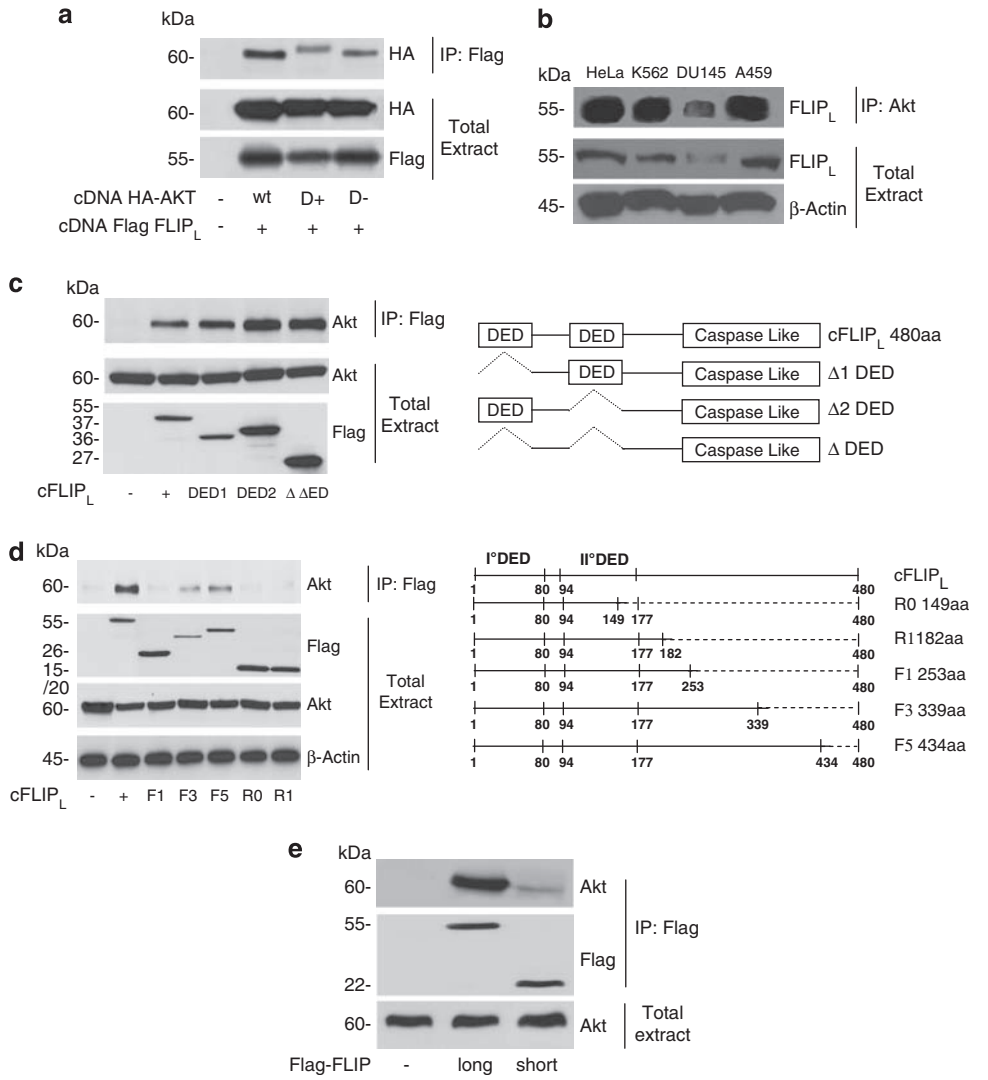

Figure 1 Akt interacts with c-FLIP$_L$. (**a**) HeLa cells were co-transfected with HA–Akt WT, Akt D+ or Akt D cDNAs and c-FLIP$_L$ for 48 h, as indicated. Protein extracts were immunoprecipitated (IP) with anti-Flag antibody and blotted with an anti-HA antibody. As negative control, proteins were incubated with beads without antibody. Total lysates were immunoblotted with the indicated antibody. (**b**) Co-immunoprecipitation of endogenous proteins. Equal amounts of total cell proteins from HeLa, K562, DU145 and A459 cell lines were immunoprecipitated with anti-Akt antibody and blotted with anti- c-FLIP$_L$ antibody. Total lysates (50 μg) were immunoblotted with anti-c-FLIP$_L$ or anti-β-actin antibodies. (**c** and **d**) Identification of FLIP–Akt interaction site. HEK-293 cells were transfected with 2 μg of either wt c-FLIP$_L$ cDNA or the N-terminal deletion mutants, c-FLIP$_L$ I-DED, c-FLIP$_L$ II-DED, c- FLIP$_L$ Δ-DED (**c**), or the C-terminal deletion mutants c-FLIP$_L$-F1, c-FLIP$_L$ -F3, c-FLIP$_L$ -F5, c-FLIP$_L$ -R0 and c-FLIP$_L$ -R1 (**d**), as indicated. Protein extracts were immunoprecipitated with anti-Flag antibody and blotted with anti-Akt antibody. Total extracts were loaded as control, and blotted with anti-Akt or anti-Flag antibodies. Akt was not able to interact with F1, R0 and R1 mutants, indicating that Akt–c-FLIP interacting region is included from a.a. 253 to a.a. 339. (**e**) HEK-293T cells were transfected with c-FLIP$_L$ or c-FLIP$_s$ cDNA. Total lysates were immunoprecipitated with an anti-Flag antibody and then blotted with an anti-Akt antibody

immunoprecipitated using a monoclonal anti-Flag antibody and subsequently blotted using an anti-HA antibody. As shown in Figure 1a, c-FLIPL interacted at comparable levels with both the activated kinase and the kinase-dead Akt.

c-FLIP$_L$ is characterized by two death effector domains (DEDs), which are important for interaction with members of the apoptosis cascade. We examined whether these DED domains were important for the interaction with Akt. For this purpose, we generated three different mutants: cFLIP$_L$ I-DED, missing the first DED; cFLIP$_L$ II-DED, missing the second DED; and cFLIP $\Delta-$DED, missing both DEDs. The three mutants were transfected together with HA–Akt cDNA into HeLa cells. Extracts were immunoprecipitated using anti-Flag antibody and blotted with an anti-HA antibody. As shown in Figure 1c, all the c-FLIP$_L$ deletion mutants interacted with Akt, indicating that neither DED domain is necessary for the interaction with Akt.

We next investigated whether the carboxy terminal of c-FLIP$_L$ was the region of interaction with Akt. For this purpose, we generated different carboxy-terminal c-FLIP$_L$ mutants named: c-FLIP$_L$ F1 (a.a. 1–253), c-FLIP$_L$ F3 (a.a. 1–339), c-FLIP$_L$ F5 (a.a. 1–434), c-FLIP$_L$ R0 (a.a. 1–149) and c-FLIP$_L$ R1 (a.a. 1–182). Each mutant was transfected together with HA–Akt cDNA in HEK-293 cells. Extracts were immunoprecipitated after 48 h with anti-Flag antibody and blotted with anti-HA antibody. Akt interacted with F3 and F5 mutants but not with F1, R0 or R1 mutants (Figure 1d). The interaction of Akt with the short c-FLIP isoform (FLIPs) was barely detectable (Figure 1e). This suggests that the Akt–c-FLIP-interacting region is located between a.a. 253 and a.a. 339, within the caspase-like domain.

Role of c-FLIP$_L$ on growth factor-mediated Akt signaling. Beside cell death, c-FLIP$_L$ also regulates other DR-mediated signals. Thus, we set out to verify whether Akt–c-FLIP$_L$ interaction might modulate Akt activation. For this purpose, we first transfected increasing amounts of c-FLIP$_L$ cDNA and assessed the levels of the activated Akt using specific phospho-Akt antibodies. The overexpression of c-FLIP$_L$ did not induce significant differences in insulin-induced Akt phosphorylation (Figure 2a), even though it modified the phosphorylation of Gsk3β. As shown in Figure 2b, c-FLIP expression induced a reduction in endogenous Gsk3β basal phosphorylation level, in a dose-dependent manner. A similar inhibition of Gsk3β phosphorylation, both basal and upon insulin stimulation, was observed on co-transfecting the HA–Gsk3β together with c-FLIP (Figure 2c). Such inhibition was not observed in the presence of c-FLIP$_s$ (Figure 2f).

This inhibition was not observed in HeLa cells transfected with c-FLIP$_L$ mutants that do not interact with Akt, suggesting that Akt–c-FLIP interaction is necessary for this effect (Figure 2d and e).

Role of c-FLIP modulation of Gsk3β pathway on TRAIL-induced cell death. Although it has been clearly shown that c-FLIP$_L$ overexpression may cause resistance to TRAIL, the effects of Gsk3β on cell death are more controversial.[19] However, recently it was described that Gsk3β is involved in the resistance to TRAIL-induced apoptosis. Therefore, we investigated whether c-FLIP$_L$-induced apoptosis resistance upon extrinsic pathway activation was at least in part mediated by its effects on Gsk3β activation.

For this purpose, HeLa cells were transfected with Flag c-FLIP$_L$ cDNAs alone or in the presence of lithium chloride, an inhibitor of Gsk3 activity.[20] The cells were subsequently incubated with TRAIL, and cell death was assessed using a cell viability assay or with propidium iodide staining followed by FACS analysis. As shown in Figure 3a and b, c-FLIPL overexpression decreased the sensitivity of HeLa to TRAIL-induced apoptosis. However, treatment with LiCl completely counteracted the protective effect of c-FLIP on cell death (Figure 3a and b). To exclude unspecific effects of LiCl on cell death, the role of the Gsk3β pathway in the anti-apoptotic effect of c-FLIP was further evaluated using a specific Gsk3β kinase-inactive cDNA (Gsk3β-KI) and measuring caspase-8 activation. As shown in Figure 3c and d, c-FLIP$_L$ overexpression reduced TRAIL-induced caspase-8 activation, and this effect was counteracted by both LiCl and Gsk3β-KI cDNA. LiCl and Gsk3β-KI or GSk3β WT cDNA did not produce any effects on endogenous c-FLIP$_L$ levels (Supplementary Figure 1a).

Effects of c-FLIP$_L$ on p27^{Kip1} expression. Recently, Gsk3β inhibition has been suggested to regulate the cell cycle through regulation of p27^{Kip1} levels.[21] In addition, we have recently shown that miRNAs regulate p27^{Kip1} expression and TRAIL sensitivity.[22] Therefore, we addressed the question of whether the effect of c-FLIP$_L$ on TRAIL resistance was mediated through Gsk3β activity and thus on p27 expression levels.

As shown in Figure 4a, we observed that the levels of p27^{Kip1} were drastically reduced in HEK-293 cells stably overexpressing c-FLIP$_L$. A similar result was observed also in HeLa cells stably (HeLa Tween FLIP) or transiently overexpressing c-FLIP$_L$ (Flag FLIP; Figure 4b). However, overexpression of c-FLIP$_L$ deletion mutants of the Akt interaction site did not induce reduction in p27^{Kip1} levels (Figure 4c). Moreover, this effect was not observed in the presence of c-FLIP$_s$ (Figure 4f).

The downregulation of Gsk3β, by a specific siRNA or inactivation with LiCl, induced an increase in p27^{Kip1} levels in HeLa Tween FLIP$_L$ compared to cells transfected with a scrambled siRNA (Figure 4d). Taken together these results indicate that the effect of c-FLIP on p27^{Kip1} is mediated by Gsk3β activity. We next investigated whether c-FLIP$_L$–Gsk3 regulate p27^{Kip1} at mRNA levels. To assess this point, HeLa cells were transfected with 5 μg of Flag c-FLIP$_L$ cDNA or a control vector for 48 h, and p27^{Kip1} cDNA levels were evaluated by real-time PCR. Interestingly, we observed a significant reduction of *p27^{Kip1}* mRNA levels in HeLa cells transfected with c-FLIP$_L$ but not with its mutant (Figure 4e), suggesting that the c-FLIP$_L$–Gsk3 pathway regulates p27^{Kip1} expression levels through a transcriptional mechanism.

The effect of p27^{Kip1} on TRAIL-mediated apoptotic signaling. We recently provided evidence that p27^{Kip1} is involved in TRAIL resistance in non-small cell lung cancer (NSCLC).[22] We demonstrated that in TRAIL-resistant CALU-1 cells, miR-222 and miR-221 are overexpressed and target

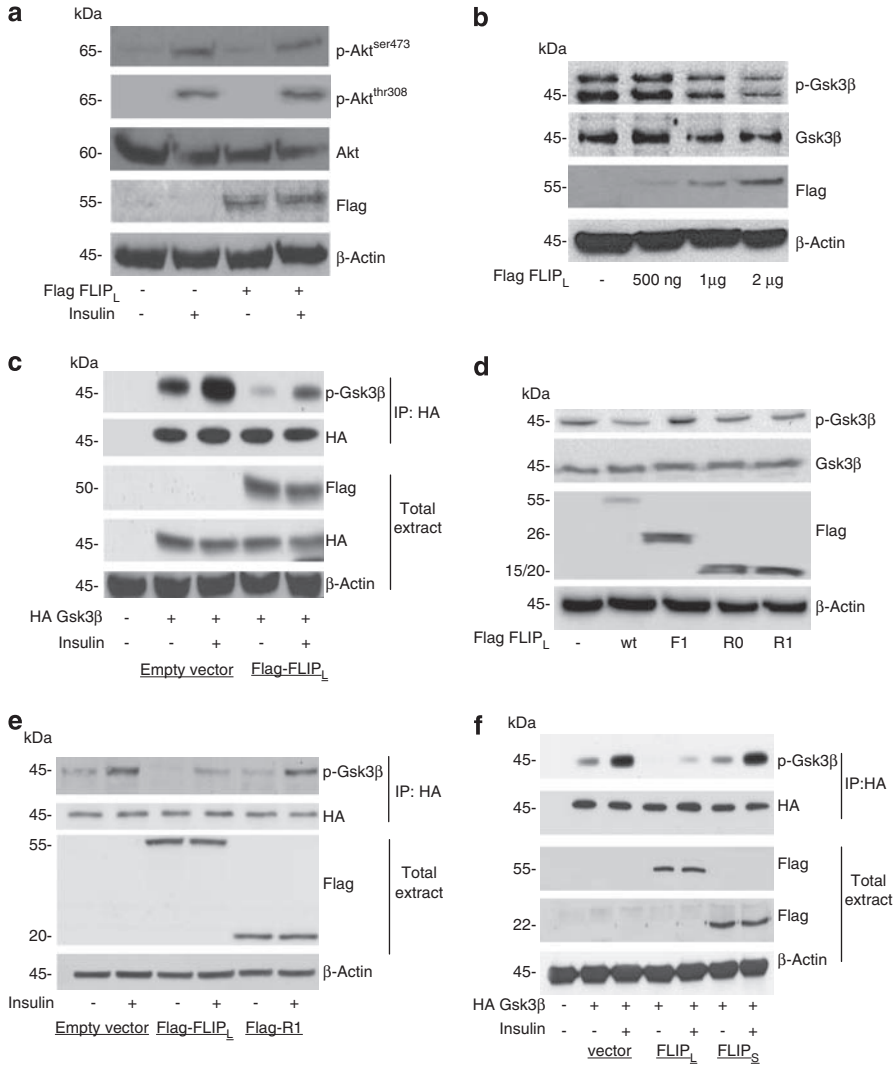

Figure 2 Role of c-FLIP$_L$ on Akt–Gsk3β signaling pathway. (**a**) c-FLIP effects on Akt activation. HeLa cells were transfected with c-FLIP$_L$ cDNA for 24 h, serum-starved for 12 h and then treated with insulin (100 nM) for 15 min. Total cellular extracts were resolved by western blot and analyzed with the indicated antibodies. FLIP overexpression does not affect Akt phosphorylation. (**b**) Western blot analysis of p-Gsk3β and Gsk3β expression in HeLa WT or transfected with different concentrations of c-FLIP$_L$ cDNA (500 ng, 1 μg and 2 μg) for 48 h. We observed a strong reduction of Gsk3β phosphorylation. (**c**) HeLa cells were transfected with HA–Gsk3β cDNA, and c-FLIP$_L$ cDNA or control vector, as indicated for 24 h. Cells were starved for 12 h and then treated with insulin (100 nM) for 15 min. Cell lysates were immunoprecipitated with anti-HA antibody and blotted with phospho-Gsk3β antibody. (**d**) Western blot analysis of HeLa cells transfected with c-FLIP-WT, c-FLIP-F1, c-FLIP-R0 or c-FLIP-R1 cDNA. Total lysates were analyzed with anti-phospho-Gsk3β, Gsk3, Flag and β-actin antibodies. c-FLIP mutants were not able to decrease phospho Gsk3β levels. (**e**) HeLa cells were transfected with HA–Gsk3β and c-FLIP-R1 cDNA or with a control vector, treated with insulin (100 nM) for 15 min, immunoprecipitated with anti-HA antibodies, and blotted with p-Gsk3β antibodies. Total lysates were analyzed with the indicated antibodies. c-FLIP mutant overexpression did not reduce Gsk3β phosphorylation. (**f**) HeLa cells were transfected with HA–Gsk3β cDNA, and c-FLIP$_L$ cDNA, c-FLIP$_s$ cDNA or control vector, as indicated for 24 h. Cells were serum starved for 12 h and then treated with insulin (100 nM) for 15 min. Cell lysates were immunoprecipitated with anti-HA antibody and blotted with anti-phospho-Gsk3β antibody

p27^{Kip1}, inducing its downregulation. However, TRAIL-sensitive H460 cells exhibited reduced levels of miR-222 and miR-221 and increased p27^{Kip1} expression. We therefore investigated whether p27^{Kip1} modulated sensitivity to TRAIL-mediated cell death through the regulation of the apoptotic machinery molecules. To this aim, HeLa Tween FLIP cells, which express p27^{Kip1} at very low levels, were transfected with HA–p27 cDNA, and caspase-3 levels were investigated by western blot analysis. We observed a significant increase in caspase-3 levels (Figure 5a). Furthermore, silencing of p27^{Kip1} using a specific siRNA in H460 cells, which express p27^{Kip1} at high levels, resulted in reduction in caspase-3 level (Figure 5b).

To further confirm the role of the FLIP–Gsk3 pathway on TRAIL apoptotic machinery, we evaluated caspase-3 levels in HeLa Tween c-FLIP-overexpressing cells, Gsk3 pathway of which was inhibited either by *Gsk3* siRNA or by LiCl treatment. Both inhibitions resulted in an increase in caspase-3 expression levels, whereas no differences were observed in FADD levels (Figure 5c).

We investigated whether c-FLIP$_L$ modulated caspase-3 transcript levels through a transcriptional mechanism by

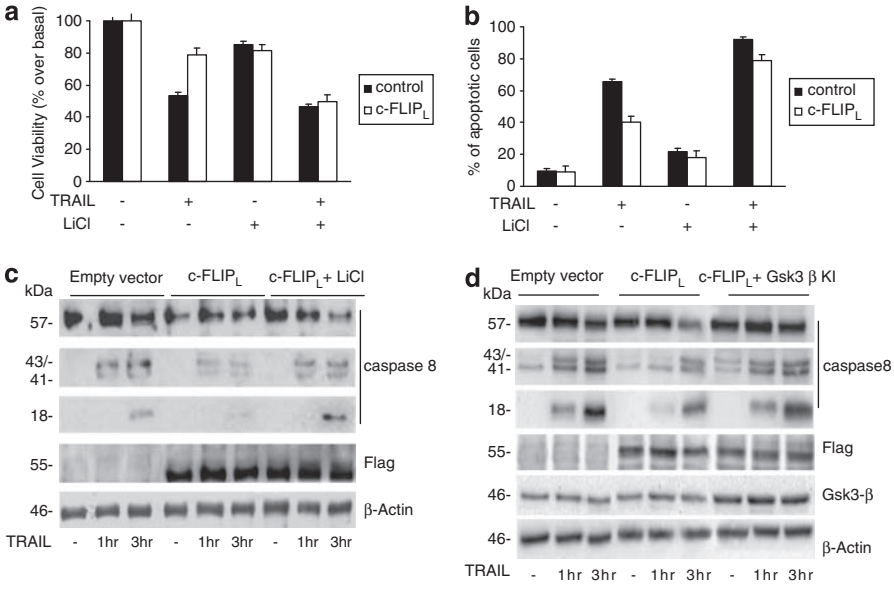

Figure 3 Role of c-FLIP$_L$ and Gsk3β signaling pathway on TRAIL-induced cell death. Cell death quantification – HeLa cells were transfected with 2 μg of c-FLIP$_L$ cDNA for 24 h, plated in 96-well plates in triplicate and then treated with SuperKiller TRAIL (500 ng/ml) and lithium chloride (20 mmol) for 48 h, as indicated. Cell viability was assessed by Cell Vitality assay (**a**) or by propidium iodine staining and FACS analysis (**b**). (**c** and **d**) Western blot analysis of caspase-8 activation. The inhibition of Gsk3β was obtained by transfection of HeLa cells with kinase-inactive Gsk3β cDNA or by treatment with 20 mmol lithium chloride for 24 h. Cells were incubated with 500 ng/ml TRAIL for 1 or 3 h. The inhibition of Gsk3β induced an increase of caspase-8 activation in c-FLIP-overexpressing cells

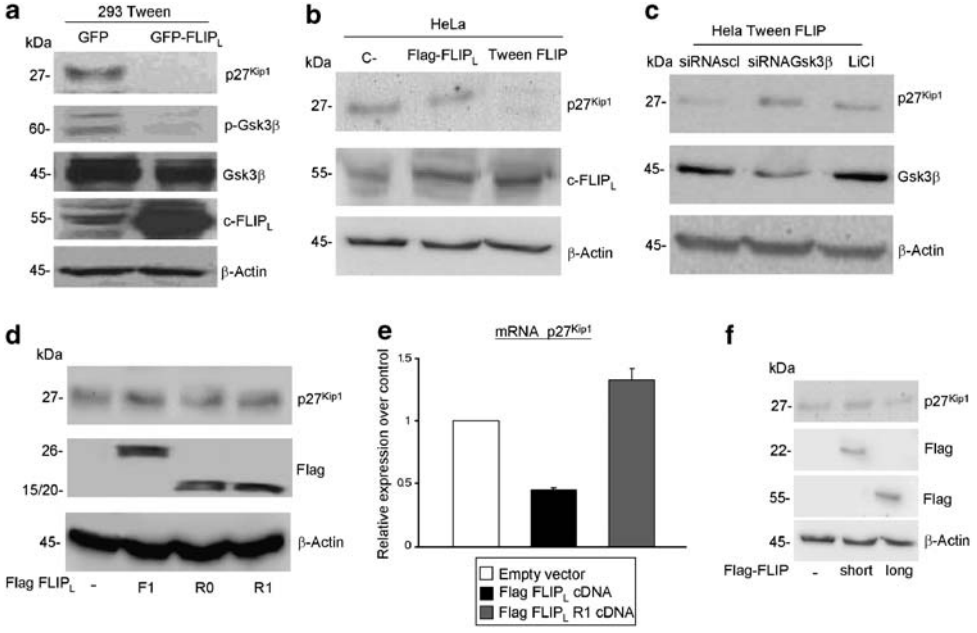

Figure 4 c-FLIP overexpression regulates p27^{Kip1} levels through Gsk3β. Western blot analysis of Gsk3β, p-Gsk3β and p27^{Kip1} levels in different cell lines. (**a**) HEK-293–Tween GFP and tween–GFP c-FLIP$_L$; (**b**) HeLa cells transfected with c-FLIP$_L$ cDNA and HeLa Tween c-FLIP$_L$. There is an inverse correlation between FLIP and p-Gsk3 levels. (**c**) Western blot analysis of p27^{Kip1} levels in HeLa cells transfected with c-FLIP$_L$ mutants F1, R0 and R1 cDNA. (**d**) Effects of inhibition of Gsk3β on p27^{Kip1} expression. HeLa Tween FLIP cells were transfected with Gsk3β siRNA or scrambled siRNA or treated with 20 mmol lithium chloride for 24 h. Levels of p27^{Kip1} and Gsk3β were analyzed by immunoblotting. (**e**) Real time PCR analysis of *p27^{Kip1}* mRNA with transfection of FLIP$_L$ cDNA in HeLa cells. c-FLIP reduces p27 ^{Kip1} levels through Gsk3β. c-FLIP deletion mutants were not able to reduce p27^{Kip1} levels. (**f**) Total lysates of HeLa cells transfected with c-FLIP$_L$, c-FLIP$_s$ or control vector were analyzed for p27 expression

real-time PCR. Interestingly, we observed a significant reduction in *caspase-3* mRNA levels in HeLa cells transfected with c-FLIP$_L$ compared with controls, whereas this effect was not observed in FLIP R1 mutant (Figure 5d).

Finally, we also examined the activity of caspase-3 by the colorimetric CaspACE assay in HeLa cells transfected with an empty vector or with c-FLIP$_L$ cDNA. The expression of c-FLIP$_L$ induced a reduction of caspase-3 activity

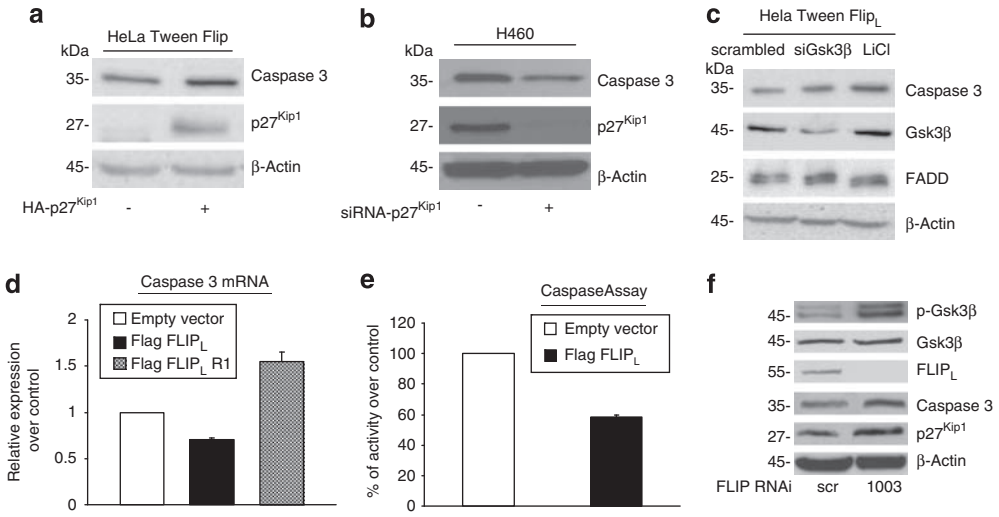

Figure 5 Role of $p27^{Kip1}$ on caspase-3 expression. (**a**) HeLa Tween FLIP cells transfected with HA–$p27^{Kip1}$ cDNA were analyzed by western blotting for caspase-3. Loading and transfection control were analyzed with anti-$p27^{Kip1}$ and anti-β-actin antibodies. p27 overexpression induced an increase in caspase-3 expression levels. (**b**) Western blot analysis of caspase-3 and -8 in H460 cells on transfection of *$p27^{Kip1}$* siRNA. The inhibition of p27 decreases caspase-3 levels. (**c**) Immunoblotting of HeLa Tween FLIP cells upon transfection of scrambled siRNA (sc-si), Gsk3β siRNA or treatment with 20 mM lithium chloride for 24 h with caspase-3, FADD or Gsk3β antibodies. The inhibition of Gsk3 pathway resulted in an increase in expression levels of caspase-3, whereas no differences were observed in FADD and caspase-8 expression. (**d**) Real-time PCR of *caspase-3* mRNA on transfection in HeLa cells with Flag–$FLIP_L$ cDNA. FLIP overexpression induced a significant reduction of *caspase-3* mRNA levels. (**e**) Quantification of caspase-3 activity by Colorimetric CaspACE Assay System in HeLa cells transfected with an empty vector or Flag–$FLIP_L$ cDNA. (**f**) Total lysate of HeLa cells expressing RNAi constructs for c-FLIP (FLIP 1003) or with a scrambled control. A total of 40 μg of proteins were loaded and blotted with the indicated antibodies. β-Actin was used as the loading control. FLIP downregulation induced an increase of GSK3β phosphorylation, p27 and caspase-3 levels. Representative experiment was performed in triplicates

(Figure 5e). All these effects were reverted when c-$FLIP_L$ endogenous levels were downregulated by a specific c-$FLIP_L$ siRNA (Figure 5f). The effects of specific RNAi constructs for c-FLIP on FLIP expression levels are shown in Supplementary Figure 1b.

Discussion

In this study, we provide evidence for a new role of c-$FLIP_L$. c-$FLIP_L$ has been identified as an inhibitor of apoptosis triggered by the engagement of death receptors, such as Fas or TRAIL.[23,24] c-$FLIP_L$ has also been implicated in other cellular functions, such as control of gene expression by ERK and NF-κB.[9,25]

We demonstrate, to the best of our knowledge, for the first time that Akt interacts with c-$FLIP_L$, and that this interaction functionally regulates Gsk3β activation and apoptosis. Recently, Giampietri *et al*.[26] described that in c-FLIP transgenic mice, the phosphorylation of Akt and Gsk3β were reduced compared with control animals, even though caspase-3 activity was unchanged, highlighting an apoptosis-independent role of c-FLIP on pressure overload-mediated cardiac hypertrophy. The role of c-FLIP in heart development has been previously described in c-FLIP ko mice that, similar to FADD ko mice, developed severe defects of heart development.[27,28] These studies identify c-FLIP as a new regulator of heart development and the hypertrophic response, possibly through Gsk3 signaling.

In this study, by genetic and biochemical methodologies, we have demonstrated that Akt is able to interact with c-$FLIP_L$ in the region stretching from a.a. 253 to a.a. 339 of the c-$FLIP_L$ protein. We observed that overexpression of c-$FLIP_L$, although does not interfere with insulin-induced Akt activation, almost abolishes Gsk3β phosphorylation. The effects on Gsk3β were abrogated when we overexpressed c-$FLIP_L$ mutants that do not bind Akt. This may means that, by binding to Akt, c-$FLIP_L$ relegates the kinase in a different cellular compartment, and abolishes its ability to bind and phosphorylate its substrates. It is interesting that the phosphorylation of other Akt substrates besides Gsk3β, such as BAD, was reduced in c-$FLIP_L$-overexpressing cells (data not shown).

It has been reported that Gsk3β contributes both to cell death and cell survival, depending on the cellular system and the appropriate stimuli.[19] Several studies indicated that inhibition of Gsk3β activity in cancer cells potentates apoptosis stimulated by death receptor.[29–32] Furthermore, knocking out Gsk3β or inhibiting Gsk3β using lithium chloride, potentates TNF-induced apoptosis, indicating an anti-apoptotic role for Gsk3β.[30]

Therefore, we asked whether c-$FLIP_L$-mediated reduction of Gsk3β phosphorylation, and thus increase in its kinase activity, might be necessary for the anti-apoptotic function of c-$FLIP_L$. Interestingly, when we interfered with Gsk3β activity, either using LiCl or with overexpression of a kinase-inactive form of Gsk3, anti-apoptotic c-$FLIP_L$ effects were significantly reduced. Thus, Gsk3β may act as an important mediator that participates in FLIP's anti-apoptotic function in human cancer.

We have recently demonstrated that p27 expression is linked to TRAIL resistance in NSCLC cells overexpressing miR-222.[22] We therefore investigated the level of p27 in different cells overexpressing c-$FLIP_L$. Interestingly, we observed an inverse correlation between the c-$FLIP_L$ and

p27 expression levels, as well as Gsk3β phosphorylation. This was also true in forced c-FLIP$_L$-expressing cells (HEK-293 and HeLa). We then investigated whether c-FLIP could affect p27 levels through the activation of Gsk3β. For this purpose, we interfered with Gsk3β expression levels or activity in c-FLIP$_L$-overexpressing cells and evaluated p27 levels. We observed that Gsk3β inhibition increased protein and mRNA levels of p27. The effects of FLIP$_L$ on p27 depend on its interaction with Akt, as c-FLIP$_L$ WT overexpression, but not its Akt-binding-site deletion mutants, was able to reduce *p27* mRNA level. Recently, Wang *et al*.[21] described that Gsk3β negatively regulates p27 protein in MLL leukemia cells, thus being critical for the maintenance of MLL leukemia, and prospecting Gsk3 as an interesting target for this form of cancer. In the MLL cellular system, the effects were mainly at the protein level because the inhibition of Gsk3β did not affect mRNA levels. Therefore, although the final effect is similar, the functional relationships of Gsk3β with p27 seem to be cell type dependent. Gsk3β is a negative regulator of heart hypertrophy.[33] Interestingly, Hauck[34] recently described that silencing p27 induced cardiomyocyte hypertrophyc growth in the absence of growth-factor stimulation. It is interesting to speculate that Gsk3β mediates negative regulation of hypertrophyc growth through its effects on p27 expression levels.

Finally, we investigated the mechanisms of c-FLIP–Gsk3β–p27-mediated inhibition of cell death, by the evaluation of protein and mRNA levels of apoptosis-signaling molecules.

We showed that the absence of p27 induces a reduction in caspase-3 levels. This effect was mediated by Gsk3β because its inactivation induced an increase in caspase-3 level. The effect was specific on caspase-3 because other apoptosis-signaling molecules, such as FADD, were not affected. This effect occurred at the transcriptional level because c-FLIP$_L$ overexpression, but not its mutants, was able to reduce *caspase-3* mRNA level, as assessed by RT-PCR. The overexpression of c-FLIP$_L$ also induces a significant reduction in the amount of the active caspase in untreated cells. Thus, taken together these data depict a model in which in c-FLIP-overexpressing cells, the activation of Gsk3β induces a reduction in p27^{Kip1} and caspase-3 expression and activity levels, and thus a reduction in TRAIL-induced cell death (Figure 6).

Recently, Gsk3β has been described as a protein complex associated with death receptors, DDX3, and cellular inhibitor of apoptosis protein-1 (cIAP-1).[29] In that study, Gsk3β inhibited apoptosis by interfering with DISC formation and caspase-8 activation. Our data reveal other possible mechanisms through which Gsk3 might inhibit apoptosis, that is, through regulation of p27 expression and that of downstream caspase-3 (Figure 6).

Our data show that c-FLIP overexpression strongly reduces Akt-mediated Gsk3β phosphorylation. Furthermore, it's down-regulation by a specific c-FLIP siRNA resulted in an increase in Gsk3β phosphorylation, as well as in p27 and caspase-3 levels.

In conclusion, this study demonstrates that anti-apoptotic functions of c-FLIP$_L$ are mediated by its effects on Gsk3β activity, and p27 and caspase-3 levels. These findings may be of importance in optimizing a strategy for the treatment of TRAIL-resistant human cancer.

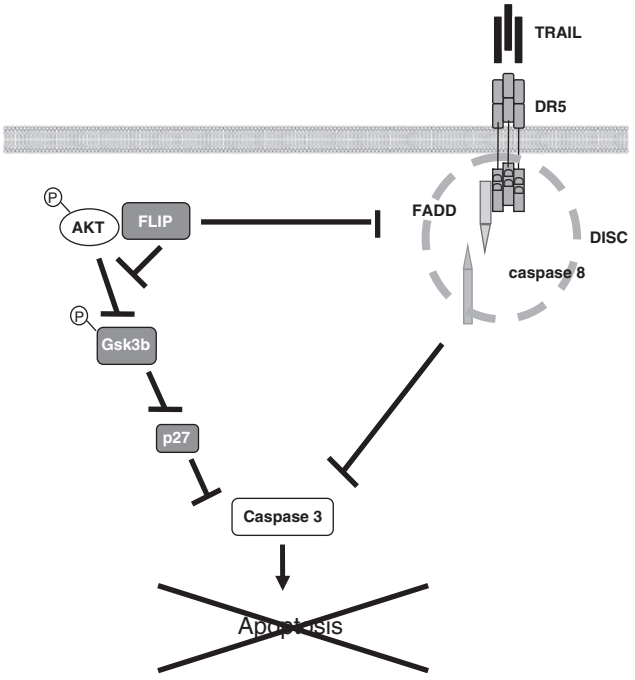

Figure 6 Role of cFLIP–Gsk3 signaling pathway in the regulation of cell death. In FLIP-overexpressing cells, activation of Gsk3β induces a reduction in p27^{Kip1} and caspase-3 expression levels and a reduction in TRAIL-induced cell death

Materials and Methods

Materials. Media, sera and antibiotics for cell culture were purchased from Life Technologies (Grand Island, NY, USA). Protein electrophoresis reagents were obtained from Bio-Rad (Richmond, VA, USA). Western blotting and ECL reagents were procured from GE Healthcare (Pixcataway, NJ, USA). All other chemicals were from Sigma (St. Louis, MO, USA). The antibodies: anti-caspase-8 antibody (1C12), anti-Akt, anti-P-Akt, anti-P-Gsk3β, anti-Gsk3β and anti-p27^{Kip1} were purchased from Cell Signaling Technology (Danvers, MA, USA); anti-caspase-3 antibody was obtained from Abcam (Cambridge, MA, USA); anti-c-FLIP (NF6) antibody was purchased from Alexis (Lausen, Switzerland); anti-Flag M2 and anti-β-actin antibodies were obtained from Sigma; anti-HA antibody was obtained from Covance (Berkeley, CA, USA). SuperKiller TRAIL was purchased from Alexis.

Plasmids. The plasmids pcDNA3 Flag(hs)FLIP$_L$ and FLIP$_s$ were kindly provided by Professor Pasquale Vito and Henning Walczack, respectively. Akt WT, Akt E40K (constitutively active, HA–Akt D+) and Akt K179M (dominant-negative HA–Akt D) with an HA tag were a kind gift of Professor Gianluigi Condorelli. Gsk3β WT and Gsk3β kinase inactive (KI) cDNAs were kindly provided by Professor Junichi Sadoshima. p27 cDNA was kindly provided by Professor Alfredo Fusco. pRetroSuper vectors expressing RNAi for c-FLIP were obtained from Professor Simone Fulda.

Cell culture. Human HeLa, HEK-293, K562 and A459 cell lines were grown in DMEM containing 10% heat-inactivated FBS with 2 mM L-glutamine and 100 U/ml penicillin–streptomycin. DU145 and H460 cell lines were grown in RPMI containing 10% heat-inactivated FBS with 2 mM L-glutamine and 100 U/ml penicillin–streptomycin.

Yeast two-hybrid system. All experiments were performed in the yeast reporter MaV203. The human heart cDNA library was obtained from Invitrogen (Carlsbad, CA, USA). Screening of the library was performed essentially following instructions for the ProQuest two-hybrid system (Life Technologies) and has been previously described.[35] The GAL4 DNA-binding domain/human Akt fusion was obtained from Dr. Alfonso Bellacosa (Fox Chase Cancer Center, Philadelphia, PA, USA). Subsequently, yeast pLEx4-Akt plasmid was transformed with the pPC86AD cDNA library and plated onto plates lacking histidine in the presence of 3AT

(aminotriazole; 10 mM). Approximately 1.2×10^6 individual clones were plated, and about 200 grew on the selective medium. Resistant colonies were grown on a master plate and then replica-plated onto selection plates to determine their ability to induce three independent reporters (*HIS3*, *URA3* and *lacZ*). A total of 80 independent clones were isolated after this first screening. The DNA was isolated from each positive clone and sequenced to identify the inserts. Independent clones were retransformed into yeast and tested for interaction with a fresh Akt clone.

c-FLIP$_L$ deletion mutants generation. We generated three deletion mutants of c-FLIP$_L$ by PCR, using as template the plasmid pcDNA3-3 × Flag-FLIP$_L$. c-FLIP l-DED mutant, encoding a.a. 81–480, which lacks the first DED, was generated using the primers: Fw: 5′-cccaagcttacccacctgctcaggaaccct-3′ and Rv: 5′-gctctagattatgtgtaggagaggata -3′; c-FLIP-II-DED, encoding a.a. 1–93 and a.a. 178–480, which lacks the second DED, was generated using the primers: Fw: 5′-cccaagcttatgtctgctgaagtcatccat-3′ and Rv: 5′-tgtccctgcatagtccgaaacaaggtgagg-3′ for amino acids 1–93 and Fw: 5′-tcggactatgcagggacaagttacaggaat-3′ and Rv: 5′-gctctagattatgtgtaggagaggata-3′ for amino acids 178–480; FLIP$_L$-ΔDED, encoding a.a. 178–488, which lacks both DEDs, was generated using the primers: Fw: 5′-cccaagcttgcagggacaagttacaggaat-3′ and Rv: 5′-gctctagattatgtgtaggagaggata-3′. The amplified sequences were cloned in p3 × -Flag-CMV previously linearized with the restriction enzymes *Hin*DIII and *Xba*I. The following deletion mutants were generated: c-FLIP$_L$-F1, encoding a.a. 1–253, was generated using the primers: Fw: 5′- tgacgataaagaattcatgtctgc-3′ and Rv: 5′-gattcctaggggcttgctctt-3′; c-FLIP$_L$-F3, encoding a.a. 1–339, was generated using the primers: Fw: 5′-tgacgata aagaattcatgtctgc-3′ and Rv: 5′-catcctcctgatgtgatgca-3′; cFLIP$_L$-F5, encoding a.a. 1–434, was generated using the primers: Fw: 5′-tgacgataaagaattcatgtctgc-3′ and Rv: 5′-ttcttgtctcagtttctggg-3′; c-FLIP$_L$-R0, encoding a.a. 1–177, was generated using the primers: Fw: 5′-tgacgataaagaattcatgtctgc-3′ and Rv: 5′-gccctcgagttatc cagttgatctggggcaac-3′; c-FLIP$_L$-R1, encoding a.a. 1–182, was generated using the primers: Fw: 5′-tgacgataaagaattcatgtctgc-3′ and Rv: 5′-gccctcgagttactgtaacttgt ccctgctcc-3′. Temperature cycles used were as follows: 95°C for 1 min; 95°C for 50 s, 60°C for 50 s, 68°C for 7 min for 35 cycles; 68°C for 2 min.

Production of retroviral particles and infection of HeLa and HEK-293 cells. The c-FLIP$_L$ cDNA was cloned in PINCO vector.[36] The amphotropic packaging cell line Phoenix was transfected by standard calcium phosphate/chloroquine method, and culture supernatants containing retroviral particles were collected at 48 h after transfection. Transduction was carried out by culturing (thrice) 5×10^5 cells in 1 ml of 0.45-mmol/l filtered supernatant containing viral particles. Gene-transfer efficiency was evaluated by flow cytometry analysis based on the expression of the GFP reporter. The levels of c-FLIP expression were evaluated by immunoblot analysis using lysates of cells infected with the empty Tween vector (HeLa Tween and HEK-293 Tween) for comparison.

Western blotting. Total proteins from cells was extracted with RIPA buffer (0.15 mM NaCl, 0.05 mM Tris-HCl (pH 7.5), 1% Triton X-100, 0.1% SDS, 0.1% sodium deoxycolate and 1% Nonidet P40). A total of 50 μg of sample extract were resolved on 7.5–12% SDS-PAGE using a mini-gel apparatus (Bio-Rad Laboratories, Richmond, CA, USA) and transferred to Hybond-C extra nitrocellulose. Membranes were blocked for 1 h with 5% non-fat dry milk in TBS containing 0.05% Tween-20, incubated for 2 h with primary antibody, washed and incubated with secondary antibody, and visualized by chemiluminescence.

Phosphorylation experiments. HeLa cells were transiently transfected with different cDNAs as indicated. After 24 h, the cells were incubated in serum-free culture medium for 16 h at 37°C. Insulin (final concentration, 100 nM) was then added, and the cells were rapidly rinsed with ice-cold saline followed by solubilization with 0.5 ml of RIPA buffer per dish for 1 h at 4°C. Lysates were centrifuged at 5000 × *g* for 20 min, and solubilized proteins were precipitated with the indicated antibodies, separated by SDS-PAGE, and revealed by western blot with antibodies recognizing the phosphorylated proteins.

Immunoprecipitation. Cells were cultured at a final concentration of 90% in p100 plates. The cells were collected with RIPA Buffer on a shaker for 30 min. A total of 1 mg of total extract was immunoprecipitated using the indicated antibodies (5 μg/ml anti-Flag, 2 μg/ml anti-HA, 3 μg/ml anti-Akt and 3 μg/ml anti-Gsk3β) for 16 h on shaker. Then, A/G beads (Santa Cruz Biotechnology, Santa Cruz, CA, USA) were added for 2 h. The beads were washed for three times with washing buffer (50 mM Tris-HCl (pH 7.5), 150 mM NaCl, 0.1% Triton X-100, 10% glycerol), and then 20 μl of sample buffer was added; the samples were boiled at 100°C for 5 min and then the supernatants resolved by SDS-PAGE.

Caspase assay. The assay was performed using the Colorimetric CaspACE Assay System (Promega, Madison, WI, USA) as reported in the instruction manual. Briefly, HeLa cells were transfected with lipofectamine 2000; 48 h after transfection, cells were collected in caspase assay buffer and protein was quantified by Bradford Assay. A total of 50 μg of protein were used.

Cell death and cell proliferation quantification. Cells were plated in 96-well plates in triplicate and incubated at 37°C in a 5%CO_2 incubator. To induce apoptosis, Superkiller TRAIL (Alexis) was used for 24 h at 500 ng/ml. Cell viability was evaluated with the CellTiter 96 AQ_{ueous} One Solution Cell Proliferation Assay (Promega), according to the manufacturer's protocol. Metabolically active cells were detected by adding 20 μl of MTT to each well. After 30 min of incubation, the plates were analyzed in a Multilabel Counter (Bio-Rad, Richmond, VA, USA). Apoptosis was also assessed using annexin V–FITC Apoptosis Detection Kit followed by flow cytometric analysis. Cells were seeded at a density of 1.8×10^6 cells per 100-mm dish, grown overnight in 10% FBS/RPMI, washed with PBS, and then treated for 24 h with 200 ng TRAIL. After incubation, cells were washed with cold PBS and removed from the plates using very mild trypsinization conditions (0.01 % trypsin/EDTA). The resuspended cells were washed with cold PBS and stained with FITC-conjugated annexin V antibody and propidium iodide (PI), according to the instructions provided by the manufacturer (Roche Applied Science, Indianapolis, IN, USA). Cells (50 000 per sample) were then subjected to flow cytometry analysis. Flow cytometry analysis and PI staining were performed as described previously.[16] To quantify caspase activation, cells were transfected with the indicated cDNA or treated with lithium chloride (20 mM) and then incubated with superkiller TRAIL for the indicated times. Lysates were examined by western blotting with anti-caspase-8 antibodies.

siRNA transfection. HeLa cells were cultured to 80% confluence, kept in antibiotic-free, serum-containing medium, and transiently transfected using Lipofectamine 2000 with 150 nmol anti-Gsk3-β siRNA (Invitrogen), a pool of two target-specific 20–25 nt siRNAs, or with siCONTROL oligonucleotides, as indicated. Cells were incubated with siRNAs for the indicated times.

The siRNAs were transfected with 6 μl transfection reagent, as described in the manufacturer's protocol. Anti $p27^{Kip1}$ siRNA was purchased from Santa Cruz Biotechnology. siCONTROL Non-Targeting siRNA Pool #2 (D-001206–14–05) was from obtained from Dhamarcon (Lafayette, CO, USA) and comprised four siCONTROL Non-Targeting siRNAs. Each individual siRNA within this pool was characterized by genome-wide microarray analysis and found to have minimal off-target signatures.

c-FLIP$_L$ knockdown. Stable knockdown of c-FLIP$_L$ in HeLa cells was obtained with siRNAs (complementary sense and antisense oligonucleotides): FLIP-909 (5′-GGAGCAGGGACAAGTTACA-3′) and FLIP-1003 (5′-GTAAAGAAC AAAGACTTAA-3′) or scrambled oligonucleotide were cloned in the pRSC retroviral vector as described previously.[37] Cells were selected with 10 μg/ml puromycin.

RNA isolation and real-time PCR analysis. The RNA was extracted using TRIzol solution (Invitrogen) followed by DNAse treatment (DNA free, Ambion, Austin, TX, USA). The quality and quantity of RNA was determined by measuring the absorbance of the total RNA at 260 and 280 nm, and by 1% agarose electrophoresis under reducing conditions and visualized with ethidium bromide. For mRNA profiling, reverse transcription (RT) was performed by using Superscript II First Stand Synthesis Kit (Invitrogen). Real-time PCR to assay mRNA level was performed in an iQ Real Time PCR Detection System (Bio-Rad, Hercules, CA, USA) with iQ SYBR Green Supermix (Bio-Rad). All primers were synthesized commercially (PRIMM, Milan, Italy). Polymerase chain reactions were performed in triplicate and fold changes were calculated with the following formula: $2^{(\text{sample 1}\Delta C_t\ \text{sample 2}\Delta C_t)}$, where ΔC_t is the difference between the amplification fluorescent thresholds of the mRNA of interest and the mRNA of β-actin used as an internal reference. All reactions were performed according to manufacturer's protocol.

Conflict of interest

The authors declare no conflict of interest.

Acknowledgements. We thank Dr. V de Franciscis and M Latronico for paper revision; and LR Vitiani for preparation of c-FLIP-overexpressing cells. This study was partially supported by funds from: Associazione Italiana Ricerca sul Cancro (AIRC) (to GC), MIUR-FIRB (RBIN04J4J7) and EU grant EMIL (European Molecular Imaging Laboratories Network) contract number 503569.

1. Hengartner MO. The biochemistry of apoptosis. *Nature* 2000; **407**: 770–776.
2. Okada H, Mak TW. Pathways of apoptotic and non-apoptotic death in tumour cells. *Nat Rev Cancer* 2004; **4**: 592–603.
3. Ghobrial IM, Witzig TE, Adjei AA. Targeting apoptosis pathways in cancer therapy. *CA Cancer J Clin* 2005; **55**: 178–194.
4. Peter ME. The flip side of FLIP. *Biochem J* 2004; **382** (Part2): e1–e3.
5. Scaffidi C, Schmitz I, Krammer PH, Peter ME. The role of c-FLIP in modulation of CD95-induced apoptosis. *J Biol Chem* 1999; **274**: 1541–1548.
6. Irmler M, Thome M, Hahne M, Schneider P, Hofmann K, Steiner V *et al.* Inhibition of death receptor signals by cellular FLIP. *Nature* 1997; **388**: 190–195.
7. Safa AR, Day TW, Wu CH. Cellular FLICE-like inhibitory protein (C-FLIP): a novel target for cancer therapy. *Curr Cancer Drug Targets* 2008; **8**: 37–46.
8. Lin Y, Liu X, Yue P, Benbrook DM, Berlin KD, Khuri FR *et al.* Involvement of c-FLIP and survivin down-regulation in flexible heteroarotinoid-induced apoptosis and enhancement of TRAIL-initiated apoptosis in lung cancer cells. *Mol Cancer Ther* 2008; **7**: 3556–3565.
9. Kataoka T, Budd RC, Holler N, Thome M, Martinon F, Irmler M *et al.* The caspase-8 inhibitor FLIP promotes activation of NF-kappaB and Erk signaling pathways. *Curr Biol* 2000; **10**: 640–648.
10. Maedler K, Fontana A, Ris F, Sergeev P, Toso C, Oberholzer J *et al.* FLIP switches Fas-mediated glucose signaling in human pancreatic beta cells from apoptosis to cell replication. *Proc Natl Acad Sci USA* 2002; **99**: 8236–8241.
11. Fang LW, Tai TS, Yu WN, Liao F, Lai MZ. Phosphatidylinositide 3-kinase priming couples c-FLIP to T cell activation. *J Biol Chem* 2004; **279**: 13–18.
12. Franke TF, Hornik CP, Segev L, Shostak GA, Sugimoto C. PI3K/Akt and apoptosis: size matters. *Oncogene* 2003; **22**: 8983–8998.
13. Datta SR, Dudek H, Tao X, Masters S, Fu H, Gotoh Y *et al.* Akt phosphorylation of BAD couples survival signals to the cell-intrinsic death machinery. *Cell* 1997; **91**: 231–241.
14. Cardone MH, Roy N, Stennicke HR, Salvesen GS, Franke TF, Stanbridge E *et al.* Regulation of cell death protease caspase-9 by phosphorylation. *Science* 1998; **282**: 1318–1321.
15. Brunet A, Bonni A, Zigmond MJ, Lin MZ, Juo P, Hu LS *et al.* Akt promotes cell survival by phosphorylating and inhibiting a Forkhead transcription factor. *Cell* 1999; **96**: 857–868.
16. Garofalo M, Quintavalle C, Zanca C, De Rienzo A, Romano G, Acunzo M *et al.* Akt regulates drug-induced cell death through Bcl-w downregulation. *PLoS ONE* 2008; **3**: e4070.
17. Doble B, Woodgett J. GSK-3: tricks of the trade for a multi-tasking kinase. *J Cell Sci* 2003; **116** (Part 7): 1175–1186.
18. Cohen P, Frame S. The renaissance of GSK3. *Nat Rev Mol Cell Biol* 2001; **2**: 769–776.
19. Beurel E, Jope RS. The paradoxical pro- and anti-apoptotic actions of GSK3 in the intrinsic and extrinsic apoptosis signaling pathways. *Prog Neurobiol* 2006; **79**: 173–189.
20. Jope RS. Lithium and GSK-3: one inhibitor, two inhibitory actions, multiple outcomes. *Trends Pharmacol Sci* 2003; **24**: 441–443.
21. Wang Z, Smith KS, Murphy M, Piloto O, Somervaille TC, Cleary ML. Glycogen synthase kinase 3 in MLL leukaemia maintenance and targeted therapy. *Nature* 2008; **455**: 1205–1209.
22. Garofalo M, Quintavalle C, Di Leva G, Zanca C, Romano G, Taccioli C *et al.* MicroRNA signatures of TRAIL resistance in human non-small cell lung cancer. *Oncogene* 2008; **27**: 3845–3855.
23. Bélanger C, Gravel A, Tomoiu A, Janelle ME, Gosselin J, Tremblay MJ *et al.* Human herpesvirus 8 viral FLICE-inhibitory protein inhibits Fas-mediated apoptosis through binding and prevention of procaspase-8 maturation. *J Hum Virol* 2001; **4**: 62–73.
24. Djerbi M, Screpanti V, Catrina AI, Bogen B, Biberfeld P, Grandien A. The inhibitor of death receptor signaling, FLICE-inhibitory protein defines a new class of tumor progression factors. *J Exp Med* 1999; **190**: 1025–1032.
25. Lens SM, Kataoka T, Fortner KA, Tinel A, Ferrero I, MacDonald RH *et al.* The caspase 8 inhibitor c-FLIP(L) modulates T-cell receptor-induced proliferation but not activation-induced cell death of lymphocytes. *Mol Cell Biol* 2002; **22**: 5419–5433.
26. Giampietri C, Petrungaro S, Musumeci M, Coluccia P, Antonangeli F, De Cesaris P *et al.* c-Flip overexpression reduces cardiac hypertrophy in response to pressure overload. *J Hypertens* 2008; **26**: 1008–1016.
27. Yeh WC, Itie A, Elia AJ, Ng M, Shu HB, Wakeham A *et al.* Requirement for Casper (c-FLIP) in regulation of death receptor-induced apoptosis and embryonic development. *Immunity* 2000; **12**: 633–642.
28. Yeh WC, Pompa JL, McCurrach ME, Shu HB, Elia AJ, Shahinian A *et al.* FADD: essential for embryo development and signaling from some, but not all, inducers of apoptosis. *Science* 1998; **279**: 1954–1958.
29. Sun M, Song L, Li Y, Zhou T, Jope RS. Identification of an antiapoptotic protein complex at death receptors. *Cell Death Differ* 2008; **15**: 1887–1900.
30. Hoeflich KP, Luo J, Rubie EA, Tsao MS, Jin O, Woodgett JR. Requirement for glycogen synthase kinase-3beta in cell survival and NF-kappaB activation. *Nature* 2000; **406**: 86–90.
31. Liao X, Zhang L, Thrasher JB, Du J, Li B. Glycogen synthase kinase-3beta suppression eliminates tumor necrosis factor-related apoptosis-inducing ligand resistance in prostate cancer. *Mol Cancer Ther* 2003; **2**: 1215–1222.
32. Rottmann S, Wang Y, Nasoff M, Deveraux QL, Quon KC. A TRAIL receptor-dependent synthetic lethal relationship between MYC activation and GSK3beta/FBW7 loss of function. *Proc Natl Acad Sci USA* 2005; **102**: 15195–15200.
33. Markou T, Cullingford TE, Giraldo A, Weiss SC, Alsafi A, Fuller SJ *et al.* Glycogen synthase kinases 3alpha and 3beta in cardiac myocytes: regulation and consequences of their inhibition. *Cell Signal* 2008; **20**: 206–218.
34. Hauck L, Harms C, An J, Rohne J, Gertz K, Dietz R *et al.* Protein kinase CK2 links extracellular growth factor signaling with the control of p27(Kip1) stability in the heart. *Nat Med* 2008; **14**: 315–324.
35. Missero C, Pirro MT, Simeone S, Pischetola M, Di Lauro R. The DNA glycosylase T:G mismatch-specific thymine DNA glycosylase represses thyroid transcription factor-1-activated transcription. *J Biol Chem* 2001; **276**: 33569–33575.
36. Todaro M, Zerilli M, Ricci-Vitiani L, Bini M, Perez Alea M, Maria Florena A *et al.* Autocrine production of interleukin-4 and interleukin-10 is required for survival and growth of thyroid cancer cells. *Cancer Res* 2006; **66**: 1491–1499.
37. Brummelkamp TR, Bernards R, Agami R. Stable suppression of tumorigenicity by virus-mediated RNA interference. *Cancer Cell* 2002; **2**: 243–247.

Supplementary Information accompanies the paper on Cell Death and Differentiation website (http://www.nature.com/cdd)

European Heart Journal (2008) **29**, 2569–2576
doi:10.1093/eurheartj/ehn197

PRECLINICAL RESEARCH

Contrast agents and renal cell apoptosis

Giulia Romano[1,2†], Carlo Briguori[3,4*†], Cristina Quintavalle[1], Ciro Zanca[1], Natalia V. Rivera[5], Antonio Colombo[4], and Gerolama Condorelli[1*]

[1]Department of Cellular and Molecular Biology and Pathology, 'Federico II' University of Naples, Via Pansini, 5, I-80121 Naples, Italy; [2]Fondazione SDN, Naples, Italy; [3]Laboratory of Interventional Cardiology, Department of Cardiology, Clinica Mediterranea, Via Orazio, 2, I-80121 Naples, Italy; [4]Laboratory of Interventional Cardiology, 'Vita e Salute' University School of Medicine, San Raffaele Hospital, Milan, Italy; and [5]University School of Molecular Medicine, University of Milan, Milan, Italy

Received 25 December 2007; revised 14 April 2008; accepted 18 April 2008; online publish-ahead-of-print 8 May 2008

Aims Contrast media (CM) induce a direct toxic effect on renal tubular cells. This toxic effect may have a role in the pathophysiology of contrast nephropathy.

Methods and results We evaluated (i) the cytotoxicity of CM [both low-osmolality (LOCM) and iso-osmolality (IOCM)], of iodine alone, and of an hyperosmolar solution (mannitol 8%) on human embryonic kidney (HEK 293), porcine proximal renal tubular (LLC-PK1), and canine Madin–Darby distal tubular renal (MDCK) cells; and (ii) the effectiveness of various antioxidant compounds [N-acetylcysteine (NAC), ascorbic acid and sodium bicarbonate] in preventing CM cytotoxicity. The cytotoxicity of CM was assessed at different time points, with different methods: cell viability, DNA laddering, flow cytometry, and caspase activation.

Both LOCM and IOCM produced a concentration- and time-dependent increase in cell death as assessed by the different methods. On the contrary, iodine alone and hyperosmolar solution did not induce any significant cytotoxic effect. There was not any significant difference in the cytotoxic effect between LOCM and IOCM. Furthermore, both LOCM and IOCM caused a marked increase in caspase-3 and -9 activities and poly(ADP-ribose) fragmentation, while no effect on caspase-8/-10 was observed, thus indicating that the CM activated apoptosis mainly through the intrinsic pathway. Both CM induced an increase in protein expression levels of pro-apoptotic members of the Bcl2 family (Bim and Bad). NAC and ascorbic acid but not sodium bicarbonate had a dose-dependent protective effect on renal cells after 3 h incubation with high dose (200 mg iodine/mL) of both LOCM and IOCM.

Conclusion Both LOCM and IOCM induce a dose-dependent renal cell apoptosis. NAC and ascorbic acid but not sodium bicarbonate prevent this contrast-induced apoptosis.

Keywords Contrast media • Kidney • Apoptosis • Prevention

Introduction

Contrast-induced nephropathy (CIN) accounts for 10% of all causes of hospital-acquired renal failure, causes a prolonged in-hospital stay, and represents a powerful predictor of poor early and late outcome.[1,2] Haemodynamic changes of renal blood flow, which lead to hypoxia of the renal medulla, and direct toxic effects of contrast media (CM) on renal cells are thought to contribute to the pathogenesis of CIN.[3] A predominant toxic effect of CM on renal tubules has been shown in both clinical trials and animal experiments.[4–6] Furthermore, administration of compounds with antioxidant properties [such as N-acetylcysteine (NAC), ascorbic acid, and sodium bicarbonate] has emerged as an effective strategy to prevent CIN.[7–11] Little is known about cellular mechanisms underlying CIN, and, as a consequence, about the mechanism(s) for the protective effect of compounds, such as NAC, ascorbic acid, and sodium bicarbonate.

In the present study, we assessed the apoptotic effect of both iso-osmolar (IOCM) and low-osmolar (LOCM) CM on human embryonic kidney (HEK 293), porcine proximal renal tubular (LLC-PK1), and canine Madin–Darby distal tubular renal (MDCK) cells and determined the role of various antioxidant compounds in preventing CM-induced apoptosis.

* Corresponding authors. Tel: +39 081 7259 764, Fax: +39 081 7259 777, Email: briguori.carlo@hsr.it or carlo.briguori@hsr.it (C.B.); Tel: +39 081 7464416, Fax: +39 081 7701016, Email: gecondor@unina.it (G.C.)

† The first two authors contributed equally to this work.

Methods

Culture conditions and reagents

Three different cell lines were utilized: (i) human embryonic kidney (HEK 293), which are undifferentiated human renal cells; (ii) porcine proximal renal tubular (LLC-PK1) and canine Madin–Darby renal epithelial (MDCK) cells which have the characteristics of proximal and distal tubule cells, respectively. Cells were grown in a 5% CO_2 atmosphere in Dulbecco's Modified Eagle Medium (DMEM) containing 10% heat-inactivated FBS, 2 mM L-glutamine, and 100 U/mL penicillin–streptomycin. Cells were routinely passaged when they reached 80–85% confluent. Media, sera, and antibiotics for cell culture were from Life Technologies, Inc. (Grand Island, NY, USA). Protein electrophoresis reagents were from Bio-Rad (Richmond, VA, USA) and western blotting and ECL reagents (GE Health care, Europe SA). All other chemicals were from Sigma (St Louis, MO, USA).

Contrast agents

Two different CM were tested: (i) iodixanol (Visipaque®, GE Healthcare Europe; 320 mg iodine/mL) non-ionic, IOCM (290 mOsm/kg of water) and (ii) iobitridol (Xenetix®, Guerbet, France; 250 mg iodine/mL) non-ionic, LOCM (915 mOsm/kg of water).

Experimental design

Experiments were driven in the following phases: (i) assessment of cytotoxicity of both LOCM (iobitridol) and IOCM (iodixanol). In order to assess the impact of contrast dose, two different doses of CM were tested, 100 and 200 mg iodine/mL. The cytotoxicity of CM was tested at 15, 30, 45, 60, 90, 120, 150, 180. The osmolality of DMEM alone was 355 mOsm/L, when compared with 395 mOsm/L for DMEM plus IOCM and 830 mOsm/L for DMEM plus LOCM. In order to clarify the potential major determinants of the cytotoxic effect, we further assessed the effect of iodine alone (by incubation with 100 and 200 mg/mL sodium iodine)[12] and hyperosmolality (by incubation in DMEM/8% mannitol, having an osmolality of 830 mOsm/L); (ii) assessment of the effectiveness of various antioxidant compounds (that is, NAC, ascorbic acid, and sodium bicarbonate) in preventing contrast cytotoxicity. Different doses of all tested compounds were utilized, in order to elicit any dose-dependent effect. The doses tested were selected according to the available data in the clinical setting. NAC was tested at 1, 10, and 100 mM.[13,14] Ascorbic acid was tested at 2, 4, and 8 mM.[15] Sodium bicarbonate was tested at 75, 150, and 300 mM.[10] Each concentration was done in triplicate.

Protein isolation and western blotting

Cellular pellets from a singular cell line at time were washed twice with cold PBS and resuspended in JS buffer (HEPES 50 mM, NaCl 150 nM, 1% glycerol, 1% Triton X-100, 1.5 mM $MgCl_2$, 5 mM EGTA) containing Proteinase Inhibitor Cocktail (Roche). Solubilized proteins were incubated for 1 h on ice. After centrifugation at 13 200 rpm for 10 min at 4°C, lysates were collected as supernatants. Eighty micrograms of sample extract were resolved on a 12% SDS-polyacrylamide gel using a mini-gel apparatus (Bio-Rad Laboratories, Richmond, CA, USA) and transferred to Hybond-C extra nitrocellulose (GE Healthcare Europe). Membrane was blocked for 1 h with 5% non-fat dry milk in TBS containing 0.05% Tween-20 and incubated over night at 4°C with specific antibodies. The following antibodies were used for immunoblotting: anti-pro-caspase-3 (recognizing only the inactive pro-caspase-3) (cell signalling), anti-beta Actin (Sigma), anti-PARP (Sigma), anti-Bim (Santa Cruz), anti Bad (Santa cruz), and anti-Caspase-9, -10, and -8 from Stressgen. Washed filters were then incubated for 60 min with HRP-conjugated anti-rabbit or anti-mouse secondary antibodies (GE Healthcare, Europe) and visualized using chemioluminescence detection (GE Healthcare Europe). The activation of caspase was followed by the disappearance of the band corresponding to the inactive pro-caspase enzyme, utilizing a specific antibody that recognizes this form.

Cell-death quantification

Cell death was evaluated with the CellTiter 96® AQ_{ueous} One Solution Cell Proliferation Assay (Promega, Madison, WI, USA), according to the manufacturer's protocol. The assay is based on reduction of 3-(4,5-dimethylthiazol-2-yl)-5-(3-carboxymethoxyphenyl)-2-(4-sulfophenyl)-2H-tetrazolium, inner salt (MTS) to a coloured product that is measured spectrophotometrically. Cells were plated in 96-well plates in triplicate, stimulated, and incubated at 37°C in a 5% CO_2 incubator. Iobitridol, iodixanol, NAC, sodium bicarbonate, and ascorbic acid were used *in vitro* at the doses and time indicated. Metabolically active cells were detected by adding 20 μL of MTS to each well. After 30 min of incubation, the plates were analysed on a Multilabel Counter (Bio-Rad, Richmond, VA, USA). DNA laddering was also used to confirm the apoptotic death induced by CM. Briefly, after CM exposure, the cells were harvested with 500 μL of DNA lysis buffer [5 mM Tris–HCl (pH 7.5), 20 mM EDTA (pH 8.0), 0.5% NP40], and were incubated on ice for 20 min. After centrifugation at 13 200 rpm for 30 min, the DNA was then extracted with phenol chloroform isoamyl alcohol and finally precipitated with the addition of 1.25 mL of cold ethanol 100% and 50 μL sodium acetate (pH 5.2) on dry ice for 20 min. The precipitates were centrifuged (30 min, 13 200 rpm, 4°C), dried at room temperature, solubilized in 10 μl of TE, and then incubated with RNase A for 30 min at 37°C. The DNA samples were finally separated on 1.5% agarose gel containing ethidium bromide (Sigma, St Louis). The gel was photographed under UV light. Apoptosis was also analysed via propidium iodide incorporation in permeabilized cells by flow cytometry. The cells (2×10^5) were washed in PBS and resuspended in 200 μL of a solution containing 0.1% sodium citrate, 0.1% Triton X-100, and 50 μg/mL propidium iodide (Sigma). Following incubation at 4°C for 30 min in the dark, nuclei were analysed with a Becton Dickinson FACScan flow cytometer. Cellular debris was excluded from analyses by raising the forward scatter threshold, and the DNA content of the nuclei was registered on a logarithmic scale. The percentage of elements in the hypodiploid region was calculated.

Statistical analysis

Continuous variables are expressed as mean values ± SD. We performed a multiple comparison test using the information derived by performing one-way analysis of variance (ANOVA) test on groups of independent variables having cell viability as our dependent variable. In an ANOVA, we compared the means of several groups to test the hypothesis that they are all the same, against the general alternative that they are not all the same. However, since the alternative hypothesis may be too general and more information is needed about which pairs of means are significantly different, and which are not, we used the multiple comparison procedure, which allows us to comparing all group mean pairs at the same time. Throughout the analysis, we have specified a significance level $\alpha = 0.001$ and we performed priori comparisons on the outputs derived from ANOVA test. Also, main focus was given on the ANOVA outputs where the F test resulted significantly. We performed the priori comparisons using the Bonferroni t method for both orthogonal and non-orthogonal comparisons to reduce multiplicity between group comparisons.

The Bonferroni *t* method increases the critical *F* value needed for the comparison to be declared significant. Data were analysed with SPSS 13.0 (Chicago, IL, USA) for Windows.

Results

Effects of contrast medium on cell viability

As shown in *Figure 1A*, both LOCM and IOCM produced a concentration-dependent decrease in cell viability as assessed by MTS assay. This effect was identical in all the three renal cell lines utilized (*Figure 2*). Indeed, the amount of cell death was significantly higher with 200 mg iodine/mL than with 100 mg iodine/mL of contrast at each time-point of the experiment ($P = 0.0025$; by paired *t*-test with $\alpha = 0.001$). There was a significant interaction between time of exposure and the effect of CM on cell viability ($P = 9.51 \times 10^{-5}$; $F = 5.93$ by ANOVA model with $\alpha = 0.001$). The toxic effect of CM was further evaluated by DNA laddering (*Figure 1B*) and propidium staining and FACS analysis (*Figure 1C*). Both methods confirmed that exposure of cells to LOCM and IOCM induces apoptosis of renal cells.

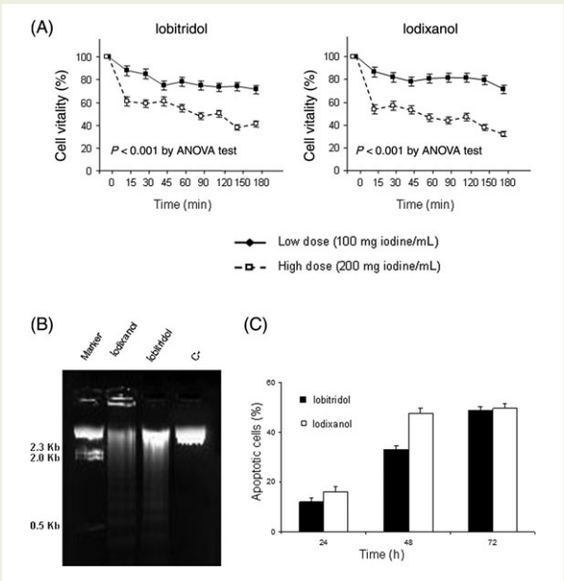

Figure 1 Effects of contrast media on renal cell viability. (*A*) HEK 293, LCC-PK1, and MDCK cells were incubated in the presence of either 100 (low dose) or 200 (high dose) mg iodine/mL of iobitridol or iodixanol for the indicated time. Cell viability was then assessed with CellTiter Proliferation Assay. By the ANOVA model and multiple comparison test, there was a significant interaction between cell viability and time of exposure ($P < 0.001$; $F = 285.02$) and dose of contrast media ($P < 0.001$; $F = 5.93$). (*B*) HEK 293, LCC-PK1, and MDCK cells were incubated in the presence of 200 mg iodine/mL of iobitridol or iodixanol for 3 h. DNA was extracted and loaded on 1.5% agarose gel. (*C*) HEK 293, LCC-PK1, and MDCK cells were incubated in the presence of 100 and 200 mg iodine/mL of iobitridol or iodixanol for 24, 48, or 72 h and then DNA fragmentation was measured by flow cytometry. Data represent the mean ± SD of two separate experiments performed in triplicate.

The cytotoxic effect, although maximum at 3 h, was mostly (≈85%) observed already at 15 min of incubation (*Figure 1A*). In order to better clarify the time-dependency effect, we performed a further control experiment in which cells were exposed for a short period (only 15 min), then washed free of CM, and studied for viability immediately or 3 h later, and compared these effects to those observed upon 3 h of incubation. Interestingly, we found that the cytotoxic effect induced by 15 min of high dose (200 mg iodine/mL) of CM exposure was similar whether it was observed immediately or 3 h later (cell viability: 12 ± 6 vs. 13 ± 6%, respectively; $P = 1.0$) (data not shown).

There was not any interaction between the cytotoxic effect and the type of contrast used ($P = 0.22$; $F = 1.87$ by ANOVA model with $\alpha = 0.001$). Furthermore, neither sodium iodine alone nor hyperosmolar solution decreased cell viability or induced cell apoptosis (*Figure 2*). All cell lines were exposed to the same concentrations of CM. On the contrary, *in vivo*, cell apoptosis was mostly found in the more distal tubular cells (MDCK) which may be exposed to higher concentrations of CM.

Role of caspases in contrast-induced cytotoxicity

To test whether CM stimulate caspase activity, HEK 293 cells were incubated in the presence of either LOCM or IOCM at different time points and then the activation of caspases-8, -10, -3, -9 was assessed by western blot (*Figure 3A*). Both LOCM and IOCM caused a marked increase in caspase-3 and -9 activities at 7 h of exposure, as assessed by the reduction of the pro-caspase form (*Figure 3A*). No effect on caspases-8 and -10 was observed, thus indicating that the CM activated apoptosis mainly through the intrinsic, or 'mitochondrial', pathway (*Figure 3A*). This pathway of apoptosis is regulated by Bcl2 family members. Hence, we studied the expression of Bad and Bim, two pro-apoptotic members of the Bcl2 family, after incubation with the CM. Western blotting revealed that exposure to CM induce an increase in both Bad and Bim expression (*Figure 3B*). Similar results were obtained in the other cell types (data not shown).

Effects of NAC on contrast-induced cytotoxicity

HEK 293, LLC-PK1, and MDCK cells were pre-incubated with different concentrations of NAC and cell viability was assessed with the cell proliferation assay. We observed a dose-dependent protective effect of NAC on renal cells after 3 h incubation with the high dose (200 mg iodine/mL) of both LOCM and IOCM ($P < 0.001$; $F = 396.22$ by ANOVA test; *Figure 4A*). As compared to baseline, after 3 h of incubation, cell viability was <10% in the CM-treated cells, <25% with the lowest (1 mM) dose of NAC, <30% with the middle (10 mM), and approximately 80% with the highest (100 mM) dose of NAC. There was not any interaction between the protective effect of NAC (for dose 1 and 10 mM) and the type of CM ($P = 0.75$; $F = 0.12$ and $P = 0.32$; $F = 1.31$,

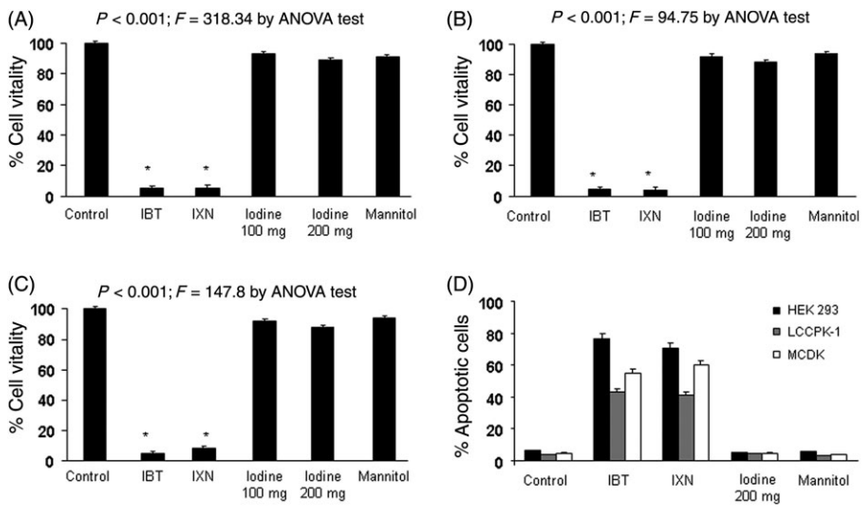

Figure 2 Effects of contrast media, iodine, and mannitol on renal cells. HEK 293 (*A*), LCC-PK1 (*B*), and MCDK (*C*) cells were incubated in the presence of 200 mg iodine/mL of iobitridol (IBT) or iodixanol (IXN), of iodine alone (sodium iodine, 100 and 200 mg) and 8% mannitol (hyperosmolar solution) for 3 h. Cell viability was then assessed with CellTiter Proliferation Assay. *$P < 0.001$ vs. all the other groups; (*D*) HEK 293, LCC-PK1, and MDCK cells were incubated in the presence of 200 mg iodine/mL of iobitridol or iodixanol for 72 h and then DNA fragmentation was measured by flow cytometry. Data represent the mean ± SD of two separate experiments performed in triplicate.

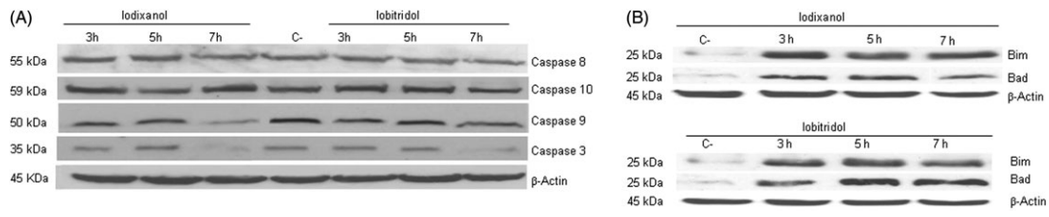

Figure 3 Effect of contrast media on caspase activation and on Bcl2 family proteins expression. HEK 293 cells were incubated in the presence of 200 mg iodine/mL of iobitridol or iodixanol for the indicated time. Eight micrograms of protein were loaded onto 12% SDS–PAGE gel. (*A*) The membranes were incubated with anti-caspase-3, -8, -9, -10 antibodies and visualized by chemioluminescence detection. Contrast media induced an activation of caspases-3 and -9 and not of caspases-8 and -10 as assessed by the reduction of the pro-caspase levels. (*B*) Membranes were incubated with anti-Bim or anti-Bad antibodies and visualized by chemioluminescence detection. Loading control was controlled with anti-β-actin.

respectively, both by ANOVA test with $\alpha = 0.001$). However, results for NAC 100 mM with LOCM appears to be slightly better for cell viability when compared with NAC 100 mM with IOCM ($P = 0.006$; $F = 28.22$). In order to clarify the mechanism by which NAC prevented contrast-induced apoptosis, we analysed the effect of NAC pre-treatment on Poly(ADP-ribose) (PARP), a final substrate of caspase-3. We found that the CM induced the activation of PARP as assessed by the marked reduction of the 116 kDa PARP pro-form. On the contrary, NAC completely prevented this activation, suggesting that NAC acts through the inhibition of the intrinsic pathway of apoptosis (*Figure 4B*).

Effects of ascorbic acid on contrast-induced cytotoxicity

We observed a dose-dependent protective effect of ascorbic acid on renal cells exposed after 3 h of incubation with the high dose (200 mg iodine/mL) of both LOCM (HEK 293: $P = 2.99 \times 10^{-5}$; $F = 1552.67$; LLC-PK1: $P = 0.04$; $F = 10.85$; MDCK: $P = 0.04$; $F = 18.57$) and IOCM (HEK 293: $P = 6.43 \times 10^{-5}$; $F = 933.55$; LLC-PK1: $P = 0.02$; $F = 16.29$; MDCK: $P = 0.01$; $F = 19.98$) (*Figure 5A*). When compared to baseline, at 3 h of incubation cell viability was <6% in the control group, <15% with the lowest (2 mM) dose of ascorbic acid, and <60% with in both 4 mM and

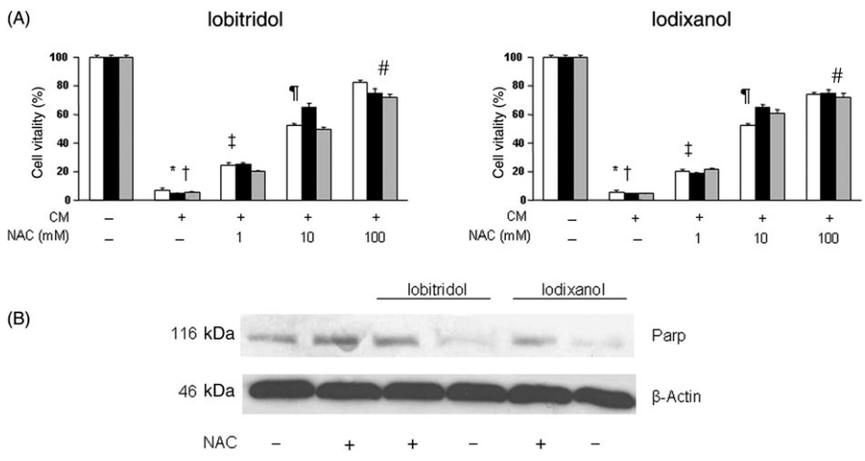

Figure 4 Pre-treatment with NAC and contrast-induced cell death. (*A*) HEK 293 (open columns), LCC-PK1 (black columns), and MDCK (grey columns) cells were pre-treated for 2 h with different concentration of N-acetylcysteine (NAC) as indicated (1, 10, and 100 mM) and then incubated for 3 h with 200 mg iodine/mL of iobitridol or iodixanol. Cell viability was then assessed with CellTiter Proliferation Assay. NAC protects the cells from contrast-induced cell death in a dose-dependent fashion (HEK 293: $P < 0.001$; $F = 143.51$ with iobitridol; $P < 0.001$; $F = 122.43$ with iodixanol. LCC-PK1 cells: $P < 0.04$; $F = 12.9$ with iobitridol; $P < 0.03$; $F = 14.79$ with iodixanol; MDCK cells: $P < 0.006$; $F = 41.19$ with iobitridol; $P < 0.01$; $F = 25.24$ with iodixanol). $^{*}P = <0.001$ vs. baseline (CM−/NAC−) and [CM+/NAC 100 mM]; $^{\dagger}P < 0.05$ vs. (CM+/NAC 1 mM) and (CM+/NAC 10 mM); $^{\ddagger}P = 0.003$ vs. (CM+/NAC 100 mM); $^{\P}P < 0.03$ vs. (CM+/NAC 100 mM); $^{\#}P < 0.05$ vs. baseline (CM−/NAC−). (*B*) HEK 293 cells were pre-incubated with NAC for 2 h and then incubated in the presence of 200 mg iodine/mL of iobitridol or iodixanol for 3 h. Eighty microgram of protein was loaded onto 10% SDS–PAGE. The membranes were incubated with anti-PARP antibody and visualized by chemioluminescence detection. PARP activation was detected by the reduction of the 116 kDa non-cleaved form of PARP. Loading was controlled with anti-b-actin.

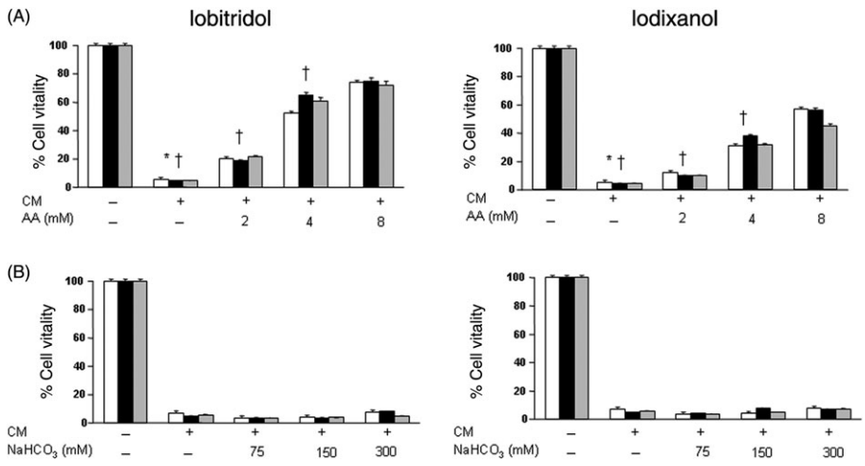

Figure 5 Effects of ascorbic acid and sodium bicarbonate on contrast-induced cell death. HEK 293 (open columns), LCC-PK1 (black columns), and MDCK (grey columns) were pre-treated for 2 h with different concentrations of ascorbic acid (AA) (2, 4, and 8 mM) or sodium bicarbonate (75, 150, and 300 mM) as indicated and then incubated for 3 h with 200 mg iodine/mL of iobitridol or iodixanol. Cell viability was then assessed with CellTiter Proliferation Assay. $^{*}P < 0.03$ vs. (CM+/AA 2 mM+), $^{\dagger}P < 0.001$ vs. all the other groups.

8 mM doses of ascorbic acid, respectively. There was a significant interaction between the protective effect of ascorbic acid and cell viability for both types of CM (Iobitridol: $P = 0.0017$, $F = 10.09$, and Iodixanol: $P = 0.0002$, $F = 16.46$, both by the ANOVA model).

Effects of sodium bicarbonate on contrast-induced cytotoxicity

We did not find any protective effect of sodium bicarbonate on HEK 293 (LOCM: $P = 0.53$; $F = 0.78$; IOCM: $P = 0.02$;

$F = 23.02$); LCC-PK1 (LOCM: $P = 0.09$; $F = 6$; IOCM: $P = 0.94$; $F = 0.06$); and MDCK (LOCM: $P = 0.88$; $F = 0.13$; IOCM: $P = 0.71$; $F = 0.38$) after 3 h of incubation with the high dose of either LOCM or IOCM. Cell viability was quite similar even in the presence of high (300 mM) dose of sodium bicarbonate (*Figure 5B*). This lack of any protective effect was similar with LOCM and IOCM. There was no difference in pH in the medium from the various groups (*Table 1*) and there was no effect on cell viability (Iobitridol: $P = 0.72$, $F = 0.33$; Iodixanol: $P = 0.49$, $F = 0.73$ by the ANOVA model).

Effects of co-incubation of NAC with ascorbic acid or with sodium bicarbonate

The protective effect of NAC (100 mM) was greater than that of ascorbic acid (8 mM) LOCM: $P = 1.25 \times 10^{-8}$, $F = 52.21$; and IOCM $P = 9.90 \times 10^{-9}$, $F = 54.03$ by the ANOVA model; *Figure 6*). We performed a further experiment to investigate the effect on cell death of 2 h of NAC pre-treatment (100 mM), in the presence of either ascorbic acid (8 mM), or sodium bicarbonate (150 mM) on cell death after 3 h of incubation with the high dose (200 mg iodine/mL) of either LOCM or IOCM. As shown in *Figure 6*, the combination of NAC with another antioxidant agent was less effective than NAC alone ($P = 0.95$; $F = 0.54$ by the ANOVA test).

Table 1 pH in the various treatment groups

Group	Iobitridol*	Iodixanol**
Contrast media alone	7.34 (7.18–7.50)	7.25 (7.06–7.50)
Contrast media plus NAC	7.29 (6.97–7.60)	7.03 (6.96–7.10)
Contrast media plus AA	6.90 (6.80–7.01)	7.04 (7.06–7.10)
Contrast media plus $NaHCO_3$	7.30 (7.21–7.40)	7.24 (7.08–7.50)

Values are expressed as median and interquartile range.
NAC, N-acetylcysteine; AA, ascorbic acid; $NaHCO_3$, sodium bicarbonate.
*$P = 0.57$ through the groups by ANOVA test, after transforming pH values into proton H^+ concentrations.
**$P = 0.65$ through the groups by ANOVA test after transforming pH values into proton H^+ concentrations.

Discussion

The main conclusions of the present study are (i) CM induce dose- and time-dependent renal cell apoptosis through the activation of the intrisinc pathway, (ii) this cytotoxic effect does not seem to be caused by iodine or osmolality $\leq$830 mOsm/L, and (iii) pre-treatment with NAC and ascorbic acid but not with sodium bicarbonate prevents apoptosis in a dose-dependent fashion.

Contrast media and renal cell apoptosis

Our study confirms that the CM induce renal cell apoptosis.[4–6,16–18] In order to strengthen this finding, we used three different renal cell lines, namely, human epithelial cells (HEK 293) and two cell lines with the characteristics of proximal and distal tubule cells [porcine kidney proximal tubular epithelial cells (LLC-PK1) and Madin–Darby canine kidney cells (MDCK)]. The activation of caspase-9 and -3, but not of caspases-8 and -10 observed after exposure to CM supports the concept that CM induce apoptosis through the intrinsic, or 'mitochondrial', pathway. This finding was also supported by the activation of PARP, a final substrate of caspase-3. In a rat model of CIN, cellular injury of the renal medulla consisted of extensive DNA fragmentation, which has been attributed to medullary hypoxia.[17,19] Yano *et al.*[19] have shown that CM induced apoptosis in the porcine tubular cell line, LLC-PK-1, and that the injuries might be due to de-regulation in Bax/Bcl-2 expression, followed by increases in caspases-9 and -3 activities. In agreement with these previous observations, we found that CM induce an increase of at least two Bcl-2 pro-apoptotic family members, i.e. Bim and Bad.[20,21]

Role of contrast dose and osmolality

CM induce renal cell apoptosis in a dose- and time-dependent manner.[18] Guidelines recommend to limit the volume of CM

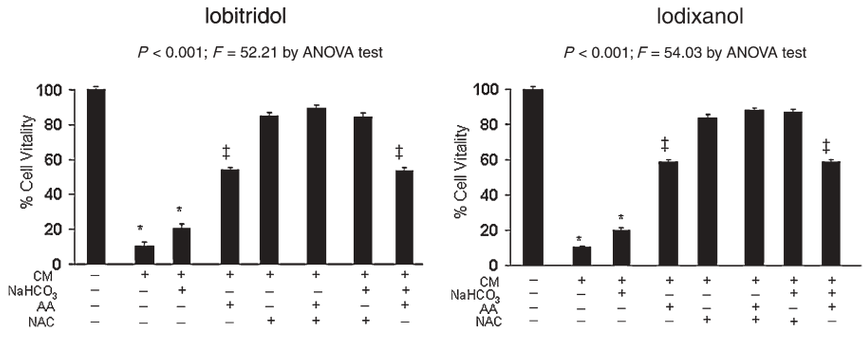

Figure 6 Effect of NAC, ascorbic acid, and sodium bicarbonate alone and in combinations on contrast-induced cell death. HEK 293 cells were pre-treated for 2 h in the presence of N-acetylcysteine (NAC, 100 mM), ascorbic acid (AA, 8 mM), and sodium bicarbonate ($NaHCO_3$, 150 mM) alone or in combination and then incubated for 3 h with 200 mg iodine/mL of iobitridol or iodixanol. Cell viability was then assessed with CellTiter Proliferation Assay. *$P < 0.001$ vs. (CM+/AA+), (CM+/NAC+), (CM+/NAC+/AA+), (CM+/NAC+/$NaHCO_3$+), and (CM+/AA+/$NaHCO_3$+); ‡ $P < 0.001$ vs. (CM+/NAC+), (CM+/NAC+/$NaHCO_3$+), and (CM+/NAC+/AA).

usage in order to prevent contrast-associated nephrotoxicity.[22,23] It has been suggested that using the iodine dose/glomerular filtration rate ratio may be a more expedient way of improving risk assessment of CIN than the more common practice of estimating CM dose from volume alone.[23] After intravascular administration of CM in rabbits, a urinary concentration higher than 100 mg/mL of iodine has been measured.[12] However, we found that the iodine alone does not cause renal cell apoptosis.

We observed that the cytotoxic effect, although maximum at 3 h, was mostly (≈85%) observed already at 15 min of incubation. This suggests that even a short period of exposure activates the cascade leading to apoptosis and therefore what is being observed at the later time periods represents mostly the cumulative effect of that initial exposure. This finding highlights the importance of strategies limiting the exposure of the kidney to the toxins contained in the contrast agent by generating high urine flow in patients.

The contribution of osmolality to contrast-induced apoptosis is controversial.[18,24,25] Although previous studies demonstrated that the cytotoxicity of high-osmolality contrast media (HOCM) is higher than that of LOCM,[18] we did not find any difference in the extent of cell injury between IOCM and LOCM. Furthermore, the cytotoxic effect may be related to CM hypertonicity, since equally hyperosmolal but less hypertonic urea solution failed to induce DNA fragmentation.[18] Factors other than osmolality may contribute to the toxic effect. Ionicity and/or molecular structure (monomeric or dimeric) may be of importance. Heinrich *et al.*[26] demonstrated that at an equal iodine concentration, no significant differences exist between the direct toxic effects of non-ionic monomeric and dimeric CM on renal proximal tubular cells *in vitro*. On the contrary, when comparing the data on a molar basis, the dimeric CM showed a significantly stronger effect on the tubular cells than did the non-ionic monomeric CM. This suggests a greater cytotoxic effect of the dimeric CM molecules. In the last generation of CM (which has a non-ionic, dimeric structure), iso-osmolality has been achieved at the price of an increased viscosity. Indeed viscosity is inversely related to osmolality. High viscous CM compromise renal medullary blood flux, renal medullary erythrocyte concentration, and renal medullary pO_2.[27] Our *in vitro* experiments allow us to examine the cytotoxic effects of CM on renal cells, eliminating the effects of confounding variables (e.g. hypoxia due to haemodynamic changes or viscosity), which can be found *in vivo*. Therefore, additional studies are necessary to assess whether molecular structure and/or other components of the CM may induce this cytotoxic effect.

Antioxidant compounds and contrast-induced apoptosis

In the last few years, a number of clinical studies have suggested that NAC may prevent CIN.[7,8] Recently, two additional antioxidant strategies have aroused considerable interest: sodium bicarbonate[10] and ascorbic acid.[11] It has been hypothesized that all these compounds may be effective due to their antioxidant properties. Our study supports the clinical observation of the effectiveness of NAC and ascorbic acid in preventing contrast-induced apoptosis. This effect is dose-dependent: indeed, the greater the dose, the larger the cellular benefit. This finding supports the clinical observation of the dose-dependency of NAC in preventing CIN.[8,28] The plasma level of NAC ranges from 10 mM (with a dosing regimen of 600 mg/day) to 100 mM (with a dosing regimen of 1200 mg BID).[13,14] Of note, NAC was more effective against contrast-induced apoptosis than ascorbic acid. In contrast, sodium bicarbonate does not prevent contrast-induced apoptosis. However, recent clinical studies suggest that the sodium bicarbonate seems to be effective in preventing CIN.[10] This discordance may be explained by alternative mechanisms. We recently demonstrated that the combined prophylactic strategy of sodium bicarbonate plus NAC, but not the combination of ascorbic acid and NAC, is more effective than NAC alone in preventing CIN. We speculated that NAC and ascorbic acid may work through similar pathways while the protective action of bicarbonate may be different in comparison to NAC and, therefore, additive.[9] The lack of benefit of the combination of NAC and ascorbic acid in preventing contrast-induced apoptosis observed in the present study supports this hypothesis. Free-radical formation is promoted by an acidic environment typical of distal tubular urine, but is inhibited by the higher pH of normal extracellular fluid.[29] It has been hypothesized that alkalinizing renal tubular fluid with bicarbonate[10] may reduce injury. At physiologic concentrations, bicarbonate scavenges peroxynitrite and other reactive species generated from nitric oxide.[10] In the clinical setting, the higher concentration of HCO_3 in the proximal convoluted tubule may (i) buffer the higher production of H^+ due to cellular hypoxia and (ii) facilitate Na^+ reabsorption through the electrogenic Na/HCO_3 co-transporter.[29] The result of our *in vitro* study does not support the former mechanism. It may be that $NaHCO_3$ may facilitate Na^+ reabsorption: this would mitigate the increase in sodium delivery to the macula densa induced by CM, an effect that results in vasoconstriction of the afferent arteriola through the oricess of tubuloglomerular feedback. Furthermore, in our *in vitro* model, $NAHCO_3$ did not raise the pH of the media in comparison to CM alone.

Study limitations

Hizoh *et al.*[18] observed that NAC failed to reduce the DNA fragmentation rate caused by HOCM. This discordance may be explained by (i) the lower dose of NAC utilized (10 mM) and (ii) the use of a HOCM. Additional data are necessary to address the issue of which CM component (other than iodine) and chemical property (such as viscosity) causes renal cell apoptosis. The investigators who evaluated the cellular damage were not blinded to the contrast type, the iodine dose, or the protective strategy attempted.

In conclusion, CM induce apoptosis through the activation of the intrinsic pathway. Pre-treatment with NAC and ascorbic acid but not with sodium bicarbonate prevents apoptosis in a dose-dependent fashion.

Acknowledgements

Giulia Romano is recipient of Fondazione SDN fellowship. We thank M. Fiammetta Romano, MD, for her invaluable help in FACS analysis, and Michael Latronico, PhD, for paper revision.

Conflict of interest: none declared.

Funding

This work was partially supported by funds from Associazione Italiana Ricerca sul Cancro, AIRC (G.C.), MIUR-FIRB (RBIN04J4J7).

References

1. McCullough PA, Wolyn R, Rocher LL, Levin RN, O'Neill WW. Acute renal failure after coronary intervention: incidence, risk factors, and relationship to mortality. *Am J Med* 1997;**103**:368–375.
2. Tepel M, Aspelin P, Lameire N. Contrast-induced nephropathy: a clinical and evidence-based approach. *Circulation* 2006;**113**:1799–1806.
3. Persson PB, Hansell P, Liss P. Pathophysiology of contrast medium-induced nephropathy. *Kidney Int* 2005;**68**:14–22.
4. Andersen KJ, Christensen EI, Vik H. Effects of iodinated x-ray contrast media on renal epithelial cells in culture. *Invest Radiol* 1994;**29**:955–962.
5. Humes HD, Hunt DA, White MD. Direct toxic effect of the radiocontrast agent diatrizoate on renal proximal tubule cells. *Am J physiol* 1987;**252**:F246–F255.
6. Messana JM, Cieslinski DA, Nguyen VD, Humes HD. Comparison of the toxicity of the radiocontrast agents, iopamidol and diatrizoate, to rabbit renal proximal tubule cells in vitro. *J Pharmacol Exp Ther* 1988;**244**:1139–1144.
7. Tepel M, van der Giet M, Schwarzfeld C, Laufer U, Liermann D, Zidek W. Prevention of radiographic-contrast-agent-induced reductions in renal function by acetylcysteine. *New Engl J Med* 2000;**343**:180–184.
8. Briguori C, Colombo A, Violante A, Balestrieri P, Manganelli F, Paolo Elia P, Golia B, Lepore S, Riviezzo G, Scarpato P, Focaccio A, Librera M, Bonizzoni E, Ricciardelli B. Standard vs double dose of N-acetylcysteine to prevent contrast agent associated nephrotoxicity. *Eur Heart J* 2004;**25**:206–211.
9. Briguori C, Airoldi F, D'Andrea D, Bonizzoni E, Morici N, Focaccio A, Michev I, Montorfano M, Carlino M, Cosgrave J, Ricciardelli B, Colombo A. Renal Insufficiency Following Contrast Media Administration Trial (REMEDIAL): a randomized comparison of 3 preventive strategies. *Circulation* 2007;**115**:1211–1217.
10. Merten GJ, Burgess WP, Gray LV, Holleman JH, Roush TS, Kowalchuk GJ, Bersin RM, Van Moore A, Simonton CA 3rd, Rittase RA, Norton HJ, Kennedy TP. Prevention of contrast-induced nephropathy with sodium bicarbonate: a randomized controlled trial. *JAMA* 2004;**291**:2328–2334.
11. Spargias K, Alexopoulos E, Kyrzopoulos S, Iokovis P, Greenwood DC, Manginas A, Voudris V, Pavlides G, Buller CE, Kremastinos D, Cokkinos DV. Ascorbic acid prevents contrast-mediated nephropathy in patients with renal dysfunction undergoing coronary angiography or intervention. *Circulation* 2004;**110**:2837–2842.
12. Spataro RF, Fischer HW, Boylan L. Urography with low-osmolality contrast media: comparative urinary excretion of Iopamidol, Hexabrix, and diatrizoate. *Invest Radiol* 1982;**17**:494–500.
13. Longo A, Di Toro M, Galimberti C, Carenzi A. Determination of N-acetylcysteine in human plasma by gas chromatography-mass spectrometry. *J Chromatogr* 1991;**562**:639–645.
14. Flanagan RJ, Meredith TJ. Use of N-acetylcysteine in clinical toxicology. *Am J Med* 1991;**91**:131S–139S.
15. Levine GN, Frei B, Koulouris SN, Gerhard MD, Keaney JF Jr, Vita JA. Ascorbic acid reverses endothelial vasomotor dysfunction in patients with coronary artery disease. *Circulation* 1996;**93**:1107–1113.
16. Haller C, Schick CS, Zorn M, Kubler W. Cytotoxicity of radiocontrast agents on polarized renal epithelial cell monolayers. *Cardiovasc Res* 1997;**33**:655–665.
17. Beeri R, Symon Z, Brezis M, Ben-Sasson SA, Baehr PH, Rosen S, Zager RA. Rapid DNA fragmentation from hypoxia along the thick ascending limb of rat kidneys. *Kidney Int* 1995;**47**:1806–1810.
18. Hizoh I, Strater J, Schick CS, Kubler W, Haller C. Radiocontrast-induced DNA fragmentation of renal tubular cells in vitro: role of hypertonicity. *Nephrol Dial Transplant* 1998;**13**:911–918.
19. Yano T, Itoh Y, Sendo T, Kubota T, Oishi R. Cyclic AMP reverses radiocontrast media-induced apoptosis in LLC-PK1 cells by activating A kinase/PI3 kinase. *Kidney Int* 2003;**64**:2052–2063.
20. Adams JM, Cory S. The Bcl-2 apoptotic switch in cancer development and therapy. *Oncogene* 2007;**26**:1324–1337.
21. Tanaka T, Miyata T, Inagi R, Kurokawa K, Adler S, Fujita T, Nangaku M. Hypoxia-induced apoptosis in cultured glomerular endothelial cells: involvement of mitochondrial pathways. *Kidney Int* 2003;**64**:2020–2032.
22. Solomon R, Deray G. How to prevent contrast-induced nephropathy and manage risk patients: practical recommendations. *Kidney Int* 2006;**100**:S51–S53.
23. Nyman U, Almen T, Aspelin P, Hellstrom M, Kristiansson M, Sterner G. Contrast-medium-induced nephropathy correlated to the ratio between dose in gram iodine and estimated GFR in ml/min. *Acta Radiol* 2005;**46**:830–842.
24. Chan WH, Yu JS, Yang SD. PAK2 is cleaved and activated during hyperosmotic shock-induced apoptosis via a caspase-dependent mechanism: evidence for the involvement of oxidative stress. *J Cell Physiol* 1999;**178**:397–408.
25. Solomon R. The role of osmolality in the incidence of contrast-induced nephropathy: a systematic review of angiographic contrast media in high risk patients. *Kidney Int* 2005;**68**:2256–2263.
26. Heinrich MC, Kuhlmann MK, Grgic A, Heckmann M, Kramann B, Uder M. Cytotoxic effects of ionic high-osmolar, nonionic monomeric, and nonionic iso-osmolar dimeric iodinated contrast media on renal tubular cells in vitro. *Radiology* 2005;**235**:843–849.
27. Seeliger E, Flemming B, Wronski T, Ladwig M, Arakelyan K, Godes M, Mockel M, Persson PB. Viscosity of contrast media perturbs renal hemodynamics. *J Am Soc Nephrol* 2007;**18**:2912–2920.
28. Marenzi G, Assanelli E, Marana I, Lauri G, Campodonico J, Grazi M, De Metrio M, Galli S, Fabbiocchi F, Montorsi P, Veglia F, Bartorelli AL. N-acetylcysteine and contrast-induced nephropathy in primary angioplasty. *New Engl J Med* 2006;**354**:2773–2782.
29. Boron WF. Acid-base transport by the renal proximal tubule. *J Am Soc Nephrol* 2006;**17**:2368–2382.

Journal of Cellular Physiology

PED Interacts With Rac1 and Regulates Cell Migration/ Invasion Processes in Human Non-Small Cell Lung Cancer Cells

CIRO ZANCA,[1] FLORA COZZOLINO,[2,3] CRISTINA QUINTAVALLE,[1] STEFANIA DI COSTANZO,[1] LUCIA RICCI-VITIANI,[4] MARGHERITA SANTORIELLO,[1] MARIA MONTI,[2,5] PIERO PUCCI,[2,5] AND GEROLAMA CONDORELLI[1,6,7]*

[1]*Department of Cellular and Molecular Biology and Pathology, "Federico II" University of Naples, Naples, Italy*

[2]*CEINGE Biotecnologie Avanzate, Naples, Italy*

[3]*Istituto Nazionale Biosistemi e Biostrutture (INBB), Rome, Italy*

[4]*Department of Hematology, Oncology and Molecular Medicine, Istituto Superiore Sanità, Rome, Italy*

[5]*Department of Organic Chemistry and Biochemistry, "Federico II" University of Naples, Naples, Italy*

[6]*IEOS, CNR, Naples, Italy*

[7]*Facoltà di Scienze Biotecnologiche, "Federico II" University of Naples, Naples, Italy*

PED (phosphoprotein enriched in diabetes) is a 15 kDa protein involved in many cellular pathways and human diseases including type II diabetes and cancer. We recently reported that PED is overexpressed in human cancers and mediates resistance to induced apoptosis. To better understand its role in cancer, we investigated on PED interactome in non-small cell lung cancer (NSCLC). By the Tandem Affinity Purification (TAP), we identified and characterized among others, Rac1, a member of mammalian Rho GTPase protein family, as PED-interacting protein. In this study we show that PED coadiuvates Rac1 activation by regulating AKT mediated Rac1-Ser^{71} phosphorylation. Furthermore, we show that the expression of a constitutively active Rac, affected PED-Ser^{104} phosphorylation, which is important for PED-regulated ERK 1/2 nuclear localization. Through specific Rac1-siRNA or its pharmacological inhibition, we demonstrate that PED augments migration and invasion in a Rac1-dependent manner in NSCLC. In conclusion, we show for the first time that PED and Rac1 interact and that this interaction modulates cell migration/invasion processes in cancer cells through ERK1/2 pathway.
J. Cell. Physiol. 225: 63–72, 2010.

PED, (phosphoprotein enriched in diabetes), also known as PEA15, (phosphoprotein enriched in astrocytes), is a 15 kDa protein involved in many cellular pathways, included apoptosis and survival (Condorelli et al., 1999; Hao et al., 2001; Ricci-Vitiani et al., 2004; Stassi et al., 2005; Garofalo et al., 2007; Zanca et al., 2008; Peacock et al., 2009), senescence (Gaumont-Leclerc et al., 2004), autophagy (Bartholomeusz et al., 2008), proliferation and migration (Renault et al., 2003; Renault-Mihara et al., 2006; Glading et al., 2007). PED function is regulated by phosphorylation on two different serine residues: Ser^{104}, phosphorylated by PKC (Protein Kinase C) (Araujo et al., 1993), and Ser^{116}, phosphorylated by AKT/PKB (Protein Kinase B) (Trencia et al., 2003) and CamKII (Calcium Calmodulin Kinase II) (Kubes et al., 1998). PED is member of Death Effector Domain (DED) containing protein family. These domains regulate cell death through protein-protein interaction (Valmiki and Ramos, 2009). PED inhibits DISC (Death Inducing Signaling Complex) formation and caspase 8 activation upon death cytokines stimulation (FasL, TNFα, TRAIL) in different cell types (Condorelli et al., 1999; Hao et al., 2001; Garofalo et al., 2007; Zanca et al., 2008). We recently demonstrated that PED expression is increased in B-CLL (B-cell chronic lymphocytic leukemia) (Garofalo et al., 2007) and non-small cell lung cancer (NSCLC) (Zanca et al., 2008), where it mediates resistance to TRAIL (TNF-Related Apoptosis Inducing Ligand) induced apoptosis. Moreover, PED can contribute to apoptosis resistance to chemotherapies in breast cancer (Stassi et al., 2005).

The molecular mechanisms that regulate PED expression in human cancer are still unclear. Recent studies revealed that PED expression can be regulated by several transcription factors. Hepatocyte nuclear factor 4 alpha (HNF-4α), which is involved in induction of apoptosis in pancreatic INS-1 beta-cell line (Erdmann et al., 2007), negatively regulates PED expression (Ungaro et al., 2008), while its expression is upregulated by

Additional Supporting Information may be found in the online version of this article.

Contract grant sponsor: Italian Ministry of Education (MIUR) Progetto FIRB Rete Nazionale di Proteomica Umana (Italian Human Proteomenet);
Contract grant number: RBRN07BMCT.
Contract grant sponsor: Associazione Italiana Ricerca sul Cancro (AIRC).
Contract grant sponsor: MIUR-FIRB;
Contract grant number: RBIN04J4J7.

*Correspondence to: Gerolama Condorelli, Department of Cellular and Molecular Biology and Pathology, "Federico II" University of Naples, Via Pansini, 5, 80131 Naples, Italy.
E-mail: gecondor@unina.it

Received 12 March 2010; Accepted 30 March 2010

Published online in Wiley InterScience (www.interscience.wiley.com.), 21 May 2010.
DOI: 10.1002/jcp.22197

Chicken Ovalbumin Upstream Promoter-Transcription Factor II (COUP-TFII) (Ungaro et al., 2008), by vitamin D receptor (VDR) upon vitamin D_3 treatment (Obradovic et al., 2009) and by IL-4 (interleukin-4) (Todaro et al., 2008). More recently we demonstrated that PED expression levels in lung cancer are regulated by microRNAs (Incoronato et al., 2010).

PED interacts with different molecules, among these ERK 1/2, altering their nuclear localization by sequestering them into the cytosol, thus preventing their nuclear translocation (Formstecher et al., 2001). PED augments ERK phosphorylation acting as a scaffold protein for RSK2 and ERK 1/2 (Vaidyanathan et al., 2007). In order to get further insights on the role of PED in cancer, we aimed to find new PED interactors through the tandem affinity purification (TAP) method (Rigaut et al., 1999) in NSCLC. Upon mass spectrometry analysis, we identified several new PED interactors.

In this article we describe the functional role of the interaction between PED and Rac1, a member of mammalian Rho GTPase protein family. Rac1 regulates a wide range of cellular effects such as secretory processes, phagocytosis of apoptotic cells, epithelial cell polarization, growth factor-induced formation of membrane ruffles, ROS generation, lamellipodia formation and cell migration (Bosco et al., 2009; Heasman and Ridley, 2008). We investigate the downstream effects of PED/Rac1 interaction, focusing our attention on cell migration processes.

Materials and Methods

Reagents

Media, sera, and antibiotics for cell culture were from Life Technologies, Inc. (Grand Island, NY). Protein electrophoresis reagents were from Bio-Rad (Richmond, VA), and Western blotting and ECL reagents were from GE Healthcare (Piscataway, NJ). All other chemicals were from Sigma (St. Louis, MO).

Plasmids

Expression vectors for Rac wild type, RacQL, Rac12V, RasN17 and Vav1 were kindly provided by Dr. Mario Chiariello. pBS1761 was kindly provided by Dr. Ingram Iaccarino. PED-MYC expression plasmid was previously described (Condorelli et al., 2002). PED-MYC S104G was realized through AGT-GGT single nucleotide substitution (QuikChange Site-Directed Mutagenesis Kit, Stratagene, La Jolla, CA). ShRNAi-PED and shRNAi-scrambled were from Open Biosystems (Huntsville, AL), GST-CRIB has been previously described (Benard et al., 1999).

Virus production

We produced vector stocks by calcium phosphate transient transfection, cotransfecting three plasmids in 293 T human embryonic kidney cells, since these cells are good DNA recipients. The three plasmids are: the packaging plasmid, pCMVDR8.74 designed to provide the HIV proteins needed to produce the virus particle; the envelope-coding plasmid, pMD.G, for pseudotyping the virion with VSV-G and TWEEN PED-TAP vector, the transgene coding plasmid.

The calcium phosphate–DNA precipitate was allowed to stay on the cells for 14–16 h, after which the medium was replaced, collected 48 h later, centrifuged at 1,000 rpm for 5 min at room temperature and filtered through 0.22 mm pore nitrocellulose filters.

Generation of lentiviral vectors and gene transfer

For PED-TAP plasmid, we PCR-amplified PED cDNA from PED-MYC expressing vector and subcloned into the pBS1761 plasmid for TAP-tagging of proteins at the N-terminus. For TWEEN PED-TAP vector, we PCR-amplified PED-TAP cDNA from PED-TAP expressing vector and subcloned into the lentiviral vector TWEEN17 under control of the cytomegalovirus promoter.

On the day of infection, the medium was removed and replaced with viral supernatant to which 4 mg/ml of Polybrene had been added. Cells were then centrifuged in their plate for 45 min in a Beckman GS-6KR centrifuge, at 1,800 rpm and 32°C. After centrifugation, cells were kept for either 1 h 15 min or ON in a 5% CO2 incubator at 32 or 37°C, respectively. After exposure, cells were washed twice with cold PBS and fresh medium added. At either 12 or 48 h after the infection, cells were washed with PBS, harvested with trypsin/EDTA and analyzed by FACS for GFP expression.

Cell culture

Human A459, A459 TWEEN, A459 TWEEN PED-TAP and HeLa cell lines were grown in DMEM containing 10% heat-inactivated FBS and with 2 mM L-glutamine and 100 U/ml penicillin-streptomycin. PEDshRNA A459 clones (A459 shPED#1 and A459 shPED #2) and SCRAMBLEDshRNA A459 clone (A459 shSCR) were grown in DMEM medium containing 10% heat-inactivated FBS, with 2 mM L-glutamine and 100 U/ml penicillin–streptomycin and selected with 2.5 μg/ml puromycin from Sigma.

Tandem affinity purification

A459 PED-TAP cells were lysed in TEB buffer (50 mM Tris–HCl, pH 8, 150 mM NaCl, 5% glycerol, 1% Triton X-100, 1.5 mM $MgCl_2$, 2 mM EGTA and protease inhibitors from Roche (Indianapolis, IN)) for 2 h under gently mix and cleared by centrifugation for 30 min at 13,000 rpm. The lysate was incubated with rabbit-IgG agarose beads (Sigma) overnight at 4°C. Beads were collected by centrifugation (3,000 rpm for 5 min), and then extensively washed firstly with TEB buffer and then with TEV-protease cleavage buffer (TCB: 10 mM Tris–HCl (pH 8), 150 mM NaCl and 0.1% Triton X-100, 0.5 mM EGTA). Beads were then incubated with 150 μl TEV protease in 1.5 mL of TCB overnight at 4°C. The TEV-protease cleavage products were collected and then loaded onto Calmodulin sepharose beads (GE Healthcare) in Calmodulin Binding Buffer (CBB: 10 mM Tris–HCl, pH 8, 150 mM NaCl, 0.1% Triton X-100, 1 mM MgAcetate, 1 mM Imidazole, 2 mM $CaCl_2$) supplemented with 250 mM $CaCl_2$ at 4°C for 1.5 h. Beads were recovered by centrifugation at 3,000 rpm for 5 min and then extensively washed with CBB. Proteins retained on the beads were eluted by incubation with Calmodulin Eluition Buffer (CEB: 10 mM Tris–HCl, pH 8, 150 mM NaCl and 0.1% Triton X-100, 1 mM MgAcetate, 1 mM Imidazole) with three different $CaCl_2$ concentrations (2, 10, and 20 mM). The eluate was collected and concentrated by methanol/chloroform precipitation before loading onto a 12% SDS–PAGE.

Mass spectrometry analysis and protein identification

The gel was stained with colloidal Coomassie blue (Sigma). Protein bands were excised from the gel, reduced, alkylated and digested with trypsin (Zito et al., 2007). Peptide mixtures were extracted from the gel and analyzed by nano-chromatography tandem mass spectrometry (nanoLC–MS/MS) on a CHIP MS Ion Trap XCT Ultra equipped with a capillary 1100 HPLC system and a chip cube (Agilent Technologies, Palo Alto, CA). Peptide analysis was performed using data-dependent acquisition of one MS scan (mass range from 400 to 2,000 *m/z*) followed by MS/MS scans of the three most abundant ions in each MS scan. Raw data from nanoLC–MS/MS analyses were employed to query a non-redundant protein database using in house MASCOT software (Matrix Science, Boston, MA).

Western blotting

Total proteins from A459 and HeLa cells were extracted with RIPA buffer (0.15 mM NaCl, 0.05 mM Tris–HCl, pH 7.5, 1% Triton, 0.1% SDS, 0.1% sodium deoxycolate and 1% Nonidet P40). Fifty

micrograms of sample extract were resolved on 10–15% SDS–polyacrilamide gels using a mini-gel apparatus (Bio-Rad Laboratories, Richmond, CA) and transferred to Hybond-C extra nitrocellulose. Membranes were blocked for 1 h with 5% non-fat dry milk in TBS containing 0.05% Tween-20, incubated over night with primary antibody, washed and incubated with secondary antibody, and visualized by chemiluminescence. The following primary antibodies were used: anti-PAP (Peroxidase-Anti-Peroxidase Soluble Complex), anti-β-actin antibodies from Sigma, anti-Rac1 antibody from Abcam (Cambridge, MA); anti-phospho ser71 Rac1, anti-phospho ser104 PED, anti-ERK 1/2, anti-phospho ERK 1/2, anti-ELK1, anti-phospho-ELK1, anti-MYC-tag antibodies from Cell Signalling (Danvers, MA), anti-phospho ser116 PED antibody from Biosource International Inc. (Camarillo, CA), anti-PED antibody (Condorelli et al., 2002), anti-AU5, anti-HA antibodies from Covance (Emeryville, CA), anti-Ras antibody from Upstate (Temecula, CA).

Immunoprecipitation

Cells were cultured at a final concentration of 90% in p100 plates. The cells were harvested with RIPA Buffer on a shaker for 30 min. One milligram of total extract was immunoprecipitated using the indicated antibodies (4 μg/ml Anti-Rac1, 4 μg/ml Anti-PED), for 16 h on shaker. Then, A/G beads (Santa Cruz Biotechnology Inc., Santa Cruz, CA) were added for two hrs. The beads were washed for three times with washing buffer (50 mM Tris–HCl pH 7.5, 150 mM NaCl, 0.1% Triton, 10% glycerol), and then 20 μl of sample buffer was added; the samples were boiled at 100°C for 5 min and then the supernatants resolved by SDS–PAGE.

siRNA and plasmid transfection

A459 cells were cultured to 80% confluence and transiently transfected using LIPOFECTAMINE 2000 (Invitrogen, Carlsbad, CA) with 150 nM anti-PED siRNAs and anti-Rac1 siRNAs (Dharmacon, Lafayette, CO), or with control vector, PED, PED S104G, Rac, RacQL, Rac12V, Vav1 cDNAs as reported in the paper, as described in the manufacturer's protocol.

Rac1 pull-down assay

Plates were starved for 24 h and then treated as indicated. After a quick wash with iced-cold PBS, cells were lysed with GST-Fish buffer (50 mM Tris–HCl ph 7.4, 2 mM $MgCl_2$, 1% NP-40, 10% glycerol, 100 mM NaCl, 1 μg/ml leupeptin, 1 μg/ml pepstatin, 1 μg/ml aprotinin, 1 mM PMSF, and 2 mM DTT). After 10 min at 4°C under agitation, cells were scraped and lysates were cleared by centrifugation in a precooled rotor. One hundred fifty micrograms of total protein extract was mixed with 10 μg of GST-PAK-CRIB domain coupled to glutathione-sepharose beads and incubated 30 min at 4°C under agitation. Beads were then rinsed three times rapidly with 1 ml of iced-cold GST-Fish buffer. The amounts of total Rac and Rac-GTP were estimated by immunoblot against Rac1.

Migration assay

Transwell Permeable Supports, 6.5 mm diameter inserts, 8.0 μM pore size, polycarbonate membrane (Corning Incorporate, Corning, NY) were used to perform migration assay. A459 and HeLa cells were grown as indicated above, then harvested by TrypLE™ Express (Invitrogen) and 10^5 cells were washed three times and then resuspended in 1% FBS containing DMEM medium and seeded in the upper chamber. Lower chamber of the Transwell was filled with 600 μl of culture medium containing 10% FBS, 5 μg/ml fibronectin, as an adhesive substrate. Cells were incubated at 37°C for 24 h. Transwell were then removed from 24-well plates and stained with 0.1% Crystal Violet in 25% methanol. Nonmigrated cells were scraped off on the top of the Transwell with a cotton swab. % of migrated cells was evaluated by eluiting crystal violet with 1% SDS and reading the absorbance at $\lambda = 570$ nm.

Invasion assay

A similar procedure as in migration assay was used. The upper chamber of the Transwell was filled with 100 μl of BD Matrigel™ (BD Biosciences, San Jose, CA). BD Matrigel™ was diluted to 1mg/ml in serum free culture medium and put into the top of the Transwell. Then it was incubated for 4 h for gelling. Cells were counted and treated as indicated above. Invaded cells were measured as % over control cells, transfected with empty vector.

Wound healing

Cells were cultured as confluent monolayers, synchronized in 1% FBS for 24 h, and wounded by pipette tip. Wounded monolayers were washed twice with PBS to remove nonadherent cells. Wound healing was followed up to 24 h. For these studies, cells were seeded in 35 mm Petri dishes and kept at 37°C in a humidified atmosphere with 5% CO_2.

Adhesion assay

4×10^5 cells were plated onto Fibronectin coated 96-well plate and incubated at 37°C with 5% CO_2 for 30 min. Then cells were fixed with 4% PFA for 20 min at RT and stained with 0.1% Crystal Violet in 25% methanol. % of adherent cells was evaluated by eluiting crystal violet with 1% SDS and reading the absorbance at $\lambda = 570$ nm.

Microscope image acquisition

Cells were fixed with 4% PFA for 20 min, blocked with 1% BSA and incubated with rhodamine-labeled phalloidin (Sigma). Fluorescent images of cells were captured on Confocal Laser Scanner Microscope LSM510 (Carl Zeiss MicroImaging, Thornwood, NY). (Objective lens: plan-apochromat 63×/1.4 oil dic).The samples were hold at room temperature. The acquisition software was Zeiss LSM510 Version 2.8 and the image was adapted using Photoshop® imaging software.

Results

PED interacts with Rac1

In order to discover new PED interactors, A459 cells were infected with the tween PED-TAP construct or, as control, tween vector. Total protein lysate was incubated with immunoglobulin derivatised agarose beads (IgG) and the retained sample eluted by hydrolysis with TEV protease. PED containing complexes were finally purified onto Calmodulin derivatised beads. After these two purification steps, the sample and the control were fractionated by SDS–PAGE, the entire lanes from the gel were cut in slices and each gel slice was submitted to the identification procedure (Fig. 1A,B) (Pisa et al., 2009). The resulting peptide mixtures were directly analyzed by mass spectrometry (LC–MS/MS) and identified by MASCOT protein database search. Proteins identified in both the control and the sample lanes were discarded, whereas those proteins solely identified in the sample and absent in the control were selected as putative PED interactors.

Several new candidate proteins were identified (data not shown) and among these we focused our attention on Rac1, because of its involvement in cancer signaling pathways. PED and Rac1 interaction was also confirmed by immunoprecipitation experiments from A459-tween PED-TAP cells (Fig. 1C), from A459 transfected with Rac1 (Fig. 1D) and from wild type A459 cells (Fig. 1E). PED and Rac1 co-immunoprecipitation was evident either with exogenous or with endogenous proteins.

PED affects Rac1 activation

In order to investigate the effects of PED on Rac1 activation, A459 cells were transfected with PED-MYC cDNA or control

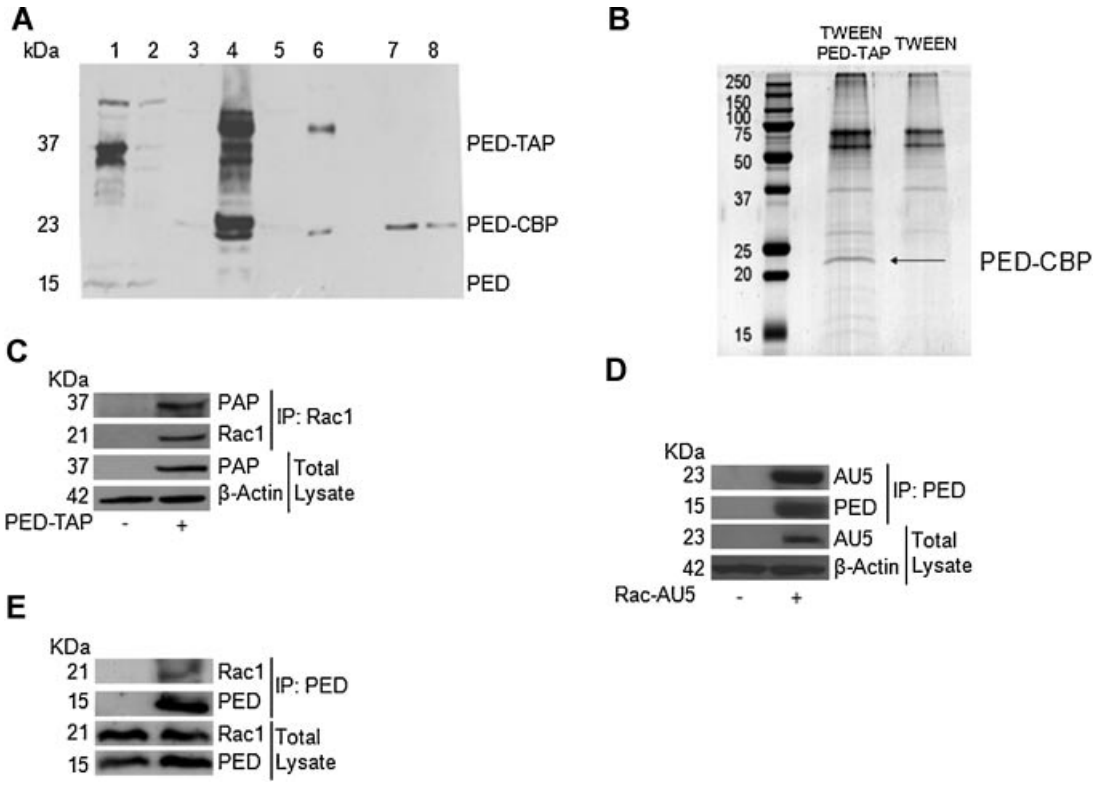

Fig. 1. PED interacts with Rac1. A459 cells infected with PED-TAP cDNA has been subjected to tap purification as described in the method's section. A: Samples from Tandem Affinity Purification collected at each step of the protocol. Lanes: (1) 40 μg of total extract; (2) 40 μg of supernatant after IgG incubation; (3) TEV cleavage control; (4) IgG beads after TEV cleavage; (5) supernatant after Calmodulin beads; (6) Calmodulin beads before final eluition; (7,8) eluition with 2, and 10 mM EGTA. B: Coomassie staining of preparative polyacrilamide gel. Our PED-CBP bait is indicated at 23 kDa. A459 cells infected with TWEEN vector were used as negative control. C: Co-immunoprecipitation of endogenous Rac1 with exogenous PED-TAP. One milligram of total extract immunoprecipitated using an anti-Rac1 antibody. Immunoprecipitated and input samples were loaded on 12% SDS polyacrilamide gel and blotted with an antibody (PAP) to identify the external part of the TAP tag. As negative control (C−), proteins were incubated with beads without antibody. D: Co-immunoprecipitation of endogenous PED with exogenous Rac-AU5 tagged. E: Co-immunoprecipitation between endogenous PED and Rac1. Samples from A459 wild type cells were immunoprecipitated with anti-PED antibody. Samples incubated with beads only were used as negative control for each immunoprecipitation.

vector. After 24 h cells were serum starved for 16 h and then treated with 20% FBS for 5 or 15 min. The activity of Rac1 was assessed using the p21-binding domain (CRIB) of p21-activated kinase 1 (PAK1) in a GST-pull down assay (Benard et al., 1999). As shown in Figure 2A, after 5 min of stimulation, a larger amount of Rac1-GTP could be observed in PED overexpressing cells, compared to the control cells, transfected with an empty vector. This activation decreased after 15 min. Similar results have been obtained upon EGF stimulation, a Rac1 specific activator (Dise et al., 2008), with a similar kinetics (Supplementary Data, Fig. S1).

Mechanisms of PED-mediated Rac1 activation

The removal of bound GDP and the subsequent GTP loading are catalyzed by guanine nucleotide exchange factors (GEFs proteins) (Bernards and Settleman, 2007). We therefore asked whether PED could act as a scaffold protein in Rac1 activation by promoting the interaction between Rac1 and its GEFs. A459 cells were transfected with PED-MYC cDNA, starved for 24 h and then incubated for 16 h with 100 μM of NSC23766, a Rac1 GTPase specific inhibitor that inhibits GEFs binding to Rac1 (Gao et al., 2004). Subsequently cells were treated with 20% FBS for 5 min and Rac1-GTP pull down assay was performed. As shown in Figure 2A, PED overexpression increased Rac1 activation upon serum stimulation. However, this effect was inhibited by pretreating cells with NSC23766 (Fig. 2B), suggesting that Rac1 is activated by PED through a mechanism involving GEFs action. Since PED can stimulate Ras activation, thereby promoting Rac activation, A459 were transfected with empty vector, PED or RasN17 dominant negative cDNAs, starved for 24 h and then Rac1-GTP pull down assay was performed as shown in Figure 2C. RasN17 transfection did not alter PED-induced Rac1 activation.

Role of PED in AKT-mediated Rac1 phosphorylation

AKT is serine/threonine kinase downstream PTEN/PI3K pathway involved in many cellular processes, for example, survival, apoptosis and migration (Tokunaga et al., 2008). AKT phosphorylates Rac1 on Ser^{71} and thus inhibits its GTP-loading (Kwon et al., 2000). Because PED interferes the Rac1-GTP loading, we asked whether this effect was mediated through the regulation of Rac1 phosphorylation on Ser^{71}. To this aim, A459 cells were transfected with control vector or PED-MYC cDNA. After 24 h, the cells were serum starved and then treated for 5 min with 20% FBS. As shown in Figure 2D, PED overexpression resulted in a strong reduction of serum mediated Rac1 phosphorylation on Ser^{71}. Similar results were obtained with EGF stimulation (Supplementary Data, Fig. S2).

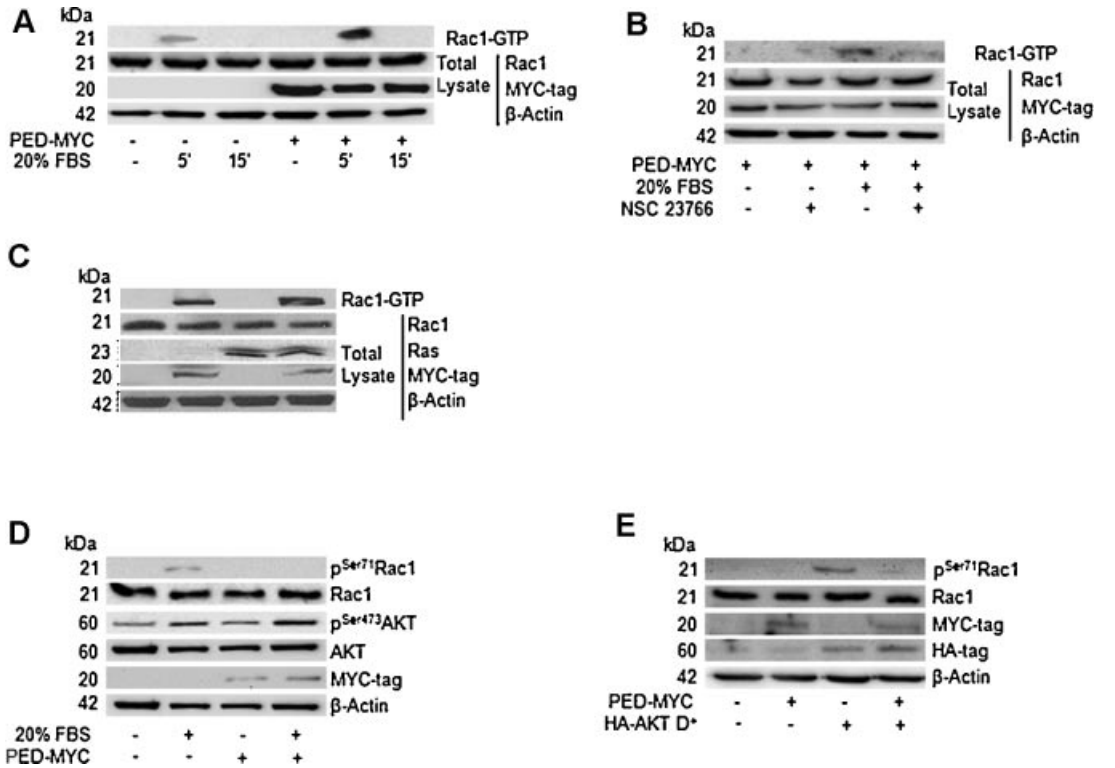

Fig. 2. PED regulates Rac1-GTP loading. A–C: Rac pull down experiments. A: A459 cells were transfected with 2 μg empty vector as control or 2 μg PED-MYC cDNA as indicated. After 24 h cells were serum starved and then treated for 5 and 15 min with 20% FBS respectively. Rac1-GTP pull down assay was performed as described in Materials and Methods Section. The amounts of total Rac1 and Rac1-GTP were estimated by immunoblotting with Rac1. B: Cells were transfected as described and then treated with 20% FBS stimulation, with or without 100 μM NSC23766 pretreatment for 16 h as indicated. C: A459 cells were transfected with 2 μg of PED, Ras17N cDNAs or control vector, then starved for 24 h and treated with 20% FBS. Then 150 μg of total lysate was subjected to Rac1-GTP pull down assay. D: A459 cells were transfected with 2 μg of PED cDNA or control vector, then starved for 16 h and treated as indicated. The phosphorylation of Rac1 was evaluated by immunoblotting with specific phospho Ser^{71} Rac1 antibody. E: Evaluation of Rac1 phosphorylation levels upon transfection with 2 μg of PED-MYC or AKT D+. The total amount of transfected plasmids is normalized with co-transfection of empty vector. PED cDNA expression inhibits AKT-induced Ser^{71} Rac1 phosphorylation upon serum stimulation.

To further confirm this observation, we evaluated basal Rac1 phosphorylation levels in A459 cells transfected with a constitutive active AKT (AKT D+) (Stassi et al., 2005) and PED-MYC cDNAs (Fig. 2E). AKT D+ increased Rac1-Ser^{71} phosphorylation, while co-transfection of AKT D+ and PED-MYC cDNAs resulted in a reduction of Rac1 phosphorylation levels. These results suggest that PED can enhance Rac1-GTP bound state by interfering with AKT-mediated Rac1 phosphorylation.

Effects of Rac1 activation on PED phosphorylation status

We also asked whether Rac/PED interaction could result in a Rac-1 modulation of PED cellular function. In order to be recruited to the DISC and inhibit the apoptotic process, PED needs to be phosphorylated in Ser^{104} and Ser^{116} (Condorelli et al., 1999; Trencia et al., 2003). On the other hand, in its non-phosphorylated status PED can bind and sequester ERK 1/2 into the cytosol (Renganathan et al., 2005; Glading et al., 2007). Therefore we asked whether Rac1 could alter PED phosphorylation status and thus its function. To this aim, we transfected A459 cells with wild type Rac or constitutively active Rac (RacQL) cDNAs. Interestingly, PED-Ser^{104} phosphorylation was increased upon transfection of wild type Rac and more strongly by RacQL compared to control, while Serine^{116} phosphorylation was not modified (supplementary data, Fig. S3). Furthermore, Ser^{104}-PED phosphorylation was also increased by transfection with another constitutively active Rac (Rac12V) and with Vav1 overexpression, one of Rac1 GEFs (Crespo et al., 1997; Fig. 3A). Because PKC is the major kinase involved in PED-Ser^{104} phosphorylation (Araujo et al., 1993; Renganathan et al., 2005), we investigated whether Rac1 may regulate PED phosphorylation through PKC. To this aim, A459 cells were transfected with constitutively active Rac and then treated with 108 nM Ro-32-0432, a cell-permeable and selective PKC inhibitor. PED phosphorylation levels on serine 104 were evaluated by blotting with specific anti-phospho-serine 104 PED antibody. As shown in Figure 3B, RacQL-mediated PED phosphorylation was completely abolished when the cells were treated with the PKC inhibitor. These results suggest that Rac1 augments PED phosphorylation on serine 104 by regulating PKC activity.

Role of PED and Rac1 interaction on ERK 1/2 activation

In order to investigate the downstream effects of PED and Rac1 interaction, we investigated ERK 1/2 pathway. PED can promote ERK 1/2 phosphorylation and is able to retain them into cytosol and thus avoiding their nuclear translocation and thus their transcriptional effects (Renganathan et al., 2005; Glading et al., 2007). The mechanism by which PED allows ERK 1/2 phosphorylation is not clear yet. Rac1 activation leads to

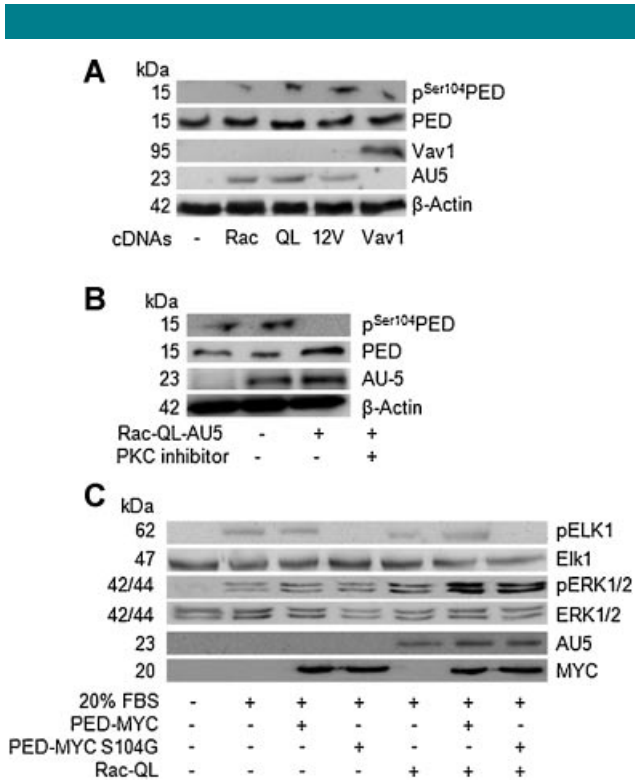

Fig. 3. Rac1 activation induces PED-Ser^{104} phosphorylation. A: A459 cells were transfected with control vector, Rac, RacQL, Rac12V or Vav1 respectively. Expression of constitutively active Rac resulted in a strong increase of Ser^{104}–PED phosphorylation, as attested by immunoblotting with specific Ser^{104}–PED antibody, compared to empty vector and wild type Rac. B: A459 cells were transfected with 2 μg of RacQL and then treated with 108 nM PKC inhibitor Ro-32-0432 for 16 h. PKC inhibition resulted in abolishment of Rac-induced Ser^{104}–PED phosphorylation. C: A459 cells were transfected with control vector, PED, PED S104G or RacQL. Then cells were starved for 16 h and treated with 20% FBS. Expression of PED and Rac-QL resulted in an increase of ERK 1/2 phosphorylation and ELK1 activation upon serum stimulation.

ERK 1/2 phosphorylation through a pathway involving PAK1-MEK1-ERK1/2 (Eblen et al., 2002; Alahari, 2003). To determine the effect of PED and Rac1 interaction on ERK 1/2 activation, we transfected A459 cells with control vector, PED-MYC or RacQL cDNAs and then evaluated the downstream effects on ERK 1/2 phosphorylation. PED and RacQL alone were able to activate ERK 1/2. Interestingly, when PED and RacQL were co-transfected the levels of ERK 1/2 phosphorylation were even stronger (Fig. 3C). As previously described (Glading et al., 2007), we found that PED transfection resulted in an inhibitory effect on ERK 1/2 nuclear translocation, as attested by the reduction of the phosphorylation of their nuclear substrate ELK1 (Hill and Treisman, 1995; Reddy et al., 2003; Fig. 3C). On the contrary, when PED was overexpressed together with RacQL, ELK1 phosphorylation was stronger compared to control. In order to evaluate whether this effect was due to Rac1-induced phosphorylation on PED Serine 104, we generated a mutant PED protein which could not be phosphorylated in Ser^{104} (S104G PED). Interestingly, transfection of S104G PED mutant, alone or co-transfected with RacQL, abolished the phosphorylation of ELK1 (Fig. 3C). These results suggest that PED, upon Rac-induced Ser^{104} phosphorylation, loses its capability to retain ERK 1/2 into cytosol and thus to phosphorylate ELK1, while its unphosphorylable mutant S104G retains ERK 1/2 into cytosol, even in the presence of constitutively active Rac.

Role of PED on cell migration

One of the most important effects of the activation of ERK1/2 pathway is regulation of cellular migration and invasion (Reddy et al., 2003). For this reason we asked whether PED/Rac1 interaction was involved in these phenomena. Overexpression of PED-MYC resulted in increased migration and invasion of A459 cells. The effect was similar to that obtained with constitutive active Rac (Fig. 4A). When PED-MYC and RacQL were cotransfected, the effects on cell migration and invasion were even stronger. Similar results were obtained by transfecting the same constructs into HeLa cells (data not shown). Moreover, unphosphorylable S104G PED mutant was able to inhibit both cell migration and invasion, even when co-transfected with constitutively active Rac (Fig. 4A). These results suggest that RacQL effects on PED phosphorylation may regulate its effects on migration/invasion.

To determine the pathway involved in the regulation of PED-mediated migration and invasion, PED overexpressing A459 cells were treated with Rac1 inhibitor NSC23766, PKC inhibitor Ro-32-0432 or MEK1 inhibitor U0126 for 16 h. PED-MYC transfected cells lost their capability to migrate and invade upon treatment with all the inhibitors used (Fig. 4B), suggesting that PED requires either Rac1, PKC and MEK1 activity to promote migration and invasion. To confirm Rac1 involvement in PED-mediated cell migration and invasion, we down-regulated Rac1 by transfection of specific siRNAs and then we tested cell migration and invasion in A459 cells. Upon Rac1 downregulation, PED lost its effects on cell migration and invasion (Fig. 4C). These results show for the first time that PED expression promotes cell migration and invasion through a mechanism involving the activation of Rac1, PKC and MEK1.

Effects of PED downregulation on cell migration

In order to evaluate the direct effect of PED on cell migration and invasion processes, we performed migration assays on PED knock down clones A459 ShPED#1 and A459 ShPED#2. As attested by western blotting analysis, we obtained a strong reduction of PED expression upon silencing, compared to the scrambled ShRNA clone (A459 ShSCR; Fig. 5A). PED silencing resulted in a reduction of cell capability for adhering, migrating and invading compared to control cells (Fig. 5A). Interestingly, PED knock down clones failed in Rac1-activation upon serum stimulation, as shown in Figure 5B.

Moreover, reduction of migration capability was also confirmed by wound healing assay, where the cells were induced to repair upon serum stimulation (Fig. 5C). We next analyzed F-actin structures in PED knock down clones using Rhodamine-conjugated phalloidin. Interestingly, as show in Figure 5D, cellular morphology of PED knock down clones was strongly altered, with the increase of cortical actin structures and rounder, less elongated phenotype. These data support the pivotal role of PED in regulating cell shape and migration processes in A459 cells.

Discussion

Several observations support the important role of PED in human cancer. PED, being a member of DED protein family (Valmiki and Ramos, 2009), induces resistance to TRAIL, FasL, TNFα-mediated death in cancer cells (Condorelli et al., 1999; Hao et al., 2001; Ricci-Vitiani et al., 2004; Garofalo et al., 2007; Zanca et al., 2008; Valmiki and Ramos, 2009), making therapy often ineffective. PED is overexpressed in many types of human cancer, among which lung cancers. The ability of PED to bind ERK 1/2 was the focus of many studies indicating that PED

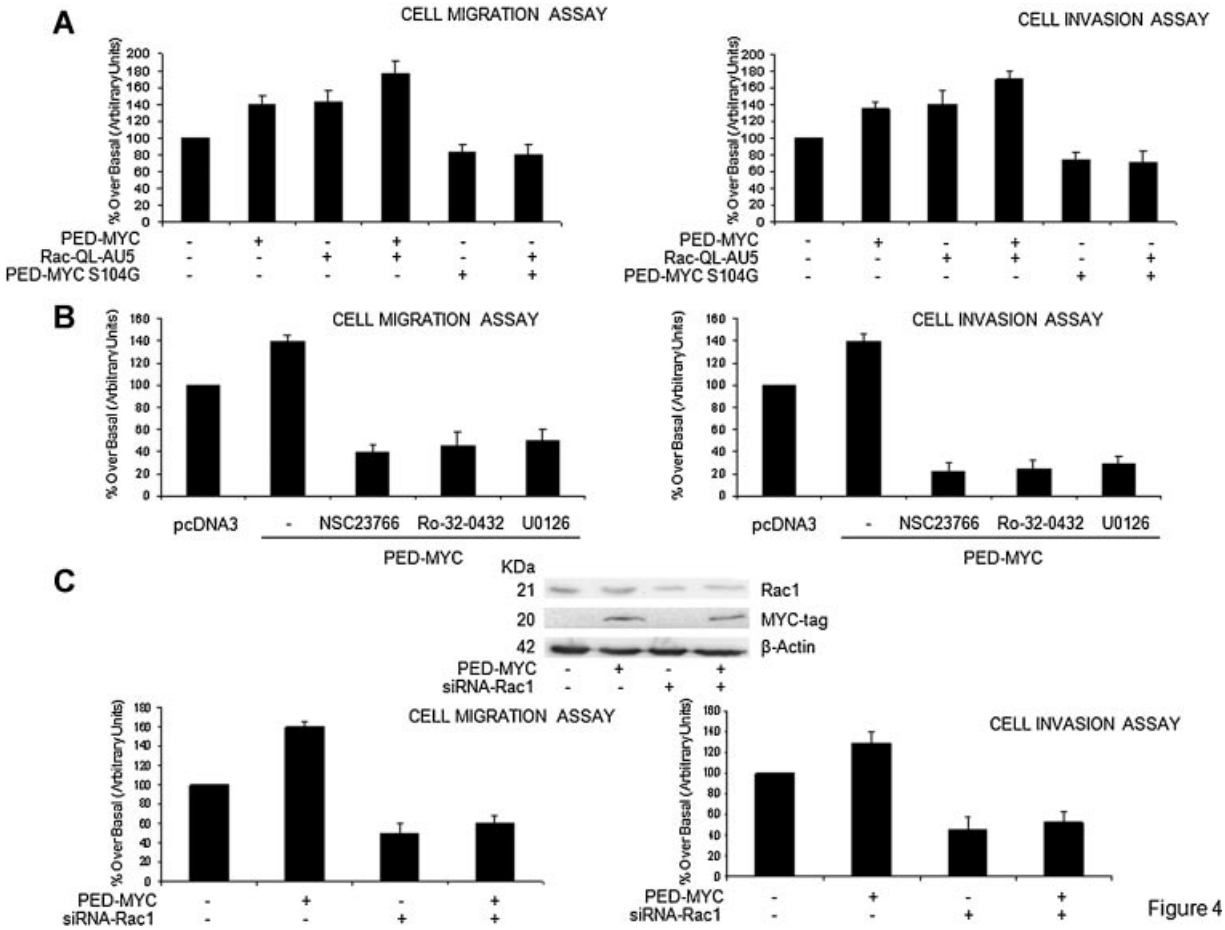

Fig. 4. Pathways of PED-mediated migration and invasion. A: A459 cells were transfected with control vector, PED, PED S104G or mutant RacQL, and Transwell migration and invasion assay was performed as described in Materials and Methods Section. Percentage of migrated cells is indicated as increase/decrease compared to control sample. B: A459 cells were transfected with control vector or PED cDNA. Then cells were plated on Transwell chambers to perform migration and invasion assays and treated with Rac1, PKC and MEK1 inhibitors (NSC23766, Ro-32-0432 and U0126 respectively). Migrated cells were evaluated 24 h later. Cells were stained in 25% methanol and 0.1% crystal violet. Then it was eluted with 1% SDS and the migration rate was established by reading absorbance at λ = 570 nm. (C) A459 cells were transfected with control vector, PED-MYC and Rac1-siRNAs. Rac1 downregulation was evaluated by immunoblotting with Rac1 antibody. Transwell chambers were used to perform migration and invasion assays. 10^5 cells were plated onto the upper chamber of Transwell and cells were incubated for 24 h. Rac1 downregulation blocked PED-mediated migration and invasion. Each assay was performed three times in independent experiments (n = 3). Error bars indicate standard deviation.

restrains ERK 1/2 within the cytosol, avoiding their nuclear translocation and thus ERKs nuclear effects, included transcription, migration, invasion (Ramos et al., 2000; Formstecher et al., 2001; Condorelli et al., 2002; Gaumont-Leclerc et al., 2004; Renganathan et al., 2005; Glading et al., 2007). PED is also able to bind RSK2 in a phosphorylation-regulated manner and act as a scaffold protein to strengthen its role in ERK activation (Vaidyanathan et al., 2007). In order to give new insights in PED's role in cancer, in this article we aimed to find new PED interactors. We performed a two steps purification method, the tandem affinity purification method for protein complexes characterization (Rigaut et al., 1999) and identified several new candidate partners of PED, one of which was Rac1. We first confirmed the interaction between PED and Rac1 through independent immunoprecipitation experiments, using both exogenous and endogenous proteins. In order to investigate the effect of PED on Rac1 GDP/GTP bound state, we performed a GST-pull down assay using the p21-binding domain (CRIB) of p21-activated kinase 1 (PAK1) to isolate the active GTP-bound Rac1 from the total extract (Benard et al., 1999). We demonstrated that PED augmented GTP-bound state upon stimulation with both 20% serum and specific Rac1 activator as EGF (Supplementary Data, Fig. S1) in a mechanism probably involving GEFs action. Even though our data show that GEFs action is necessary for Rac activation, we suggest that PED does not act as a scaffold protein in promoting GEFs-Rac1 binding, since in co-immunoprecipitation experiments, PED could not bind neither Tiam1 nor TrioN, two of the most abundant Rac1 GEFs (Bernards and Settleman, 2007). Moreover, we did not identify any GEFs from tandem affinity purification analysis and mass spectrometry experiments that bind to PED. Therefore, the mechanism of GEF involvement needs to be clarified. Since it was reported that AKT inhibits Rac1 activation (Kwon et al., 2000), we hypothesize that PED promotes GTP loading to Rac1 by reducing AKT inhibitory effects on Rac1, thus allowing its binding with GEFs. Our data are supported by the finding that PED downregulation in two stable knock down clones resulted in 30% increase in Rac1 phosphorylation, compared to control cells (Supplementary Data, Fig. S4). PED is AKT substrate (Trencia et al., 2003) and reduces AKT-mediated

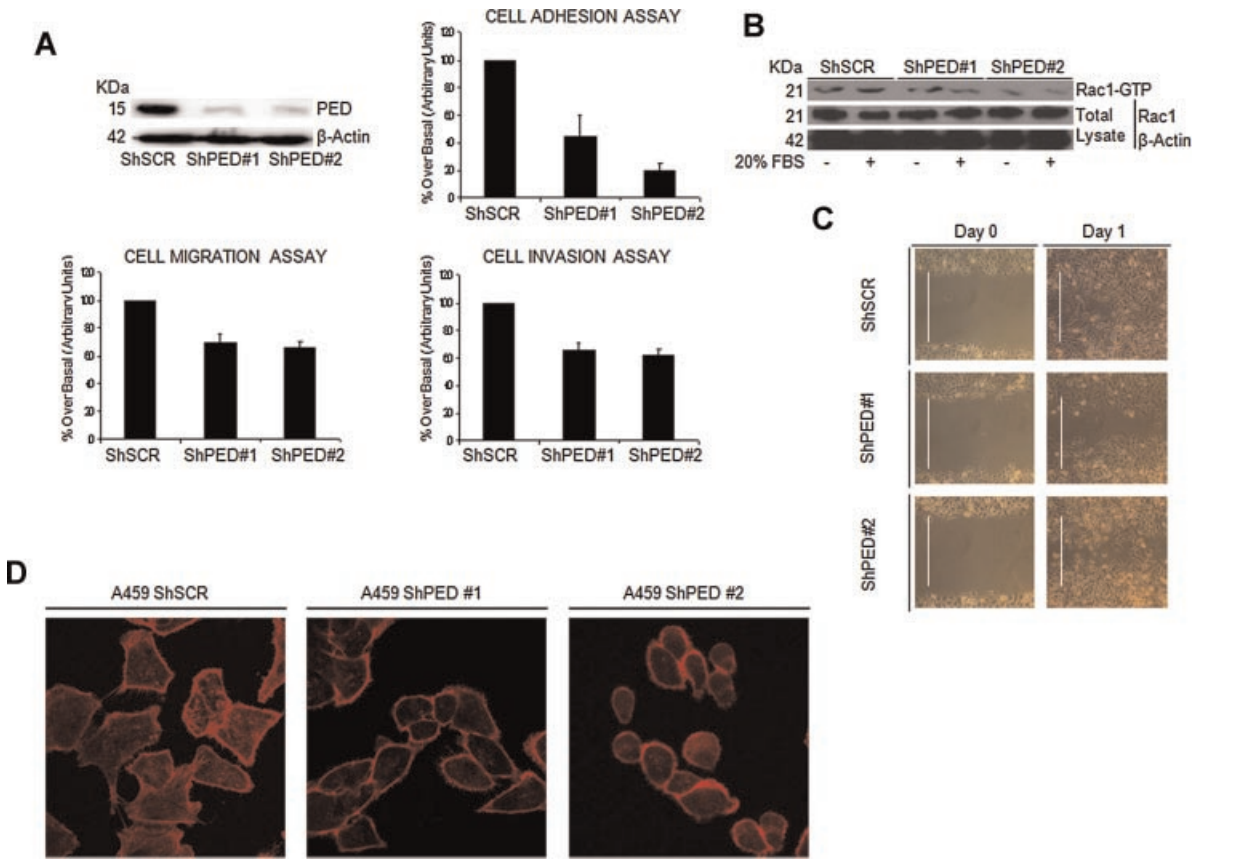

Fig. 5. Effects of PED downregulation on cell migration and cell morphology. A: A459-PED KO clones, obtained with transfection of specific PEDshRNA vector and then selected with 2.5 μg/ml of Puromycin. PED downregulation was evaluated by immunoblot against PED. Two clones were obtained and are indicated as ShPED#1 and ShPED#2. Control ShRNA cells is indicated as ShSCR. A459-PED KO clones showed a reduction of migration, invasion and adhesion upon serum stimulation, compared to control cells expressing Scrambled shRNA (ShSCR). Each assay was performed three times in independent experiments (n = 3). Error bars indicate standard deviation. B: ShSCR, ShPED#1 and ShPED#2 A459 clones were serum starved for 24 h and then treated with 20% FBS for 5 min. Cells were subjected to Rac1-GTP pull down assay in order to evaluate the amount of activated Rac1. Rac1-GTP was detected by blotting with Rac1 antibody. Total lysate was examined by western blotting to exclude variations in the total amount of Rac1. C: Wound healing assay of A459 ShSCR cells and PED shRNA clones (ShPED#1 and ShPED#2). Cells were grown to confluence and then wound was performed using a pipette tip. Then cells were incubated and grown for 24 h. D: Analysis of cell morphology. Cells were fixed with 4% PFA for 20 min, blocked with 1% BSA and incubated with rhodamine-labeled phalloidin.

phosphorylation of Rac1 probably competing with Rac1 for AKT binding or through a direct binding to the AKT binding site of Rac1. Many evidences show that AKT and its regulatory pathway can sustain migration process of tumor cells (Tokunaga et al., 2008; Garofalo et al., 2009) and then it was also found to be activated in vivo in human lung cancers (Mukohara et al., 2003; Balsara et al., 2004). Our observations, coupled with the AKT-mediated increased stability of PED (Trencia et al., 2003), gives new insights of the mechanism by which AKT augments cell migration/invasion: that is, increasing PED levels which promotes Rac1 activation.

Moreover, PED and Rac1 interfered with each other's function once bound together. In facts, when Rac1 is active, promotes PED Ser^{104} phosphorylation, through a mechanism involving PKC activation. The mechanism through which Rac1 promotes PKC-dependent PED phosphorylation is under investigation in our lab.

PED and Rac1 are involved in many cellular processes. To understand the biological meaning of their interaction we focused on the regulation of ERK 1/2 activation status as well as their cellular localization. We observed that co-expression of PED and constitutively active Rac induced a strong ERKs activation as well as Elk-1 phosphorylation (Hill and Treisman, 1995), indicating that ERKs were able to translocate from the cytosol into the nucleus. We propose that PED alone coadiuvates Rac1-mediated ERKs activation and the expression of active Rac facilitates PED phosphorylation on Ser^{104} and the consequent release of ERKs. In fact, PED Ser104 mutant blocked ELK phosphorylation when co-expressed with RacQL. Interestingly, EGFR/K-Ras activating mutations, an upstream regulator of Rac1 (Yip et al., 2007), often found in human NSCLC (Slebos et al., 1990; Mukohara et al., 2003), can contribute to the activation of Rac1 and thus promote the Rac1-mediated PED phosphorylation.

In this article we demonstrated that PED is involved in promoting cell migration and invasion. Previous findings described that PED mediated inhibition of cell migration/invasion (Renault-Mihara et al., 2006; Glading et al., 2007). Our data suggest that Rac1's effects on PED phosphorylation determine a reduction of PED's inhibitory role of ERK 1/2 nuclear translocation, which is required to promote migration/invasion (Hill and Treisman, 1995; Reddy et al., 2003). The importance of PED in controlling of ERK 1/2 localization was recently highlighted in a study in which PED, according to its phosphorylation status, is one of the main regulator of ERK 1/2 activity in response to treatment of EGF or NGF during

neuronal differentiation (von Kriegsheim et al., 2009). Moreover Haling et al. proposed that PED could sustain ERK 1/2 activation by regulating FRS2alpha phosphorylation status by retaining ERK 1/2 within the cytosol and preventing their localization to plasma membrane (Haling et al., 2009). Ramos et al. previously reported that PED activates ERK MAP Kinase through a Ras-dependent pathway (Ramos et al., 2000). In our experiment we found that PED-mediated Rac1-activation is independent from Ras activity. PED-Rac1 interaction gives a new explanation of how PED can mediate its effects on MAPK signaling.

In order to clarify PED role in migration and invasion processes, we generated two stable A459 PED knock down clones and evaluated the adhesion, migration and invasion capabilities of the cells. We found that PED silencing reduced these phenomena. Cell shape of PED knock down clones was strongly altered compared to control cells. In fact, cell showed a rounder and less elongated shape, as well as cortical actin structures, in accordance with a reduced migratory capability. Cells need multiple protrusions and well-organized lamellipodia structures to migrate (Petrie et al., 2009). The actin based cytoskeleton structures are dynamically controlled by several stimuli and Rac1 is one of the main effectors of this process, acting in the generation of focal adhesions and lamellipodia (Ridley et al., 1992; Machesky, 1997; Nobes and Hall, 1999; Heasman and Ridley, 2008; Bosco et al., 2009). The lost of these structures in PED knock down cells correspond to a reduced Rac1 activity. Furthermore, similar phenotypes can be observed in Rac1 deficient fibrosarcoma cells HT1080, endothelial cells or platelets, that show an impairment in lamellipodia formation (McCarty et al., 2005; Heasman and Ridley, 2008; Tan et al., 2008; Niggli et al., 2009) supporting the role of Rac1 in migration process.

Our findings about PED interactome demonstrate that PED overexpression is linked to cancer not only because of its anti-apoptotic role but also because this promotes migration and invasion of malignant cells.

Acknowledgments

We thank Prof. C. Garbi for his support in fluorescence imaging analysis. This work was supported in part by the Italian Ministry of Education (MIUR) Progetto FIRB Rete Nazionale di Proteomica Umana (Italian Human Proteomenet) RBRN07BMCT and by Associazione Italiana Ricerca sul Cancro (AIRC) and MIUR-FIRB (RBIN04J4J7).

Literature Cited

Alahari SK. 2003. Nischarin inhibits Rac induced migration and invasion of epithelial cells by affecting signaling cascades involving PAK. Exp Cell Res 288:514–524.

Araujo H, Danziger N, Cordier J, Glowinski JH. 1993. Characterization of PEA-15, a major substrate for protein kinase C in astrocytes. J Biol Chem 268:5911–5920.

Balsara BR, Pei J, Mitsuuchi Y, Page R, Klein-Szanto A, Wang H, Unger M, Testa JR. 2004. Frequent activation of AKT in non-small cell lung carcinomas and preneoplastic bronchial lesions. Carcinogenesis 25:2053–2059.

Bartholomeusz C, Rosen D, Wei C, Kazansky A, Yamasaki F, Takahashi T, Itamochi H, Kondo S, Liu J, Ueno NT. 2008. PEA-15 induces autophagy in human ovarian cancer cells and is associated with prolonged overall survival. Cancer Res 68:9302–9310.

Benard V, Bohl BP, Bokoch GM. 1999. Characterization of rac and cdc42 activation in chemoattractant-stimulated human neutrophils using a novel assay for active GTPases. J Biol Chem 274:13198–13204.

Bernards A, Settleman J. 2007. GEFs in growth factor signaling. Growth Factors 25:355–361.

Bosco EE, Mulloy JC, Zheng Y. 2009. Rac1 GTPase: A "Rac" of all trades. Cell Mol Life Sci 66:370–374.

Condorelli G, Vigliotta G, Cafieri A, Trencia A, Andalo P, Oriente F, Miele C, Caruso M, Formisano P, Beguinot F. 1999. PED/PEA-15: An anti-apoptotic molecule that regulates FAS/TNFR1-induced apoptosis. Oncogene 18:4409–4415.

Condorelli G, Trencia A, Vigliotta G, Perfetti A, Goglia U, Cassese A, Musti AM, Miele C, Santopietro S, Formisano P, Beguinot F. 2002. Multiple members of the mitogen-activated protein kinase family are necessary for PED/PEA-15 anti-apoptotic function. J Biol Chem 277:11013–11018.

Crespo P, Schuebel KE, Ostrom AA, Gutkind JS, Bustelo XR. 1997. Phosphotyrosine-dependent activation of Rac-1 GDP/GTP exchange by the vav proto-oncogene product. Nature 385:169–172.

Dise RS, Frey MR, Whitehead RH, Polk DB. 2008. Epidermal growth factor stimulates Rac activation through Src and phosphatidylinositol 3-kinase to promote colonic epithelial cell migration. Am J Physiol Gastrointest Liver Physiol 294:276–285.

Eblen ST, Slack JK, Weber MJ, Catling AD. 2002. Rac-PAK signaling stimulates extracellular signal-regulated kinase (ERK) activation by regulating formation of MEK1-ERK complexes. Mol Cell Biol 22:6023–6033.

Erdmann S, Senkel S, Arndt T, Lucas B, Lausen J, Klein-Hitpass L, Ryffel GU, Thomas H. 2007. Tissue-specific transcription factor HNF4alpha inhibits cell proliferation and induces apoptosis in the pancreatic INS-1 beta-cell line. Biol Chem 388:91–106.

Formstecher E, Ramos JW, Fauquet M, Calderwood DA, Hsieh JC, Canton B, Nguyen XT, Barnier JV, Camonis J, Ginsberg MH, Chneiweiss H. 2001. PEA-15 mediates cytoplasmic sequestration of ERK MAP kinase. Dev Cell 1:239–250.

Gao Y, Dickerson JB, Guo F, Zheng J, Zheng Y. 2004. Rational design and characterization of a Rac GTPase-specific small molecule inhibitor. Proc Natl Acad Sci USA 101:7618–7623.

Garofalo M, Romano G, Quintavalle C, Romano MF, Chiurazzi F, Zanca C, Condorelli G. 2007. Selective inhibition of PED protein expression sensitizes B-cell chronic lymphocytic leukaemia cells to TRAIL-induced apoptosis. Int J Cancer 120:1215–1222.

Garofalo M, Di Leva G, Romano G, Nuovo G, Suh SS, Ngankeu A, Taccioli C, Pichiorri F, Alder H, Secchiero P, Gasparini P, Gonelli A, Costinean S, Acunzo M, Condorelli G, Croce CM. 2009. miR-221&222 regulate TRAIL resistance and enhance tumorigenicity through PTEN and TIMP3 downregulation. Cancer Cell 16:498–509.

Gaumont-Leclerc MF, Mukhopadhyay UK, Goumard S, Ferbeyre G. 2004. PEA-15 is inhibited by adenovirus E1A and plays a role in ERK nuclear export and Ras-induced senescence. J Biol Chem 279:46802–46809.

Glading A, Koziol JA, Krueger J, Ginsberg MH. 2007. PEA-15 inhibits tumor cell invasion by binding to extracellular signal-regulated kinase 1/2. J Biol Chem 279:46802–46809.

Haling JR, Wang F, Ginsberg MH. 2010. Phosphoprotein enriched in astrocytes 15 kDa (PEA-15) reprograms growth factor signaling by inhibiting threonine phosphorylation of fibroblast receptor substrate 2alpha. Mol Biol Cell. 21:664–673.

Hao C, Beguinot F, Condorelli G, Trencia A, Van Meir EG, Yong VW, Parney IF, Roa WH, Petruk KC. 2001. Induction and intracellular regulation of tumor necrosis factor-related apoptosis-inducing ligand (TRAIL) mediated apotosis in human malignant glioma cells. Cancer Res 61:1162–1170.

Heasman SJ, Ridley AJ. 2008. Mammalian Rho GTPases: New insights into their functions from in vivo studies. Nat Rev Mol Cell Biol 9:690–701.

Hill CS, Treisman R. 1995. Transcriptional regulation by extracellular signals: Mechanisms and specificity. Cell 80:199–211.

Kubes M, Cordier J, Glowinski J, Girault JA, Chneiweiss H. 1998. Endothelin induces a calcium-dependent phosphorylation of PEA-15 in intact astrocytes: Identification of Ser104 and Ser116 phosphorylated, respectively, by protein kinase C and calcium/calmodulin kinase II in vitro. J Neurochem 71:1307–1314.

Kwon T, Kwon DY, Chun J, Kim JH, Kang SS. 2000. Akt protein kinase inhibits Rac1-GTP binding through phosphorylation at serine 71 of Rac1. J Biol Chem 275:423–428.

Machesky LMHA. 1997. Role of actin polymerization and adhesion to extracellular matrix in Rac- and Rho-induced cytoskeletal reorganization. J Cell Biol 138:913–926.

McCarty OJ, Larson MK, Auger JM, Kalia N, Atkinson BT, Pearce AC, Ruf S, Henderson RB, Tybulewicz VL, Machesky LM, Hall A, Watson SP. 2005. Rac1 is essential for platelet lamellipodia formation and aggregate stability under flow. J Biol Chem 280:39474–39484.

Mukohara T, Kudoh S, Yamauchi S, Kimura T, Yoshimura N, Kanazawa H, Hirata K, Wanibuchi H, Fukushima S, Inoue K, Yoshikawa J. 2003. Expression of epidermal growth factor receptor (EGFR) and downstream-activated peptides in surgically excised non-small-cell lung cancer (NSCLC). Lung Cancer 41:123–130.

Niggli V, Schlicht D, Affentranger S. 2009. Specific roles of Rac1 and Rac2 in motile functions of HT1080 fibrosarcoma cells. Biochem Biophys Res Commun 386:688–692.

Nobes CD, Hall A. 1999. Rho GTPases control polarity, protrusion, and adhesion during cell movement. J Cell Biol 144:1235–1244.

Obradovic D, Zanca C, Vogl A, Trümbach D, Deussing J, Condorelli G, Rein T. 2009. Vitamin D(3) signalling in the brain enhances the function of phosphoprotein enriched in astrocytes—15 kDa (PEA-15). J Cell Mol Med 13:3315–3328.

Peacock JW, Palmer J, Fink D, Ip S, Pietras EM, Mui AL, Chung SW, Gleave ME, Cox ME, Parsons R, Peter ME, Ong CJ. 2009. PTEN loss promotes mitochondrially dependent type II Fas-induced apoptosis via PEA-15. Mol Cell Biol 29:1222–1234.

Petrie RJ, Doyle AD, Yamada KM. 2009. Random versus directionally persistent cell migration. Nat Rev Mol Cell Biol 10:538–549.

Pisa V, Cozzolino M, Gargiulo S, Ottone C, Piccioni F, Monti M, Gigliotti S, Talamo F, Graziani F, Pucci P, Verrotti AC. 2009. The molecular chaperone Hsp90 is a component of the cap-binding complex and interacts with the translational repressor Cup during Drosophila oogenesis. Gene 432:67–74.

Ramos JW, Hughes PE, Renshaw MW, Schwartz MA, Formstecher E, Chneiweiss H, Ginsberg MH. 2000. Death effector domain protein PEA-15 potentiates Ras activation of extracellular signal receptor-activated kinase by an adhesion-independent mechanism. Mol Biol Cell 11:2863–2872.

Reddy KB, Nabha SM, Atanaskova N. 2003. Role of MAP kinase in tumor progression and invasion. Cancer Metastasis Rev 22:395–403.

Renault F, Formstecher E, Callebaut I, Junier MP, Chneiweiss H. 2003. The multifunctional protein PEA-15 is involved in the control of apoptosis and cell cycle in astrocytes. Biochem Pharmacol 66:1581–1588.

Renault-Mihara F, Beuvon F, Iturrioz X, Canton B, De Bouard S, Léonard N, Mouhamad S, Sharif A, Ramos JW, Junier MP, Chneiweiss H. 2006. Phosphoprotein enriched in astrocytes-15kDa expression inhibits astrocyte migration by a protein kinase C delta-dependent mechanism. Mol Biol Cell 17:5141–5152.

Renganathan H, Vaidyanathan H, Knapinska A, Ramos JW. 2005. Phosphorylation of PEA-15 switches its binding specificity from ERK/MAPK to FADD. Biochem J 390: 729–735.

Ricci-Vitiani L, Pedini F, Mollinari C, Condorelli G, Bonci D, Bez A, Colombo A, Parati E, Peschle C, De Maria R. 2004. Absence of caspase 8 and high expression of PED protect primitive neural cells from cell death. J Exp Med 200:1257–1266.

Ridley AJ, Paterson HF, Johnston CL, Diekmann D, Hall A. 1992. The small GTP-binding protein rac regulates growth factor-induced membrane ruffling. Cell 70:401–410.

Rigaut G, Shevchenko A, Rutz B, Wilm M, Mann M, Séraphin B. 1999. A generic protein purification method for protein complex characterization and proteome exploration. Nat Biotechnol 17:1030–1032.

Slebos RJ, Kibbelaar RE, Dalesio O, Kooistra A, Stam J, Meijer CJ, Wagenaar SS, Vanderschueren RG, van Zandwijk N, Mooi WJ., et al. 1990. K-ras oncogene activation as a prognostic marker in adenocarcinoma of the lung. N Engl J Med 10:538–549.

Stassi G, Garofalo M, Zerilli M, Ricci-Vitiani L, Zanca C, Todaro M, Aragona F, Limite G, Petrella G, Condorelli G. 2005. PED mediates AKT-dependent chemoresistance in human breast cancer cells. Cancer Res 65:6668–6675.

Tan W, Palmby TR, Gavard J, Amornphimoltham P, Zheng Y, Gutkind JS. 2008. An essential role for Rac1 in endothelial cell function and vascular development. FASEB J 22:1829–1838.
Todaro M, Lombardo Y, Francipane MG, Alea MP, Pammareri P, Iovino F, Di Stefano AB, Di Bernardo C, Agrusa A, Condorelli G, Walczak H, Stassi G. 2008. Apoptosis resistance in epithelial tumors is mediated by tumor-cell-derived interleukin-4. Cell Death Differ 15:762–772.
Tokunaga E, Oki E, Egashira A, Sadanaga N, Morita M, Kakeji Y, Maehara Y. 2008. Deregulation of the Akt pathway in human cancer. Curr Cancer Drug Targets 8:27–36.
Trencia A, Perfetti A, Cassese A, Vigliotta G, Miele C, Oriente F, Santopietro S, Giacco F, Condorelli G, Formisano P, Beguinot F. 2003. Protein kinase B/Akt binds and phosphorylates PED/PEA-15, stabilizing its antiapoptotic action. Mol Cell Biol 23:4511–4521.
Ungaro P, Teperino R, Mirra P, Cassese A, Fiory F, Perruolo G, Miele C, Laakso M, Formisano P, Beguinot F. 2008. Molecular cloning and characterization of the human PED/PEA-15 gene promoter reveal antagonistic regulation by hepatocyte nuclear factor 4alpha and chicken ovalbumin upstream promoter transcription factor II. J Biol Chem 283:30970–30979.
Vaidyanathan H, Opoku-Ansah J, Pastorino S, Renganathan H, Matter ML, Ramos JW. 2007. ERK MAP kinase is targeted to RSK2 by the phosphoprotein PEA-15. Proc Natl Acad Sci USA 104:19837–19842.
Valmiki MG, Ramos JW. 2009. Death effector domain-containing proteins. Cell Mol Life Sci 66:814–830.
von Kriegsheim A, Baiocchi D, Birtwistle M, Sumpton D, Bienvenut W, Morrice N, Yamada K, Lamond A, Kalna G, Orton R, Gilbert D, Kolch W. 2009. Cell fate decisions are specified by the dynamic ERK interactome. Nat Cell Biol 11:1458–1464.
Yip SC, El-Sibai M, Coniglio SJ, Mouneimne G, Eddy RJ, Drees BE, Neilsen P, Goswami S, Symons M, Condeelis JS, Backer JM. 2007. The distinct roles of Ras and Rac in PI 3-kinase-dependent protrusion during EGF-stimulated cell migration. J Cell Sci 120:3138–3146.
Zanca C, Garofalo M, Quintavalle C, Romano G, Acunzo M, Ragno P, Montuori N, Incoronato M, Tornillo L, Baumhoer D, Briguori C, Terracciano L, Condorelli G. 2008. PED mediates TRAIL resistance in human non small cell lung cancer. J Cell Mol Med 12:2416–2426.
Zito E, Buono M, Pepe S, Settembre C, Annunziata I, Surace EM, Dierks T, Monti M, Cozzolino M, Pucci P, Ballabio A, Cosma MP. 2007. Sulfatase modifying factor 1 trafficking through the cells: From endoplasmic reticulum to the endoplasmic reticulum. EMBO J 26:2443–2453.